

Strategic energy planning under uncertainty

THÈSE N° 7961 (2017)

PRÉSENTÉE LE 20 OCTOBRE 2017
À LA FACULTÉ DES SCIENCES ET TECHNIQUES DE L'INGÉNIEUR
GROUPE SCI STI FM
PROGRAMME DOCTORAL EN ENERGIE

ÉCOLE POLYTECHNIQUE FÉDÉRALE DE LAUSANNE

POUR L'OBTENTION DU GRADE DE DOCTEUR ÈS SCIENCES

PAR

Stefano MORET

acceptée sur proposition du jury:

Prof. J. A. Schiffmann, président du jury
Prof. F. Maréchal, Prof. M. Bierlaire, directeurs de thèse
Prof. A. P. C. Faaij, rapporteur
Dr T. G. Kreutz, rapporteur
Prof. D. Kuhn, rapporteur

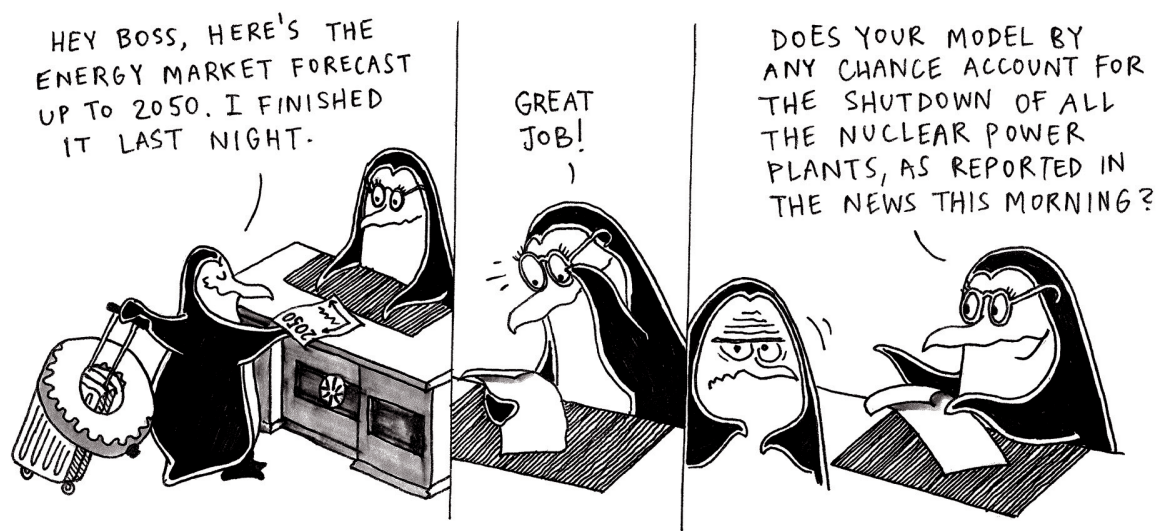


ÉCOLE POLYTECHNIQUE
FÉDÉRALE DE LAUSANNE

Suisse
2017

“At the time we were all convinced that we had to speak, write, and publish as quickly as possible and as much as possible and that this was necessary for the good of mankind. Thousands of us published and wrote in an effort to teach others, all the while disclaiming and abusing one another. Without taking note of the fact that we knew nothing, that we did not know the answer to the simplest question of life, the question of what is right and what is wrong, we all went on talking without listening to one another. At times we would indulge and praise each other on the condition that we be indulged and praised in return; at other times we would irritate and shout at each other exactly as in a madhouse.”

Lev Nikolajevič Tolstoj. *A Confession*



by Outi Supponen

Acknowledgments

On paper, doing a PhD sounds like the best of deals, and it probably is: you are given four years and a fair amount of freedom to fully focus on a topic you are passionate about - and you even get paid for it! Yet, for many, a PhD is also a difficult and challenging time. Of course, there is difficulty associated with the chosen research topic *per se*, but that is not the kind of difficulty I am talking about. The fact is that this very privileged status comes with the burden of constantly being confronted with yourself, of having to create your own meaning. Or, at least, that was the case for me: several days, I woke up in the morning, had coffee, sat at my desk, and found myself able to decide what I would do in the next eight-hours-and-twelve-minutes, which made me progressively pretty aware of the fact that, had I done nothing at all, the world would have still managed to go on. This implies that, although I humbly hope that someone will eventually be able to find value in the work I have collated in the forthcoming pages, I sincerely think that the significance of a PhD thesis is ultimately personal and relative to its author.

But don't get me wrong - I had a lot of fun. And this is mostly due to the fantastic people I have had the luck of being surrounded by - starting from my mentors. François, thank you for making it so easy to interact on both the personal and the professional level. Thank you for the special environment you do create in our group, the guitar playing, the interesting discussions, the bright insights, and above all for the freedom and trust I always felt granted from your side - I don't think that there are many supervisors you can openly say *no* to, while being confident that you will still have an office the following day. And Michel, your very rigorous yet friendly guidance has been a constant reference point for me during this journey. Thank you for your truly impressive knowledge, for welcoming me in your lab's activities, and especially for being so honest, sometimes to the point of being harsh, in reviewing and criticizing my work - I really feel that it brought a substantial improvement to the quality of my papers and of my writing.

During my first months at EPFL, I also had the pleasure of working closely with Prof. Favrat. Looking back at those months, I am surprised at how you put me at ease while working, although I was quite honestly intimidated by your knowledge. Thank you also for your availability and support whenever I needed it throughout the rest of my thesis.

Acknowledgments

I feel humbled when thinking of the - many - people who managed to find time from their busy schedules for me and my research work. First of all, I am sincerely honored by the dedication and passion that the jury members - Daniel Kuhn, André Faaij and Thomas Kreutz - have devoted to the review of this work, and I am thankful for the precious insights they provided. I am also grateful to Frédéric Babonneau, whose advice and help on the topic of robust optimization have been fundamental in the writing of the last chapter of this thesis. Thank you also to Philippe Thalmann, for the interesting discussions, and from whom I have “stolen” - with permission! - the proof of the formula to approximate the annualization factor (Section 4.1.2); to Stefano Tarantola and Rossana Rosati, for sharing their deep expertise on sensitivity analysis; to Melvyn Sim, for the Skype calls late at night to discuss about the application of his method to energy systems; to Bernard Gendron, for the office discussions about the beauty of Swiss trains and for the insights on tackling complex integer optimization problems; to Stéphane Joost, for his valuable collaboration and expertise on the use of georeferenced data; to the people at the Services Industriels de Lausanne and in particular to Francesco Barone, who often took time out of his personal schedule, moved by a genuine interest in making the heat supply of Lausanne more renewable. I would also like to take this opportunity to thank the various authors of the papers cited in this thesis whom, as a believer in scientific collaboration, I have disturbed with emails and questions, and who were often kind enough to reply and provide more details about their work.

A thought also goes to Arturo Lorenzoni. Although we could never publish the - I would dare say, good - work done together, I am very grateful for your support and for believing in me in a rather difficult period of my life. It is reassuring to know that people of your moral loftiness are working to make our beloved “*serva Italia*” a better place.

As the limit between the professional and personal spheres gradually blurs and becomes less defined, I should mention some of the extremely talented students I had the luck of supervising, who - rather surprisingly - did not end up hating me as much as they probably should. Frédéric, Jérémy, I am really proud of your work, and I hope to have been able to give you as much as I have received from you.

And, of course, there are the past and present members of the lab. First of all, the *télétravail-ers*, mastering the art of working on boats and airplanes, across rivers and oceans, on beaches and mountains, proving to the world out there that fixed working stations are overrated. Thank you Sophia, for always being there when I needed you the most - your crazy existence is a gift to humanity; Steph, for always being the coolest, and for making a wonderful couple when we travel together; Raman, for the highly nonlinear discussions and for your brilliant mind; Víctor, for the entertaining stories and for bringing us back on track when we care too much about things - I am not angry at you for CTRL+F-ing these acknowledgements.

Among the lab members who still prefer a stationary work station my thoughts fly to our dove Ema who, in her strong fragility, had also to withstand me as a *coloc* for some months, and unexpectedly lived to talk about it; to our secretaries, Brigitte and Sylvie, always busy saving the boat from sinking;

to Matthias (and Myriam), who used to love me, but then made the terrible mistake of inviting me to their marriage; to Elfie, best Vivapoly co-organizer ever; to Léda, who introduced me to the lab and shared all her work to get me started; to Lindsay, for being such a cool mum and human being; to Jean-Loup, for the unforgettable - really! - Christmas dinner after-party; to super-Nils, for caring about important things, such as good beer; to Ivan, for having suffered reading some of my papers; and then to Nicolas (the problem solver), Leandro (whom I still need to see dance tango), Samuel (the only real engineer in the lab, let's face it), Alberto (terminator), Mazi (great sufferer), Hür (the fate of the lab is in your hands), Hossein & Morgane (and Bardia!), Francesco/a, TiVi (Duolingo master), Priscilla & Manuel, Giorgio & Cecilia, Thierry (brother in uncertainty), JB and Arata (dear officemates), Fabio (good people eat late), Katie & Guillaume, Dilan, Raluca, and all the other members of our - extended - lab. I hope that in the future you will think of me with - or, even better, without - a smile, reminiscing about the rays of sunshine and positivity I used to bring to the lab in the (late) morning.

My first contact with Lausanne was definitely not the easiest, but I was lucky enough to meet a bunch of lovely people here, who helped me to gradually make it home. Thank you to Elena, who started off catastrophically by destroying everything she could in the house, including Italian grammar, but ended up being the loveliest flatmate I could have asked for; to Claudia, for hosting me during my first nights in Lausanne, the late night beers, the ghosts and the lost telephones; to Outi, "*dottor professor truffatore imbroglione*", for the brilliant Passi drawing and for simply being amazing at everything you do; to Irene, for always giving me a reason to visit Barcelona; to the Bing, for the delicious Ethiopian dinners, the drawings on the table and your calculation skills; and to the Panques, Marta, and *los locos*, the Couchsurfers (Katerina and Janine), Diego and his enchanting piano, Helena, Cathy (*meine tandem-Partnerin*), Riccardo, Claudia B., Mirja, Marc & Sara, Laurent, Olivier, Philip, Emiliano, Valentin, Marine, Sam & Julie (*deuxième étage*). You made Switzerland a more memorable and entertaining place in the last four years.

One of the best things that happened to me during this last one year has been the decision to set out and work with the *hoaxers*: Eugenio (*no problem!*), Gabriele, Marco, and the American cowboys - Luca and Massimo. After some years over which I have gotten used to working on my own, you have given me back the pleasure of working together as a team. In this case, this is particularly special as it also happens to be a team of true friends. I am sincerely proud of the results we were able to achieve together - and of how we achieved them - and I look forward to a day, maybe not so far in the future, when we will hopefully be sharing the same office space.

And then, of course, there are the friends of forever, where *forever* means that, even if we do not necessarily meet that often, I simply know that you are there and you will be there, and that is enough for me. Thanks to Pippo for his insults full of love - I have taken this sentence verbatim from the Master's Thesis acknowledgments, as things have not changed ("*what are you doing this?*"); to


Acknowledgments

Fiore, for mixing politics and poker with apparent *nonchalance*; to Davide & Claudia, *gli svizzeri*; to Marcus and Cima - I am very proud of how our friendship has managed and continues to last over time and distance; to Vix, Ilaria, Lova, Taty, Gec; to my friends from Belluno (Alessandra, Isabella, Spes, Marcello, Isa, Giorgia, Fabrizia, Giulia, Rossella), with whom I have still managed to keep in touch and meet over the many years whenever we are all back to our little paradise in the mountains; to Enzo & Nerina and Cice & Cristina, who have always followed my steps with sincere affection; to Ale & Luana, and to my lovely curly smiling niece - I am now thinking of you reading these pages by yourself in a few years.

I am looking at the list of people that I have here on my desk by a glass of whisky - list which I have written in order to not forget anybody in these pages - and I realize that I have failed badly at dividing people into different categories. It is amazing, to the point of making me almost break into a smile, seeing how most colleagues are also dear friends; how friends that I have met at different points in my life have now met each other and constitute a new group of friends on their own; how old friends are now becoming workmates. So, even if I did not put you in the right category, if you read your name in these pages, be sure that you are important to me, for what it matters. Most of you have enjoyed my highest highs and some of you have witnessed my lowest lows - I do not need to make a list, you know it already. The fact is that the older I become, the less certain I am about things, but in your sincere friendship I find comfort and meaning, and words cannot express how grateful and lucky I feel for having such amazing human beings in my life.

There are still two names which I have not yet erased from my list - the names of my parents, Dorino and Nilva. The mere knowledge that you will be present at the faintest sign of difficulty, ready to offer unconditional love and support, has been the basis on which I have built the rest of my otherwise fragile existence. I know that I will always be indebted to you, and I hope that I will be able to give back a tiny bit of what you did and are doing for me. Thank you for being your loving and caring selves - I honestly do not know what it would have been of me without you.

Bateau Henry-Dunant, Lac Léman
September 30th, 2017



Abstract

Various countries and communities are defining or rethinking their energy strategy driven by concerns for climate change and security of energy supply. Energy models, often based on optimization, can support this decision-making process. In the current energy planning practice, most models are deterministic, i.e. they do not consider uncertainty and rely on long-term forecasts for important parameters. However, over the long time horizons of energy planning, forecasts often prove to be inaccurate, which can lead to overcapacity and underutilization of the installed technologies. Although this shows the need of considering uncertainty in energy planning, uncertainty is to date seldom integrated in energy models. The main barriers to a wider penetration of uncertainty are *i)* the complexity and computational expense of energy models; *ii)* the issue of quantifying input uncertainties and determining their nature; *iii)* the selection of appropriate methods for incorporating uncertainties in energy models. To overcome these limitations, this thesis answers the following research question

How does uncertainty impact strategic energy planning and how can we facilitate the integration of uncertainty in the energy modeling practice?

with four novel methodological contributions. First, a mixed-integer linear programming modeling framework for large-scale energy systems is presented. Given the energy demand, the efficiency and cost of energy conversion technologies, the availability and cost of resources, the model identifies the optimal investment and operation strategies to meet the demand and minimize the total annual cost or greenhouse gas emissions. The concise formulation and low computational time make it suitable for uncertainty applications. Second, a method is introduced to characterize input uncertainties in energy planning models. Third, the adoption of a two-stage global sensitivity analysis approach is proposed to deal with the large number of uncertain parameters in energy planning models. Fourth, a complete robust optimization framework is developed to incorporate uncertainty in optimization-based energy models, allowing the consideration of uncertainty both in the objective function and in the other constraints.

To evaluate the impact of uncertainty, the presentation of the methods is systematically associated to their validation on the real case study of the Swiss energy system. In this context, a novelty is represented by the consideration of *all* uncertain parameters in the analysis. The main finding is

Abstract

that uncertainty dramatically impacts energy planning decisions. The results reveal that uncertainty levels vary significantly for different parameters, and that the way in which uncertainty is characterized has a strong impact on the results. In the case study, economic parameters, such as the discount rate and the price of imported resources, are the most impacting inputs; also, parameters which are commonly considered as fixed assumptions in energy models emerge as critical factors, which shows that it is crucial to avoid an *a priori* exclusion of parameters from the analysis. The energy strategy drastically changes if uncertainty is considered. In particular, it is demonstrated that robust solutions, characterized by a higher penetration of renewables and of efficient technologies, can offer more reliability and stability compared to investment plans made without accounting for uncertainty, at the price of a marginally higher cost.

Keywords

Strategic energy planning; uncertainty; national energy systems; energy modeling; mixed-integer linear programming; uncertainty characterization; global sensitivity analysis; robust optimization; Switzerland; geothermal energy.

Résumé

Divers pays et communautés sont actuellement en train de définir ou repenser leur stratégie énergétique, poussés par des préoccupations liées au changement climatique et à la sécurité d’approvisionnement en énergie. Les modèles énergétiques, souvent basés sur l’optimisation, peuvent soutenir ce processus décisionnel. Dans la pratique actuelle en matière de planification énergétique, la plupart des modèles sont déterministes, c’est-à-dire qu’ils se basent sur des prévisions à long terme en ne prenant pas en compte l’incertitude des paramètres. Cependant, sur les longs horizons temporels liés à la planification énergétique, ces prévisions se révèlent souvent inexactes, ce qui peut donner lieu à une surcapacité et à une sous-utilisation des technologies installées. Bien que cela montre la nécessité de considérer l’incertitude dans la planification énergétique, celle-ci est jusqu’à présent rarement intégrée dans les modèles énergétiques. Les obstacles principaux à une pénétration majeure de l’incertitude sont *i)* la complexité et les temps de calcul élevés des modèles énergétiques; *ii)* la question de la quantification des incertitudes et de la détermination de leur nature; *iii)* la sélection des méthodes appropriées pour intégrer les incertitudes dans les modèles énergétiques. Pour surmonter ces limitations, cette thèse répond à la question de recherche suivante

Comment l’incertitude affecte-t-elle la planification stratégique en matière d’énergie et comment pouvons-nous faciliter l’intégration de l’incertitude dans les modèles énergétiques?

à travers quatre contributions méthodologiques novatrices. Premièrement, un cadre de modélisation pour les systèmes énergétiques à grande échelle basé sur la programmation linéaire en nombre entiers est présenté. En considérant la demande en services énergétiques, l’efficacité et le coût des technologies, la disponibilité et le coût des ressources, le modèle identifie les stratégies optimales d’investissement et d’exploitation afin de satisfaire la demande et minimiser le coût total annuel ou les émissions de gaz à effet de serre du système énergétique. La formulation concise et le faible temps de calcul le rendent approprié pour des applications prenant en compte l’incertitude. Deuxièmement, une nouvelle méthode est introduite pour caractériser les incertitudes des données dans les modèles de planification énergétique. Troisièmement, l’utilisation d’une approche d’analyse de sensibilité globale en deux étapes est proposée pour traiter le grand nombre de paramètres incertains dans ce type de modèle. Quatrièmement, un cadre complet d’optimisation robuste est développé pour intégrer l’incertitude dans les modèles énergétiques basés sur l’optimisation, permettant de considérer l’incertitude à la fois dans la fonction objective et dans les autres contraintes.

Résumé

Pour évaluer l'impact de l'incertitude, la présentation des méthodes est systématiquement associée à leur validation par une étude de cas réelle du système énergétique suisse. Dans ce contexte, la prise en compte de *tous* les paramètres incertains dans l'analyse présente un caractère novateur. L'incertitude affecte considérablement les décisions de planification énergétique. Les résultats montrent que les niveaux d'incertitude varient sensiblement selon les différents paramètres et que la manière dont l'incertitude est caractérisée a un impact important sur les résultats. Dans l'étude de cas, les paramètres économiques, tels que le taux d'intérêt et le prix des ressources importées, sont les éléments les plus influents; de plus, des paramètres qui sont généralement considérés comme des hypothèses fixes dans les modèles énergétiques apparaissent comme des facteurs critiques, ce qui montre qu'il est essentiel d'éviter une exclusion *a priori* des paramètres de l'analyse. La stratégie énergétique change radicalement lorsque l'incertitude est prise en compte. En particulier, il est démontré que des solutions robustes, caractérisées par une plus grande pénétration des énergies renouvelables et des technologies efficaces, peuvent offrir plus de fiabilité et de stabilité par rapport aux stratégies d'investissement définies sans tenir compte de l'incertitude, au prix d'un coût marginalement plus élevé.

Mots-clefs

Planification énergétique; stratégie énergétique; incertitude; systèmes énergétiques nationaux; modélisation énergétique; programmation linéaire en nombre entiers; Caractérisation de l'incertitude; analyse de sensibilité globale; optimisation robuste; Suisse; géothermie.

Abstract

Diversi Paesi e comunità locali stanno definendo o ripensando la propria strategia energetica spinti da preoccupazioni per il cambiamento climatico e per la sicurezza dell'approvvigionamento energetico. I modelli energetici, sovente basati sull'ottimizzazione, possono supportare questo processo decisionale. Ad oggi, i modelli energetici comunemente utilizzati per la pianificazione energetica sono deterministici; ciò significa che non prendono in considerazione l'incertezza dei parametri in input, e che si basano su previsioni a lungo termine. Tuttavia, queste previsioni si rivelano spesso inesatte, causando errori decisionali che possono dar luogo a sovraccapacità e sottoutilizzazione delle tecnologie installate. Benché ciò dimostri la necessità di tener conto dell'incertezza nella definizione della strategia energetica, questo avviene di rado nella pratica. I principali fattori che ostacolano una penetrazione maggiore dell'incertezza sono *i)* la complessità ed i tempi di calcolo elevati dei modelli energetici; *ii)* la difficoltà nel quantificare e caratterizzare l'incertezza; *iii)* l'identificazione dei metodi più appropriati per integrare l'incertezza nei modelli energetici. Per contribuire al superamento di questi ostacoli, questa tesi risponde alla seguente domanda di ricerca

Qual è l'impatto dell'incertezza sulla definizione della strategia energetica e come possiamo rendere più sistematica la considerazione dell'incertezza nei modelli energetici?

presentando quattro metodi innovativi. Il primo contributo consiste in un approccio basato sulla programmazione lineare intera per la modellizzazione di sistemi energetici urbani e nazionali. Dati in input la domanda energetica, l'efficienza ed i costi delle tecnologie, e la disponibilità ed i costi delle risorse, il modello calcola la strategia energetica ottimale, che soddisfa la domanda minimizzando al contempo il costo totale del sistema o le emissioni di gas a effetto serra. La formulazione compatta ed il limitato tempo di calcolo rendono questo modello ideale per l'integrazione dell'incertezza. In secondo luogo, è presentato un metodo per la caratterizzazione dell'incertezza dei parametri in input dei modelli energetici. Il terzo contributo consiste nell'utilizzo di un metodo a due stadi per l'analisi di sensitività globale, che permette di includere nell'analisi l'elevato numero di parametri che tipicamente caratterizza questo tipo di modelli. Infine, è presentato un metodo per integrare l'incertezza nei modelli di pianificazione energetica attraverso l'ottimizzazione robusta; il metodo permette di tener conto dell'incertezza sia nella funzione obiettivo sia negli altri vincoli del problema

Abstract

di ottimizzazione.

Per valutare l'impatto dell'incertezza, la presentazione di questi quattro metodi è sistematicamente associata alla loro validazione sul caso studio del sistema energetico svizzero. In questo contesto, uno degli elementi di carattere maggiormente innovativo è la presa in considerazione di *tutti* i parametri incerti nell'analisi. Il risultato principale è che l'incertezza ha un impatto determinante sulla definizione della strategia energetica. I risultati mostrano che vi sono differenze significative tra i livelli di incertezza dei diversi parametri del modello, e che il modo in cui l'incertezza viene caratterizzata impatta fortemente l'output. Nel caso studio, i parametri di tipo economico, come il tasso d'interesse ed il prezzo dei combustibili fossili, emergono come i fattori più impattanti. Inoltre, alcuni tra i parametri più impattanti sono parametri a cui sono spesso assegnati dei valori di default nei modelli energetici; ciò dimostra l'importanza di considerare tutti i parametri incerti, i.e. di non tralasciare ed escludere *a priori* alcuni di essi dall'analisi. La strategia energetica cambia radicalmente quando l'incertezza viene presa in considerazione. In particolare, le soluzioni robuste, caratterizzate da una maggiore penetrazione di energie rinnovabili e tecnologie efficienti, possono garantire maggiore stabilità ed affidabilità rispetto a strategie energetiche definite senza tener conto dell'incertezza, al prezzo di un costo totale marginalmente più elevato.

Parole chiave

Pianificazione energetica; strategia energetica; incertezza; sistemi energetici nazionali; modellizzazione energetica; programmazione lineare intera; caratterizzazione dell'incertezza; analisi di sensitività globale; ottimizzazione robusta; Svizzera; energia geotermica.

Contents

Acknowledgments	i
Abstract (English/Français/Italiano)	v
List of figures	xv
List of tables	xix
Acronyms and abbreviations	xxiii
List of Symbols	xxvii
Introduction	1
Energy forecasting: learning from the past	2
State of the art: uncertainty in the energy modeling practice	6
Contributions and outline of the thesis	8
1 Modeling for uncertainty	13
Contributions	14
1.1 MILP modeling framework	15
1.1.1 Sets, parameters, variables	15
1.1.2 Constraints	19
1.2 Case study: the Swiss energy system in 2035	24
1.2.1 Additional constraints	25
1.2.2 Model validation	27
2 Uncertainty characterization	31
Contributions	32
2.1 Uncertainty characterization method	33
2.1.1 Preliminary screening and grouping	35
2.1.2 Uncertainty characterization criteria	36
2.1.3 Calculation of the uncertainty range	38
2.2 Application to the case study	42

Contents

2.2.1 Preliminary screening and grouping	42
2.2.2 Uncertainty characterization results	42
Discussion	48
3 Global sensitivity analysis	49
Contributions	51
3.1 Two-stage GSA method	52
3.1.1 First stage: factor fixing	52
3.1.2 Second stage: factor prioritization	53
3.2 Application to the case study	54
3.2.1 Factor fixing	54
3.2.2 Factor prioritization	55
3.2.3 Does uncertainty characterization matter in energy planning?	56
Discussion	57
4 Robust optimization	59
Contributions	63
4.1 Uncertainty in the objective function	65
4.1.1 The robust formulation by Bertsimas and Sim [62]	65
4.1.2 Novel robust formulation	67
4.1.3 Application to the case study	74
4.1.4 Evaluation of the robust solutions	80
4.2 Uncertainty in the constraints	83
4.2.1 The robust formulation by Babonneau et al. [154]	84
4.2.2 Application to the case study	85
4.2.3 Evaluation of the robust solutions	89
4.3 Decision-making for energy systems	91
4.3.1 A target-oriented perspective on robust optimization	92
4.3.2 First feasibility, then optimality	93
4.3.3 Robust investment strategies and overcapacity in the electricity sector	98
4.3.4 Comparison with stochastic programming	100
Discussion	103
Conclusions	105
Main results summary	105
Recommendations and guidance	106
Future perspectives	108

A	Swiss energy system data	111
A.1	Energy demand	113
A.1.1	Heating	113
A.1.2	Electricity	115
A.1.3	Mobility	115
A.2	Electricity production and storage	116
A.2.1	Renewables	116
A.2.2	Non-renewable electricity supply technologies	120
A.2.3	Seasonal storage	120
A.2.4	Electricity grid	120
A.3	Heating and cogeneration technologies	122
A.4	Transport	125
A.5	Resources	125
A.6	Other parameters	126
A.7	2011 data for model validation	128
B	Uncertainty characterization data	131
B.1	Discount rate	131
B.2	End-use energy demand	131
B.3	Technology efficiency	133
B.4	Resources availability and maximum capacity of technologies	134
B.5	Capacity factor	135
B.6	Technologies investment cost	136
B.7	Resources cost	137
B.8	Other parameters: technologies lifetime	138
C	Urban energy modeling - Integration of deep geothermal energy and woody biomass conversion pathways in cities	139
C.1	Methodology	143
C.1.1	Urban energy system model	143
C.1.2	MILP model formulation	146
C.1.3	Performance Indicators	149
C.1.4	Scenarios	151
C.2	Results	153
C.2.1	Individual scenarios: geothermal and biomass alone	153
C.2.2	Combined scenarios: combination of biomass and geothermal options	157
C.2.3	Evaluation of hybrid processes	162
C.2.4	Discussion	164

Contents

D Urban energy modeling - data	167
D.1 Lausanne case study	167
D.1.1 Excess heat from the municipal solid waste incinerator (MSWI)	169
D.1.2 Evolution of the energy system to 2035	171
D.2 MILP model	172
D.2.1 Sets	172
D.2.2 Parameters	172
D.2.3 Variables	172
D.3 Unit models	174
D.3.1 Resources	174
D.3.2 Energy demand	177
D.3.3 Biomass technologies	178
D.3.4 Geothermal resources and technologies	184
D.3.5 Boilers	187
D.3.6 Electricity production & Cogeneration (CHP)	190
D.3.7 Storage	194
D.3.8 Waste treatment and District Heating Network	196
D.3.9 Mobility	200
D.4 Additional results	203
Bibliography	211
Curriculum Vitae	235

List of Figures

1	Analysis of errors in the yearly US Energy Information Administration (EIA) Annual Energy Outlook (AEO) energy demand forecasts for the years 1994-2014	3
2	Natural gas for electricity production price in the US: comparison between the yearly Energy Information Administration (EIA) Annual Energy Outlook (AEO) price forecasts and the actual values for the years 1985-2015	4
3	Thesis structure overview.	10
1.1	Overview of the MILP modeling framework	13
1.2	Application of the MILP modeling framework to the energy system of Switzerland. . .	16
1.3	Visual representation of the sets and indices of the MILP framework.	18
1.4	EndUses calculation starting from yearly demand model input	19
1.5	Conceptual representation of a layer	23
1.6	Monthly net electricity production vs. demand in Switzerland in the year 2011.	24
1.7	Energy flows in Switzerland in the year 2011	28
2.1	Overview of the proposed uncertainty characterization method	31
2.2	Uncertainty characterization method flowchart.	34
2.3	Uncertainty characterization: application in parallel of the five criteria to each uncertain parameter in a model.	37
2.4	Different types of uncertainty over the planning horizon.	40
2.5	Application of the scaling procedure for <i>Type I</i> , <i>Type II</i> and <i>Type III</i> parameters.	41
3.1	Overview of the two-stage global sensitivity analysis approach.	49
3.2	GSA results: factor fixing with the EEs method	55
3.3	Comparison of elementary effect (EE) method results: input uncertainty characterization as in Table 2.1 vs. identical uncertainty of $\pm 20\%$ for all parameters	57
4.1	Chapter overview	59
4.2	Energy flows in Switzerland in the year 2035: cost optimal deterministic solution . . .	64
4.3	Annualization factor of the investment cost (τ): comparison between exact calculation and two possible approximations	70

List of Figures

4.4	Evolution of the energy system configuration vs. protection level Γ_{obj} : annual consumption of resources.	77
4.5	Performance indicators (cost, GHG emissions, installed capacity, electricity in the system, consumption of fossil fuels.) vs. protection level Γ_{obj} : ratio vs. deterministic solution ($\Gamma_{obj} = 0$).	78
4.6	Evolution of the energy system configuration vs. protection level Γ_{obj} : electricity production.	78
4.7	Evolution of the energy system configuration vs. protection level Γ_{obj} : DHN, decentralized and industrial heat production.	79
4.8	Simulation results for the robust solutions in Table 4.2	82
4.9	Evolution of the energy system configuration vs. objective (C_{tot}): annual consumption of resources	93
4.10	Flowchart of the proposed decision-making method	94
4.11	Simulation results for the robust solutions with uncertainty in the objective and in the constraints	96
4.12	Average additional installed capacity and electricity imports for the robust solutions obtained at different values of Γ_{obj}	99
4.13	Example of scenario tree for a two-stage stochastic programming problem	101
4.14	Simulation results: stochastic vs. representative robust solutions	102
B.1	Implementation of a cogeneration unit in the example MILP model.	134
C.1	Overview of the scenario-based methodology	144
C.2	Urban energy system model.	145
C.3	DHN heat supply and demand in the reference scenario (scenario 0).	154
C.4	Results of the individual scenarios listed in Table C.1: individual assessment of geothermal and biomass options.	155
C.5	ΔC_{tot} and ΔGWP_{tot} for the geothermal-biomass combined scenarios.	159
C.6	$\Delta_{Hybrid}C_{tot}$ and $\Delta_{Hybrid}GWP_{tot}$ for the hybrid biomass-geothermal processes.	163
D.1	Energy flow Sankey diagram of the city of Lausanne (Switzerland) for the year 2012	168
D.2	Lausanne MSWI thermal and electricity production compared to the DHN demand in the year 2012.	170
D.3	Sets of the MILP model with the corresponding indices	172
D.4	Wood dryer unit model.	178
D.5	Pyrolysis unit model.	179
D.6	Fischer-Tropsch unit models for wet and dry wood input.	180
D.7	Gasification to SNG unit model.	182
D.8	Geological profile of the city of Lausanne	184
D.9	Simplified input-output representation of the geothermal ORC and Kalina cycles models.	186

D.10 Centralized and decentralized NG boiler unit models.	187
D.11 Centralized and decentralized Oil-BioOil boiler unit models.	188
D.12 Centralized wet and dry wood boiler unit models.	189
D.13 Natural gas CHP unit model.	191
D.14 BioOil CHP unit model.	192
D.15 Wet and dry wood CHP unit model.	193
D.16 SNG storage unit model.	194
D.17 Oil and BioOil storage unit models.	195
D.18 Dry wood storage unit model.	196
D.19 MSWI unit model.	196
D.20 WWTP unit model.	198
D.21 Private mobility unit models.	200
D.22 Public mobility unit models.	201
D.23 Results of the individual scenarios listed in Table C.1: individual assessment of geother- mal and biomass options.	203
D.24 Results for all scenarios: Total annual cost vs GWP emissions.	204
D.25 Results for all scenarios: Total annual cost vs human health emissions	205

List of Tables

1	Comparison of existing large-scale energy planning models	7
1.1	Parameter list with description.	17
1.2	Independent decision variable list with description.	17
1.3	Dependent decision variable list with description.	18
1.4	Model validation: MILP model output vs. actual 2011 values for the Swiss energy system	29
2.1	Application of the uncertainty characterization method to the example MILP model. .	43
3.1	Review of application of sensitivity and uncertainty analysis methods to energy models.	50
3.2	Factor prioritization results: S_i and S_{T_i} for the first 10 parameters with respect to the objective value.	56
3.3	Results of the EE method: average of μ^* ($\overline{\mu^*}$) for the different parameter categories with respect to the objective value (Y_1) and the investment decision (Y_2)	58
4.1	Review of application of robust optimization methods to energy models.	61
4.2	Characterization of the representative energy system configurations selected via <i>k-medoids</i> clustering.	81
4.3	Simulation results for uncertainty in the constraints: price of robustness against constraint violations	90
4.4	Characterization of the representative energy system configurations for $\Gamma_{lb} = 1$ and $\Gamma_{lb} = 2$	97
4.5	Optimal investment strategy of the stochastic programming problem.	102
A.1	CEPCI values	112
A.2	Data for the calculation of the end use energy demand in the households sector. . . .	113
A.3	FEC and EUD in the household, industry and service sectors.	114
A.4	Monthly distribution factors for SH demand ($\%_{heating}$) and electricity demand for lighting ($\%_{lighting}$).	115
A.5	Electricity demand not related to heating by sector.	115
A.6	Renewable electricity production technologies	116
A.7	Monthly electricity production share from renewable energy sources.	117

List of Tables

A.8	Data for the calculation of the future capacity factors for hydro run-of-river and dams.	117
A.9	Development potential for hydroelectricity in Switzerland	118
A.10	Development potential for hydroelectricity in Switzerland by 2050	118
A.11	Net hydroelectricity production and installed power in Switzerland in the years 2012 and 2050.	118
A.12	Development potential of hydroelectricity in Switzerland by 2050	119
A.13	Investment cost data for the new hydro power plants in Switzerland.	119
A.14	O&M cost data for the new hydroelectric power plants in Switzerland.	120
A.15	Non-renewable electricity supply technologies.	121
A.16	Data for the seasonal storage cost calculation.	121
A.17	Industrial heating and cogeneration technologies.	122
A.18	District heating technologies.	123
A.20	Monthly heat production share from decentralized solar thermal panels.	123
A.19	Decentralized heating and cogeneration technologies.	124
A.21	Fuel and electricity consumption for transport technologies in 2035, and minimum/- maximum shares allowed in the model.	125
A.22	Price and GHG emissions of resources.	126
A.23	Hydrogen production technologies.	127
A.24	Woody biomass to synthetic fuels conversion technologies	127
A.25	End-uses demand in Switzerland ($endUses_{year}$) in 2011.	128
A.26	$\%_{Public}$, $\%_{Rail}$ and $\%_{Dhn}$ for the Swiss energy system in the year 2011.	128
A.27	Yearly shares of public mobility technologies for the Swiss energy system in 2011.	129
A.28	Yearly shares of private mobility technologies for the Swiss energy system in 2011.	129
A.29	Yearly shares of decentralized low temperature heat & CHP technologies for the Swiss energy system in 2011.	130
A.30	Yearly shares of DHN low temperature heat & CHP technologies for the Swiss energy system in 2011.	130
A.31	Yearly shares of industrial high temperature heat & CHP technologies for the Swiss energy system in 2011.	130
B.1	Maximum yearly potential of woody biomass in Switzerland from different sources.	135
B.2	Analysis of yearly capacity factors (c_p) of Swiss nuclear power plants.	135
B.3	Technologies specific investment cost: sources for the definition of the uncertainty range.	136
B.4	Projection for the investment cost of rooftop residential PV systems in 2035 from different sources.	137
B.5	Lifetime (n) of boilers from different sources.	138
C.1	List of individual scenarios	152

C.2	Avoided GWP emissions (resources only) associated to the different uses of 1 kWh of electricity.	153
D.1	Parameter list with description. Set indices as in Figure D.3	173
D.2	Variable list with description. All variables are continuous and non-negative, unless otherwise indicated.	173
D.3	Resources properties	176
D.4	Characterization of end-uses in energy services for the city of Lausanne in 2035.	177
D.5	Wood dryer parameters	179
D.6	Fast pyrolysis parameters	180
D.7	Fischer-Tropsch synthesis from biomass gasification parameters	181
D.8	Gasification to SNG parameters	183
D.9	Geothermal resources and energy conversion cycles emission parameters.	185
D.10	Geothermal resources parameters.	185
D.11	NG-SNG DHN and decentralized boilers parameters	187
D.12	Oil and decentralized boilers parameters	189
D.13	Centralized wet and dry wood boilers parameters	190
D.14	Fixed hydroelectricity power production in each period.	191
D.15	Hydroelectricity parameters	191
D.16	Natural Gas CHP parameters.	192
D.17	Oil-BioOil CHP parameters	193
D.18	Wet and dry wood CHP parameters	194
D.19	Oil and BioOil storage tanks parameters	195
D.20	Dry wood storage parameters	196
D.21	MSWI parameters	197
D.22	WWTP parameters	198
D.23	DHN parameters	199
D.24	Public mobility model parameters.	201
D.25	Private and public mobility model emission parameters.	202
D.26	δPI calculated for each performance indicator (Eq. C.19). Performance of each with respect to the reference (scenario 0).	206

Acronyms and abbreviations

ADP	Approximate dynamic programming
AEO	Annual Energy Outlook
ARO	Adjustable robust optimization
BEV	Battery electric vehicle
BtL	Biomass to liquids
CCGT	Combined cycle gas turbine
CCS	Carbon capture and storage
CEPCI	Chemical Engineering's Plant Cost Index
CHP	Cogeneration of heat and power
COP	Coefficient of performance
DH	District heating
DHN	District heating network
DM	Decision-maker
EE	Elementary effect
EFAST	Extended Fourier Amplitude Sensitivity Test
EGS	Enhanced geothermal system
EIA	Energy Information Administration
EO	Expert opinion
EU	European Union
EUD	End-use demand
FC	Fuel cell
FEC	Final energy consumption
FRILP	Fuzzy radial interval linear programming
FT	Fischer-Tropsch
GHG	Greenhouse gas
GSA	Global sensitivity analysis
GWP	Global warming potential
HEV	Hybrid electric vehicle
HFO	Heavy fuel oil
HH	Households

Acronyms and abbreviations

hh	Human health
HHV	Higher heating value
HP	Heat pump
HW	Hot water
I	Industry
IEA	International Energy Agency
IGCC	Integrated gasification combined cycle
LCA	Life cycle assessment
LDR	Linear decision rules
LFO	Light fuel oil
LHV	Lower heating value
LNG	Liquefied natural gas
LP	Linear programming
LSA	Local sensitivity analysis
MILP	Mixed-integer linear programming
MINLP	Mixed-integer non linear programming
MPG	Miles-per-gallon
MSW	Municipal solid waste
MSWI	Municipal solid waste incinerator
NEMS	National Energy Modeling System
NG	Natural gas
O&M	Operation and maintenance
OAT	One-at-a-time
OECD	Organisation for Economic Co-operation and Development
ORC	Organic Rankine cycle
PDF	Probability density function
PHEV	Plug-in hybrid electric vehicle
PI	Performance indicator
PoR	Price of robustness
PV	Photovoltaic
RO	Robust optimization
S	Services
SA	Sensitivity analysis
SFOE	Swiss Federal Office of Energy
SFOS	Swiss Federal Office of Statistics
SH	Space heating
SiL	Services Industriels de Lausanne
SNG	Synthetic natural gas

SP	Stochastic programming
TL	Transport Lausannois
TR	Transportation
U-S	Ultra-supercritical
UA	Uncertainty analysis
UCTE	Union for the Co-ordination of Transmission of Electricity
WWT	Waste-water treatment
WWTP	Waste-water treatment plant

List of Symbols

A	Constant annuity of a discounted investment
C	Construction
c_v	Coefficient of variation
db	Dry basis
\mathbb{E}	Expected value
E	End-of-life
e	Error factor
I	Annuity component: interest
kgoe	kilogram of oil equivalent
M	Annuity component: amortization of the capital cost
MC	Moisture content
M	Molar mass
O	Operation
pkm	passenger-kilometer
R	Range of variation
R_0	Nominal value
R_{min}	Lower bound of the range
R_{max}	Upper bound of the range
$R\%$	Relative range
$R_{\%,min}$	Lower bound of the range (in relative values)
$R_{\%,max}$	Upper bound of the range (in relative values)
S	First-order effect sensitivity index
S_T	Total effect sensitivity index
tkm	ton-kilometer
V	Variance
wb	Wet basis
\bar{x}	Mean
Y	Output of interest

List of Symbols

Greek Letters

α	Aleatory uncertainty
ε	Epistemic uncertainty
η	Efficiency
μ^*	Sensitivity index of the EE method
σ	Standard deviation
θ	Parameter
Φ	Humidity
ξ	Magnitude of constraint violation

Introduction

“It is difficult to make predictions, especially about the future.”

Danish proverb

Overview

- Why should uncertainty be incorporated in strategic energy planning models?
- State of the art: key barriers to a wider penetration of uncertainty in the energy field.
- Contributions and novelty of this thesis.
- Thesis structure overview.

Every day, we consume energy to satisfy our needs: we consume energy to move, to heat and cool our houses, to power our laptops and to cook our food, among others. To be precise, the World Bank estimates that a citizen of an OECD member country consumes every day the equivalent of 11.3 kg of oil [1]¹. This corresponds to fifty-six times the amount of energy needed daily by the human body². Today, this energy is mostly provided by the combustion of fossil fuels, which in 2014 accounted for 81.1% of the world primary energy supply [3]. Combustion of such fuels is the primary source of anthropogenic greenhouse gas (GHG) emissions [4], and thus of climate change.

Extending current energy consumption trends to 2050, the International Energy Agency (IEA) projects a 70% increase in global energy demand and an associated 60% increase of GHG emissions against 2011 levels, mainly due to growth of non-OECD countries [5]. To mitigate the associated catastrophic effects of climate change, the “2DS” scenario, which aims at an 80% chance of limiting the increase of the global average temperature below 2°C compared to pre-industrial times, requires a 50% reduction of GHG emissions compared to today’s levels [6]. Thus, various countries and communities are defining strategic energy plans to increase the share of renewables and efficient technologies, reducing dependency on fossil fuels while ensuring security of energy supply.

¹ Average primary energy consumption in OECD countries in 2015. 41868 kJ/kilogram of oil equivalent (kgoe) [2]

² Assuming a diet of 2000 kcal/day.

Introduction

Strategic energy planning for large-scale energy systems defines investment roadmaps for energy conversion technologies. In other words, making a strategic energy plan means deciding which resources and technologies will supply our future energy service needs. Due to the lifetime of these technologies, energy plans at urban and national scale have a time horizon of 20 to 50 years.

Energy models can support this decision-making process. These models are often based on *optimization* [7], which means that they aim at identifying optimal investment strategies, e.g. meeting minimum cost or emission targets. Examples of well known and widely used optimization-based energy models are the US National Energy Modeling System (NEMS) [8], the MARKet ALlocation (MARKAL) [9], the MESSAGE [10] and the META*Net [11] models. These models are in origin *deterministic* [12]. This means that they do not consider uncertainty and rely on long-term forecasts for important parameters. But, how accurate are these forecasts?

Energy forecasting: learning from the past

Koomey et al. [13], analyzing available retrospectives on long-term energy models, argue that forecasting models are inevitably inaccurate as they fail to account for pivotal events. Krugman [14], recently revisiting the pioneering work by Nordhaus [15] on the allocation of energy resources, comments that “*looking back [...] after four decades, what’s striking is how wrong the technical experts were about future technologies*”. Based on the classification proposed by Hodges and Dewar [16], Craig et al. [17] define energy forecasting model as *nonvalidatable*, i.e. likely to yield low accuracy and low precision.

Errors in energy demand forecasts

Forecasting models are usually made to estimate future energy demand and prices. Sohn [18] analyzes the consumption projections of fossil fuels over a 19-year time horizon based on a global economic model. Linderoth [19] assesses the IEA’s errors in estimating future energy consumption of member countries. Bezdek and Wendling [20] analyze major US energy forecast errors in the years 1950-2000. O’Neill and Desai [21] evaluate the accuracy of the US Energy Information Administration (EIA) energy consumption forecasts in the years 1982-2000. These various studies highlight relevant errors in energy demand forecasts. Furthermore, Winebrake and Sakva [22] performing similar analyses found no evidence that energy forecasts for the studied time period were becoming more accurate over time.

The same conclusion can be drawn from the latest annual retrospective report by the EIA, which analyzes errors in its own past predictions: Figure 1 illustrates the errors in the energy demand forecasts published yearly in the EIA Annual Energy Outlook (AEO) in the period 1994-2014 [23]. Each AEO report includes forecasts for the following 15-20 years. The average of errors in absolute values (full lines) and the minimum/maximum errors (dotted lines) in energy demand forecasts

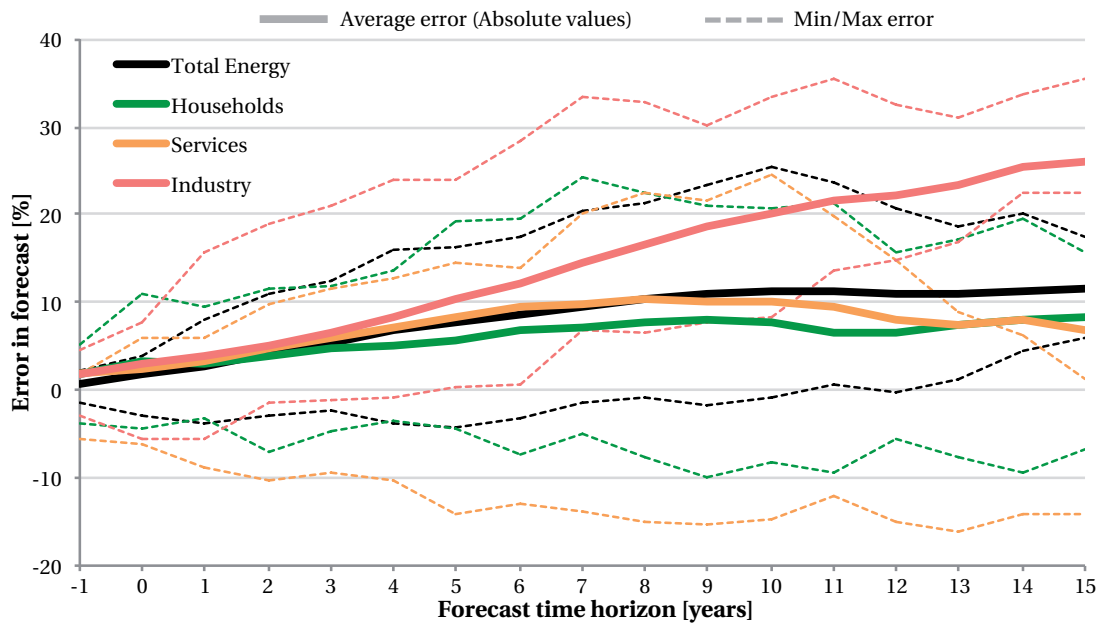


Figure 1 – Analysis of errors in the yearly US Energy Information Administration (EIA) Annual Energy Outlook (AEO) energy demand forecasts for the years 1994-2014 [23]. Full lines indicate the average of errors in absolute values, dotted lines indicate minimum/maximum errors. Errors are calculated for the different sectors with respect to the forecast time horizon. The time horizon is the difference between the target year of the forecast and the year of publication of the AEO. A positive error indicates an overestimation, i.e. the forecast is higher the actual value in a given year. EIA (www.eia.gov).

are calculated for the different sectors with respect to the forecast time horizon. The time horizon is the difference between the target year of the forecast and the year of publication of the AEO. As an example, the 10-year time horizon includes the errors calculated after 10 years from the publication of the reports (such as the forecast for 2003 published in the 1993 AEO, the forecast for 2004 published in the 1994 AEO, etc.). A positive error indicates an overestimation, i.e. the forecast is higher the actual value in a given year. Forecast errors are as high as 24.3% for households total energy demand, 24.7% for services, and 35.5% for industry.

Errors in forecasts of fuel prices

Forecasts on energy prices suffer even higher volatility, as shown by Bezdek and Wendling [20], who find error factors³ as high as five in long-term oil price forecasts. Oil price fluctuations remain, to date, extremely difficult to predict [24].

³ If $\hat{y}(t)$ is the predicted value at time t and $y(t)$ is the actual value, the *error factor* $e(t)$ of a forecast is defined as $e(t) = \hat{y}(t)/y(t)$ if $\hat{y}(t) \geq y(t)$, and $e(t) = y(t)/\hat{y}(t)$ if $\hat{y}(t) < y(t)$.

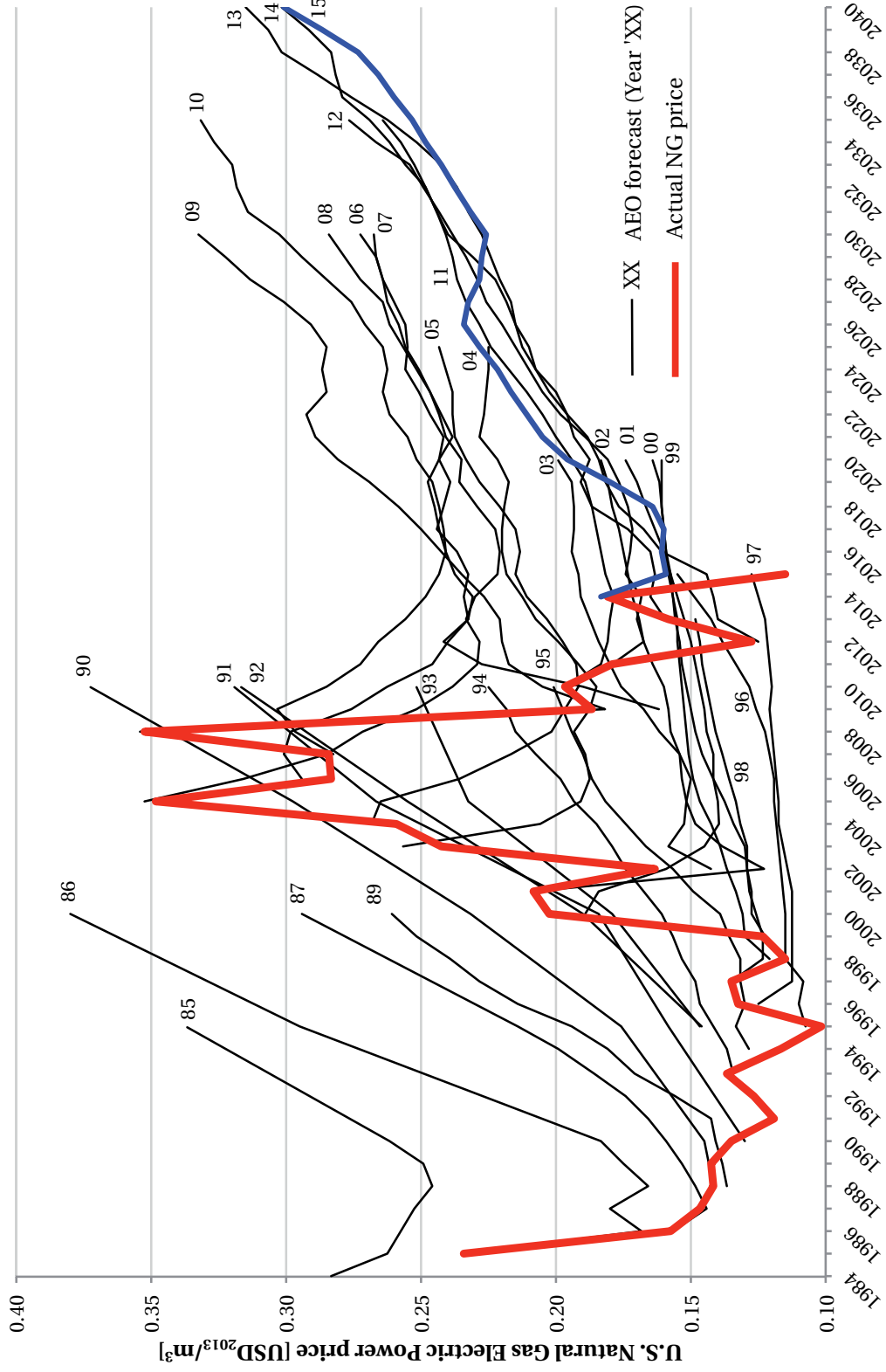


Figure 2 ? Natural gas for electricity production price in the US: comparison between the yearly EIA Annual Energy Outlook (AEO) price forecasts and the actual values for the years 1985-2015. The black lines are the forecasts made in different years. The red line indicates the actual NG price. The blue line is the last available forecast. Sources: forecasts 1994-2014 taken from the AEO retrospective review [23], older and more recent forecasts taken from the corresponding AEOs. Actual price data from the EIA monthly energy review. EIA (www.eia.gov). Conversion to USD₂₀₁₃ with the GDP deflator from the US Department of Commerce, Bureau of Economic Analysis [25].

Wiser and Bolinger [26] show errors in the EIA predictions for wellhead US natural gas (NG) prices up to the year 2003. Siddiqui and Marnay [27] updated the analysis of Wiser and Bolinger in 2006. In Figure 2, the analysis is extended by comparing the yearly EIA AEO forecasts for the US NG electric power price⁴ with the actual prices for the years 1985-2015. Up to the analysis by Siddiqui and Marnay [27] forecasts were heavily overestimating fuel prices. The figure shows that the trend was opposite in the following years, as predictions failed to capture the increase in NG prices. Errors range from the maximum overestimation by a factor of 3.32 in 1995, to the maximum underestimation by a factor of 2.95 in 2005. Furthermore, there is no strong evidence that forecasts perform better in the short term compared to the long term.

Considering uncertainty in strategic energy planning

Forecasting errors can dramatically impact strategic energy planning decisions. In particular, they can lead to overcapacity and underutilization of the installed technologies. This is the case with the current overcapacity of NG cogeneration of heat and power (CHP) plants in Europe [28], caused by past expectations of low NG prices. As an extreme example, in the Netherlands newly constructed combined cycle gas turbine (CCGT) power plants were shut down in 2014 because non economically viable to operate [29].

As Craig et al. [17] conclude, *“long-run forecasting methods for energy [...] will likely fall prey to the inherent unpredictability of pivotal events”*, i.e. it is unlikely that by investing more time and resources we will ever be able to accurately predict the future evolution of energy systems. Thus, long time horizons and forecast unreliability reveal the inevitable pitfalls of the “traditional” - deterministic - energy modeling approach, and motivate the need for accounting of uncertainty in energy planning. For example, Hirst and Schweitzer [30] consider uncertainty a *“critical element of integrated resource planning”*. Overall, the consideration of uncertainty is an emerging topic in the literature, and various authors recommend its systematic integration in energy modeling [31, 32, 33].

Nonetheless, uncertainty is to date seldom integrated in energy models. In a recent review of urban energy system models, Keirstead et al. [34] highlight that only three of the 219 reviewed works explicitly mentioned uncertainty or sensitivity analysis; Goel and Grossmann [35] point out that most of the available literature for planning of oil and gas field infrastructures uses a deterministic approach.

⁴ The natural gas price to the electric power sector is taken instead of the wellhead price, since starting from 2013 the wellhead price of natural gas is no longer reported by the EIA.

State of the art: uncertainty in the energy modeling practice

As reviewed by Grossmann et al. [36] in the field of process system engineering, the main barriers to a wider penetration of uncertainty are *i)* the complexity and computational expense of energy models; *ii)* the issue of quantifying input uncertainties and determining their nature; *iii)* the selection of appropriate methods for incorporating uncertainties in energy models. The state of the art concerning these challenges is here briefly summarized, while a more detailed review is presented in the dedicated chapters.

Energy models and uncertainty

Connolly et al. [37] perform an extensive review of existing energy models and tools. Table 1 reports an extract of their analysis, limited to the models which are at regional/national scale and are based on optimization. The SMART model [12] is additionally included in the analysis. The models are compared based on the following criteria: *i)* is the model freely available or commercial? *ii)* Does it optimize the investment and/or the operation strategy of the energy system? *iii)* Is it a market-equilibrium model? *iv)* Computational time. *v)* Do stochastic versions of the model exist?

The analysis reveals that the most common approach is based on economic modeling, entirely (as for NEMS and MARKAL) or partially aiming at reaching equilibrium in one or several energy markets. The main issue with this approach is the difficulty of forecasting the future evolution of energy markets. Also, models belonging to this category are - at least partly - commercial. A different, energy-based, modeling approach is adopted in EnergyPlan [38], a freely downloadable tool to evaluate the future operation of energy systems given the investment strategy as an input. Although it can be indirectly used to evaluate different investment options, EnergyPlan cannot be considered a strategic energy planning tool (as defined at the beginning of this chapter) as it does not optimize the investment strategy.

The main shortcoming of most energy models is that they were originally conceived to be deterministic. Thus, adapting them to incorporate uncertainty can be difficult under both the formulation and the computational points of view. Integrating uncertainty in optimization models, e.g. via sensitivity analysis or stochastic optimization techniques, leads very quickly to heavy computational burdens. Siddiqui and Marnay [27] comment that the run time of NEMS limits its use for uncertainty applications to a few well-designed scenarios. Similarly, Usher and Strachan [39] note that the size of the MARKAL model limits the maximum number of uncertain parameters to be considered. SMART is an exception, as it was originally developed as a stochastic model, with a remarkable computational performance. However, it mostly focuses on the electricity sector. Focusing only on electricity, and thus neglecting heating and transportation, is quite common in energy decision-making [40] and it characterizes various other energy planning modeling frameworks, such as [41, 42].

Table 1 – Comparison of existing large-scale energy planning models. Legend: ✓ criterion satisfied; ✓ criterion partly satisfied; ✗ criterion not satisfied. Adapted from Connolly et al. [37], unless otherwise specified.

Model	Free	Investment & Operation	Market Equilibrium	Run time	Stochastic ^a
EnergyPlan [38]	✓	Operation only	✗	Seconds	✗
MARKAL/TIMES [9]	✗	Investment only	✓	5-35 min [43]	✓ [44]
MESSAGE [10]	✓ ^b	✓	✓	-	✓ [45]
NEMS [8]	✓ ^b	✗	✓	1-12 h [46]	✗
SMART [12]	✓ ^c	✓	✓ ^d	1-20 h ^e	✓

^a If the model is in origin deterministic, the criterion is considered partly satisfied if stochastic or partially-stochastic versions of the model exist (indicated as references).

^b Model is freely available, while the associated simulation tools need to be purchased.

^c Model not available, but documented in the supplementary material of [12].

^d The model is a stochastic extension of META*Net [11], which is market equilibrium model.

^e For a 4-year time horizon. The lower bound (1h) is the approximate dynamic programming (ADP) version of the model, the upper bound (20h) is the linear programming (LP) one.

Uncertainty characterization

In order to integrate uncertainties in energy models, the uncertainty of input parameters needs to be quantified. In the context of strategic energy planning, this is often made difficult by the scarce quantity and quality of available data, as highlighted by Pye et al. [47] in the context of the UK energy transition. As an example, looking at the past projections of NG prices in Figure 2, it is indeed challenging to quantify the uncertainty of the latest available forecasts. The difficulty of defining probability density functions (PDFs) for uncertain parameters is underlined by various authors [27, 48].

The quantitative definition of input uncertainties is here defined as *uncertainty characterization*. The way in which uncertainty is quantified can strongly affect model outputs. Various approaches have been used in the literature for this purpose, ranging from the definition of PDFs to the use of qualitative ranges of variation [47, 48, 49, 50, 51, 52, 53]. However, in most of the energy planning literature, uncertainty characterization is not the main focus; instead, it is often marginally addressed as an input to other analyses. Also, in most cases it is only applied to a subset of arbitrarily selected parameters and the data used for uncertainty characterization are rarely fully documented, which limits reproducibility and use in similar applications.

Sensitivity analysis and optimization under uncertainty

The impact of uncertainty in optimization models can be evaluated via sensitivity analysis; else, uncertainty can be directly incorporated into the problem formulation using optimization under

uncertainty techniques.

Sensitivity analysis studies “how uncertainty in the output of a model can be apportioned to different sources of uncertainty in the model input”. It differs from *uncertainty analysis*, a related practice focusing on quantifying uncertainty in model output [54]. In both cases, the deterministic optimization model is run several times sampling the values of input parameters from distributions.

Sensitivity analysis is seldom applied to energy models [34], and it is often limited to an *a priori* selected set of uncertain parameters [55]. A reason of this, along with computational barriers and the difficulty in characterizing input uncertainties, is the lack of a general framework to carry out global sensitivity analysis (GSA) studies in energy planning models.

The review works by Zhou et al. [40] and Soroudi and Amraee [56] illustrate a variety of decision-making under uncertainty methods for energy systems. The classical method to incorporate uncertainty in optimization problem formulations is *stochastic programming* [57]. First proposed by Dantzig [58], it is a scenario-based approach optimizing the expected value over the possible realizations of the uncertain parameters [36]. Problems with stochastic programming are the need of defining PDFs for the uncertain parameters, and the fact that it quickly leads to intractable model sizes [59]. *Robust optimization* is an alternative approach able to cope with large numbers of uncertain parameters and scarcity of data to characterize their uncertainty, which are common issues in strategic energy planning applications. Differently from stochastic programming, it considers the worst-case realizations of uncertainty in the optimization problem. It was first proposed by Soyster [60], and more recently extended by various contributions [61, 62] aiming at reducing the over-conservatism of robust solutions.

Although robust optimization methods are well established in the mathematical programming literature, their application to energy planning problems is, to date, rather limited. Furthermore, most applications only consider the electricity sector [56] and uncertain parameters - often cost parameters - in the objective function.

Contributions and outline of the thesis

This thesis contributes to overcoming these limitations, thus enabling a systematic consideration of uncertainty in energy planning applications. The main research question is:

*How does uncertainty impact strategic energy planning and
how can we facilitate the integration of uncertainty in the energy modeling practice?*

To answer this question, the thesis proposes the following methodological contributions:

- **“Modeling for uncertainty” (Chapter 1):** a mixed-integer linear programming (MILP) modeling framework for large-scale energy systems planning is presented. Given the end-use

energy demand, the efficiency and cost of energy conversion technologies, the availability and cost of energy resources, the model identifies the optimal investment and operation strategies to meet the demand and minimize the total annual cost or GHG emissions of the energy system. It is a simplified, yet complete, representation of an energy system, including electricity, heating and mobility, with a multiperiod formulation accounting for seasonality and energy storage. The concise formulation and low computational time make it suitable for uncertainty applications, and complementary to existing and more complex energy models.

- **Uncertainty characterization (Chapter 2):** a novel application-driven uncertainty characterization method for strategic energy planning problems is introduced. Through a set of criteria, the method aids the definition of ranges of variation for the uncertain parameters, taking into account the nature of the uncertainty and how uncertainty develops over the planning time horizon. The use of ranges instead of PDFs is motivated by the lack of data highlighted in the literature.
- **Global sensitivity analysis (Chapter 3):** the adoption of a two-stage GSA method [63] is proposed to deal with the large number of uncertain parameters in energy planning models. The application of a two-stage approach and the consideration of *all* parameters in the analysis represents a novelty in the energy planning field.
- **Robust optimization (Chapter 4):** the robust formulation by Bertsimas and Sim [62] is applied for the first time in the context of strategic energy planning. A general framework is provided, allowing to consider uncertainty for all parameters, both in the objective function and in the other constraints, and a decision-support method is proposed. In this context, the original formulation by Bertsimas and Sim [62] is extended to consider the case of multiplied uncertain parameters.

To evaluate the impact of uncertainty on strategic energy planning, the presentation of the methods is systematically associated to their validation on a real case study. The national energy system of Switzerland is chosen as a representative application. After the decision of the Swiss government to phase out nuclear power plants at the end of their lifetime [64], the country is defining its future energy strategy. As most national and urban energy systems present common features, both the model and the data are fully documented to allow reproducibility and use in similar applications.

Figure 3 illustrates the outline of the thesis. In Chapter 1, the MILP modeling framework is applied and validated for the case of the Swiss energy system. In Chapter 2, the uncertainty of the main parameters in the model is characterized. The generated ranges of variation serve as input to the GSA (Chapter 3), allowing to identify the most impacting parameters in the model and the most influential model assumptions, and to the robust optimization (Chapter 4). The latter generates robust investment strategies which are then evaluated and compared through simulation. Finally, concluding remarks summarize the main findings, provide recommendations and guidance to integrate uncertainty in energy models, and envision future perspectives.

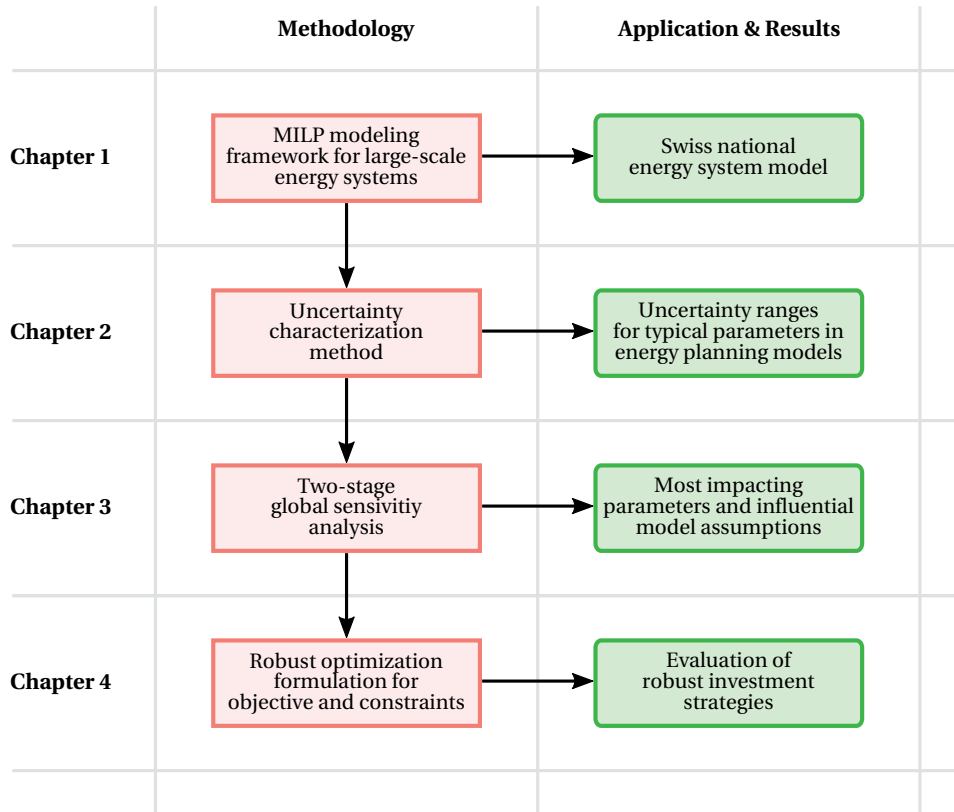


Figure 3 – Thesis structure overview.

Appendix A and Appendix B are complementary to Chapter 1 and Chapter 2, respectively: Appendix A reports the nominal input data for the case study of the Swiss energy system, while Appendix B documents the sources used for the characterization of their uncertainty. Appendix C is complementary to Chapter 1, as it proposes a MILP modeling framework for urban energy systems and applies it to the integration of geothermal and biomass resources. The model structure is conceptually equivalent to the modeling framework presented in Chapter 1; however, the level of detail is higher, as the formulation accounts for process integration [65] - and thus for the temperature levels of the thermal streams - and for the fixed cost of technologies. Appendix D documents the nominal input data for the urban energy system of Lausanne (Switzerland), which is used as example application in Appendix C.

Terminology, conventions and tools

The terminology used in the current work is the terminology commonly used in the optimization field [66]. Eq. 1 shows the general form of an optimization problem.

$$\begin{aligned} \min_{\mathbf{x} \in \mathbb{R}^n} f(\mathbf{x}, \theta) \\ \text{s.t. } h(\mathbf{x}, \theta) = 0 \\ g(\mathbf{x}, \theta) \leq 0 \end{aligned} \tag{1}$$

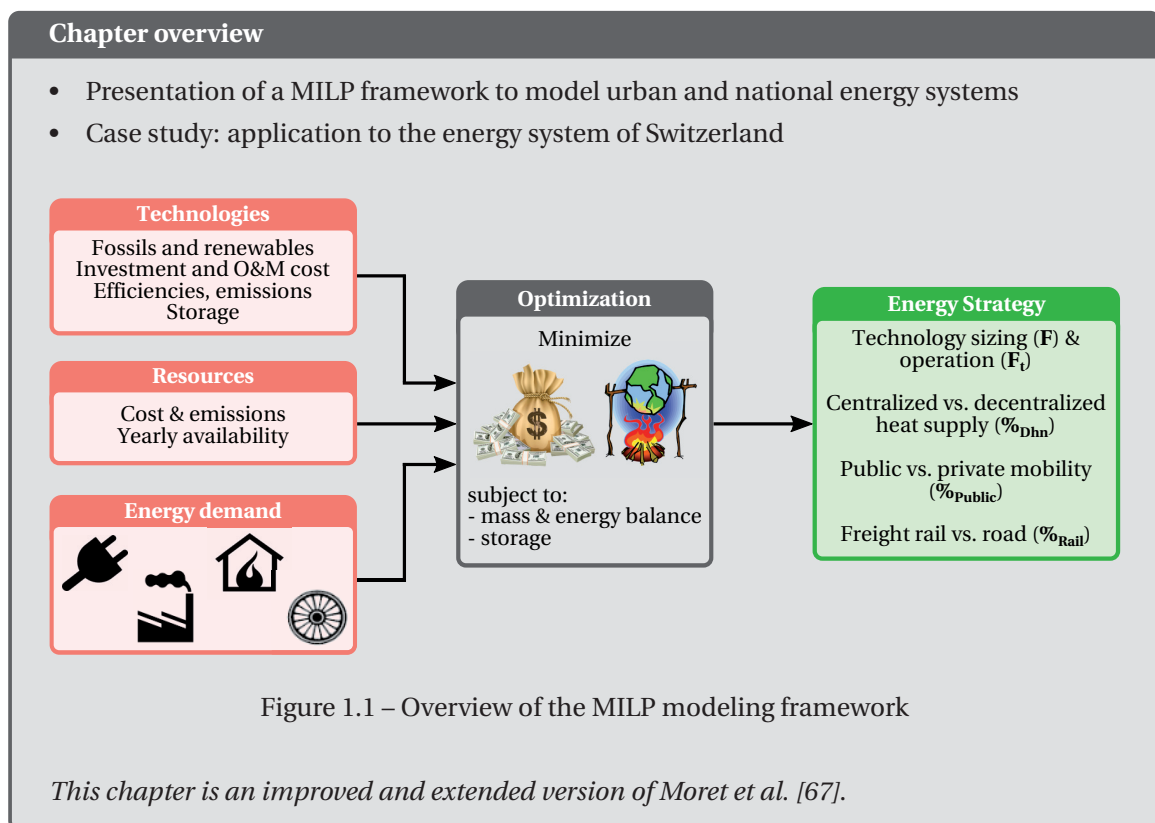
Solving an optimization problem consists in finding the optimal value of the *decision variables* \mathbf{x} , which minimizes the value of the *objective function* f subject to equality and inequality constraints. The input data of the problem θ are called *parameters*. *Outputs of interest* (Y) of an optimization problem can be the value of the objective or of the decision variables. The *model* is defined by the constraints. If no optimization is performed, the model is in the form $Y = h(\theta)$.

Throughout the thesis, sets are written in all capital letters (e.g. “SET”), parameters in italic lowercase (e.g. “*parameter*”), decision variables in bold lowercase with capitalized first letter (e.g. “**Variable**”). The optimization problem formulations are written in AMPL [66], using CPLEX 12.6 or higher as a solver.

1 Modeling for uncertainty

*“[...] Cui flavam religas comam
simplex munditiis? [...]”*

Quintus Horatius Flaccus. *Ad Pyrrham*. Ode I, 5



As briefly reviewed in the Introduction, various optimization-based modeling frameworks have been proposed in the literature to support strategic energy planning at urban and national level. The most diffused modeling strategy is the *market equilibrium* approach, balancing demand and supply to reach equilibrium in energy markets. According to Powell et al. [12], the application of this approach to energy systems dates back to the 1970s with the PIES model [68]. More recent examples are the NEMS [8], which simulates US energy markets and their interactions with the rest of economy, and the MARKAL/TIMES [9] family of models, minimizing the total discounted cost of the energy system. META*Net [11] is a LP model combining the features of NEMS and MARKAL. SMART [12] is a stochastic extension of META*Net, optimizing investment planning as well as operation in the electricity sector. MESSAGE [10] only partly relies on market equilibrium, as it supports medium- to long-term planning of energy systems to determine cost-effective climate change mitigation strategies.

Differently from these examples, other modeling frameworks are not based on seeking equilibrium in energy markets. These other approaches are here defined as *energy-based*, to distinguish them from the economic modeling strategies. As an example, EnergyPlan [38] adopts (partly) optimization to find the best operating strategies for energy systems, given the investment decisions as an input and taking one future year as reference.

Energy-based modeling frameworks to support strategic energy planning are often formulated as MILP problems, as it emerges from the analysis by Koltsaklis et al. [41], who propose a MILP model for the optimal long-term energy planning of a national power generation system. An alternative MILP framework for long-term power systems planning is also presented by Wierzbowski et al. [42]. The focus of these latter works is only on the planning of the electricity sector. MILP frameworks are also used to plan the optimal integration of specific energy resources, such as biomass, in urban systems [69, 70].

As also shown in Table 1, the different modeling frameworks proposed in the literature feature one or more of the following limitations: *i)* not optimizing both the investment and operation strategy; *ii)* being commercial, i.e. not freely available; *iii)* being limited to only one sector (normally the electricity sector) or to one specific resource. Most importantly, being originally conceived as deterministic, *iv)* most existing models are rather complex and computationally demanding. When incorporating uncertainties, this poses problems both in terms of formulation and of computational tractability. These limitations impede the direct application of existing modeling frameworks in the context of this thesis.

Contributions

Thus, a novel energy-based MILP modeling framework for large-scale energy systems is presented in this chapter. The conceptual structure of the model is illustrated in Figure 1.1: given the end-use

energy demand, the efficiency and cost of energy conversion technologies, the availability and cost of energy resources, the model identifies the optimal investment and operation strategies to meet the demand and minimize the total annual cost or GHG emissions of the energy system. It is a simplified, yet complete, representation of an energy system, including electricity, heating and mobility, with a multiperiod formulation accounting for seasonality and energy storage. The concise formulation and low computational time make it suitable for uncertainty applications, and complementary to existing and more complex energy models.

The model is validated on the real energy system of Switzerland today, and then applied to the strategic energy planning for the country with a 20-year time horizon. Urban and national energy systems worldwide have similar features. Thus, as an additional contribution, both the MILP formulation and the data are documented in detail (in the following pages and in Appendix A) and made publicly available¹ to ensure full reproducibility and use in similar applications.

1.1 MILP modeling framework

Adopting the definition by Keirstead et al. [34] for the field of urban systems, an energy model can be defined as “*a formal system that represents the combined processes of acquiring and using energy to satisfy the energy service demands of a given [...] area*”. Thus, the proposed modeling framework is a simplified representation of an urban or national energy system accounting for the energy flows within its boundaries. According to the classification proposed by Codina Gironès et al. [71], the modeling framework belongs to the *snapshot* category, as it models the energy system in a target year. This year represents all the years in which the system is operated.

Figure 1.2 illustrates its application to the case study of Switzerland, which is discussed more in detail later in this chapter (Section 1.2). The energy system is modeled in its entirety. Imported and indigenous resources can be converted with energy conversion technologies to satisfy end-use demand in energy services: heat, mobility and electricity. Heating demand is divided between industrial, centralized and decentralized; mobility is divided into passenger (public and private) and freight (rail and road). The modeling framework is the MILP equivalent of the sequential modeling framework by Codina Gironès et al. [71].

1.1.1 Sets, parameters, variables

Figure 1.3 is a visual representation of the sets of the proposed formulation with their relative indices used throughout the paper; Table 1.1 lists the parameters; Table 1.2 and Table 1.3 list and describe the independent and dependent decision variables, respectively. Units should be proportionally scaled based on the specific application.

¹ The code is available at <https://github.com/stefanomoret>

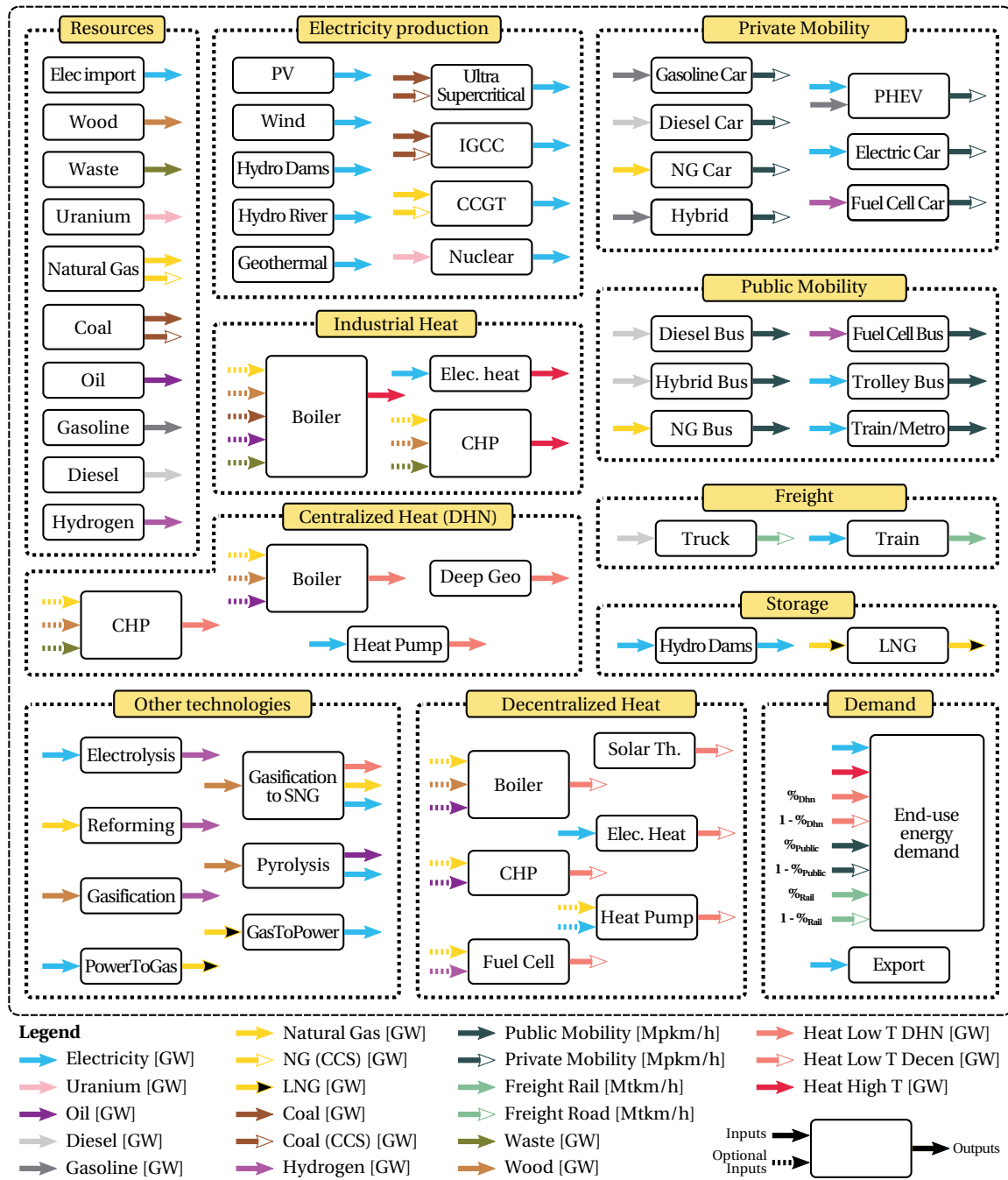


Figure 1.2 – Application of the MILP modeling framework to the energy system of Switzerland. Abbreviations: natural gas (NG), liquified natural gas (LNG), carbon capture and storage (CCS), liquified natural gas (LNG), synthetic natural gas (SNG), combined cycle gas turbine (CCGT), photovoltaic (PV), temperature (T), plug-in hybrid electric vehicle (PHEV), cogeneration of heat and power (CHP).

Table 1.1 – Parameter list with description. Set indices as in Figure 1.3

Parameter	Units	Description
$endUses_{year}(eui, s)$	[GWh/y] ^a	Annual end-uses in energy services per sector
$endUsesInput(eui)$	[GWh/y] ^a	Total annual end-uses in energy services
$\tau(tech)$	[-]	Investment cost annualization factor
i_{rate}	[-]	Real discount rate
$\%_{public,min}, \%_{public,max}$	[-]	Upper and lower limit to $\%_{Public}$
$\%_{rail,min}, \%_{rail,max}$	[-]	Upper and lower limit to $\%_{Rail}$
$\%_{dhn,min}, \%_{dhn,max}$	[-]	Upper and lower limit to $\%_{Dhn}$
$t_{op}(t)$	[h]	Time periods duration
$\%_{lighting}(t)$	[-]	Yearly share (adding up to 1) of lighting end-uses
$\%_{sh}(t)$	[-]	Yearly share (adding up to 1) of SH end-uses
$f(res \cup tech \setminus sto, l)$	[GW] ^b	Input from (< 0) or output to (> 0) layers. $f(i, j) = 1$ if j is main output layer for technology/resource i
$f_{ref}(tech)$	[GW] ^{bc}	Reference size with respect to main output
$c_{inv}(tech)$	[MCHF/GW] ^{bc}	Technology specific investment cost
$c_{maint}(tech)$	[MCHF/GW/y] ^{bc}	Technology specific yearly O&M cost
$gwp_{constr}(tech)$	[ktCO ₂ -eq./GW] ^{bc}	Technology construction specific GHG emissions
$n(tech)$	[y]	Technology lifetime
$f_{min}, f_{max}(tech)$	[GW] ^{bc}	Min./max. installed size of the technology
$f_{min,\%}, f_{max,\%}(tech)$	[-]	Min./max. relative share of a technology in a layer
$avail(res)$	[GWh/y]	Resource yearly total availability
$c_{p,t}(tech, t)$	[-]	Period capacity factor (default 1)
$c_p(tech)$	[-]	Yearly capacity factor
$c_{op}(res, t)$	[MCHF/GWh]	Specific cost of resources
$gwp_{op}(res)$	[ktCO ₂ -eq./GWh]	Specific GHG emissions of resources
$\eta_{sto,in}, \eta_{sto,out}(sto, l)$	[-]	Efficiency [0; 1] of storage input from/output to layer. Set to 0 if storage not related to layer.
$\%_{loss}(eut)$	[-]	Losses [0; 1] in the networks (grid and DHN)
$\%_{PeakDHN}$	[-]	Ratio peak/max. average DHN heat demand

Table 1.2 – Independent decision variable list with description. All variables are continuous and non-negative, unless otherwise indicated.

Variable	Units	Description
$\%_{Public}$	[-]	Ratio [0; 1] public mobility over total passenger mobility
$\%_{Rail}$	[-]	Ratio [0; 1] rail transport over total freight transport
$\%_{Dhn}$	[-]	Ratio [0; 1] centralized over total low-temperature heat
$F(tech)$	[GW] ^{bc}	Installed capacity with respect to main output
$F_t(tech \cup res, t)$	[GW] ^{bc}	Operation in each period
$Sto_{in}, Sto_{out}(sto, l, t)$	[GW]	Input to/output from storage units
$Y_{Solar}(tech) \in \{0; 1\}$	[-]	If 1, $tech$ is backup technology for decentralized solar

^a [Mpkm] (millions of passenger-km) for passenger, [Mtkm] (millions of ton-km) for freight mobility end-uses

^b [Mpkm/h] for passenger, [Mtkm/h] for freight mobility end-uses

^c [GWh] if $tech \in STO$

Chapter 1. Modeling for uncertainty

Table 1.3 – Dependent decision variable list with description. All variables are continuous and non-negative, unless otherwise indicated.

Variable	Units	Description
$\text{EndUses}(l, t)$	[GW] ^a	End-uses demand. Set to 0 if $l \notin \text{EUT}$
$\text{N}(tech) \in \mathbb{N}$	[-]	Number of installed units of size f_{ref}
C_{tot}	[MCHF/y]	Total annual cost of the energy system
$\text{C}_{inv}(tech)$	[MCHF]	Technology total investment cost
$\text{C}_{maint}(tech)$	[MCHF/y]	Technology yearly O&M cost
$\text{C}_{op}(res)$	[MCHF/y]	Total cost of resources
GWP_{tot}	[ktCO ₂ -eq./y]	Total yearly GHG emissions of the energy system
$\text{GWP}_{constr}(tech)$	[ktCO ₂ -eq.]	Technology construction GHG emissions
$\text{GWP}_{op}(res)$	[ktCO ₂ -eq./y]	Total GHG emissions of resources
$\text{Loss}(eut, t)$	[GW]	Losses in the networks (grid and DHN)

^a [Mpkm/h] for passenger, [Mtkm/h] for freight mobility end-uses

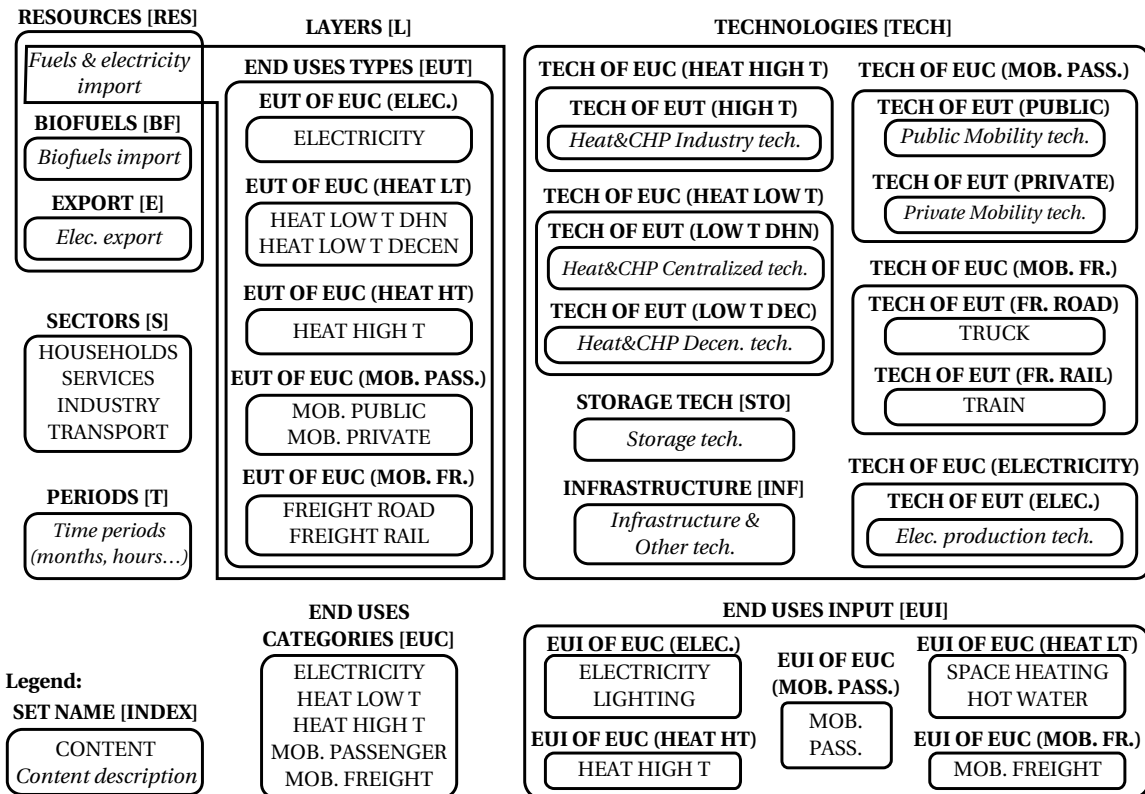


Figure 1.3 – Visual representation of the sets and indices of the MILP framework. Abbreviations: space heating (SH), hot water (HW), temperature (T), mobility (MOB)

1.1.2 Constraints

The model formulation is expressed by the equations in Figure 1.4 and Eq. 1.1-1.20.

End-uses demand

In the energy modeling practice, the energy demand is often expressed in terms of *final energy consumption (FEC)*. FEC is defined as “the energy which reaches the final consumer’s door” [72]. In other words, the FEC is the amount of input fuel needed to satisfy the *end-use demand (EUD)* in energy services. As an example, in the case of decentralized heat production with a NG boiler, the FEC is the amount of NG consumed by the boiler; the EUD is the amount of heat produced by the boiler, i.e. the heating service needed by the final user.

The input to the proposed modeling framework is the EUD in energy services, represented as the sum of three components: electricity, heating and mobility; this also replaces the classical sector-based representation of energy demand. This modeling choice has two advantages. First, it introduces a clear distinction between demand and supply. On the one hand, the demand concerns the definition of the end-uses, i.e. the requirements in energy services (e.g. the mobility needs). On the other hand, the supply concerns the choice of the energy conversion technologies to supply these services (e.g. the types of vehicles used to satisfy the mobility needs). Based on the technology choice, the same EUD can be satisfied with a different FEC, depending on the efficiency of the chosen energy conversion technology. Second, it facilitates the inclusion in the model of electric technologies for heating and transportation (such as heat pumps and electric vehicles).

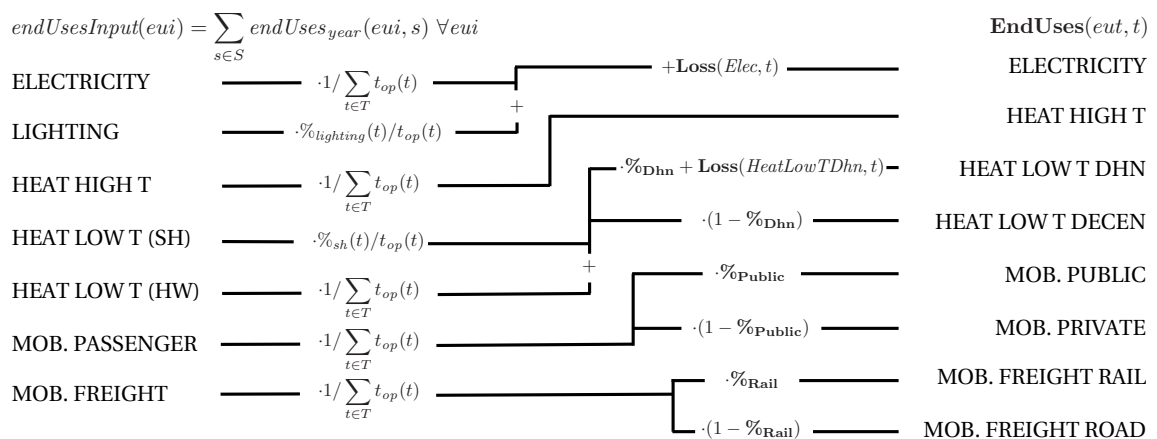


Figure 1.4 – **EndUses** calculation starting from yearly demand model input (*endUsesInput*)

$$\min \mathbf{C}_{\text{tot}} = \sum_{j \in \text{TECH}} (\tau(j) \mathbf{C}_{\text{inv}}(j) + \mathbf{C}_{\text{maint}}(j)) + \sum_{i \in \text{RES}} \mathbf{C}_{\text{op}}(i) \quad (1.1)$$

$$\text{s.t. } \tau(j) = \frac{i_{\text{rate}}(i_{\text{rate}} + 1)^{n(j)}}{(i_{\text{rate}} + 1)^{n(j)} - 1} \quad \forall j \in \text{TECH} \quad (1.2)$$

$$\mathbf{C}_{\text{inv}}(j) = c_{\text{inv}}(j) \mathbf{F}(j) \quad \forall j \in \text{TECH} \quad (1.3)$$

$$\mathbf{C}_{\text{maint}}(j) = c_{\text{maint}}(j) \mathbf{F}(j) \quad \forall j \in \text{TECH} \quad (1.4)$$

$$\mathbf{GWP}_{\text{constr}}(j) = gwp_{\text{constr}}(j) \mathbf{F}(j) \quad \forall j \in \text{TECH} \quad (1.5)$$

$$f_{\text{min}}(j) \leq \mathbf{F}(j) \leq f_{\text{max}}(j) \quad \forall j \in \text{TECH} \quad (1.6)$$

$$\mathbf{N}(j) f_{\text{ref}}(j) = \mathbf{F}(j) \quad \forall j \in \text{TECH} \quad (1.7)$$

$$\mathbf{F}_t(j, t) \leq \mathbf{F}(j) c_{p,t}(j, t) \quad \forall j \in \text{TECH}, \forall t \in T \quad (1.8)$$

$$\sum_{t \in T} \mathbf{F}_t(j, t) t_{\text{op}}(t) \leq \mathbf{F}(j) c_p(j) \sum_{t \in T} t_{\text{op}}(t) \quad \forall j \in \text{TECH} \quad (1.9)$$

$$\mathbf{C}_{\text{op}}(i) = \sum_{t \in T} c_{\text{op}}(i, t) \mathbf{F}_t(i, t) t_{\text{op}}(t) \quad \forall i \in \text{RES} \quad (1.10)$$

$$\mathbf{GWP}_{\text{op}}(i) = \sum_{t \in T} gwp_{\text{op}}(i, t) \mathbf{F}_t(i, t) t_{\text{op}}(t) \quad \forall i \in \text{RES} \quad (1.11)$$

$$\sum_{t \in T} \mathbf{F}_t(i, t) t_{\text{op}}(t) \leq \text{avail}(i) \quad \forall i \in \text{RES} \quad (1.12)$$

$$\sum_{i \in \text{RES} \cup \text{TECH} \setminus \text{STO}} f(i, l) \mathbf{F}_t(i, t) + \sum_{j \in \text{STO}} (\mathbf{Sto}_{\text{out}}(j, l, t) - \mathbf{Sto}_{\text{in}}(j, l, t)) - \mathbf{EndUses}(l, t) = 0 \quad \forall l \in L, \forall t \in T \quad (1.13)$$

$$\mathbf{F}_t(j, t) = \mathbf{F}_t(j, t-1) + t_{\text{op}}(t) \cdot \left(\sum_{l \in L | \eta_{\text{sto}, \text{in}}(j, l) > 0} \mathbf{Sto}_{\text{in}}(j, l, t) \eta_{\text{sto}, \text{in}}(j, l) - \sum_{l \in L | \eta_{\text{sto}, \text{out}}(j, l) > 0} \mathbf{Sto}_{\text{out}}(j, l, t) / \eta_{\text{sto}, \text{out}}(j, l) \right) \quad \forall j \in \text{STO}, \forall t \in T \quad (1.14)$$

$$\mathbf{Sto}_{\text{in}}(j, l, t) (\lceil \eta_{\text{sto}, \text{in}}(j, l) \rceil - 1) = 0 \quad \forall j \in \text{STO}, \forall l \in L, \forall t \in T \quad (1.15)$$

$$\mathbf{Sto}_{\text{out}}(j, l, t) (\lceil \eta_{\text{sto}, \text{out}}(j, l) \rceil - 1) = 0 \quad \forall j \in \text{STO}, \forall l \in L, \forall t \in T \quad (1.16)$$

$$\left[\sum_{l \in L | \eta_{\text{sto}, \text{in}}(j, l) > 0} \mathbf{Sto}_{\text{in}}(j, l, t) / m(j, l, t) \right] + \left[\sum_{l \in L | \eta_{\text{sto}, \text{out}}(j, l) > 0} \mathbf{Sto}_{\text{out}}(j, l, t) / m(j, l, t) \right] \quad \forall j \in \text{STO}, \forall t \in T \quad (1.17)$$

$$\mathbf{Loss}(eut, t) = \left(\sum_{i \in \text{RES} \cup \text{TECH} \setminus \text{STO} | f(i, eut) > 0} f(i, eut) \mathbf{F}_t(i, t) \right) \%_{\text{loss}}(eut) \quad \forall eut \in \text{EUT}, \forall t \in T \quad (1.18)$$

$$\mathbf{F}_t(j, t) + \mathbf{F}_t(k, t) \mathbf{Y}_{\text{Solar}}(j) \geq \frac{\mathbf{EndUses}(\text{HeatLowTDHn}, t) + \mathbf{EndUses}(\text{HeatLowTDec}, t)}{\text{endUsesInput}(\text{HeatLowTSH}) + \text{endUsesInput}(\text{HeatLowTHW})} \sum_{t \in T} \mathbf{F}_t(j, t) t_{\text{op}}(t) \quad k = \text{Dec}_{\text{Solar}}, \forall j \in \text{TECH OF EUT}(\text{HeatLowTDec}) \setminus \{k\}, \forall t \in T \quad (1.19)$$

$$\sum_{j \in \text{TECH}} \mathbf{Y}_{\text{Solar}}(j) \leq 1 \quad (1.20)$$

Figure 1.4 shows the constraints relative to the calculation of the EUD in each period t (**EndUses**) starting from the projected total yearly demand ($endUsesInput$, input from demand-side model) summed across the different energy sectors (households, services, industry, transport).

Electricity end-uses result from the sum of the electricity-only demand, assumed constant throughout the year, and the demand for lighting, distributed across the periods according to $\%_{lighting}$. Low-temperature heat demand results from the sum of yearly demand for hot water (HW), evenly shared across the year, and space heating (SH), distributed across the periods according to $\%_{sh}$. The percentage repartition between centralized (district heating network (DHN)) and decentralized heat demand is defined by the variable $\%_{Dhn}$. High temperature process heat and mobility demand are evenly distributed across the periods. Passenger mobility demand is expressed in passenger-kilometers (pkms), freight transportation demand is in ton-kilometers (tkms). The variables $\%_{Public}$ and $\%_{Rail}$ define the penetration of public transportation in passenger mobility and of train in freight, respectively.

Total cost and GHG emissions

In the proposed formulation, the objective is the minimization of the total annual cost of the energy system (C_{tot}), defined as the sum of the annualized investment and operation and maintenance (O&M) cost (C_{maint}) of technologies, and the operating cost of resources (C_{op}) (Eq. 1.1). The total investment cost (C_{inv}) of each technology results from the multiplication of its specific investment cost (c_{inv}) and installed size (F), the latter defined with respect to the main end-uses output type (Eq. 1.3). C_{inv} is annualized with the factor τ , calculated based on the interest rate (i_{rate}) and the technology lifetime (n) (Eq. 1.2). The total O&M cost is calculated in the same way (Eq. 1.4). Upper and lower limits to the installed capacity of each technology are set by f_{max} and f_{min} , respectively. The latter allows accounting for old technologies still existing in the target year (Eq. 1.6). Eq. 1.7 forces the number of installed units of a technology to be an integer multiple (N) of the reference size f_{ref} . The total cost of resources is calculated as the sum of the use over different periods multiplied by the period duration (t_{op}) and the specific cost of the resource (c_{op}) (Eq. 1.10).

The global annual GHG emissions are calculated using a life cycle assessment (LCA) approach, i.e. taking into account emissions of technologies and resources “from cradle to grave”. For climate change, the natural choice as indicator is the global warming potential (GWP), expressed in ktCO₂-eq./year. In Eq. 1.21 the total yearly emissions of the system (GWP_{tot}) are defined as the sum of the emissions related to the construction and end-of-life of the energy conversion technologies (GWP_{constr}), allocated to one year based on the technology lifetime, and the emissions related to resources (GWP_{op}).

$$GWP_{tot} = \sum_{j \in TECH} \frac{GWP_{constr}(j)}{n(j)} + \sum_{i \in RES} GWP_{op}(i) \quad (1.21)$$

The total emissions related to the construction of technologies are the product of the specific emissions (gwp_{constr}) and the installed size (Eq. 1.5). The total emissions of resources are the emissions associated to fuels (from cradle to combustion) and imports of electricity. They are calculated as the sum of the use over different periods multiplied by the period duration and the specific emissions of the resource (gwp_{op}) (Eq. 1.11). Operating emissions of technologies, mainly corresponding to auxiliary materials and maintenance, can also be additionally added to the formulation. As MILP problems have only one objective, \mathbf{GWP}_{tot} can be used as objective instead of \mathbf{C}_{tot} . Alternatively, the two objectives can be combined using the ϵ -constraint method [73]. This method seeks trade-off solutions by formulating a bi-objective problem in which one of the objectives is minimized, and the other is constrained by an upper value ϵ , which is made vary parametrically.

The conceptual separation between technologies and resources for GWP calculation allows an easy integration of biofuels and carbon capture and storage (CCS) technologies. As an example, Figure 1.2 shows that when synthetic natural gas (SNG) is produced it can be input in the NG layer, thus replacing its fossil equivalent. As a consequence, the total NG emissions are reduced as the utilization of the fossil natural gas resource is lower. The GHG emission reduction from CCS technologies can be accounted for by adding “CCS resources”, i.e. resources with lower gwp_{op} , corresponding to the carbon capture potential of the associated CCS technologies.

Operational constraints: layers and storage

The operation of resources and technologies in each period is determined by the decision variable \mathbf{F}_t . The *capacity factor* of technologies is conceptually divided into two components: a capacity factor for each period ($c_{p,t}$) depending on resource availability (e.g. renewables) and a yearly capacity factor (c_p) accounting for technology downtime and maintenance. For a given technology, the definition of only one capacity factor is needed, the other one being fixed to the default value of 1. Eqs. 1.8 and 1.9 link the installed size of a technology to its actual use in each period (\mathbf{F}_t) via the two capacity factors, respectively. The total use of resources is limited by the yearly availability (*avail*) (Eq. 1.12).

Layers are defined as all the elements in the system that need to be balanced in each period, such as resources and end-uses demand. The matrix f defines for all technologies and resources outputs to (positive) and inputs from (negative) layers. Eq. 1.13 expresses the balance for each layer: all outputs from resources and technologies (including storage) are used to satisfy the EUD or as inputs to other resources and technologies. Figure 1.5 offers an intuitive representation of the constraint. Each layer can be conceptually thought of as a pool in which the water level must be the same at the end of each period. In Figure 1.2 different colors represent different layers. As an example, the electricity which is imported or produced in the system is used to satisfy the electricity EUD; additionally, it can be stored in hydroelectric dams or used as input to other energy conversion technologies (such as heat pumps or electric vehicles) to satisfy other EUD types.

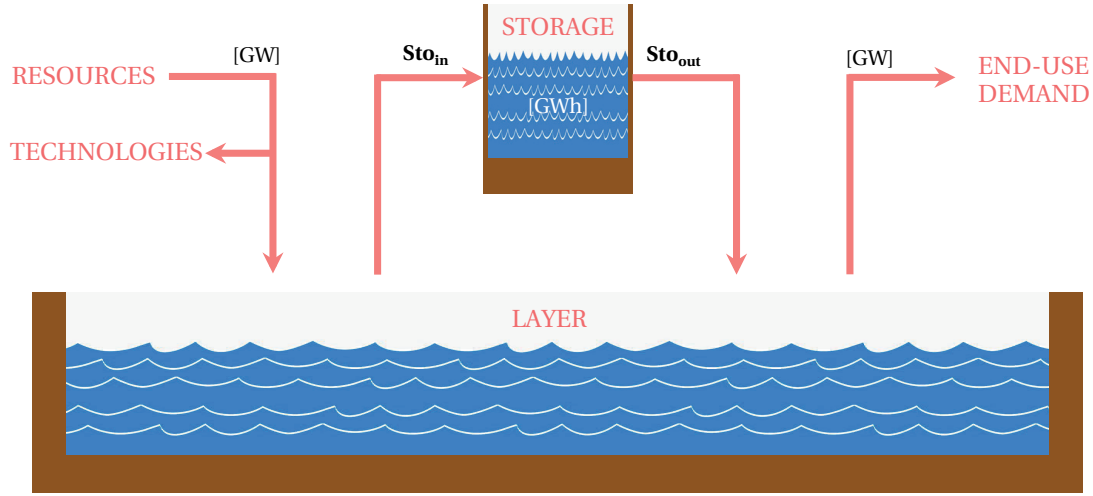


Figure 1.5 – Conceptual representation of a *layer*: all outputs from resources and technologies (including storage) are used to satisfy end-uses demand or as inputs to other resources and technologies (Eq. 1.13).

Storage technologies allow storage across different periods and layers. The storage is modeled as a “tank” whose level (F_t) in period t is equal to the level at the end of the previous period plus input to the storage (Sto_{in}) minus output (Sto_{out}) in t (Eq. 1.14). The parameters $\eta_{sto,in}$ and $\eta_{sto,out}$ define efficiencies for storage inputs and outputs, respectively: if the efficiency is 0 then the storage technology and the layer are incompatible (Eqs. 1.15-1.16). Eq. 1.17, displayed in a compact non-linear formulation², ensures that the storage is not used as a transfer unit within a given period. In the equation, the parameter m must be big enough to ensure that the arguments of the ceiling operators are lower or equal than 1. As an example, $m(j, l, t) = \max \left\{ \frac{f_{max}(j)}{\eta_{sto,in}(j,l)t_{op}(t)}; \frac{\eta_{sto,out}(j,l)f_{max}(j)}{t_{op}(t)} \right\}$ satisfies this condition.

Other constraints

Losses (**Loss**) are considered for the electricity grid and for the DHN. They are calculated as a percentage ($\%_{loss}$) of the total production and import in the corresponding layers (Eq. 1.18). Eq. 1.19 (also expressed in a compact non-linear formulation) makes the model more realistic by defining the operating strategy for decentralized heating: the relative use of each technology in each period should be constant, except for solar thermal (Dec_{Solar}). If solar thermal is installed, then at maximum one technology is used as backup (Eq. 1.20).

² All equations expressed in a compact non-linear form in this chapter (Eqs. 1.19, 1.17, 1.27, 1.29) can be easily linearized.

1.2 Case study: the Swiss energy system in 2035

As an example application, the MILP framework is applied to the energy system of Switzerland with a 20-year planning horizon. In 2011, the country decided to phase out its existing nuclear power plants in the year 2034, at the end of their technical lifetime [64]. As illustrated in Figure 1.6, in that year nuclear contributed for 42.3% to the total net electricity production, the rest being supplied by hydroelectricity (51.9%), other thermal (5.5%), and a low share of photovoltaic (PV) and wind (0.3%). Although close to being autonomous on a yearly balance, the country today already suffers an electricity deficit during winter months, when electricity production is lower, due to the lower outputs of run-of-river power plants, and demand is higher, mostly due to the use of electricity for heating end-uses. The decision of gradually abandoning nuclear power has generated a vibrant energy debate in the country about the future energy strategy [74].

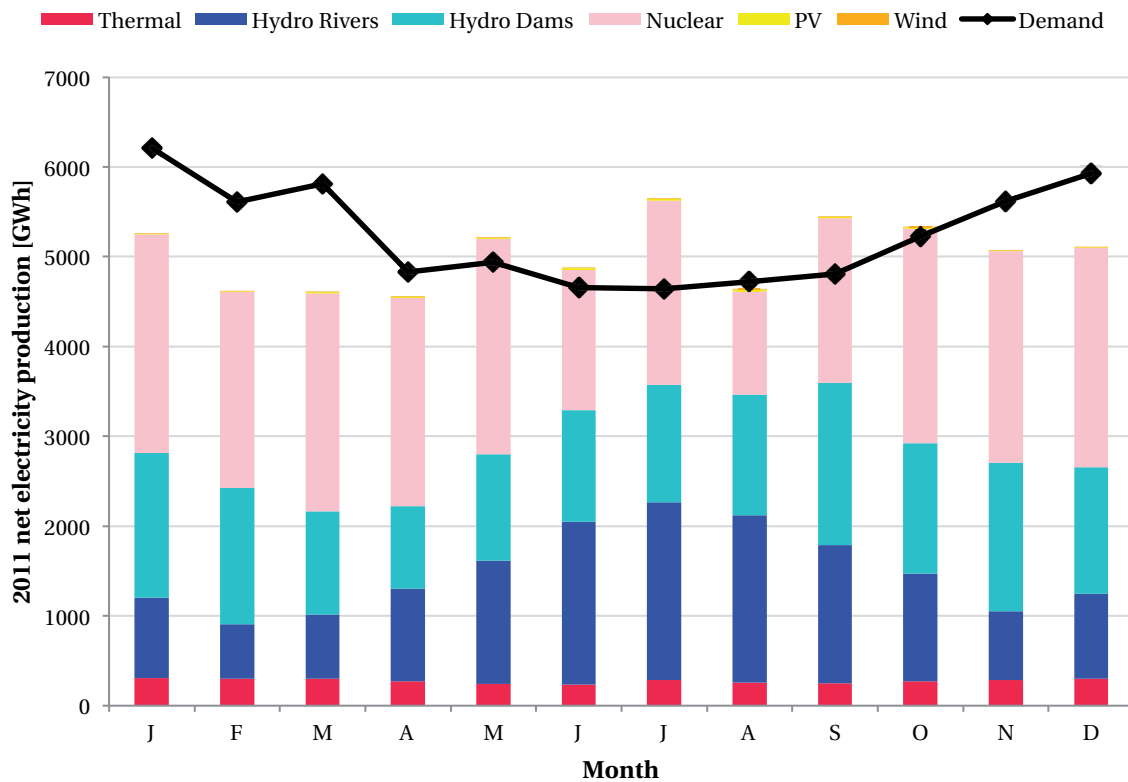


Figure 1.6 – Monthly net electricity production vs. demand in Switzerland in the year 2011.

Thus, the long-term planning of the Swiss energy system is chosen as example application in this thesis with the goal of understanding how uncertainty impacts strategic energy planning decisions. The presented MILP framework is applied to the energy system of Switzerland with a 20-year time horizon. It is assumed that the investment decisions are made today considering fuel prices, energy demand and technology development status corresponding to the last year of the planning horizon.

In other words, the values of the parameters in the model are the projections for the year 2035, and the evolution of the system during the planning horizon is not accounted for.

Figure 1.2 illustrates the case study. Wood and waste are the considered limited local resources, while import of electricity and other fuels is assumed to be unlimited. The resources can be input to different energy technology options in order to satisfy the demand. As an example, the decentralized heat demand can be met by boilers, CHP engines, direct electric heating, heat pumps, fuel cells (FCs) and solar thermal panels. For some of the technologies, such as the boilers, different fuel options are offered. Technologies already existing today, and which will still be present in 2035, such as the hydroelectric plants, are considered fixed in the model. The model has a monthly resolution, and seasonal storage is allowed by hydroelectric dams and power-to-gas systems [75]. All the values are documented Appendix A. In terms of computational requirements, the resulting MILP problem features 1633 decision variables (of which 118 binaries and 56 integers) and it is solved to optimality in approximately 0.25 seconds on a 2.7 GHz 4-core machine.

The use of the presented MILP framework to model the Swiss energy system has found application, among others, in the work by Codina Gironès et al. [76], comparing different energy conversion pathways for woody biomass in the context of a national energy system. Also, an earlier sequential version of the model (not based on optimization), presented in [71], is implemented in the online platform Swiss-EnergyScope.ch [74]. This shows the possibility of using the proposed MILP framework as a tool to assess and compare different energy strategy options, which can be forced by the addition of constraints limiting the degrees of freedom of the model.

In the next paragraphs, first the additional constraints needed for the specific case of the Swiss energy system are introduced. Second, the model is validated via a comparison to the real energy system of Switzerland in the year 2011.

1.2.1 Additional constraints

Eqs. 1.1-1.20 and Figure 1.4 define the main constraints of the MILP model. Eqs. 1.22-1.29 are added to simplify the use of the model and adapt it to the specific case study of Switzerland.

Eq. 1.22 is complementary to Eq. 1.6, as it expresses the minimum ($f_{min,\%}$) and maximum ($f_{max,\%}$) yearly output shares of each technology for each type of EUD. In fact, for a given technology, assigning a relative share (e.g. boilers providing at least a given percent of the total heat demand) is more intuitive and close to the energy planning practice than limiting its installed size. $f_{min,\%}$ and $f_{max,\%}$ are fixed to 0 and 1, respectively, unless otherwise indicated. Eq. 1.23 imposes that the share of the different technologies for mobility be the same in each period. The addition of this constraint is motivated by the fact that the investment cost of passenger and freight transport technologies is not accounted for in the model. Eq. 1.24-1.25 regulate the functioning of hydroelectric dams in Switzerland, which is further detailed in Appendix A.2.1. Increasing the installed power of the

dams, and thus their yearly production, allows also to have a margin for shifting their electricity production across the time periods. This possibility is represented in the model by *StoHydro*, a “storage” technology (with efficiency equal to 1) allowing to shift the production of hydroelectric dams across the different months. Eq. 1.24 links linearly the storage capacity to the new installed power. Eq. 1.25 ensures that the shifted production in a given time period does not exceed the electricity production by the dams in that period. Eq. 1.26 links the DHN size to the total size of the installed centralized energy conversion technologies. To avoid underestimating the cost of centralized heat production, a multiplication factor is introduced to account for peak demand, defined as a $\%_{Peak_{DHN}}$ times the maximum monthly average heat demand (Eq. 1.27). Based on the data reported in Appendix A.2.4, an additional investment cost of 9.4 billion CHF₂₀₁₅ is linked proportionally to the deployment of stochastic renewables (Eq. 1.28). The power-to-gas storage system described in Appendix A.2.3 is implemented in the model with two conversion units and a liquified natural gas (LNG) storage tank. *PowerToGas* converts electricity to LNG, *GasToPower* converts LNG back to electricity. The investment cost is associated to the *PowerToGas* unit, whose size is the maximum size of the two conversion units.

$$\sum_{j' \in TECH\ OF\ EUT(eut)} f_{min,\%}(j) \sum_{t \in T} \mathbf{F}_t(j', t) t_{op}(t) \leq \sum_{t \in T} \mathbf{F}_t(j, t) t_{op}(t) \leq \sum_{j' \in TECH\ OF\ EUT(eut)} f_{max,\%}(j) \sum_{t \in T} \mathbf{F}_t(j', t) t_{op}(t) \quad \forall eut \in EUT, \forall j \in TECH\ OF\ EUT(eut) \quad (1.22)$$

$$\mathbf{F}_t(j, t) \sum_{t \in T} t_{op}(t) \geq \sum_{t \in T} \mathbf{F}_t(j, t) t_{op}(t) \quad \forall j \in TECH\ OF\ EUC(MobPass) \cup TECH\ OF\ EUC(MobFreight), \forall t \in T \quad (1.23)$$

$$\mathbf{F}(StoHydro) \leq f_{max}(StoHydro) \frac{\mathbf{F}(NewHydroDam) - f_{min}(NewHydroDam)}{f_{max}(NewHydroDam) - f_{min}(NewHydroDam)} \quad (1.24)$$

$$\mathbf{Sto}_{in}(StoHydro, Elec, t) \leq \mathbf{F}_t(HydroDam, t) + \mathbf{F}_t(NewHydroDam, t) \quad \forall t \in T \quad (1.25)$$

$$\mathbf{F}(DHN) \geq \sum_{j \in TECH\ OF\ EUT(HeatLowTDHN)} \mathbf{F}(j) \quad (1.26)$$

$$\sum_{j \in TECH\ OF\ EUT(HeatLowTDHN)} \mathbf{F}(j) \geq \%_{Peak_{DHN}} \max_{t \in T} \{ \mathbf{EndUses}(HeatLowTDHN, t) \} \quad (1.27)$$

$$\mathbf{F}(Grid) \geq \frac{9400}{c_{inv}(Grid)} \frac{\mathbf{F}(Wind) + \mathbf{F}(PV)}{f_{max}(Wind) + f_{max}(PV)} \quad (1.28)$$

$$\mathbf{F}(PowerToGas) = \max \{ \mathbf{F}(PowerToGas); \mathbf{F}(GasToPower) \} \quad (1.29)$$

1.2.2 Model validation

As discussed in the Introduction, long-term energy models are inherently nonvalidatable. For example, they differ from the model of a physical system, for which inputs can be controlled and outputs can be measured to validate and improve the model structure. Such validation is not possible when dealing with a large-scale energy system model, especially when considering future projections. However, in the availability of past and current data about the studied energy system, it is possible to verify the degree of accuracy of the model in representing the past or present state of the system.

Thus, the model is validated on the Swiss energy system in the year 2011. The choice of the reference year is motivated by the good availability of detailed data, collected during previous work. The Sankey diagram in Figure 1.7 illustrates the energy flows in the country in 2011 [77, 78, 79, 80, 81, 82]. In that year, fossil fuels accounted for 54.2% of the country's primary energy consumption, supplying most of the heating and mobility demand; renewables had a 15.4% share, divided among hydroelectricity (10.8%), wood (3.2%), and other renewables (1.5%) [77]. The production of heat is dominated by fuel combustion in boilers and direct electric heating, while heat pumps (HPs) and CHP plants have a lower share, the latter mostly associated to the incineration of municipal solid waste (MSW). Low temperature heat demand is mostly decentralized, with a 6.4% share of district heating, and public mobility has a 20% penetration in the total passenger mobility demand.

The validation is performed as follows. Given as inputs:

- the EUD values estimated based on the FEC data;
- the relative annual production shares of the different technologies for each type of EUD;
- the share of public mobility ($\%_{\text{Public}}$), of train in freight ($\%_{\text{Rail}}$) and of centralized heat production ($\%_{\text{Dhh}}$);
- the fuel efficiency of mobility technologies

for the year 2011, the outputs of the MILP model are compared to the actual values reported for that year (as in Figure 1.7). The difference is assessed based on the following four indicators:

- primary energy consumption, global and per type of fuel;
- global GHG emissions;
- share of production per type of technology (boilers, HPs, CHP plants);
- installed size and number of installed technologies (HPs, CHP plants).

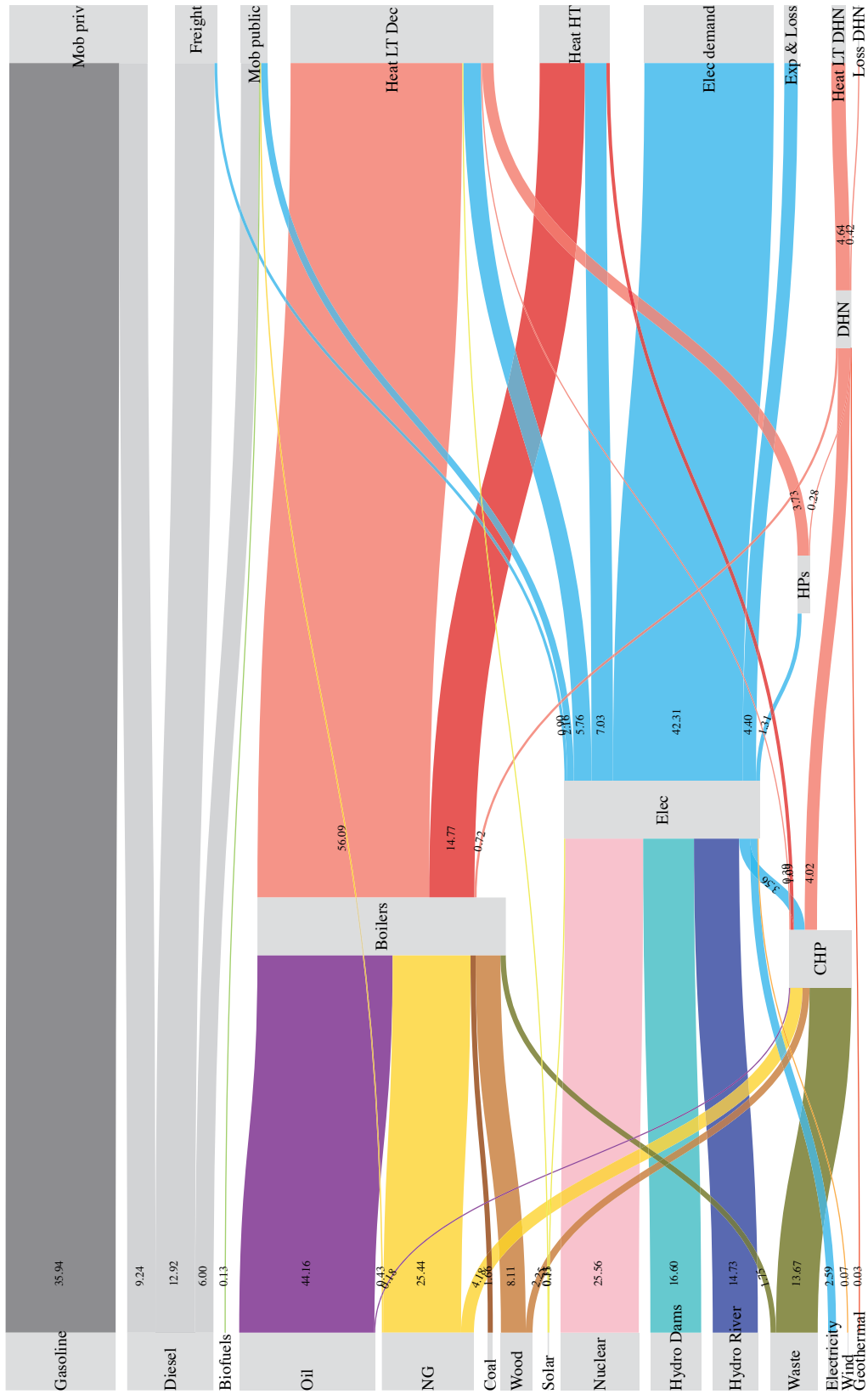


Figure 1.7 – Energy flows in Switzerland in the year 2011 [77, 78, 79, 80, 81, 82]. All values are in TWh. The methodology used to treat the data is documented in Appendix A.7.

1.2. Case study: the Swiss energy system in 2035

Table 1.4 – Model validation: MILP model output vs. actual 2011 values for the Swiss energy system. Values for the Swiss energy system in 2011 are taken from [77, 78, 79, 80, 81, 82] unless otherwise indicated. More details are provided in Appendix A.7.

		Actual 2011	MILP	Δ	Units	
Primary Energy Consumption	Gasoline	35.94	37.36	1.42	TWh	
	Diesel	28.16	26.16	-2.00	TWh	
	NG	30.05	28.40	-1.65	TWh	
	Elec. imports	2.59	2.76	0.17	TWh	
	Coal	1.66	1.43	-0.23	TWh	
	Solar	0.46	0.48	0.02	TWh	
	Geothermal	0.03	0.02	-0.01	TWh	
	Waste	15.41	10.65	-4.76	TWh	
	Oil	44.34	46.20	1.86	TWh	
	Wood	10.36	9.32	-1.04	TWh	
	Total	169.0	162.8	-6.21	TWh	
Technologies Output	Boilers	71.59	72.53	0.94	TWh	
	CHP	9.06	8.58	-0.48	TWh	
	HPs	4.02	4.23	0.21	TWh	
GHG emissions (fuels)		47.51 ^a	46.92	-0.59	MtCO ₂ -eq.	
Installed Technologies	HPs	Installed units	191.8	160.6	-31.2	kUnits
		Total	2.87	1.66	-1.21	GW _{th}
	CHP^b	Installed units	41	51	10	Units
		Total	0.96	1.02	0.06	GW _{th}

^a Total GHG emissions following the Kyoto protocol [83], removing the direct non-energy related emissions from industrial processes.

^b Large CHP installation (> 1 MW). 2011 Data for HPs and CHP in [77]

The results are reported in Table 1.4. In terms of energy consumption, the MILP offers a good approximation of the actual 2011 values. The lower values of estimated primary energy consumption are due to the fact that for electricity, heat and CHP technologies, the conversion efficiencies used for the year 2035 are also used for the validation. This difference is mostly relevant in the case of waste. Other differences are due to the fact that the MILP does not account for some minor contributions, e.g. the use of nuclear waste heat for district heating (DH) or the amount of heat classified as “other renewables” in the Swiss reports.

The total GHG emissions from fuel combustion in 2011 were 50 MtCO₂-eq., which includes 2.49 MtCO₂-eq. due to direct non-energy related emissions from industrial processes [83]. This number is accurately estimated by the model.

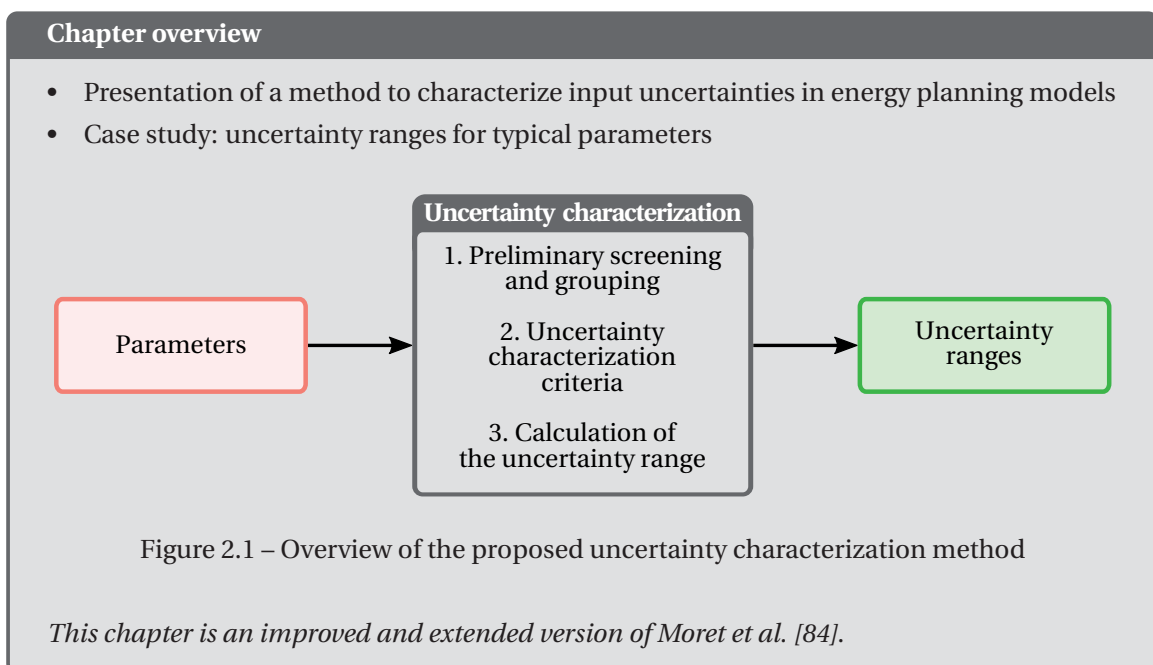
The proposed MILP formulation aims at offering a representation of the energy balance of the country. This means that, especially with a monthly resolution as in the case study, it does not aim at obtaining an accurate estimate of the installed capacity of the different technologies. However,

Chapter 1. Modeling for uncertainty

the validation results show that the model is able to capture the order of magnitude of the number installed units and total capacity of the technologies, especially in the case of large CHP plants.

Overall, the MILP formulation offers an accurate picture of a national energy system for the goal of strategic decision-making support. In fact, at the time of writing, collecting and harmonizing the needed data to close the monthly - or, even, annual - energy balance of an urban or national energy system is still a surprisingly challenging and time-consuming effort. If, on the one hand, there is a good availability of detailed data for the electricity sector, the modeling process is far more difficult for heating and mobility end-uses. This suggests that the adopted monthly resolution can be a reasonable trade-off between time and accuracy, compatible with the level of detail of available data.

2 Uncertainty characterization



In any study involving uncertainty, from sensitivity analysis to optimization, the uncertainty of input parameters needs to be quantified. In this thesis, the quantitative definition of input uncertainties is defined as *uncertainty characterization*.

In the literature, various approaches are adopted for this purpose. Tock and Maréchal [49] use normal, uniform and beta distributions to specify the uncertainty of economic parameters in two strategic design problems. Lower and upper bounds are taken from institutional reports and the distribution parameters are selected in such a way that these bounds are part of the resulting distributions. Dubuis [48] proposes a methodology for energy system design under uncertainty based on PDFs, which are assumed to be known. While being based on statistical theory, the author notes that

data are often unavailable to define the distribution parameters. Siddiqui and Marnay [27] argue that PDFs assumed in stochastic models seldom have a solid empirical basis.

Pye et al. [47], highlighting the lack of data for defining future uncertainties in the UK energy transition pathways, propose the use of triangular distributions to represent uncertainty between upper and lower bounds estimated from the literature. They consider investments costs, build rates, resource availability and prices as uncertain parameters. Kim et al. [50] account for technology uncertainty in the assessment of biomass-to-fuel strategies by assigning technologies different levels of cost uncertainty (low: 10%, medium: 30%, high: 50%) based on their maturity and complexity. This results in a range for the total cost of the evaluated alternatives. A similar approach is adopted by Sin et al. [51] for waste water treatment applications. Expert knowledge is used to assign upper and lower bounds to all the model parameters and uniform distributions are assumed. Lythcke-Jørgensen et al. [85] integrate uncertainty in the design of flexible multi-generation systems. They assume $\pm 25\%$ variations and uniform distributions for investment and operating cost parameters. Majewski et al. [86] use historical data to define ranges of uncertainty for energy prices and demand; the ranges are used for the design of a decentralized energy supply system using robust optimization. Lauinger et al. [87] consider weather data and energy demand uncertainty for the stochastic optimization of a residential energy system, assuming that the uncertainty of other parameters (cost and efficiencies) can be mitigated through careful supplier examination. Carpaneto et al. [52] discuss uncertainty characterization in depth in the context of a cogeneration planning problem. Some parameters (investment costs, efficiencies) are assumed as not uncertain, while uncertainties are classified into *large-scale* and *small-scale*. Parameters with small-scale uncertainties, such as electricity prices and energy loads, are assumed to be known at hourly resolution. Small-scale uncertainties lie in the simplifications introduced by grouping hourly data into representative aggregated time periods. To characterize them, multivariate normal distributions are used. On the other hand, large-scale uncertainties, such as energy price evolution, are characterized through a set of plausible scenarios defined by the decision-maker (DM).

In most of the reviewed literature, uncertainty characterization is not the main focus; instead, it is often marginally addressed as an input to other analyses. Also, in most cases it is only applied to a subset of arbitrarily selected parameters, and full documentation of the used data sources is seldom provided. Furthermore, various authors highlight the difficulty in finding the appropriate quantity and quality of data needed to define PDFs for the uncertain parameters, and propose simplified approaches.

Contributions

Thus, a novel application-driven uncertainty characterization method for strategic energy planning problems is presented. This type of problems is typically characterized by a large number of input parameters along with scarce availability of data to characterize their uncertainty. The method is

based on the application of a set of criteria to define ranges of variation for the uncertain parameters. The use of ranges instead of PDFs is motivated by the lack of data highlighted in the literature. Also, ranges are a necessary and sufficient input for applications such as robust optimization, as discussed in Chapter 4.

To obtain a proof of concept, the method is applied to the parameters of the MILP Swiss energy system case study introduced in Chapter 1. Uncertainty is characterized for the different types of parameters in the model. As these parameters are typically found in energy planning problems, the data sources used for the definition of the ranges are reported in Appendix B to allow reproducibility and use in similar applications. By using relative ranges, it is shown how the method can be systematically applied to models featuring a large number of input parameters. This avoids the need of an *a priori* arbitrary exclusion of some parameters from the analysis.

2.1 Uncertainty characterization method

Figure 2.2 illustrates the proposed uncertainty characterization method. After a preliminary screening and grouping of the model parameters, five criteria are applied to each uncertain parameter. Each criterion corresponds to a different method for investigating the uncertainty of a parameter. For a given parameter, more than one criterion can apply. If a given criterion applies, the corresponding information is collected for the calculation of the uncertainty range. After this, the range is calculated taking into account both the nature of the uncertainty (epistemic or aleatory) and how uncertainty develops over the planning time horizon. First, the terminology is defined and a conceptual distinction is made between the types of uncertainties in the context of strategic energy planning. Following this, the different steps of the methodology are detailed.

Definitions and terminology

The focus of this work is on the uncertainty of the parameters (θ). Each parameter has a *nominal* value (R_0), corresponding to its most likely realization. A *range* of variation is defined by assigning a lower (R_{min}) and an upper (R_{max}) bound to the parameter. The total range R is the difference between the upper and the lower bound ($R = R_{max} - R_{min}$). In order to compare ranges of variation among different parameters, upper and lower bounds can be expressed as percentages relative to the nominal value, as in Eq. 2.1.

$$R_{\%,min} = \frac{R_{min} - R_0}{R_0}, \quad R_{\%,max} = \frac{R_{max} - R_0}{R_0}, \quad R_{\%} = |R_{\%,max} - R_{\%,min}|, \quad R_0 \neq 0 \quad (2.1)$$

In which R_{min} and R_{max} are the lower and upper bound in absolute values, respectively. $R_{\%,min}$ and $R_{\%,max}$ are the lower and upper bound in relative values, respectively. $R_{\%}$ is the *relative range*, i.e.

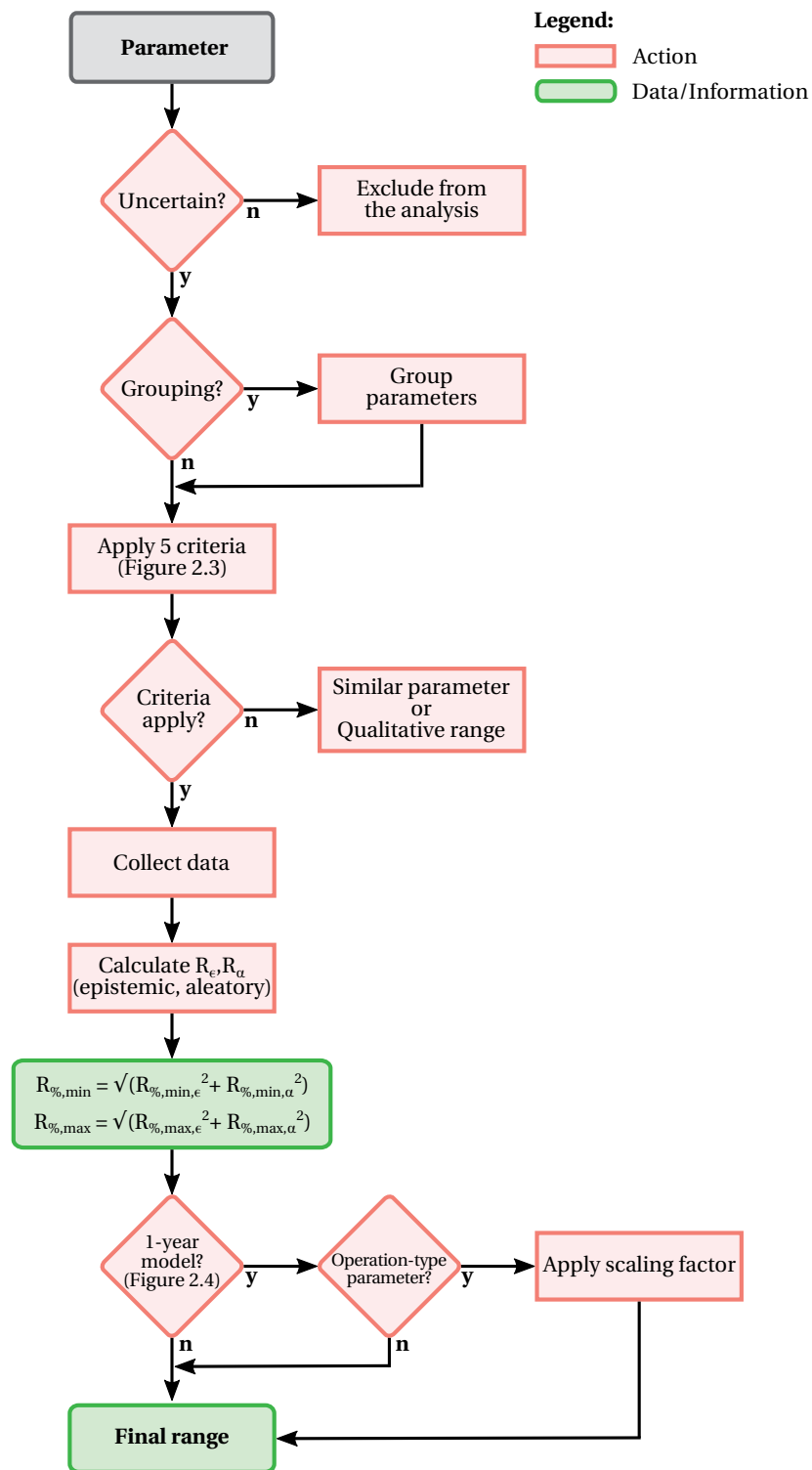


Figure 2.2 – Uncertainty characterization method flowchart.

the total range relative to the nominal value.

Types of uncertainty

In the literature, various classifications of uncertainty have been proposed, without a common agreement [32]. Adopting the terminology by Walker et al. [88], uncertainty can be classified according to its *location* (i.e. where the uncertainty manifests itself within the model complex) and its *nature*. In terms of location, Morgan et al. [89] distinguish between “uncertainty about the value of empirical quantities” (*parameter uncertainty*) and “uncertainty about model functional form” (*model structure uncertainty*) in the context of climate modeling. A model is a simplified representation of reality. Long-term energy planning models are inherently nonvalidatable. This implies that model uncertainty, i.e. how well a model represents reality, cannot be assessed; thus, the focus is only on parameter uncertainty.

In terms of nature, parameter uncertainty is further divided into *epistemic* and *aleatory*: uncertainties are characterized as epistemic if the modeler sees a possibility to reduce them by gathering more data or by increasing the level of detail; uncertainties are categorized as aleatory if the modeler does not foresee the possibility of reducing them. Der Kiureghian and Ditlevsen [90] discuss this dichotomy in detail concluding that, although relevant, it can become philosophical if treated in general terms. They recommend to pragmatically adapt this classification to the type of model under analysis. In the context of strategic energy planning, it is relevant to distinguish between *present* and *future* uncertainties. Present uncertainties can be reduced by increasing the model detail, further data collection or additional measurements (e.g. the cost of purchasing a car today). On the other hand, future uncertainties are irreducible as they are inherent to the phenomenon (e.g. the future price of oil). To be consistent with the literature, in this thesis the term *epistemic* indicates present, reducible uncertainties, and the term *aleatory* indicates future, irreducible uncertainties.

2.1.1 Preliminary screening and grouping

In this first phase, *all* model parameters are listed. This avoids an *a priori* arbitrary exclusion from the analysis. The preliminary screening consists of eliminating the parameters which are certain. These include parameters which do not present any uncertainty (e.g. the duration of a time period), which are not related to the output of interest (e.g. emission coefficients in a cost optimization problem), or parameters whose definition is only needed for the model structure (e.g. a binary parameter defining allowed exchanges between producers and consumers). A parameter can be deemed certain enough for the level of detail of the model (e.g. the chemical properties of a fuel in a strategic planning problem). Some parameters are simply assumed based on expert judgment such as the upper and lower bounds for a decision variable. In general, these latter parameters should not be excluded from the analysis, as the GSA can highlight and rank influential assumptions. This

offers the modeler a priority list for further investigating some of the initial assumptions.

The remaining parameters can be grouped to reduce their number. In the GSA, grouped parameters vary following the same pattern. As an example, hourly values of solar radiation can be grouped by defining a yearly multiplication factor. The yearly multiplication factor becomes the uncertain parameter. When this multiplication factor is varied, all associated hourly parameters change accordingly. This way of grouping parameters cancels out the effects associated to the interaction among parameters included in the same group.

2.1.2 Uncertainty characterization criteria

The five criteria (C) shown in Figure 2.3 are applied in parallel to each uncertain parameter:

- C1 *a) Can the uncertain parameter be modeled? If yes, b) is the developed model included in the main model?* A model of the uncertain parameter can be available or be developed. Modeling a parameter means defining a mathematical relation h' such that $\theta = h'(\theta'_1, \dots, \theta'_k)$, where θ is the investigated uncertain parameter and $\theta'_1, \dots, \theta'_k$ are the k parameters of h' . As a consequence, $\theta'_1, \dots, \theta'_k$ replace θ as investigated uncertain parameters. h' can be *external* or *internal*. An external parameter model is not integrated in the main model. As an example, h' can be a complex thermodynamic model, which is externally simulated to obtain an efficiency range for a technology. An internal parameter model is integrated in the main model. This means that h' becomes part of the main model. The choice whether or not to integrate h' in the main model is ultimately made by the modeler and it usually depends on the complexity of h' .
- C2 *Is a range already proposed in the literature?* Studies in the literature can have already assessed the uncertainty of the parameter, and consequently proposed a range or a PDF for it.
- C3 *a) Can a range be obtained from existing forecasts? b) Can information be gathered about past forecast accuracy?* Forecasts can be available for the future values of parameters. Some forecasts already offer an uncertainty range around the proposed nominal values. Alternatively, a range can be defined by comparing multiple forecasts. In addition, data can be found about errors in past forecasts. This information can be obtained from retrospective studies in the literature or from data analysis (as in Figure 2). Information about errors in past forecasts can help assessing the reliability of the current ones. This principle is already adopted by some forecasters [21].
- C4 *Can (historical) data be used?* Current or historical data can be used to define the uncertainty range. In a strategic energy planning context, the application of this criterion to characterize the future uncertainty of a parameter value implies that historical or current variations are representative for the future. As an example, the uncertainty of the average solar radiation in a future year can be estimated by analyzing variations from historical radiation data.

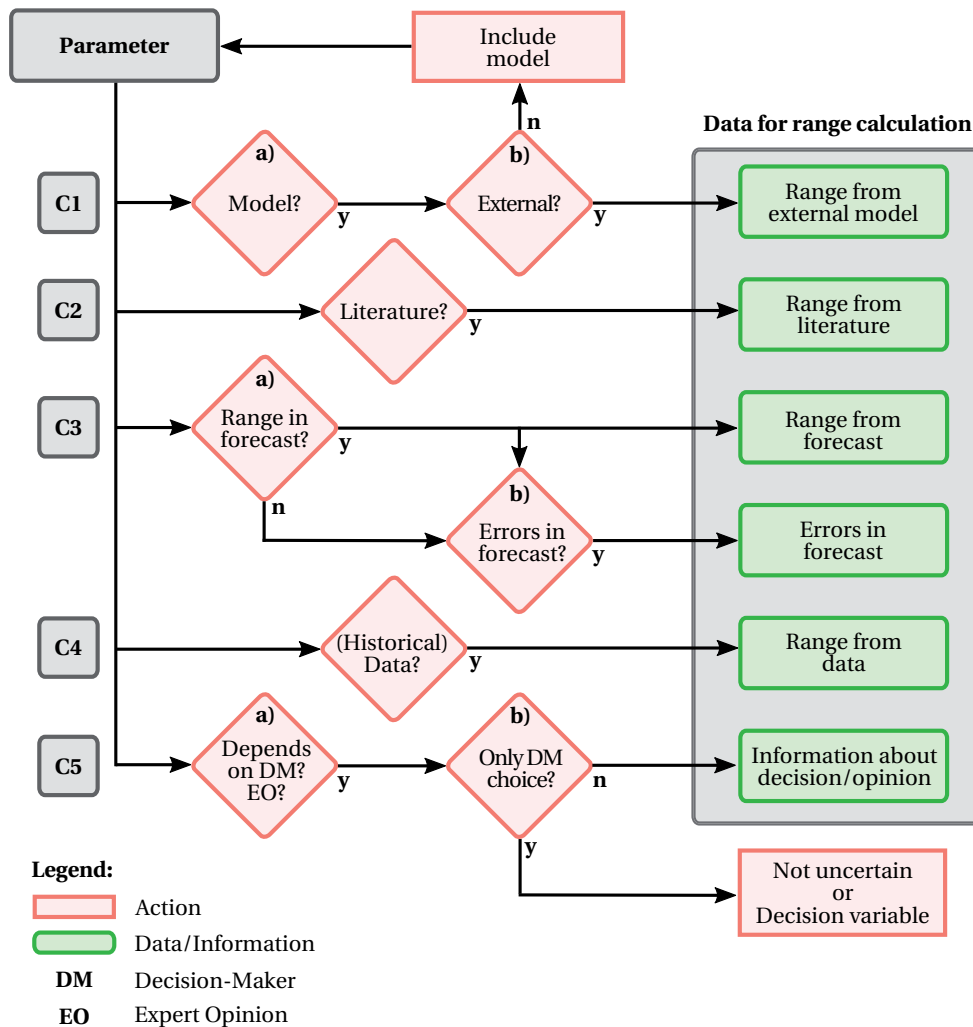


Figure 2.3 – Uncertainty characterization: application in parallel of the five criteria to each uncertain parameter in a model. Each criterion corresponds to a different method for investigating the uncertainty of a parameter.

C5 a) Does the parameter depend on the DM? Are expert opinions (EOs) available? If it depends on the DM, b) is it only a DM's choice? The DM might have an influence on the uncertainty of some parameters. As an example, if the DM is the government, a policy might be enforced. Information about the policy should be accounted for in the range definition. The same applies to expert opinions, offering informed advice about the future. In the case in which the parameter depends only on the DM and it can be known, then the parameter can be removed from the list of uncertainties or it could be modeled instead as a decision variable.

Chapter 2. Uncertainty characterization

If none of the five criteria applies, then for an initial GSA the parameter can be assigned the same relative range of a similar parameter or a qualitative range. If one or more criteria apply, the range is calculated based on the collected data.

2.1.3 Calculation of the uncertainty range

The range is calculated in a conservative way to avoid the risk of underestimating the impact. This means setting R_{max} (R_{min}) equal to the highest (lowest) value found in the different sources.

A range is defined symmetrical with reference to the nominal value if $R_{max} - R_0 = R_0 - R_{min} = R/2$. Symmetrical ranges are not always appropriate descriptions of uncertainty. As an example, there might be strong evidence that forecasts tend to overestimate or underestimate a given parameter, or that the construction costs of power plants constantly exceed expected budgets. This information can be described by asymmetrical ranges around the nominal value. In this work, a symmetrical range is used when the data sources used to define the nominal value of a parameter are not the same as the sources used to calculate its uncertainty range, or if there is no strong evidence suggesting the need of adopting an asymmetrical one.

Epistemic and aleatory uncertainty

A distinction has been previously introduced between present and future uncertainties. However, in strategic energy planning it is common practice to assume that present data can - partially or entirely - be used to define the future values of some parameters. If a given parameter is assumed not to change in the future, its uncertainty is purely epistemic. If it is assumed that present data can only be partially used for the future, then the parameter presents both epistemic and aleatory uncertainty. An example is the efficiency of future solar panels. On the one hand, solar panels available today in the market have different efficiencies, resulting in an observable distribution. Under the assumption that the shape of this distribution remains the same in the future, it can be treated as epistemic uncertainty, as data can be collected and uncertainty can be reduced by adding more types of solar panels in the model. On the other hand, the aleatory uncertainty lies in the future evolution of the technology, i.e. by how much the efficiency of these panels will increase. In the uncertainty characterization phase, information about epistemic and aleatory uncertainty is collected separately. This leads to the definition of two different ranges for the same parameter (R_ϵ and R_α). The final bounds are defined as in Eq. 2.2.

$$R_{\%,min} = \sqrt{R_{\%,min,\epsilon}^2 + R_{\%,min,\alpha}^2}, \quad R_{\%,max} = \sqrt{R_{\%,max,\epsilon}^2 + R_{\%,max,\alpha}^2} \quad (2.2)$$

In which ϵ indicates epistemic uncertainty, α indicates aleatory uncertainty. The equation is inspired by the sum of independent random variables, whose variance is the sum of the variances of the

summed variables.

Investment-type and operation-type uncertainty

Strategic energy plans define investment choices for energy technologies. Once a technology is installed, it can be operated until its end-of-life (usually 20-50 years). Strategic energy planning models, such as the MILP framework presented in Chapter 1, often analyze the energy system over one year of operation. This year represents all the years in which the system is operated. As an example, in an optimization problem having the minimum total annual cost as the objective, the total annual cost is the sum of the total annualized investment cost and the operating cost of the system over one year. In this case, a distinction is made between parameters with uncertainty realized at a specific point in time (*investment-type* uncertainty) and parameters with uncertainty spread over the whole planning horizon (*operation-type* uncertainty). The following categories are defined:

- *Type I - Investment-type uncertainty*: it characterizes parameters whose uncertainty realizes at a specific point in the considered time horizon. As an example, the investment cost uncertainty is related to the time in which technologies are purchased.
- *Type II - Operation-type uncertainty (constant uncertainty over time)*: it characterizes parameters with uncertainty spread over the operational lifetime of the system. Uncertainty is the same over time, i.e. these parameters are as uncertain in the near future as they are in the long-term. As an example, the uncertainty on fuel prices belongs in this category, as discussed in the next sections.
- *Type III - Operation-type uncertainty (uncertainty increasing over time)*: it also characterizes parameters whose uncertainty is spread over the years of operation of the system. Uncertainty increases over time, i.e. these parameters are less uncertain in the near future than in the long-term. As an example, the uncertainty on energy demand belongs in this category.

Each parameter is assigned to one of these categories. If the ranges are defined for a specific point in time (usually the last year of the planning horizon), they need to be scaled accordingly when used in the optimization model. This is shown in Figure 2.4. The ranges for the operation-type parameters are defined for the last year of the planning horizon (N). If the N -year planning horizon is represented by one year in the optimization model, these ranges cannot be directly used, as they would overestimate the uncertainty. As an example, the range R for the energy demand expresses the uncertainty of energy demand in N years. Using R as the range for the energy demand parameter in the one-year optimization model would mean assuming that the uncertainty for year N is representative for all years in the planning horizon. Thus, a scaling is proposed to avoid overestimating operation-type uncertainties. As an example, scaling factors are here analytically derived assuming uniform distributions for the parameters. If uniform distributions cannot be

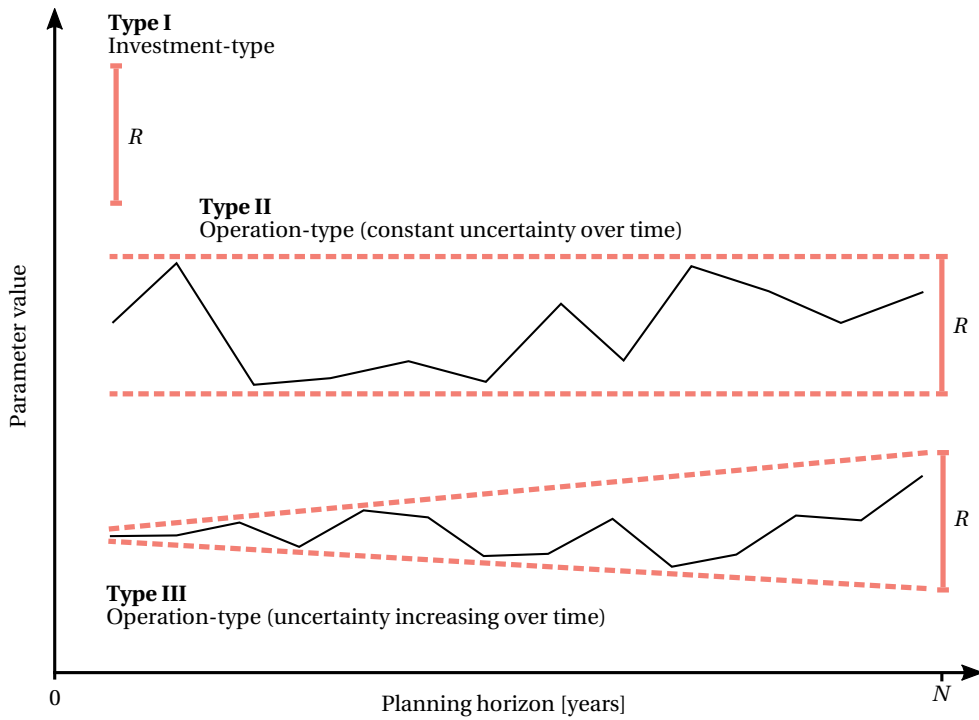


Figure 2.4 – Different types of uncertainty over the planning horizon. *Investment-type* uncertainty characterizes parameters with uncertainty defined at a given point in time. *Operation-type* uncertainty characterizes parameters with uncertainty spread over the operational lifetime of the system.

assumed, the scaling factor can be calculated via simulation.

For *Type I* uncertainties ranges do not need to be scaled, as they are calculated for the appropriate point in time. For *Type II* uncertainties, a scaling of the range is performed. Uncertainty is constant over the N -year time horizon. This means that there are N instances of the uncertainty of the parameter (each of them with range $[0, R]$ and weight $\frac{1}{N}$). The value of the parameter in the optimization model corresponds to the sum of these N instances. This is equivalent to considering that, assuming a uniform distribution, each of the N instances of the parameter can assume any value in $U[0, \frac{R}{N}]$ (the lower bound is shifted to 0 simplify the calculations). The range is scaled as 6 standard deviations (σ) of the Irwin-Hall distribution, obtained from the sum of the N uniform distributions. Eq. 2.3 shows the calculation of the variance of the sum of N independent random variables x_t uniformly distributed in $[0, \frac{R}{N}]$.

2.1. Uncertainty characterization method

$$\sigma^2\left(\sum_{t=1}^N x_t\right) = N\sigma^2\left(U\left[0, \frac{R}{N}\right]\right) = N\frac{R^2}{12N^2} = \frac{R^2}{12N} \quad (2.3)$$

Thus, the range is scaled as $6\sigma = 6\sqrt{\frac{R^2}{12N}} = R\sqrt{\frac{3}{N}}$. If $N = 20$ years, then the range of variation for this class of parameters is multiplied by a factor of approximately 0.3873. A similar procedure is applied to *Type III* parameters (e.g. energy demand). Uncertainty increases over the N -year time horizon. Assuming a linear increase, this corresponds to the sum of N independent random variables x_t uniformly distributed in $[0, t\frac{R}{N^2}]$. This is shown in Eq. 2.4.

$$\sigma^2\left(\sum_{t=1}^N x_t\right) = \sum_{t=1}^N \frac{t^2 R^2}{12N^4} = \frac{R^2}{12N^4} \sum_{t=1}^N t^2 = \frac{R^2}{12N^4} \frac{N(N+1)(2N+1)}{6} = R^2 \frac{(N+1)(2N+1)}{72N^3} \quad (2.4)$$

In this case, the range is scaled as $6\sigma = R\sqrt{\frac{(N+1)(2N+1)}{2N^3}}$. If $N = 20$ years, then the range of variation for this class of parameters is multiplied by a factor of approximately 0.2320.

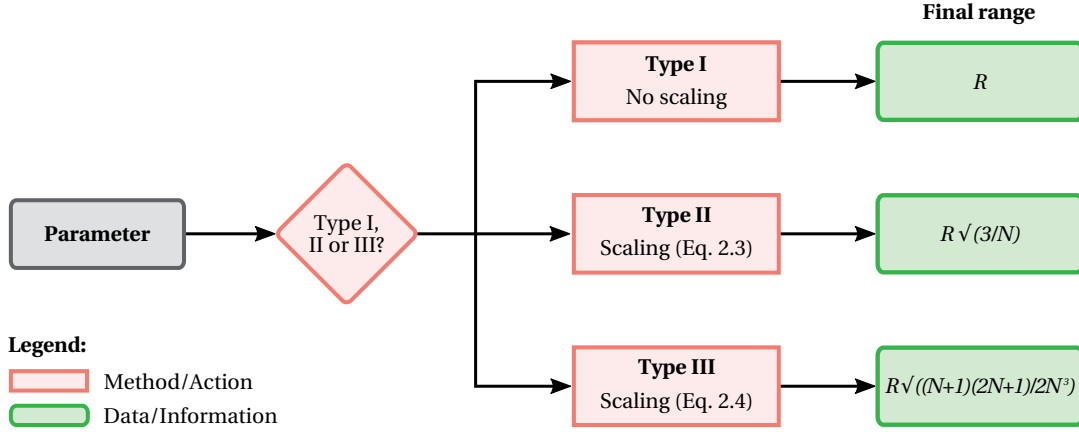


Figure 2.5 – Application of the scaling procedure for *Type I*, *Type II* and *Type III* parameters, in the case of a one-year model, and assuming uniform distributions for the uncertain parameters.

Figure 2.5 illustrates the scaling procedure in the case of a one-year model, and assuming uniform distributions for the uncertain parameters. First, each parameter is classified as *Type I*, *Type II* or *Type III*. Then, for investment-type (*Type I*) parameters, the range R is not scaled; for operation-type (*Type II* and *Type III*) parameters, the scaling factors in Eq. 2.3 and Eq. 2.4 are applied, respectively, to calculate the final range.

Scaling uncertainties by the obtained factors allows a fair comparison of investment- and operation-type uncertainties over the considered one-year time horizon in the optimization model.

2.2 Application to the case study

As an example application, the proposed uncertainty characterization method is applied to the MILP national energy planning model presented in Chapter 1.

2.2.1 Preliminary screening and grouping

Table 1.1 lists the model parameters. In total, the model has 3638 parameters. 3078 parameters are eliminated in the pre-screening phase as non-uncertain. Most of these excluded parameters are only needed for the model structure, i.e. they are assigned a default value. The following indexed parameters are entirely excluded from the analysis at this stage: the duration of the different months (t_{op}), the lower bound of the installed size of the technologies (f_{min}), the input/output efficiencies of the storage technologies ($\eta_{sto,in}$, $\eta_{sto,out}$) and the GHG emission coefficients (gwp_{constr} and gwp_{op}). The latter are excluded as there is no link between the emissions and the objective function (total cost). Parameters whose value is assumed by the modeler are excluded from the analysis only if the modeler does not envision the possibility of changing the assumed value. In the current example, a conservative approach is chosen: when in doubt, parameters are considered as uncertain and thus kept in the analysis.

Grouping is performed on the remaining 560 parameters to further reduce their number. The monthly operating cost of resources (c_{op}) and the monthly capacity factor of technologies ($c_{p,t}$) are grouped by defining a yearly multiplication factor. This means that their monthly distribution is assumed to be certain, and uncertainty is assessed for the average yearly values of these two parameters.

2.2.2 Uncertainty characterization results

The remaining 417 parameters are individually considered in the GSA; thus, their uncertainty needs to be quantified. Although possible, in practical applications it is often unaffordable to characterize the uncertainty of such a large number of inputs. To address the trade-off between time and accuracy, parameters are organized into different categories based on their similarity. Uncertainty is characterized for one representative parameter per category, and parameters belonging to the same category are assigned the same relative range. The results of the uncertainty characterization for the 21 categories of parameters are reported in Table 2.1. First, the five uncertainty characterization criteria (Section 2.1.2) are applied to each representative parameter. The relative range is then calculated, accounting for the types of uncertainties and scaling factors defined in Section 2.1.3. The application of the method is discussed, and detailed source data for each parameter are reported in Appendix B.

2.2. Application to the case study

Table 2.1 – Application of the uncertainty characterization method to the example MILP model. The 417 uncertain parameters are divided into 21 categories. Uncertainty is characterized for one representative parameter per category. The data used for the uncertainty characterization are reported in Appendix B. Abbreviations: photovoltaic (PV), fuel cell (FC), district heating network (DHN), decentralized (DEC), natural gas (NG).

Category	Representative Parameter	Criteria (section 2.1.2)					ε/α^a	Type ^b	R%	
		C1	C2	C3	C4	C5			min	max
i_{rate}	i_{rate}			✓ _a	✓	✓ _a	α	I	-46.2%	46.2%
$endUses_{year}(HH)$	$endUses_{year}(HH)^c$			✓ _{ab}			α	III	-6.9%	4.3%
$endUses_{year}(S)$	$endUses_{year}(S)^c$			✓ _{ab}			α	III	-7.4%	4.1%
$endUses_{year}(I)$	$endUses_{year}(I)^c$			✓ _{ab}			α	III	-10.5%	5.9%
$endUses_{year}(TR)$	$endUses_{year}(TR)^c$	✓ _{ab}		✓ _{ab}			α	III	-3.4%	3.4%
$\eta_{mature,standard}$	$\eta(Boilers)$				✓		ε	I	-5.7%	5.7%
$\eta_{mature,customized}$	$\eta(GASOLINE\ CAR)$				✓		ε	I	-20.6%	20.6%
$\eta_{new,standard}$	$\eta(PV)$			✓ _a	✓		$\varepsilon+\alpha$	I	-20.8%	20.8%
$\eta_{new,customized}$	$\eta(FC\ CAR)$			✓ _a	✓		$\varepsilon+\alpha$	I	-28.7%	28.7%
$avail$	$avail(WOOD)$				✓		ε	I	-32.1%	32.1%
c_p	$c_p(NUCLEAR)$				✓		α	II	-2.4%	2.4%
f_{max}	$f_{max}(PV)$				✓		ε	I	-24.1%	24.1%
$c_{inv,mature}$	$c_{inv}(DEC\ NG\ BOILER)$				✓		ε	I	-21.6%	21.6%
$c_{inv,new}$	$c_{inv}(PV)$			✓ _a	✓		$\varepsilon+\alpha$	I	-39.6%	39.6%
	$c_{inv}(NUCLEAR)$				✓		$\varepsilon+\alpha$	I	-21.6%	119.3%
	$c_{inv}(HYDRO\ DAM)$				✓		$\varepsilon+\alpha$	I	-21.6%	73.8%
	$c_{inv}(Thermal\ plants)$				✓		$\varepsilon+\alpha$	I	-21.6%	25.0%
$c_{inv,other}$	$c_{inv}(WIND)$				✓		$\varepsilon+\alpha$	I	-21.6%	22.9%
	$c_{inv}(DHN)$				✓		α	I	-39.3%	39.3%
	$c_{inv}(Geothermal)$		✓		✓		$\varepsilon+\alpha$	I	-39.7%	62.1%
c_{maint}	$c_{maint,\%}$	✓ _a		✓ _a			α	I	-48.2%	35.7%
n	$n(Boilers)$				✓		α	I	-26.5%	26.5%
$c_{op,local}$	$c_{op}(WOOD)$			✓ _a			α	III	-2.9%	2.9%
$c_{op,import}$	$c_{op}(NG)$		✓	✓ _{ab}			α	II	-47.3%	89.9%
$c_{p,t}$	$c_{p,t}(PV)$	✓ _{ab}			✓		α	II	-11.1%	11.1%
$\%_{loss}$	$\%_{loss}(Elec)$				✓		α	III	-2.0%	2.0%

^a Epistemic (ε): present, reducible uncertainty. Aleatory (α): future, irreducible uncertainty (section 2.1.3)

^b I: investment-type, II: operation-type (constant uncertainty over time), III: operation-type (uncertainty increasing over time) (section 2.1.3)

^c $\sum_{eui \in EUI} endUses_{year}(eui, s)$. Aggregated end-uses demand (eui) in the different sectors s : households (HH), services (S), industry (I), transportation (TR).

Discount rate

For the discount rate (i_{rate}), the *real*¹ interest rate of the public investor - in this case the Swiss government - is considered. Interest rate forecasts are subject to relevant errors, even in the short-term. Goodhart and Lim [91] analyze errors in nominal interest rates forecasts by central banks with a two-year time horizon, finding errors as high as 31%. In the US, since 1996 long-range private sector forecasts have exhibited a standard deviation of 2.7 percentage points relative to the nominal Treasury rate realized 10 years later [92].

Due to a lack of specific data for errors in long-term real interest rates forecasts, comparison of available long-term forecasts (*C3a*) and of current market data (*C4*) is used to define the uncertainty of the parameter based on EO (*C5a*). In [92], a model is used to forecast the US real interest rate in 2025. Different estimates are obtained by running the model with input parameters taken from various sources, resulting in interest rates ranging from a minimum value of 1.5% to a maximum value of 3.5%. Based on expert opinion, current Swiss market data can also be used to define the uncertainty of future interest rates²: a low (1.73%) and a high value (4.7%) are proposed, where the higher value is based on the official discount rate for energy in Switzerland [93] and the lower value is the estimated discount rate for Swiss electricity producers. With a conservative approach, the latter values are taken as they are specific to Switzerland and they offer a wider range than the US forecasts.

End-use energy demand

The uncertainty of the annual end-use energy demand ($endUses_{year}$) is assessed on an aggregated level for each sector. This means that, within each sector (households, services, industry, transportation) the same relative range is applied to the different end-uses (*eui*). As an example, the electricity, SH and HW end-use demand in the residential sector are assigned the same level of uncertainty. For households, services and industry, data are taken from forecasts and errors in forecasts (*C3ab*), whereas for transportation an external model is made (*C1ab*).

For households, services and industry, ranges for end-uses in 2035 can be obtained from the scenarios available in a report commissioned by the Swiss confederation [81]. These ranges are compared to errors in energy demand forecasts assessed by different sources [94, 22, 21, 95, 19, 20]. The US EIA regularly publishes a retrospective review on its own energy demand forecasts [23]. As errors in past forecasts are wider than the range proposed in the Swiss forecasts, the error factors in [23] are used to define the uncertainty ranges. In [81], asymmetric ranges are proposed. The asymmetry is maintained in the final ranges as [81] is the same source used for the definition of the nominal values. This leads to the final ranges for 2035 end-use energy demand: [-26.8%, 21.8%] for households

¹ *Real* values are expressed at the net of inflation. They differ from *nominal* values, which are the actual prices in a given year, accounting for inflation.

² Approach recommended from personal communication with Philippe Thalmann (EPFL), July 1st, 2014.

energy demand, [-27.8%, 21.5%] for services, and [-39.9%, 31.2%] for industry.

For the transportation demand, a simple model is made by decomposing the yearly passenger mobility demand in 2035, expressed in pkm, as the product of the total population and the yearly pkm/capita. For both parameters, upper and lower bounds are obtained from forecasts. The range is calculated by multiplying these extreme values, thus obtaining a range of [-14.5%, 14.5%] for passenger mobility demand in 2035.

Data show that uncertainty of energy demand is increasing over time (see Figure 1). Thus, the scaling factor calculated in Eq. 2.4 is applied to the obtained ranges.

Technology efficiency

In the uncertainty characterization phase, technologies are assigned to different categories according to two criteria. First, technologies are classified as *mature* or *new* based on their stage of development. Second, they are classified as *standard* or *customized* based on the level of customization. As an example, boilers are considered mature and standard technologies, as their efficiency cannot be substantially increased, and they are not customized goods. On the other hand, a FC car is considered a new and customized technology, as cars are customized goods and FCs are still at an early stage of commercialization.

The conversion efficiency (η) of mature technologies is assumed to remain constant in the future; thus, its uncertainty is epistemic, as it could be reduced by adding more types in the model. Epistemic uncertainties are typically characterized by collection of current data (*C4*). For the efficiency of mature and standard technologies, ranges for boilers are taken from [96]. Gasoline cars are the representative technologies for mature and customized technologies, and their efficiency ranges are taken from [97].

Uncertainty of new technologies is characterized as the sum of an epistemic and an aleatory component, combined as in Eq. 2.2. On the one hand, it is assumed that the future efficiency distribution will have the same shape as the one observed in current market data. On the other hand, the future evolution of technologies is assessed based on forecasts (*C3a*). For new technologies, PV panels are taken as representative technologies.

Resources availability and maximum installed capacity of technologies

The availability (*avail*) of imported resources is considered unlimited in the model. Thus, the availability of local resources (wood and waste) are the uncertain parameters. The availability of wood is studied for the definition of the uncertainty range. Under the assumption that the maximum availability of wood today is representative for the future, data are collected from different sources (*C4*) estimating the current availability of wood in Switzerland (Table B.1). The minimum and the maximum values are used in the definition of the range.

The uncertainty on the maximum installed size of the technologies (f_{max}) is assessed in a similar

way. f_{max} is uncertain only for renewable resources. The maximum potential for solar PV is taken as the representative parameter for this category.

Capacity factor

In the MILP formulation, the “capacity factor” is conceptually divided into two components: a capacity factor for each period ($c_{p,t}$) depending on resource availability (e.g. seasonal renewables) and a yearly capacity factor (c_p) accounting for technology downtime and maintenance (Eqs. 1.8-1.9). For each technology only one capacity factor is used, the other being set to the default value of 1. c_p is used for technologies which are not constrained by seasonality. The unavailability of these technologies depends only on shutdowns or maintenance, which are normally planned in advance. c_p is considered uncertain for all technologies for which it is defined, with the exception of decentralized ones. Analysis of historical data is used to define the future uncertainty of this parameter (C4). In particular, data for nuclear power plants in Switzerland are taken as reference due to the availability of historical data.

On the other hand, $c_{p,t}$ is defined for technologies with seasonal variations (solar, wind and hydro). The capacity factor of solar is taken as the representative parameter for this category. Under the assumption that $c_{p,t}$ depends only on solar radiation (C1ab), historical solar radiation data [98] are used to define the uncertainty range.

The uncertainty of capacity factors is constant over time, thus the scaling factor in Eq. 2.3 is applied to obtain the final ranges.

Technologies investment cost

The investment cost (c_{inv}) of mature technologies is assumed to remain the same in the future (in real currency). Thus, present market data for a decentralized gas boiler, chosen as representative technology, are used to define their uncertainty (C4, epistemic uncertainty). For new technologies, the future investment cost of residential rooftop PV systems is the representative parameter. Forecasts are used to define the future evolution (C3a, aleatory uncertainty). The final range is then calculated as the sum of an epistemic and an aleatory component, following the same approach as for the efficiency η .

Based on evidence found in the literature, some technologies are considered as exceptions (category $c_{inv,other}$). In a pioneering study published in the late 1970s, Merrow et al. [99] found that capital costs for advanced technologies were regularly underestimated. Sovacool et al. [100] analyze cost overruns in the construction of electricity production plants. Their analysis covers a total of 401 projects, divided among hydro dams, nuclear and thermal plants, wind farms, solar facilities and electricity grid. For all types of plants, the average cost exceeded the budgeted amount, by an extent ranging from 1.3% for solar projects to 117.3% for nuclear plants. Thus, the average cost overrun for each type of plant is accounted for in the definition of the corresponding uncertainty ranges. Lukawski

et al. [101] characterized the uncertainty associated with the cost of drilling and completion of geothermal wells. Thus, the ranges obtained by the application of their probabilistic approach are used to define the uncertainty of geothermal power plants (C2). The resulting range is consistent with values for wells drilled in Switzerland [102]. Finally, the uncertainty of DHN projects is based on the range between favourable and unfavourable conditions calculated in [103] from analysis of past projects in Switzerland and Austria. The range for DHNs is applied to all the infrastructure costs in the model.

Resources cost

To characterize the uncertainty of their specific cost (c_{op}), resources are divided into *local* and *imported*. In both cases, forecasts are available (C3a). Wood price is taken as representative parameter for local resources. Swiss forecasts [81] indicate a range of $\pm 12.7\%$ for wood prices in 2035. This range is scaled by applying Eq. 2.4, as uncertainty for the cost of local resources is assumed to increase over time.

NG price is taken as representative parameter for imported resources. In this case, ranges proposed in long-term price forecasts are compared with ranges proposed in the literature (C2) and with errors in past forecasts (C3b). In the European Union (EU), NG prices are expected to increase in the next decades. The relative range in EU forecasts is $[-38.0\%, 30.5\%]$ for 2035 [104]. The EIA offers similar ranges for the US market in its latest forecasts ($[-37.0\%, 33.4\%]$ for 2035 in [105]). In both cases, the proposed uncertainty ranges increase over time. Based on their analysis of past EIA forecasts, Wisner and Bolinger [26] recommend the adoption of a minimum uncertainty range of $\pm 2 \text{ USD}_{2003} / 1000 \text{ ft}_{\text{NG}}^3$ ($\pm 0.085 \text{ USD}_{2013} / \text{m}_{\text{NG}}^3$) in future forecasts, corresponding to a $\pm 33.5\%$ range over the nominal value for 2035 proposed in [105]. Errors in past EIA forecasts have been presented in Figure 2. Our analysis of past EIA forecasts in the period 1985-2015 highlights error factors as high as 3.32, corresponding to an uncertainty range of $[-69.9\%, 232\%]$. Furthermore, there is no evidence that the accuracy of forecasts is higher in the short term. Thus, the scaling factor in Eq. 2.3 is applied to the error factor. This leads to the calculation of the range $[-47.3\%, 89.9\%]$, which is chosen as the final one as it is the most conservative.

Other parameters: technologies O&M cost and lifetime, network losses

Following a common practice in energy modeling, the O&M cost (c_{maint}) of technologies is assumed to be a percentage of the initial investment. This means defining a relation of the type $c_{maint}(tech) = c_{maint,\%} * c_{inv}(tech), \forall tech \in TECH$. The equation is integrated in the model (C1a), and uncertainty is characterized for the newly defined parameter $c_{maint,\%}$. This has also the effect of reducing the number of parameters to 370. The uncertainty of this parameter is based on forecasts (C3a). The IEA forecasts future investment and O&M costs of energy technologies [106]. The ratio between O&M and investment costs is calculated for Europe in 2035. Values are in the range $[1.5\%, 4\%]$, with an

Chapter 2. Uncertainty characterization

average of 2.95% (taken as nominal value).

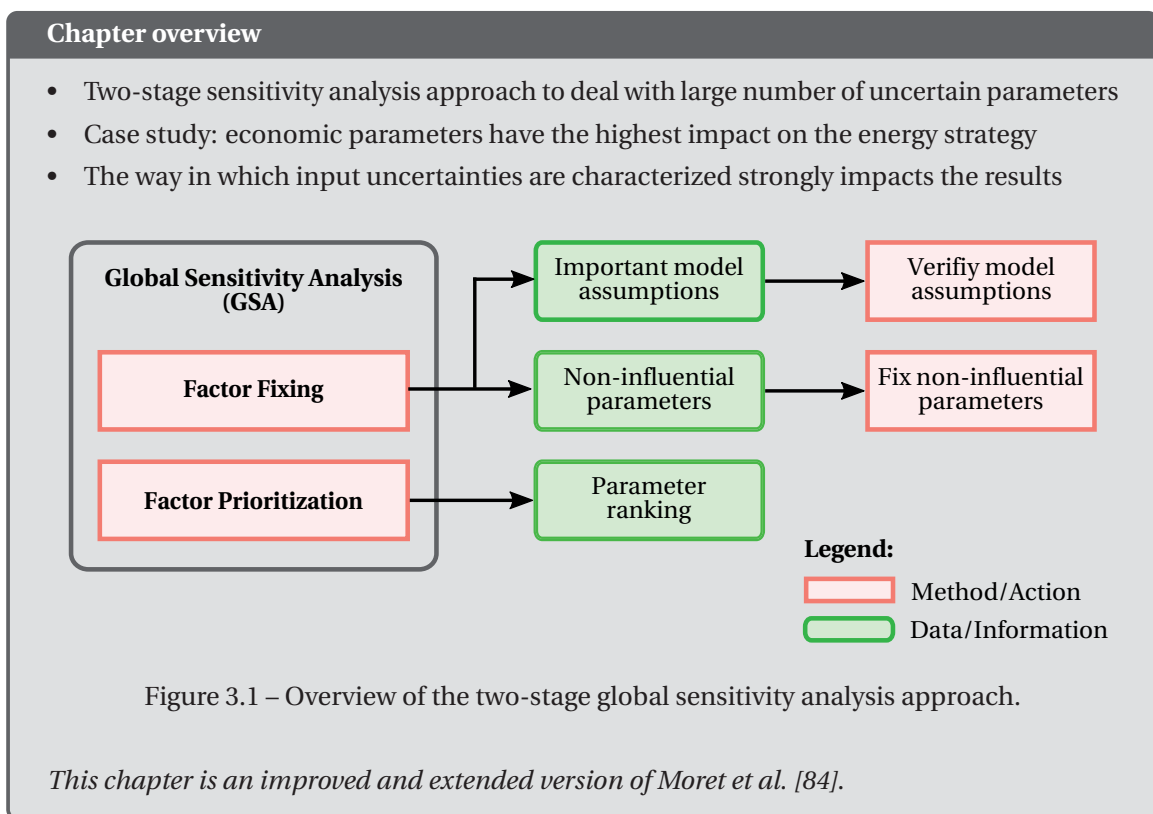
The lifetime (n) is assumed to have the same relative level of uncertainty for all technologies. The lifetime of boilers is taken as representative parameter for this category. The uncertainty range is calculated based on the data and ranges for lifetime of different boiler types collected in Table B.5. For the losses in the electricity grid ($\%_{loss}(Elec)$), historical data for Switzerland are used to define the uncertainty range [107]. Since 1960, losses have been constantly decreasing and had then negligible variations starting from the early 2000s. The uncertainty range is defined based on data in the years 1985-2015. The range is taken considering the difference between the mean value (7.62%) and the highest value (8.33% in 1985).

Parameters not belonging in any category, mostly corresponding to upper and lower bounds for the decision variables, are assigned a qualitative range of $\pm 20\%$.

Discussion

The application of the proposed uncertainty characterization method to the national energy planning model (Table 2.1) reveals substantial differences in the uncertainty ranges of the different parameters. As an example, the cost of imported fossil resources, the investment cost of hydroelectric dams, nuclear and geothermal, and interest rates have a high level of uncertainty; electricity losses, yearly capacity factors and the cost of local resources feature a low level of uncertainty. Through the application of a set of criteria, the method aids the definition of uncertainty ranges, taking into account the nature of the uncertainty (epistemic or aleatory) and how uncertainty develops over the planning time horizon. Overall, the method offers a simplified description of the input uncertainties, which is coherent with the scarce quantity and quality of available data in strategic energy planning. Although uncertainty characterization is very often problem-specific, the parameters characterized in Table 2.1 for the case of Switzerland are commonly found in strategic energy planning problems. Thus, the source data for the definition of the ranges are duly documented to allow reproducibility and adaptation to other case studies.

3 Global sensitivity analysis



Sensitivity analysis (SA) and uncertainty analysis (UA) are valuable supports to any modeling effort. As discussed in the Introduction, in the current energy modeling practice these tools still play a marginal role [34]. However, in the recent years various authors have integrated these methods in energy models.

Table 3.1 – Review of application of sensitivity and uncertainty analysis methods to energy models.

	Method(s) ^a	Uncertain Parameters	Application & Model type ^b	Output(s) of interest
Schulz et al. [108]	LSA (scenarios)	fuel prices, inv. cost, subsidies	wood-to-SNG (LP)	FEC, strategy
Kattan and Ruble [109]	LSA	fuel prices	comparison of boilers for residential heating	energy price
Siler-Evans et al. [110]	LSA	cost (fuels and inv), interest rate, efficiencies, lifetime	distributed CHP	NPV
Kim et al. [50]	LSA	feedstock and by-product prices	biomass-to-fuel (LP)	Obj. (cost)
Koltsaklis et al. [41]	LSA (scenarios)	cost (NG, emissions), inv. cost, elec. demand	national power system planning (MILP)	Obj. (cost), other
Pantaleo et al. [111]	LSA (scenarios)	demand, fuel prices, climate, infrastructure	biomass integration in urban systems (MILP)	various
Beckers et al. [112]	LSA	costs, interest rate, lifetime, geothermal resource	geothermal energy	levelized cost
Fazlollahi [113]	EFAST	cost (fuels and inv), interest rate, emissions	urban energy system (MILP+GA)	Objs. (cost, GWP, efficiency)
Pernet [114]	LSA, EE, VB	heat and exergy demand, efficiencies	urban energy system (MILP)	Obj. (exergy), Tech size
Pye et al. [47]	SP, SRC	inv. cost, build rates, resource avail. and prices	national energy model (LP)	Obj. (cost), emissions
Han et al. [115]	LSA	feedstock price, yields, solvent:biomass ratio	ethanol production	energy price
Lythcke-Jørgensen et al. [85]	EE, UA	fuel price, inv. cost, emissions	multi-generation system design (MILP+GA)	Objs. (NPV, GWP)
Mian [116]	EE, MC	cost (fuels and inv.), efficiencies, interest rate, temperatures	hydrothermal gasification plant design (MINLP)	Obj. (cost)

^aAbbreviations: local sensitivity analysis (LSA), uncertainty analysis (UA), elementary effect (EE), variance-based (VB), scatterplots (SP), standardized regression coefficients (SRC), Monte Carlo (MC)

^bOptimization model types: linear programming (LP), mixed-integer linear programming (MILP), mixed-integer non linear programming (MINLP), genetic algorithm (GA). If the model type is not indicated, the model is not based on optimization.

Table 3.1 reviews applications of sensitivity and uncertainty analysis to energy models. The reviewed works are classified according to four criteria: *i)* used methods; *ii)* considered uncertain parameters; *iii)* application and type of optimization problem, if any; *iv)* outputs of interest.

The analysis reveals that local sensitivity analysis (LSA) methods are widely diffused [108, 109, 110, 50, 41, 111, 112, 115]. LSA methods analyze how a small perturbation on an input parameter affects the output of interest [117]. In the works classified as LSA in Table 3.1, uncertain input parameters are varied in a one-at-a-time (OAT) fashion (i.e. letting the other parameters fixed at their nominal values) or through the definition of scenarios, i.e. combinations of uncertain parameters' values.

Compared to local methods, global sensitivity analysis (GSA) considers as well the effects associated to the interaction among different uncertain inputs. According to Zhou et al. [118], "*a sensitivity analysis is considered to be global when all the input factors are varied simultaneously and the sensitivity is evaluated over the entire range of each input factor*". As an example, Pye et al. [47] use scatterplots and standardized regression coefficients (SRC) to analyze the impact of uncertainties in UK energy transition pathways. Fazlollahi [113] uses the Extended Fourier Amplitude Sensitivity Test (EFAST) [119] in an urban system application. The use of methods based on the Fourier transform when dealing with optimization models is generally not recommended, as they require continuous and regular output functions. The EEs method developed by Morris [120], described more in detail in Section 3.1.1, lies in between local and global methods. It is an efficient way of screening a model to identify non-influential parameters, as demonstrated by Lythcke-Jørgensen et al. [85] and Mian [116]. Pernet [114] compares local methods, EEs and variance-based methods in an urban energy system design context.

The review reveals that the use of GSA methods is still limited in the energy field. Also, although energy models often feature a large number of input parameters, sensitivity analysis is normally carried out on a limited subset of parameters selected *a priori* by the modeler. This is a common but dangerous practice, as it "*impedes, for example, some possible misspecifications to emerge*" [55].

Contributions

As a contribution towards a wider penetration of GSA in the energy modeling practice, the adoption of a two-stage method [63] is proposed. The method, schematically illustrated in Figure 3.1, allows dealing with the large number of uncertain parameters typically found in energy planning models: the first stage, using the EEs method, performs an efficient screening of the model, highlighting non-influential parameters and important assumptions; the second stage, using variance-based methods [54], offers a ranking of the influential parameters. The application of a two-stage approach and the consideration of *all* parameters in the analysis represents a novelty in the energy planning field.

To obtain a proof of concept, the presented approach is applied to the Swiss MILP model introduced in Chapter 1. Additionally, the impact of the uncertainty characterization obtained in Chapter 2 is assessed by comparing it with the assumption of equal levels of uncertainty for all the model parameters.

3.1 Two-stage GSA method

The idea of using a two-stage GSA method to tackle quantitatively large dimensionality problems was first proposed by Campolongo et al. [63] in the late 1990s. They proposed the use of the EEs method in the first stage, and of the EFAST [119] method in the second stage. In this thesis the methods adopted in both stages are updated to the current state-of-the-art, taking into account as well the compatibility with the application to optimization models. The methods are selected following the best practices indicated by Saltelli et al. [54], who also offer a thorough background on GSA theory and methods.

3.1.1 First stage: factor fixing

The first stage corresponds to the *factor fixing* GSA setting. It aims at identifying non-influential parameters, i.e. parameters that can be fixed anywhere in their range of variation without significantly affecting the output of interest. This is normally done by calculating the *total effect* sensitivity index (S_{T_i}). Given a model in the form $Y = h(\theta_1, \theta_2, \dots, \theta_k)$, S_{T_i} , the total effect of the i -th input, is defined as the ratio between the expected value (\mathbb{E}) of the output variance $V(Y)$ when only θ_i is varying (all other parameters are fixed), and $V(Y)$ (Eq. 3.1).

$$S_{T_i} = \frac{\mathbb{E}_{\theta_{-i}}(V_{\theta_i}(Y|\theta_{-i}))}{V(Y)} \quad (3.1)$$

$S_{T_i} = 0$ is a necessary and sufficient condition to declare θ_i as a non-influential parameter. S_{T_i} is often computationally expensive to calculate even for relatively low values of k . Thus, the EEs method (Morris screening) is chosen [120], in its improved version by Sin and Gernaey [121] (as in [51]). Given a simplified description of the input uncertainties, such as the one obtained with the uncertainty characterization method proposed in Chapter 2, it allows estimating a proxy for S_T in a computationally efficient way. It is based on a discrete sampling: r trajectories are defined, each consisting of $(k + 1)$ steps. At each step of the trajectory, corresponding to one run of the model, a different parameter is made to vary (see [54] for details). In this way, all the parameters are varied once for each trajectory. At each step of the m -th trajectory, the EE of the i -th parameter with respect to the j -th output of interest is calculated as in Eq. 3.2.

$$EE_{ij}^m = \frac{\delta Y_j \sigma_{\theta_i}}{\delta \theta_i \sigma_{Y_j}} \quad (3.2)$$

In which $\delta \theta_i$ is the difference between the value of the input parameter θ_i at a given step and its nominal value, δY_j is the difference between the value of the output of interest when θ_i is varied and the value of the output of interest Y_j when all the input parameters are at nominal value. Scaling by the ratio between the standard deviations of the input (σ_{θ_i}) and the output (σ_{Y_j}) is needed when the input parameters have different orders of magnitude. The scaling also allows the comparison of the EEs on different model outputs. Once the EEs are calculated for each parameter, output and trajectory, μ_{ij}^* is calculated by averaging the absolute EE values of the i -th parameter with respect to the j -th output over the r trajectories (Eq.3.3). μ^* is a good proxy for S_T .

$$\mu_{ij}^* = \frac{1}{r} \sum_{m=1}^r |EE_{ij}^m| \quad (3.3)$$

3.1.2 Second stage: factor prioritization

The second stage corresponds to the *factor prioritization* GSA setting. It aims at ranking the most influential parameters, i.e. the parameters which, when fixed to their nominal value, lead to the greatest reduction in the variance of the output. μ^* offers an efficient yet “qualitative” ranking of the importance of input parameters. A quantitative appreciation of their influence on the outputs of interest can be obtained by using variance-based methods. Due to their significant computational requirements¹, these methods can only be applied to a limited number of parameters. Thus, in a two-stage approach they are applied to the first parameters (normally < 20) in the ranking obtained in the first stage. Factor prioritization is normally done by calculating S_i , the *first-order effect* of the i -th input, defined as the ratio between the reduction of the expected value of the output variance when fixing θ_i to its nominal value (all other parameters are varying), and $V(Y)$ (Eq. 3.4).

$$S_i = \frac{V_{\theta_i}(\mathbb{E}_{\theta_{-i}}(Y|\theta_i))}{V(Y)} \quad (3.4)$$

S_i is in the interval [0;1], and its value is directly proportional to the influence of the parameter. The calculation of both the first-order (S) and total effect (S_T) sensitivity indices by variance-based methods offers a good, synthetic characterization of the sensitivity pattern of a model. The best practices indicated by Saltelli et al. [122] are used in the current work for the calculation of these two indices.

¹ $n_{sample}(k+2)$ model runs needed with $n_{sample} \approx x100 \div x1000$ and k parameters. The EEs method requires instead $r(k+1)$ model runs, with $r \approx 15 \div 100$.

3.2 Application to the case study

The two-stage method is applied to the Swiss MILP case study (Chapter 1) using the uncertainty ranges calculated in Chapter 2. The outputs of interest (Y_j) are the value of the objective and the investment decisions. The value of the objective (Y_1) is the total annual cost of the energy system (C_{tot}). The investment decision corresponds to the value of the decision variable \mathbf{F} , indicating the total installed size of each technology. This decision variable is indexed over the technologies set. This would lead to a high number of outputs of interest, as many as the number of technologies in the model ($Y_{\text{tech}} = \mathbf{F}(\text{tech}), \forall \text{tech} \in \text{TECH}$). To limit the number of outputs of interest, an aggregated indicator (Y_2) for the investment decision is defined. As an example, Eq. 3.5 shows how this applies in the case of the calculation of the sensitivity index μ^* for the i -th parameter.

$$\mu_{iY_2}^* = \sum_{\text{tech}} \mu_{iY_{\text{tech}}}^* \quad \forall i \quad (3.5)$$

The sensitivity indices μ^* are first calculated for each technology and then summed to obtain the aggregated indicator.

3.2.1 Factor fixing

The EE method is applied to the 370 uncertain parameters with settings $r = 100$ trajectories, $p = 8$ levels (see [54] for more details). Results of the analysis are shown in Figure 3.2 for the 22 parameters having a value higher than 5% of the maximum value of $\mu_{iY_1}^*$. As the aggregated indicator $\mu_{iY_2}^*$ cannot be directly compared with $\mu_{iY_1}^*$, the value of μ^* for the i -th parameter is expressed as percentage of the maximum value with respect to j -th output of interest ($\mu_{ij}^* / \max_i(\mu_{ij}^*), \forall j \in \{Y_1, Y_2\}$). Parameters are sorted in descending order from left to right based on the value of $\mu_{iY_1}^*$.

Three main observations result from the analysis. First, the screening is effective. In fact, with respect to Y_1 , only 22 out of 370 parameters have a value of $\mu_{iY_1}^*$ higher than 5 % of the maximum, while 53 parameters are above the 1% threshold. This means that a large number of parameters has a relatively small influence on the output of interest. Second, the screening is also effective in highlighting important model assumptions. In fact, in common energy modeling practice, various parameters emerging as impacting from this analysis are often simply assumed by the modeler. It is the case, for example, of $c_{\text{maint},\%}$, and of the upper bounds of decision variables (e.g. $\%_{\text{public,max}}$, $\%_{\text{freight,max}}$). This highlights the danger of an *a priori* arbitrary exclusion of parameters in a GSA study. Third, some parameters have a strong influence on the objective, but a negligible influence on the investment decision. In this example, such a behavior is observed for the investment cost of the electricity grid and of the hydroelectric dams. Although these costs are relevant, they are fixed and thus they do not impact the investment decision.

3.2. Application to the case study

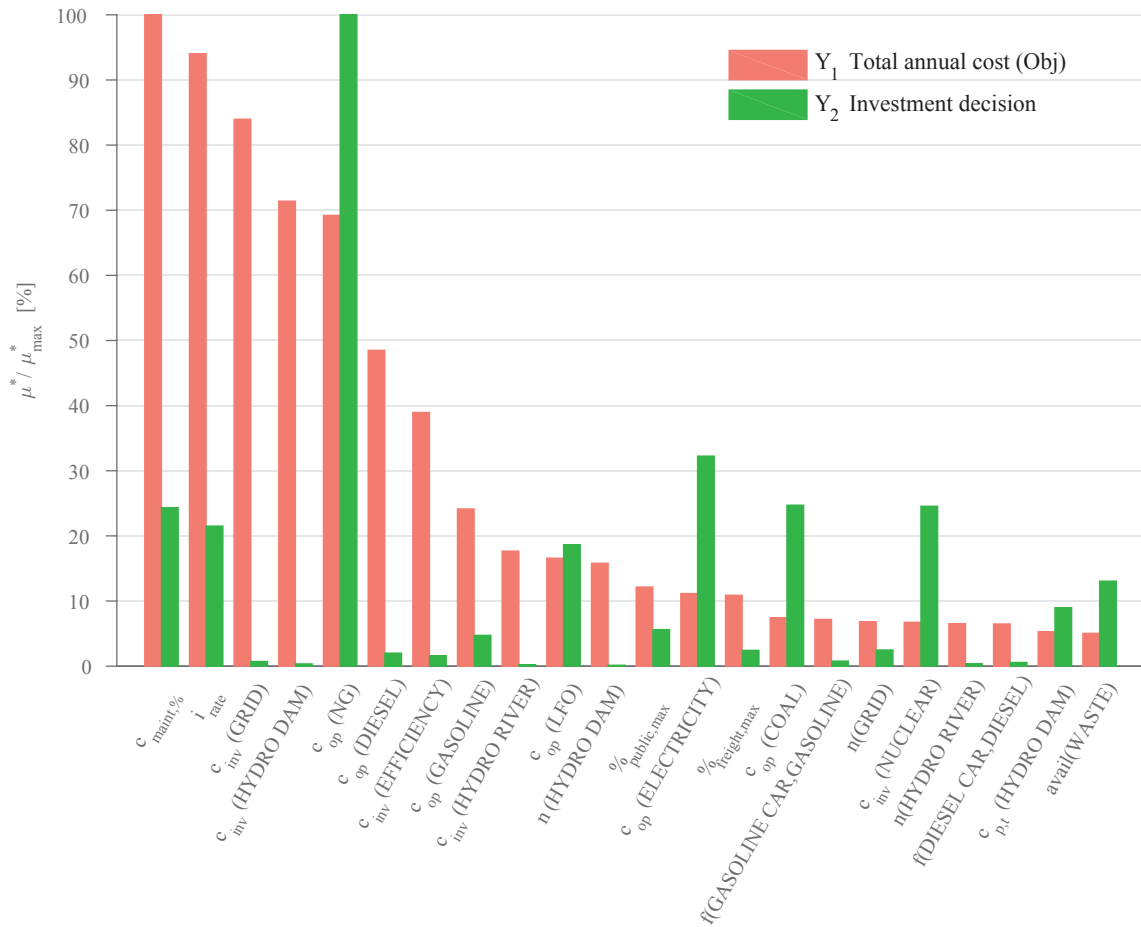


Figure 3.2 – Factor fixing with the EEs method: impact of the input parameters on the total cost (Y_1) and on the investment decision (Y_2). The value of μ^* for the i -th parameter is expressed as percentage of the maximum value with respect to the j -th output of interest ($\mu_{ij}^* / \max_i(\mu_{ij}^*), \forall j \in \{Y_1, Y_2\}$). Only the parameters having a value higher than 5% of the maximum value of $\mu_{Y_1}^*$ are shown. Parameters are sorted in descending order from left to right based on the value of $\mu_{Y_1}^*$.

3.2.2 Factor prioritization

The EE method, along with the identification of non-influential model parameters, also offers a “qualitative” ranking. This ranking can be used to select the candidate parameters for a more refined and computationally expensive analysis, aiming at ranking the parameters. At this stage, more information is normally acquired to characterize the uncertainty of the individual input parameters. As an example, a simplified factor prioritization is performed. First, parameters are ranked based on $\mu_{Y_1}^*$ and $\mu_{Y_2}^*$, respectively. Then, assuming equal importance for Y_1 and Y_2 , parameters are sorted in ascending order based on the sum of their positions in the two rankings. Parameters considered as modeler’s assumptions are excluded at this stage. Factor prioritization with respect to Y_1 is

performed on the first 10 parameters of the obtained list. Factor prioritization results are shown in Table 3.2. The first-order sensitivity index S_i , defining the parameter ranking, is calculated along with the total effect index S_{T_i} for $n_{sample} = 10000$. $S_{T_i} - S_i$ is a measure of how strongly the i -th parameter is involved in interactions with the other inputs.

Table 3.2 – Factor prioritization results: S_i and S_{T_i} for the first 10 parameters with respect to the objective value (Y_1). Parameters are selected based on the output of the first stage. S_i is used to rank the impact of parameters in the model

Rank	Parameter	S_i	S_{T_i}	$S_{T_i} - S_i$
1	i_{rate}	4.830E-01	4.906E-01	7.604E-03
2	$c_{op}(NG)$	4.412E-01	4.586E-01	1.740E-02
3	$c_{op}(LFO)$	1.900E-02	1.914E-02	1.424E-04
4	$c_{op}(ELECTRICITY)$	1.400E-02	3.398E-02	1.997E-02
5	$c_{inv}(NUCLEAR)$	5.732E-03	1.871E-02	1.298E-02
6	$c_{op}(COAL)$	5.487E-03	1.272E-02	7.232E-03
7	$c_{p,t}(HYDRO DAM)$	2.320E-03	2.137E-03	-1.830E-04
8	$avail(WASTE)$	1.501E-03	2.026E-03	5.243E-04
9	$c_{inv}(DHN)$	1.158E-03	1.310E-03	1.522E-04
10	$c_{p,t}(HYDRO RIVER)$	6.922E-04	1.744E-03	1.052E-03

3.2.3 Does uncertainty characterization matter in energy planning?

The presented methodology allows to answer an additional research question: *does uncertainty characterization matter in energy planning?* Characterizing input uncertainties (as in Table 2.1) is a time-consuming process. In the energy planning practice, this investment of time is justified only if the obtained characterization has a relevant impact on the output results. To answer this question, the GSA results are compared with the results which are obtained by assuming an identical level of uncertainty for all the input parameters. Figure 3.3 shows the results of the comparison. The EEs method is carried out assuming $\pm 20\%$ uncertainty for all parameters. Parameters are ranked with respect to the outputs of interest (Y_1 and Y_2) following the same method as in Section 3.2.2. For the first 10 parameters in the ranking, the new values of $\mu_{Y_1}^*$ and $\mu_{Y_2}^*$ are compared with the results presented in the previous section.

The comparison shows that the values of the sensitivity indices are substantially different in the two cases. Although 5 out of the 10 parameters emerge as impacting in both cases, the $\pm 20\%$ screening fails in identifying the non-influential parameters. Two observations suggest this conclusion. First, parameters which were non-influential - such as the energy demand and the efficiency of technologies - are now in the first positions of the ranking. Second, parameters previously classified among the most impacting are now classified as non-influential. The latter is a potentially dangerous error as noted in [63], as it would lead to exclusion of impacting parameters from the analysis. Overall, the

3.2. Application to the case study

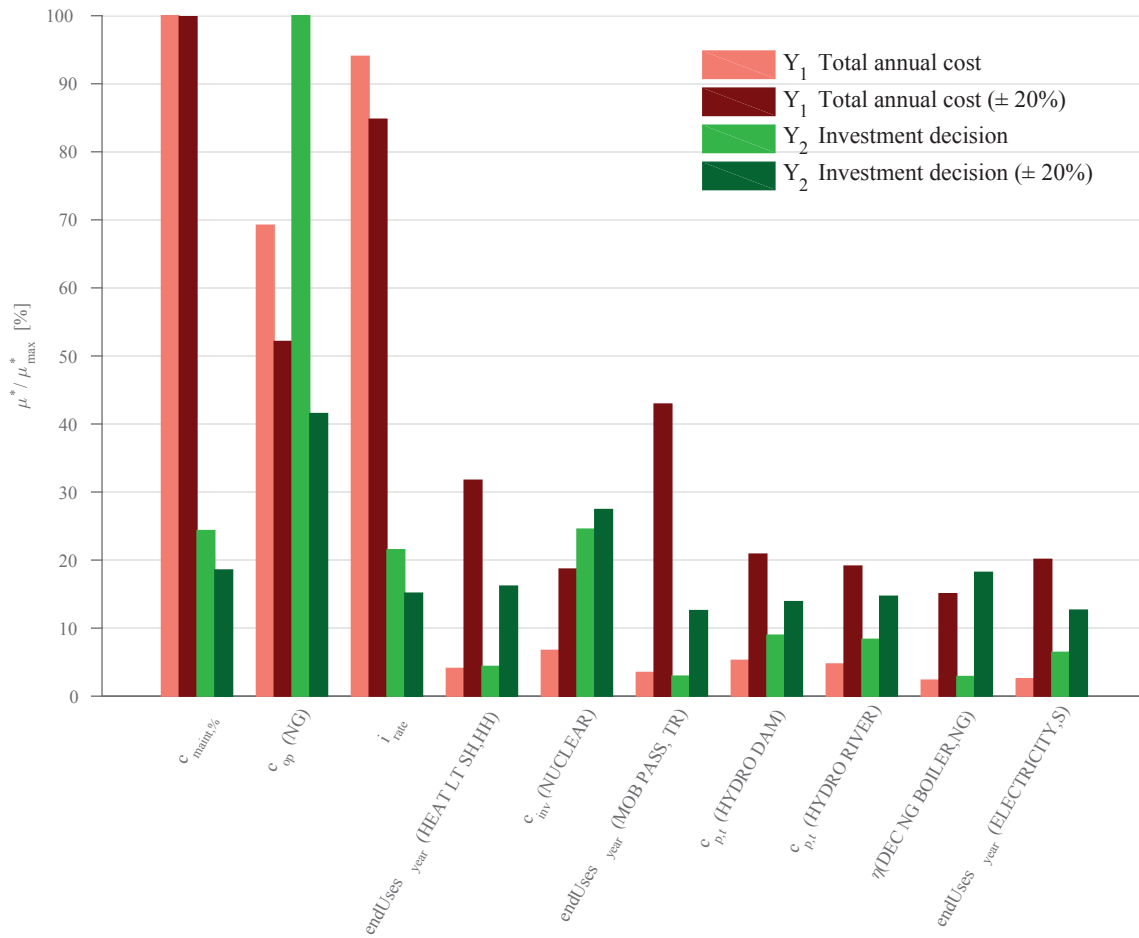


Figure 3.3 – Comparison of EE method results: input uncertainty characterization as in Table 2.1 (light colors) vs. identical uncertainty of $\pm 20\%$ for all parameters (dark colors). The value of μ^* for the i -th parameter is expressed as percentage of the maximum value with respect to the j -th output of interest ($\mu_{i,j}^* / \max_i(\mu_{i,j}^*), \forall j \in \{Y_1, Y_2\}$). Parameters are sorted in descending order from left to right based on the results of the $\pm 20\%$ GSA.

characterization of input uncertainties is proven to have a strong impact on the output results.

Discussion

The application of a two-stage approach (as in [63]) and the consideration of *all* parameters in the analysis represent a novelty in the energy planning field. To date sensitivity analysis is very seldom carried out on energy models [34], and normally only an arbitrarily defined subset of parameters is considered in the analysis.

The GSA results show that, first, the two-stage GSA is an efficient approach, as a large number of

non-influential parameters can be excluded in the first stage, reducing the problem size for the more computationally expensive second stage. Second, considering *all* parameters in the analysis is crucial. Figure 3.2 shows the risk of an arbitrary exclusion of parameters from the analysis: parameters which are commonly considered as fixed assumptions in energy models, and whose uncertainty is therefore seldom investigated, emerge as very impacting. Third, when dealing with optimization models, the outputs of interest for the GSA should be carefully defined. Selecting the value of the objective as an output of interest is a natural but often incomplete choice, as some parameters can have a strong influence on the objective but a negligible influence on other key decision variables (and *vice versa*).

Furthermore, the GSA results offer a qualitative ranking of the importance of the different parameter categories. This is shown in Table 3.3, in which the average of μ^* is calculated for the different types of parameters with respect to the two outputs of interest. The economic parameters emerge as the most impacting. In particular, the cost of resources (c_{op}) is the second most impacting parameter type with respect to the investment decisions (Y_2) and the third most impacting on the objective value (Y_1), after the assumption of the O&M cost of technologies and the interest rate.

Table 3.3 – Results of the EE method: average of μ^* ($\overline{\mu^*}$) for the different parameter categories with respect to the objective value (Y_1) and the investment decision (Y_2). Parameter categories are ranked based on $\overline{\mu_{Y_1}^*}$.

Rank	Category	$\overline{\mu_{Y_1}^*}$	$\overline{\mu_{Y_2}^*}$
1	$c_{maint,\%}$	4.749E-01	3.535E+00
2	i_{rate}	4.466E-01	3.124E+00
3	c_{op}	1.063E-01	3.421E+00
4	c_{inv}	2.162E-02	4.622E-01
5	$avail$	1.200E-02	1.185E+00
6	$c_{p,t}$	9.887E-03	7.040E-01
7	$endUses_{year}$	7.834E-03	4.820E-01
8	n	3.581E-03	2.802E-01
9	η	2.428E-03	3.540E-01
10	<i>Other</i>	1.894E-03	2.984E-01
11	$\%_{loss}$	6.157E-04	3.681E-01
12	f_{max}	4.953E-04	5.440E-01
13	c_p	5.601E-05	1.584E-01

4 Robust optimization

Chapter overview

- How can we incorporate uncertainty in strategic energy planning optimization models?
- Complete robust optimization framework: uncertainty in objective and constraints
- Uncertainty dramatically impacts energy strategy: when uncertainty is accounted for, shift towards renewables and efficient technologies
- Robust decision-making method identifies reliable and cost-effective energy strategies
- Comparison with stochastic programming

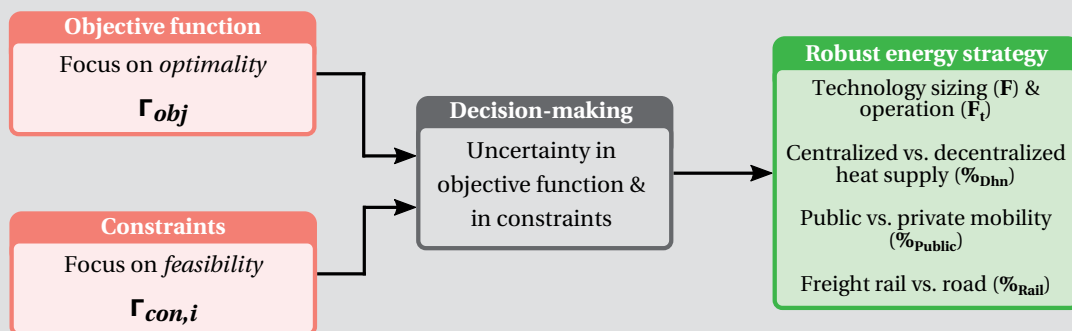


Figure 4.1 – In this chapter, first uncertainties in the objective function and in the other constraints are separately considered; then, they are put together to support decision-making.

This chapter is an improved and extended version of Moret et al. [123].

Sensitivity and uncertainty analysis offer precious insights to understand the impact of uncertainty on the output of a model. In these methods, the *deterministic* model is run several times, each time with a different combination of input parameters' values. This means that uncertainty is not directly

incorporated in the model structure; instead, it is accounted for by changing the values of the inputs at each run. In *optimization under uncertainty*, instead, uncertainty is integrated in the optimization model formulation. As Wallace [124] argues, this allows to effectively support decision-making in an uncertain context.

When dealing with optimization under uncertainty, “*a major modeling decision is whether one should rely on robust optimization, or whether one should use stochastic programming*” [36]. Historically, *stochastic programming (SP)* is the “traditional” approach [59]. In a nutshell, SP optimizes the expected value of the objective over all the possible realizations of uncertainty (modeled as a scenario tree), under the fundamental assumption that the PDFs of the uncertain parameters are known [57, 125]. First proposed by Dantzig [58] in the mid 1950s, it has found multiple applications in the contexts of multistage decision-making and long-term planning [36]. Examples of SP in the energy field are the planning of offshore gas field developments [35], the identification of optimal process integration investments in industry [126], the optimization of residential energy systems [87] and the long-term planning of national energy systems [39], among others.

The main limitations of SP are the difficulties in defining PDFs for the uncertain parameters [125], and thus the scenarios, and the fact that it quickly leads to intractable model sizes [59]. As highlighted in the previous chapters, strategic energy planning models are characterized by a large number of uncertain parameters along with scarce quantity and quality of data to characterize their uncertainty. Thus, in this context, SP applications are often limited to a handful of uncertain inputs [39], and the associated PDFs seldom have a solid empirical basis [27].

Robust optimization (RO) is an alternative approach to SP. The idea behind RO is to ensure protection against worst-case realizations of uncertainty. As a consequence, “*the main feature of this approach is that it does not resort to the calculus of probability, which makes it immune against the curse of dimensionality and computational intractability*” [59]; as previously discussed, this is a desirable feature when dealing with strategic energy planning models.

The roots of the method are found in the work by Soyster [60] for LP models in the early 1970s. In his robust formulation, all the uncertain parameters are considered at their worst case value. On the one hand, this ensures full protection against infeasibility, i.e. the obtained solution is feasible for every possible value of the uncertain parameters; on the other hand, it has the disadvantage of producing over-conservative solutions. This issue of over-conservatism was first addressed in the late 1990s by Ben-Tal and Nemirovski [61][127], whose approach offers less conservative solutions, but with the drawback of formulating a non-linear robust counterpart for a LP problem. A few years later, Bertsimas and Sim [62] also addressed the issue of over-conservatism by proposing an alternative approach, resulting in a linear formulation of the robust counterpart for MILP problems (see Section 4.1.1).

Table 4.1 – Review of application of robust optimization methods to energy models.

	Method(s)^a	Uncertain parameters	Application & Model type^b
Mulvey et al. [128]	Own (scenarios)	energy demand	power capacity expansion (LP)
Janak et al. [129]	Own	processing time, demand, prices	chemical plant scheduling (MILP)
Babonneau et al. [59]	BT&N, LDR, own	pollutant transfer, energy demand	environmental and energy planning (LP)
Ribas et al. [130]	Scenarios [131]	oil production, demand, prices	oil supply chain strategic planning (LP)
Hajimiragha et al. [132]	B&S	electricity prices	Plug-in Hybrid Electric Vehicles (MILP)
Koo et al. [133]	Scenarios [134]	fuel prices, emission targets	sustainable energy planning (LP)
Jiang et al. [135]	B&S, own	wind power production	wind & hydro unit commitment (MILP)
Parisio et al. [136]	B&S	conversion efficiencies	energy hub management (MILP)
Zhao and Zeng [137]	Own	wind production	wind unit commitment (MILP)
Dong et al. [138]	B&S, own	prices, cost, efficiencies	energy management planning (FRILP)
Street et al. [139]	ARO	generation & transmission outages	electricity market scheduling (MILP)
Akbari et al. [140]	B&S	demand, fuel costs	building energy system (MILP)
Rager [141]	B&S, own	cost, demand, efficiencies	urban energy system (MILP)
Grossmann et al. [36]	LDR	reserve demand	air separation unit scheduling (MILP)
Sy et al. [142]	Own [143]	selling prices, demand	polygeneration system (MILP)
Nicolas [144]	B&S	fuel prices, inv. cost; climate	national energy system; climate policy (LP)
Gong et al. [145]	Own	feedstock price, biofuel demand	optimal biomass conversion pathways (MINLP)
Majewski et al. [146]	Soyster [60], own	energy demand, fuel prices, emissions	decentralized energy supply system (MILP)
Majewski et al. [86]	Soyster [60], own	energy demand, fuel prices	decentralized energy supply system (MILP)

^aAbbreviations: Ben-Tal and Nemirovski [61] (BT&N), Bertsimas and Sim [62] (B&S), linear decision rules (LDR), adjustable robust optimization (ARO). ‘Own’ indicates that the paper also introduces a robust optimization (RO) framework.

^bOptimization model types: linear programming (LP), mixed-integer linear programming (MILP), mixed-integer non linear programming (MINLP), fuzzy radial interval linear programming (FRILP)

In the last 20 years, after the major contributions by Ben-Tal and Nemirovski and by Bertsimas and Sim, RO has gained increasing interest, as recently shown by Nicolas [144], and has found application in various fields, such as inventory and logistics, finance, revenue management, queueing networks, machine learning, energy systems and the public good [147]. The latest developments focused on: the consideration of *recourse*, i.e. the possibility of reactive actions after the realization of the uncertainty, via linear decision rules (LDR) [148] and adjustable robust optimization (ARO) [149]; making a link between RO and SP [150]; distributionally robust optimization [151], a paradigm where the uncertain problem data are governed by a probability distribution that is itself subject to uncertainty; the extension of RO to non-linear problems [145].

Table 4.1 reviews applications of robust optimization to energy models. The reviewed works are classified according to three criteria: *i)* used methods; *ii)* considered uncertain parameters; *iii)* application and type of optimization problem.

Among the previously discussed “classical” methods, the approach by Bertsimas and Sim [62] is the most diffused one, probably due to the linearity of their formulation. However, various authors also propose robust frameworks, which are alternative to - or combined with - the most established ones in the literature. Examples are the different scenario-based approaches to RO used in Mulvey et al. [128], Ribas et al. [130] and Koo et al. [133]; the target oriented RO framework developed by Sy et al. [142] for the synthesis of polygeneration systems; the two-stage adaptive RO approach for non-linear problems presented by Gong et al. [145], among others.

In terms of considered uncertain parameters, most applications aim at ensuring feasibility against uncertain demand, or consider market uncertainty for costs and prices in the objective function. Applications range from small scale (buildings, specific systems) to districts and industrial processes, and up to urban and national energy systems, although in the last case the focus is often on the operation of the electricity sector [128, 133, 135, 137, 139].

It is worth noting that, in the reviewed literature, the word *robust* is often adopted in contexts not related to the field of RO, for example in stochastic programming [152] or sensitivity analysis [113] applications.

The literature review reveals that, despite an increasing trend in the last years, the use of robust optimization methods is still rather limited in the energy field. Furthermore, applications are typically limited to specific cases or sectors - often the electricity sector - and consider only a subset of the uncertain parameters. This is often due to the difficulty in incorporating uncertainties in complex deterministic model formulations, initially developed without accounting for uncertainty.

Overall, the literature shows the need of a stronger link between the fields of mathematical programming and of energy systems: if works belonging in the first domain aim at fundamental methodological contributions and often simply make use of energy applications as illustrative numerical examples, energy researchers and professionals are interested in applying the developed methods to support the actual decision-making process. To date, a gap still exists between the two

worlds.

Contributions

The developments presented in this chapter aim at bridging this gap by proposing a general robust optimization framework for strategic energy planning models, with the ultimate goal of supporting decision-making. The novelty compared to the state-of-the-art is declined in five contributions.

First, the robust formulation by Bertsimas and Sim [62] is applied for the first time to the long-term planning of a large-scale energy system, accounting for electricity, heating and mobility.

Second, the formulation proposed by Kwon et al. [153] to consider the case of multiplied uncertain parameters in Bertsimas and Sim [62] is further extended to account for the uncertainty in the annualization factor of the investment cost. This is a methodological contribution, which can find application in different domains behind energy systems.

Third, the methodology proposed by Babonneau et al. [154] is integrated in the framework to systematically consider uncertainty in the constraints.

As a consequence of these developments, the proposed framework offers the possibility of considering *all* uncertain parameters, both in the objective function and in the other constraints, which constitutes an additional novelty.

Fifth, the framework is applied to the Swiss case study presented in the previous chapters to show its potential in the context of a real strategic energy planning problem. Figure 4.2 illustrates the cost optimal configuration of the Swiss energy system in 2035 in the deterministic case, i.e. with all the parameters at nominal value. Following the phase out of nuclear power plants [64], energy supply is dominated by fossil fuels, and in particular by NG (109 TWh/y), burned in CCGT power plants for electricity production and in boilers for heat supply. The high share of fossils, due to their low prices, leads to total GHG emissions of 39.9 ktCO₂-eq., while renewables and efficient conversion technologies (such as electrical HPs and CHP) play a marginal role in this scenario,

Thus, this chapter answers the following research question: “*How does the energy strategy change if we consider uncertainty and how can robust optimization aid this decision-making process?*”.

Although equivalent in terms of mathematical formulation, considering uncertainty in the objective function and in the constraints is fundamentally different [59, 147, 125]. According to Gabrel et al. [147], uncertainty in the constraints is linked to *feasibility*, i.e. the goal is obtaining “*a solution that will be feasible for any realization taken by the unknown coefficients*”; uncertainty in the objective is linked to *optimality*, i.e. the goal is obtaining “*a solution that performs well for any realization taken by the unknown coefficients*”. Thus, first the formulations and results for the objective function and constraints are separately discussed. Then, they are considered together to propose a decision-making method.

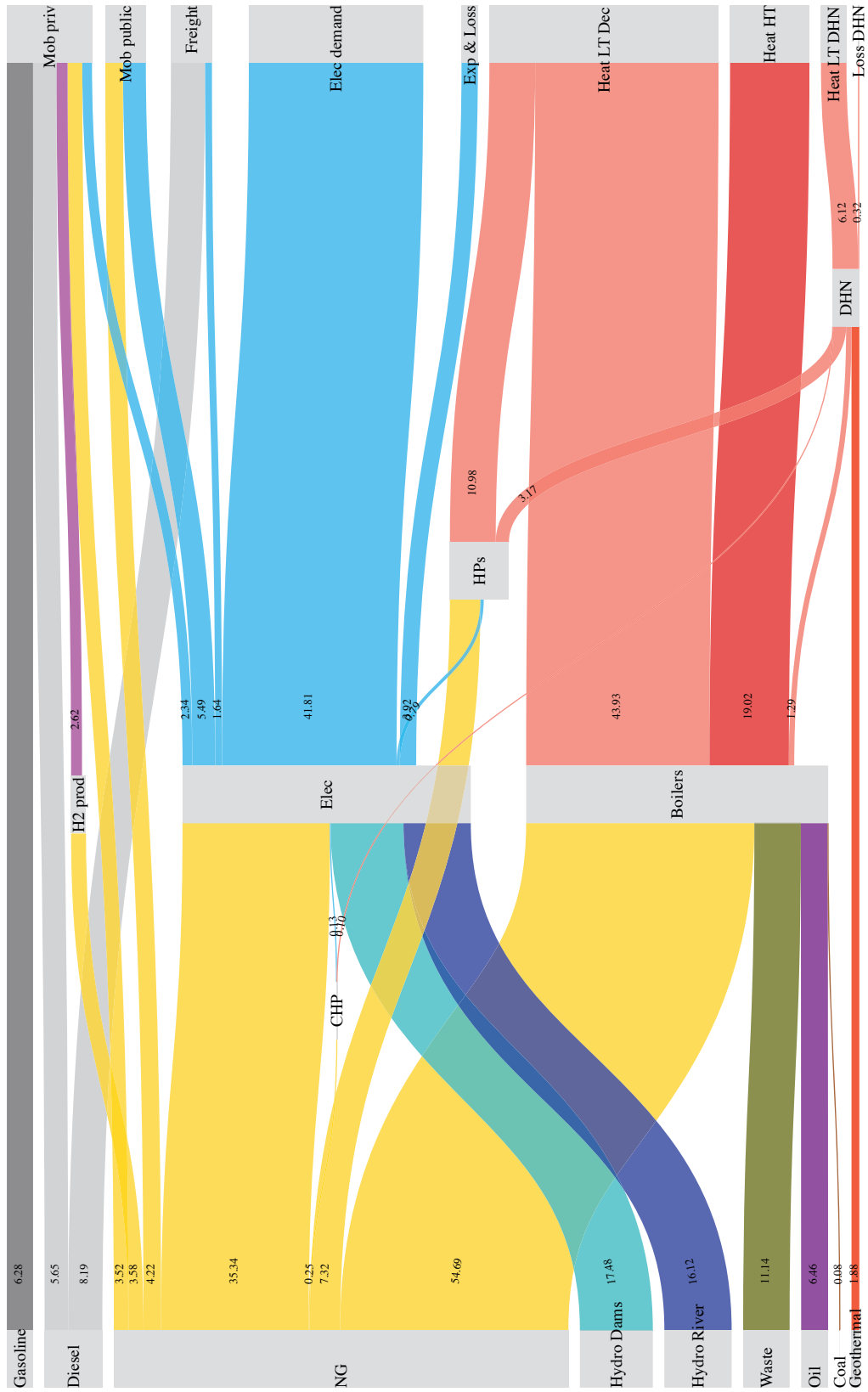


Figure 4.2 – Energy flows in Switzerland in the year 2035: cost optimal deterministic solution. All values are in TWh.

4.1 Uncertainty in the objective function

In a cost optimization model, most of the uncertain parameters are often found in the objective function [146]. The objective function of the MILP problem presented in Chapter 1 (Eq. 1.1) can be rewritten in an extended formulation as in Eq. 4.1.

$$\begin{aligned}
 \mathbf{C}_{\text{tot}} &= \sum_{j \in \text{TECH}} \mathbf{C}_{\text{inv}}(j) + \sum_{j \in \text{TECH}} \mathbf{C}_{\text{maint}}(j) + \sum_{i \in \text{RES}} \sum_{t \in T} \mathbf{C}_{\text{op}}(j, t) = & (4.1) \\
 &= \underbrace{\sum_{j \in \text{TECH}} \frac{i_{\text{rate}}(i_{\text{rate}} + 1)^{n(j)}}{(i_{\text{rate}} + 1)^{n(j)} - 1} c_{\text{inv}}(j) \mathbf{F}(j)}_{\mathbf{Obj}_1: \text{novel formulation (Section 4.1.2)}} + \underbrace{\sum_{j \in \text{TECH}} c_{\text{maint}}(j) \mathbf{F}(j) + \sum_{i \in \text{RES}} \sum_{t \in T} c_{\text{op}}(i, t) \mathbf{F}_t(i, t) t_{\text{op}}(t)}_{\mathbf{Obj}_2: \text{Application of Bertsimas and Sim [62] (Section 4.1.1)}}
 \end{aligned}$$

In which the uncertain parameters - the discount rate (i_{rate}), the technology lifetime (n), investment (c_{inv})¹ and O&M (c_{maint}) costs, and the cost of resources (c_{op}) - are highlighted in red. The GSA results in Table 3.3 reveal that these parameters are the most impacting on the model output.

As indicated in Eq. 4.1, the formulation by Bertsimas and Sim [62] can be directly applied to obtain the robust counterpart of the second half of the objective function (**Obj**₂), as there is only one uncertain parameter multiplying each decision variable. This is discussed in Section 4.1.1. However, their approach does not allow to individually consider the uncertainty of the multiplied parameters in the first half of the equation (**Obj**₁). Thus, in Section 4.1.2 novel developments are presented, extending the formulation by Bertsimas and Sim [62] to this special case.

4.1.1 The robust formulation by Bertsimas and Sim [62]

As previously discussed, in the first robust formulation proposed by Soyster [60], *all* uncertain parameters are assumed to take their worst-case values. However, in real applications it is unlikely that all uncertain parameters are at worst case. To address the over-conservatism of Soyster's approach, Bertsimas and Sim [62] proposed a robust formulation under the fundamental idea that “*nature will be restricted in its behavior, in that only a subset of the coefficients will change in order to adversely affect the solution*”.

A general MILP problem can be expressed as in Eqs. 4.2, in which \mathbf{x}_j are the decision variables (bounded by l_j and u_j) and a_{ij} are the coefficients of the constraint matrix \mathcal{A} .

¹ In the robust optimization, the instance of $c_{\text{inv}}(\text{Grid})$ in Eq. 1.28 is not considered uncertain, i.e. the parameter is fixed to its nominal value.

$$\begin{aligned}
 \min \quad & \sum_j c_j \mathbf{x}_j && (4.2) \\
 \text{s.t.} \quad & \sum_j a_{ij} \mathbf{x}_j \leq b_i && \forall i \\
 & l_j \leq \mathbf{x}_j \leq u_j && \forall j
 \end{aligned}$$

Uncertainty is considered for the coefficients of the constraint matrix \mathcal{A} , i.e. for the i -th constraint $a_{ij} \in [a_{ij} - \delta_{a,ij}, a_{ij} + \delta_{a,ij}]$, $j \in J_i$. This means that each uncertain parameter can have a $\pm \delta_{a,ij}$ variation over its nominal value a_{ij} . J_i is the *uncertainty set* of the i -th constraint, containing $|J_i|$ uncertain parameters. Considering uncertainty for the coefficients of the constraint matrix \mathcal{A} does not cause a loss of generality. In fact, as problem 4.2 is equivalent to $\min \boldsymbol{\gamma}$, s.t. $\boldsymbol{\gamma} \geq \sum_j c_j \mathbf{x}_j$, the coefficients c_j can be included in \mathcal{A} ; hence, considering uncertainty in the objective and in the constraints is mathematically equivalent.

In their formulation of the robust counterpart, a *protection parameter* $\Gamma_i \in [0, |J_i|]$ is defined for each uncertain constraint. This protection parameter controls the number of parameters at worst case. If $\Gamma_i = 0$ then no parameter is at worst case, i.e. the deterministic solution with all parameters at their nominal values a_{ij} is obtained. If $\Gamma_i = |J_i|$ then all parameters are at worst case, i.e. Soyster's solution is obtained. As shown by Bertsimas and Sim, the interest is evaluating how the solution of the optimization problem changes when varying Γ_i between these two extreme cases.

Bertsimas and Sim show that the linear robust counterpart of the MILP problem in Eqs. 4.2 is formulated as in Eqs. 4.3, in which \mathbf{p} and \mathbf{z} are positive variables², and $\mathbf{y}_j = |\mathbf{x}_j^*|$, $\forall j$ at optimality.

$$\begin{aligned}
 \min \quad & \sum_j c_j \mathbf{x}_j && (4.3) \\
 \text{s.t.} \quad & \sum_j a_{ij} \mathbf{x}_j + \mathbf{z}_i \Gamma_i + \sum_{j \in J_i} \mathbf{p}_{ij} \leq b_i && \forall i \\
 & \mathbf{z}_i + \mathbf{p}_{ij} \geq \delta_{a,ij} \mathbf{y}_j && \forall i, \forall j \in J_i \\
 & -\mathbf{y}_j \leq \mathbf{x}_j \leq \mathbf{y}_j && \forall j \\
 & l_j \leq \mathbf{x}_j \leq u_j && \forall j \\
 & \mathbf{p}_{ij} \geq 0 && \forall i, \forall j \in J_i \\
 & \mathbf{y}_j \geq 0 && \forall j \\
 & \mathbf{z}_i \geq 0 && \forall i
 \end{aligned}$$

² In Bertsimas and Sim [62], \mathbf{p} and \mathbf{z} are the dual variables of the protection function of the i -th constraint. Details are provided in their paper. For the application of the method, \mathbf{p} and \mathbf{z} can be simply seen as newly defined positive variables.

4.1. Uncertainty in the objective function

As previously shown, the same formulation can be applied to consider uncertainty in the objective function. Thus, in Eqs. 4.4-4.8, the general formulation in Eq. 4.3 is applied to the second half of the objective function in Eq. 4.1 (**Obj₂**): the original objective function is replaced by its robust counterpart (Eq. 4.4), and constraints 4.5-4.8 are added.

$$\min \mathbf{Obj}_1 + \sum_{j \in TECH} \mathbf{C}_{\text{maint}}(j) + \sum_{i \in RES} \sum_{t \in T} \mathbf{C}_{\text{op}}(j, t) + \mathbf{z}_0 \Gamma_0 + \sum_{j \in TECH} \mathbf{P}_{\text{maint}}(j) + \sum_{i \in RES} \sum_{t \in T} \mathbf{P}_{\text{op}}(j)(j, t) \quad (4.4)$$

$$\text{s.t. } \mathbf{z}_0 + \mathbf{P}_{\text{maint}}(j) \geq \delta_{\text{maint}}(j) \mathbf{y}_{\text{maint}}(j) \quad \forall j \in TECH \quad (4.5)$$

$$\mathbf{F}(j) \leq \mathbf{y}_{\text{maint}}(j) \quad \forall j \in TECH \quad (4.6)$$

$$\mathbf{z}_0 + \sum_{i \in T} \mathbf{P}_{\text{op}}(i, t) \geq \delta_{\text{op}}(i) \sum_{i \in T} \mathbf{y}_{\text{op}}(i, t) \quad \forall i \in RES \quad (4.7)$$

$$\mathbf{F}_t(i, t) t_{\text{op}}(t) \leq \mathbf{y}_{\text{op}}(i, t) \quad \forall i \in RES, \forall t \in T \quad (4.8)$$

$$\mathbf{z}_0, \mathbf{y}_{\text{op}}, \mathbf{P}_{\text{op}}, \mathbf{y}_{\text{maint}}, \mathbf{P}_{\text{maint}} \in \mathbb{R}^+$$

4.1.2 Novel robust formulation

If the uncertainty of the different parameters needs to be separately considered, the formulation by Bertsimas and Sim [62] cannot be directly applied to cases in which more than one uncertain parameter multiplies the same decision variables. In fact, the direct application of Bertsimas and Sim [62] to the first half of the objective (**Obj₁**) would imply defining a new parameter m , defined as in Eq. 4.9.

$$m(j) = [m(j) - \delta_m(j), m(j) + \delta_m(j)] \quad (4.9)$$

$$m(j) = \frac{i_{\text{rate}}(i_{\text{rate}} + 1)^{n(j)}}{(i_{\text{rate}} + 1)^{n(j)} - 1} c_{\text{inv}}(j) \quad \forall j \in TECH$$

$$\delta_m(j) = \frac{(i_{\text{rate}} + \delta_{i_{\text{rate}}})(i_{\text{rate}} + \delta_{i_{\text{rate}}} + 1)^{n(j) + \delta_n(j)}}{(i_{\text{rate}} + \delta_{i_{\text{rate}}} + 1)^{n(j) + \delta_n(j)} - 1} (c_{\text{inv}}(j) + \delta_{\text{inv}}(j)) \quad \forall j \in TECH$$

This means that for each technology, the uncertainty of its lifetime (n), of its investment cost (c_{inv}) of the interest rate (i_{rate}) are accounted for altogether in the robust optimization, which could generate excessively conservative solutions.

This issue of multiplied uncertain parameters was first addressed by Kwon et al. [153], who considered a robust shortest path problem in which the cost coefficient is the product of two uncertain factors. Given a problem such as $\min \sum_j a_j c_j \mathbf{x}_j$, with $a_j = [a_j, a_j + \delta_{a,j}]$ and $c_j = [c_j, c_j + \delta_{c,j}]$, they show that its robust counterpart is formulated as in Eqs. 4.10.

$$\begin{aligned}
 \min \quad & \sum_j a_j c_j \mathbf{x}_j + \mathbf{z}_u \Gamma_u + \mathbf{z}_v \Gamma_v + \sum_j (\mathbf{p}_j + \mathbf{q}_j) & (4.10) \\
 \text{s.t.} \quad & \mathbf{z}_u - \boldsymbol{\eta}_j + \mathbf{p}_j \geq \delta_{a,j} c_j \mathbf{x}_j & \forall j \\
 & \mathbf{z}_v - \boldsymbol{\pi}_j + \mathbf{q}_j \geq \delta_{c,j} a_j \mathbf{x}_j & \forall j \\
 & \boldsymbol{\eta}_j + \boldsymbol{\pi}_j \geq \delta_{a,j} \delta_{c,j} \mathbf{x}_j & \forall j \\
 & \mathbf{x}_j, \mathbf{p}_j, \mathbf{q}_j, \boldsymbol{\pi}_j, \boldsymbol{\eta}_j, \mathbf{z}_u, \mathbf{z}_v \in \mathbb{R}^+
 \end{aligned}$$

In which the subscripts Γ_u and Γ_v are the control parameters of the two uncertain parameters a and c , respectively; $\mathbf{p}, \mathbf{q}, \boldsymbol{\eta}, \boldsymbol{\pi}, \mathbf{z}$ are the dual variables. This formulation by Kwon et al. [153] extends Bertsimas and Sim [62] as it allows to separately consider the uncertainty of the multiplied uncertain parameters.

In this section, first it is shown how **Obj₁** can be approximated by a simpler formulation. Then, a novel robust formulation is presented, extending Kwon et al. [153] (Eq. 4.10) to obtain the robust counterpart of the studied problem.

Approximation of the annualization factor

Given a total investment C , the *constant annuity* A_t (equal for all $t = 1, \dots, n$), discounting the investment over the n -year lifetime, is calculated by Eq. 4.11, in which NPV indicates the net present value.

$$C = NPV(A_t, i_{rate}, n) = \sum_{t=1}^n \frac{A_t}{(1 + i_{rate})^t} = A_t \sum_{t=1}^n \frac{1}{(1 + i_{rate})^t} = A_t \frac{(i_{rate} + 1)^n - 1}{i_{rate}(i_{rate} + 1)^n} = \frac{A_t}{\tau} \quad (4.11)$$

The obtained formulation of the annualization factor for the investment cost (τ , Eq. 1.2), makes it difficult to develop its robust counterpart. Thus, a simplified formulation to approximate Eq. 1.2 is demonstrated.

The annuity A_t is the sum of two components (Eq. 4.12): M_t , related to the amortization of the capital; I_t , related to the payment of the interests. In the case of a constant annuity, as in Eq. 4.11, M_t increases over the time horizon, while I_t decreases.

$$A_t = M_t + I_t \quad (4.12)$$

Under the assumption of *constant amortization*, the capital cost is equally spread over the n -year

4.1. Uncertainty in the objective function

time horizon, hence $M_t = C/n, \forall t$. In this case, the capital left at the beginning of each period is $C - (t - 1)M_t$ (Eq. 4.13). Assuming that the payments are made at the end of each period, the amount of due interests at the end of each period t (I_t) is calculated based on the left capital (I_t decreases over time). In this way, the total amount of interests paid over the whole time horizon (I_{tot}) is calculated using Eq. 4.14.

$$I_t = (C - (t - 1)M_t)i_{rate} \quad \forall t \quad (4.13)$$

$$\begin{aligned} I_{tot} &= Ci_{rate} + (C - M_t)i_{rate} + (C - 2M_t)i_{rate} + \dots + (C - (n - 1)M_t)i_{rate} \\ &= Ci_{rate} + \frac{n-1}{n}Ci_{rate} + \frac{n-2}{n}Ci_{rate} + \dots + \frac{1}{n}Ci_{rate} \\ &= \frac{1}{n}Ci_{rate} \sum_{t=1}^n t = \frac{1}{n}Ci_{rate} \frac{n(n+1)}{2} = \frac{n+1}{2}Ci_{rate} \end{aligned} \quad (4.14)$$

If the annuity A_t is constant, then I_{tot} is also equally distributed over the n years, as in Eq. 4.15.

$$A_t = M_t + I_t = \frac{C}{n} + \frac{I_{tot}}{n} = \frac{C}{n} + \frac{n+1}{2n}Ci_{rate} \quad (4.15)$$

Which, for high values of n , gives:

$$\tau = \frac{A_t}{C} = \frac{M_t + I_t}{C} \approx \frac{i_{rate}}{2} + \frac{1}{n} \quad (4.16)$$

Following this simplification, Eq. 4.16 offers an approximation of the annualization factor τ as the linear sum of its two components. The exact result (without the need of assuming n big) can be obtained if the payments are made in the middle of each period.

Figure 4.3 compares the exact calculation of the annualization factor τ (Eq. 1.2) with its approximation calculated with Eq. 4.16. To reduce the margin of error in the approximation, a correction factor α is proposed in Eq. 4.17. Given N different lifetimes n , $\Delta_\tau(n)$ ($n = 1, \dots, N$) is the difference between the annualization factor calculated with equation 4.17 and with Eq. 1.2. α is determined by imposing $\sum_n \Delta_\tau(n) = 0$ (Eq. 4.18).

$$\tau = \tau_r + \tau_n = \alpha \frac{i_{rate}}{2} + \frac{1}{n} \quad (4.17)$$

$$\sum_{n=1}^N \Delta_{\tau,n} = \sum_{n=1}^N (\tau(n)[\text{Eq. 4.17}] - \tau(n)[\text{Eq. 1.2}]) = \sum_{n=1}^N \left[\alpha \frac{i_{rate}}{2} + \frac{1}{n} - \frac{i_{rate}(i_{rate} + 1)^n}{(i_{rate} + 1)^n - 1} \right] = 0 \quad (4.18)$$

$$\Rightarrow \alpha = \frac{1}{N} \sum_{n=1}^N \left[\frac{i_{rate}(i_{rate} + 1)^n}{(i_{rate} + 1)^n - 1} - \frac{1}{n} \right] \frac{2}{i_{rate}}$$

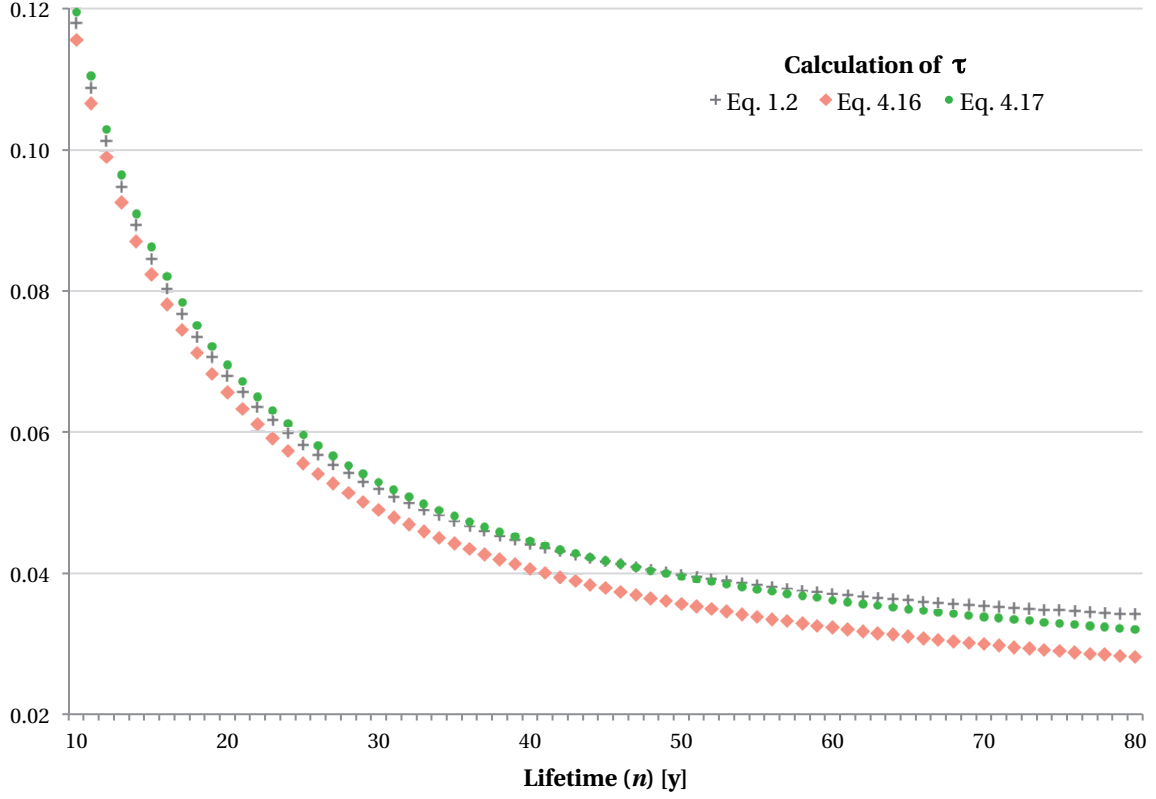


Figure 4.3 – Annualization factor of the investment cost (τ): comparison between exact calculation (Eq. 1.2) and two possible approximations (Eqs. 4.16-4.17).

As an example, for the nominal values of $i_{rate} = 3.215\%$ and considering lifetimes $n \in [10, 80]$ (typical values for energy technologies), $\alpha = 1.25$. The approximation in Eq. 4.17 is added in Figure 4.3, which reveals a good approximation of the exact calculation of τ . Thus, the formulation in Eq. 4.17 is used to derive the robust formulation of the studied MILP problem.

Robust formulation

Based on the simplification introduced in Eq. 4.18, the first half of the objective function can be rewritten as in Eq. 4.19.

$$\mathbf{Obj}_1 = \sum_{j \in \text{TECH}} \frac{i_{rate}(i_{rate} + 1)^{n(j)}}{(i_{rate} + 1)^{n(j)} - 1} c_{inv}(j) \mathbf{F}(j) \approx \sum_{j \in \text{TECH}} \left(\alpha \frac{i_{rate}}{2} + \frac{1}{n(j)} \right) c_{inv}(j) \mathbf{F}(j) \quad (4.19)$$

Thus, in this case the uncertain parameters are multiplied as in Eq. 4.20, in which $a_j = [a_j, a_j + \delta_{a,j}]$, $a'_j = [a'_j, a'_j + \delta_{a',j}]$ and $c_j = [c_j, c_j + \delta_{c,j}]$, $j \in J$.

$$\min \sum_j (a_j + a'_j) c_j \mathbf{x}_j \quad (4.20)$$

Eq. 4.20 cannot be treated with the robust formulation proposed by Kwon et al. [153] (Eq. 4.10). Thus, based on the developments in [153], the following theorem is proven.

Theorem *The robust counterpart of problem 4.20 is expressed by Eqs. 4.21.*

$$\begin{aligned} \min \quad & \sum_j (a_j + a'_j) c_j \mathbf{x}_j + \mathbf{z}_u \Gamma_u + \mathbf{z}_{u'} \Gamma_{u'} + \mathbf{z}_v \Gamma_v + \sum_j (\mathbf{p}_j + \mathbf{p}'_j + \mathbf{q}_j) & (4.21) \\ \text{s.t.} \quad & \mathbf{z}_u - \boldsymbol{\eta}_j + \mathbf{p}_j \geq \delta_{a,j} c_j \mathbf{x}_j & \forall j \\ & \mathbf{z}_{u'} - \boldsymbol{\eta}'_j + \mathbf{p}'_j \geq \delta_{a',j} c_j \mathbf{x}_j & \forall j \\ & \mathbf{z}_v - \boldsymbol{\pi}_j - \boldsymbol{\pi}'_j + \mathbf{q}_j \geq \delta_{c,j} (a_j + a'_j) \mathbf{x}_j & \forall j \\ & \boldsymbol{\eta}_j + \boldsymbol{\pi}_j \geq \delta_{a,j} \delta_{c,j} \mathbf{x}_j & \forall j \\ & \boldsymbol{\eta}'_j + \boldsymbol{\pi}'_j \geq \delta_{a',j} \delta_{c,j} \mathbf{x}_j & \forall j \\ & \mathbf{x}_j, \mathbf{p}_j, \mathbf{p}'_j, \mathbf{q}_j, \boldsymbol{\pi}_j, \boldsymbol{\pi}'_j, \boldsymbol{\eta}_j, \boldsymbol{\eta}'_j, \mathbf{z}_u, \mathbf{z}_{u'}, \mathbf{z}_v \in \mathbb{R}^+ \end{aligned}$$

Proof. Let's consider the robust optimization problem in Eq. 4.22, where the control parameters Γ_u , $\Gamma_{u'}$ and Γ_v , associated to the uncertain parameters a , a' and c , respectively, are positive integers.

$$\begin{aligned} \min_{\mathbf{x}} \max_{\mathbf{u}, \mathbf{u}', \mathbf{v}} \quad & \sum_j (a_j + \delta_{a,j} \mathbf{u}_j + a'_j + \delta_{a',j} \mathbf{u}'_j) (c_j + \delta_{c,j} \mathbf{v}_j) \mathbf{x}_j & (4.22) \\ & \mathbf{u}_j, \mathbf{u}'_j, \mathbf{v}_j \in [0, 1] & \forall j \\ & \sum_j \mathbf{u}_j \leq \Gamma_u, \quad \sum_j \mathbf{u}'_j \leq \Gamma_{u'}, \quad \sum_j \mathbf{v}_j \leq \Gamma_v \end{aligned}$$

Assuming $\mathbf{w}_j = \mathbf{u}_j \mathbf{v}_j, \forall j$ and $\mathbf{w}'_j = \mathbf{u}'_j \mathbf{v}_j, \forall j$, the maximization problem in \mathbf{u} , \mathbf{u}' and \mathbf{v} can be rewritten as in Eqs. 4.23, in which the dual variables are indicated in parentheses.

$$\begin{aligned}
 & \max_{\mathbf{u}, \mathbf{u}', \mathbf{v}, \mathbf{w}, \mathbf{w}'} \sum_j (\delta_{a,j} c_j \mathbf{u}_j + \delta_{a',j} c_j \mathbf{u}'_j + a_j \delta_{c,j} \mathbf{v}_j + \delta_{a,j} \delta_{c,j} \mathbf{w}_j + a'_j \delta_{c,j} \mathbf{v}_j + \delta_{a',j} \delta_{c,j} \mathbf{w}'_j) \mathbf{x}_j & (4.23) \\
 & \text{s.t. } \mathbf{u}_j - 1 \leq 0 \quad (\mathbf{p}_j) & \forall j \\
 & \quad \mathbf{u}'_j - 1 \leq 0 \quad (\mathbf{p}'_j) & \forall j \\
 & \quad \mathbf{v}_j - 1 \leq 0 \quad (\mathbf{q}_j) & \forall j \\
 & \quad -\mathbf{u}_j + \mathbf{w}_j \leq 0 \quad (\boldsymbol{\eta}_j) & \forall j \\
 & \quad -\mathbf{v}_j + \mathbf{w}_j \leq 0 \quad (\boldsymbol{\pi}_j) & \forall j \\
 & \quad -\mathbf{u}'_j + \mathbf{w}'_j \leq 0 \quad (\boldsymbol{\eta}'_j) & \forall j \\
 & \quad -\mathbf{v}_j + \mathbf{w}'_j \leq 0 \quad (\boldsymbol{\pi}'_j) & \forall j \\
 & \quad \sum_j \mathbf{u}_j - \Gamma_u \leq 0 \quad (\mathbf{z}_u) \\
 & \quad \sum_j \mathbf{u}'_j - \Gamma_{u'} \leq 0 \quad (\mathbf{z}_{u'}) \\
 & \quad \sum_j \mathbf{v}_j - \Gamma_v \leq 0 \quad (\mathbf{z}_v) \\
 & \quad \mathbf{u}, \mathbf{u}', \mathbf{v}, \mathbf{w}, \mathbf{w}' \in \mathbb{R}^+
 \end{aligned}$$

Problem 4.23 can be written in matrix notation as in Eq. 4.24, in which $I_{|J|}$ is the $|J| \times |J|$ identity matrix, $\mathbf{1}_{|J|}$ is a vector of size $|J| \times 1$ with all elements equal to 1, $\mathbf{0}_{|J|}$ is a vector of size $|J| \times 1$ with all elements equal to 0, $\underline{\mathbf{u}} = [\mathbf{u}_1, \mathbf{u}_2, \dots, \mathbf{u}_{|J|}]$ (the same applies to $\underline{\mathbf{u}'}$, $\underline{\mathbf{v}}$, $\underline{\mathbf{w}}$, $\underline{\mathbf{w}'}$), and empty fields are all zeros.

$$\begin{array}{l}
 \text{(Row Group 1)} \\
 \text{(Row Group 2)} \\
 \text{(Row Group 3)} \\
 \text{(Row Group 4)} \\
 \text{(Row Group 5)} \\
 \text{(Row Group 6)} \\
 \text{(Row Group 7)} \\
 \text{(Row 8)} \\
 \text{(Row 9)} \\
 \text{(Row 10)}
 \end{array}
 \left[\begin{array}{c|c|c|c|c}
 I_{|J|} & & & & \\
 & I_{|J|} & & & \\
 & & I_{|J|} & & \\
 -I_{|J|} & & & I_{|J|} & \\
 & & -I_{|J|} & I_{|J|} & \\
 & -I_{|J|} & & & I_{|J|} \\
 & & -I_{|J|} & & I_{|J|} \\
 \hline
 \mathbf{1}_{|J|}^T & & & & \\
 & \mathbf{1}_{|J|}^T & & & \\
 \hline
 & & \mathbf{1}_{|J|}^T & &
 \end{array} \right]
 \begin{bmatrix}
 \underline{\mathbf{u}} \\
 \underline{\mathbf{u}'} \\
 \underline{\mathbf{v}} \\
 \underline{\mathbf{w}} \\
 \underline{\mathbf{w}'}
 \end{bmatrix}
 \leq
 \begin{bmatrix}
 \mathbf{1}_{|J|} \\
 \mathbf{1}_{|J|} \\
 \mathbf{1}_{|J|} \\
 \mathbf{0}_{|J|} \\
 \mathbf{0}_{|J|} \\
 \mathbf{0}_{|J|} \\
 \mathbf{0}_{|J|} \\
 \mathbf{0}_{|J|} \\
 \Gamma_u \\
 \Gamma_{u'} \\
 \Gamma_v
 \end{bmatrix}
 \quad (4.24)$$

The constraint matrix \mathcal{A} is *totally unimodular*, i.e. each subdeterminant of \mathcal{A} is 0, +1, or -1. In fact, total unimodularity is preserved under the following operations: *i)* taking the transpose; *ii)* multiplying a row or column by -1; *iii)* adding an all-zero row or column, or adding a row or column

with one non-zero, being ± 1 [155]. Based on *iii*), row groups 1 to 3 can be eliminated from the analysis. Focusing on rows 4 to 10, Ghouila-Houri [156] shows that a necessary and sufficient condition for total unimodularity is that each collection of columns (or rows, based on *i*) of \mathcal{A} can be split into two parts so that the sum of the columns (rows) in one part minus the sum of the columns (rows) in the other part is a vector with entries only 0, +1, and -1 . Equivalently, for any collection of rows, if each row is multiplied by +1 or -1 (based on *ii*)), then the sum of rows must have only $-1, 0, +1$ in each column [153]. For any collection of rows 4-10 of \mathcal{A} , this is obtained by multiplying rows 5, 6 and 9 by -1 , and by appropriately multiplying row 10 by ± 1 . This proves the total unimodularity of \mathcal{A} .

Given an optimization problem as in Eq. 4.2, if the constraint matrix \mathcal{A} is totally unimodular and the coefficients b_j are all integers, a solution \mathbf{x}_j of the problem is integral. Hence, in problem Eq. 4.23 the decision variables $\mathbf{u}_j, \mathbf{u}'_j, \mathbf{v}_j, \mathbf{w}_j, \mathbf{w}'_j$ are all binaries at optimality. As a consequence, at optimality, $\mathbf{w}_j = \mathbf{u}_j \mathbf{v}_j, \forall j$ and $\mathbf{w}'_j = \mathbf{u}'_j \mathbf{v}_j, \forall j$. This proves the previously assumed equalities, and thus the equivalence between formulation 4.23 and the inner problem of Eqs. 4.22.

The dual problem of formulation 4.23 is expressed by Eqs. 4.25.

$$\begin{aligned}
 \min \quad & \mathbf{z}_u \Gamma_u + \mathbf{z}_{u'} \Gamma_{u'} + \mathbf{z}_v \Gamma_v + \sum_j (\mathbf{p}_j + \mathbf{p}'_j + \mathbf{q}_j) & (4.25) \\
 \text{s.t.} \quad & \mathbf{z}_u - \boldsymbol{\eta}_j + \mathbf{p}_j \geq \delta_{a,j} c_j \mathbf{x}_j & \forall j \\
 & \mathbf{z}_{u'} - \boldsymbol{\eta}'_j + \mathbf{p}'_j \geq \delta_{a',j} c_j \mathbf{x}_j & \forall j \\
 & \mathbf{z}_v - \boldsymbol{\pi}_j - \boldsymbol{\pi}'_j + \mathbf{q}_j \geq \delta_{c,j} (a_j + a'_j) \mathbf{x}_j & \forall j \\
 & \boldsymbol{\eta}_j + \boldsymbol{\pi}_j \geq \delta_{a,j} \delta_{c,j} \mathbf{x}_j & \forall j \\
 & \boldsymbol{\eta}'_j + \boldsymbol{\pi}'_j \geq \delta_{a',j} \delta_{c,j} \mathbf{x}_j & \forall j \\
 & \mathbf{x}_j, \mathbf{p}_j, \mathbf{p}'_j, \mathbf{q}_j, \boldsymbol{\pi}_j, \boldsymbol{\pi}'_j, \boldsymbol{\eta}_j, \boldsymbol{\eta}'_j, \mathbf{z}_u, \mathbf{z}_{u'}, \mathbf{z}_v \in \mathbb{R}^+
 \end{aligned}$$

Hence, using strong duality, the robust counterpart of problem 4.20 is expressed by Eqs. 4.21. \square

Complete formulation for the objective function

The demonstrated novel robust formulation for the first half of the objective function (**Obj₁**) is linearly combined the robust counterpart of **Obj₂** (Eqs. 4.4) to obtain the complete formulation of the robust counterpart of Eqs. 4.1.

$$\begin{aligned}
\min \quad & \sum_{j \in TECH} (\tau_r + \tau_n(j)) c_{inv}(j) \mathbf{F}(j) + \sum_{j \in TECH} c_{maint}(j) \mathbf{F}(j) + \sum_{i \in RES} \sum_{t \in T} c_{op}(i, t) \mathbf{F}_t(i, t) t_{op}(t) \quad (4.26) \\
& + \mathbf{z}_r \Gamma_r + \mathbf{z}_n \Gamma_n + \mathbf{z}_{inv} \Gamma_{inv} + \mathbf{z}_0 \Gamma_0 + \sum_{j \in TECH} (\mathbf{p}_r(j) + \mathbf{p}_n(j) + \mathbf{p}_{inv}(j) + \mathbf{p}_{maint}(j)) + \sum_{i \in RES} \sum_{t \in T} \mathbf{p}_{op}(j)(j, t) \\
\text{s.t.} \quad & \mathbf{z}_r + \sum_{j \in TECH} (-\boldsymbol{\eta}_r(j) + \mathbf{p}_r(j)) \geq \delta_{\tau_r} \sum_{j \in TECH} (c_{inv}(j) \mathbf{F}(j)) \\
& \mathbf{z}_n - \boldsymbol{\eta}_n(j) + \mathbf{p}_n(j) \geq \delta_{\tau_n}(j) c_{inv}(j) \mathbf{F}(j) \quad \forall j \in TECH \\
& \mathbf{z}_{inv} - \boldsymbol{\pi}_{inv}(j) - \boldsymbol{\pi}'_{inv}(j) + \mathbf{p}_{inv}(j) \geq \delta_{inv}(j) (\tau_r + \tau_n(j)) \mathbf{F}(j) \quad \forall j \in TECH \\
& \boldsymbol{\eta}_r(j) + \boldsymbol{\pi}_{inv}(j) \geq \delta_{\tau_r} \delta_{inv}(j) \mathbf{F}(j) \quad \forall j \in TECH \\
& \boldsymbol{\eta}_n(j) + \boldsymbol{\pi}'_{inv}(j) \geq \delta_{\tau_n}(j) \delta_{inv}(j) \mathbf{F}(j) \quad \forall j \in TECH \\
& \mathbf{z}_0 + \mathbf{p}_{maint}(j) \geq \delta_{maint}(j) \mathbf{y}_{maint}(j) \quad \forall j \in TECH \\
& \mathbf{F}(j) \leq \mathbf{y}_{maint}(j) \quad \forall j \in TECH \\
& \mathbf{z}_0 + \sum_{t \in T} \mathbf{p}_{op}(i, t) \geq \delta_{op}(i) \sum_{t \in T} \mathbf{y}_{op}(i, t) \quad \forall i \in RES \\
& \mathbf{F}_t(i, t) t_{op}(t) \leq \mathbf{y}_{op}(i, t) \quad \forall i \in RES, \forall t \in T \\
& \mathbf{z}_r, \mathbf{z}_n, \mathbf{z}_{inv}, \mathbf{z}_0, \mathbf{p}_r, \mathbf{p}_n, \mathbf{p}_{inv}, \mathbf{p}_{maint}, \mathbf{p}_{op}, \boldsymbol{\eta}_r, \boldsymbol{\eta}_n, \boldsymbol{\pi}_{inv}, \boldsymbol{\pi}'_{inv}, \mathbf{y}_{maint}, \mathbf{y}_{op} \in \mathbb{R}^+
\end{aligned}$$

In which δ is the difference between the upper bound and the nominal value of the uncertain parameters. In particular, $\delta_{\tau_r} = \frac{1}{2}(i_{rate}(\alpha' - \alpha) + \alpha' \delta_{i_{rate}})$, with $\delta_{i_{rate}}$ being the maximum worst case deviation from the nominal value of the interest rate, α being the correction factor for the nominal value of the interest rate (Eq. 4.18), and α' being the correction factor for its worst case value (Eq. 4.18); $\delta_{\tau_n}(j) = \frac{\delta_n(j)}{n(j)(n(j) - \delta_n(j))}$, with $\delta_n(j)$ being the maximum worst case deviation from the nominal value of the technologies' lifetime.

4.1.3 Application to the case study

Formulation 4.26 is applied to the example MILP model presented in Chapter 1, with the uncertainty ranges in Table 2.1. In the objective function there is a total of 160 uncertain inputs, which are controlled by four different protection parameters: $\Gamma_r \in [0, 1]$ for i_{rate} , $\Gamma_n \in [0, 51]$ for n , $\Gamma_{inv} \in [0, 52]$ for c_{inv} , $\Gamma_0 \in [0, 56]$ for c_{maint} and c_{op} . To evaluate how the energy system configuration evolves from the deterministic solution ($\Gamma_k = 0, \forall k \in K = \{r, n, inv, 0\}$) to "Soyster's" solution ($\Gamma_k = |J_k|, \forall k$), a method is needed to define the order in which the control parameters are made vary.

A first option consists in defining only one control parameter Γ_{obj} , defined as $\Gamma_{obj} = \sum_k \Gamma_k$, hence $\Gamma_{obj} \in [0, 160]$. The model is then run according to algorithm 1, in which Γ_K is a vector containing the values of all Γ_k , and Γ' indicates a temporary assignment within a loop.

```

i ← 0
 $\Gamma_{K,i} \leftarrow 0$ 
Run model ( $\Gamma_{K,i}$ ) & save output ( $\Gamma_{K,i}$ )
while i < |Jobj| do
    i ← i + 1
    for all k ∈ K do
         $\Gamma'_{K,i} \leftarrow \Gamma_{K,i-1}$ 
         $\Gamma'_{k,i} \leftarrow \Gamma_{k,i-1} + 1$ 
         $\mathbf{C}_{\text{tot}}(k) = \text{Run model } (\Gamma'_{K,i})$ 
        if  $\mathbf{C}_{\text{tot}}(k) \geq \max_k \mathbf{C}_{\text{tot}}$  then
             $\Gamma_{K,i} \leftarrow \Gamma'_{K,i}$ 
        end if
    end for
    save output ( $\Gamma_{K,i}$ )
end while

```

Algorithm 1 – Procedure followed to vary the control parameters in the objective function

Following the idea of Bertsimas and Sim [62], at each step, corresponding to a unitary increment of Γ_{obj} , the effect of incrementing a different protection parameter Γ_k is separately evaluated, and the protection parameter generating the worst case objective is identified. Overall, this option requires $(|J_{obj}| + 1) \times |K|$ model runs.

An alternative and simpler solution consists in additionally defining $\mathbf{z}_{obj} = \mathbf{z}_k, \forall k \in K$, and thus replacing $\mathbf{z}_{obj}\Gamma_{obj} = \mathbf{z}_r\Gamma_r + \mathbf{z}_n\Gamma_n + \mathbf{z}_{inv}\Gamma_{inv} + \mathbf{z}_0\Gamma_0$ in formulation 4.26. This means directly using Γ_{obj} as the control parameter of the objective function, which only requires $|J_{obj}| + 1$ model runs. On the one hand, differently from the first option in algorithm 1, this does not ensure the integrality of Γ_r , Γ_n and Γ_{inv} , which is a needed assumption to prove the previously presented novel robust formulation. On the other hand, interestingly, for the studied problem this second option is equivalent from a practical standpoint to the first option. In fact, numerical tests comparing the two alternatives reveal that the average deviation in the objective value is 0.01% ($\sigma = 0.03\%$), and reaches at maximum 0.28%. Thus, in the following, the second option is used.

Two issues are additionally addressed to apply the robust formulation to the considered case study. First, as discussed in Section 1.1.2, CCS technologies are included in the MILP model (Figure 1.2) via the definition of “CCS resources”. As an example, a standard CCGT power plant uses the NG resource as an input, while a CCGT power plant with CCS uses the NG CCS resource as an input. This means that there are two instances of the same resource (NG in this case) to account for its different use. When considering cost uncertainty, the cost variation must be identical for the two instances. For NG, this is imposed by Eq. 4.27, which equivalently applies to the other “CCS resources” included in

the model.

$$\mathbf{z}_0 + \sum_{t \in T} (\mathbf{p}_{\text{op}}(i, t) + \mathbf{p}_{\text{op}}(k, t)) \geq \delta_{\text{op}}(i) \sum_{t \in T} (\mathbf{y}_{\text{op}}(i, t) + \mathbf{y}_{\text{op}}(k, t)) \quad i = NG, k = NG \text{ (CCS)} \quad (4.27)$$

Second, in Eqs. 4.26, it is considered that c_{op} varies equally in the different months of the reference year, consistently with the parameter grouping in Section 2.2.1. Based on the GSA results (Table 3.3), c_{op} is the most impacting parameter on the investment decision. Thus, in this application, c_{op} is made vary gradually towards the worst case ($c_{\text{op}} + \delta_{\text{op}}$), i.e. in six sequential steps of size $\delta_{\text{op}}/6$. Numerical tests show that this choice allows a more gradual transition towards the worst case, without altering the trade-offs between the different robust solutions.

Results

Figures 4.4-4.7 illustrate how the optimal configuration of the energy system changes when gradually increasing (at integral steps) the protection parameter Γ_{obj} from its lower bound ($\Gamma_{\text{obj}} = 0$, deterministic solution) to its upper bound ($\Gamma_{\text{obj}} = |J_{\text{obj}}|$, “Soyster’s” solution).

The energy strategy changes dramatically when uncertainty is accounted for. In terms of energy resources (Figure 4.4), the deterministic solution (Figure 4.2) is dominated by NG. For medium levels of Γ_{obj} , there is a “risk pooling” effect, i.e. the dependency on only one resource is replaced by a mix of alternatives (coal, renewables and electricity imports) to offer more protection against worst case. For high levels of Γ_{obj} , the solution stabilizes towards a mix of NG (used in more efficient technologies) and renewables. This tendency, i.e. a diversification for medium uncertainty budgets and a stabilization on a restricted set of alternatives for very low and very high protection levels, is rather common in robust optimization. In fact, Bertsimas and Sim [62] and Nicolas [144] observe similar results in their numerical experiments.

An analysis of the output shows that the first parameter which is “activated” (at $\Gamma_{\text{obj}} = 1$) is i_{rate} , followed by fixed costs (hydro dams, grids, efficiency) and by the operating cost of resources; investment-related parameters (c_{inv} , c_{maint} , n) are activated for higher values of Γ_{obj} . This trade-off between operating and investment cost uncertainties pushes the solution in opposite directions, as showed by the performance indicators in Figure 4.5. The highest reduction of fossil fuel consumption (-42%) in the system and the lowest emissions (-23%) compared to the deterministic case are obtained at medium uncertainty budgets ($\Gamma_{\text{obj}} = 31$ and $\Gamma_{\text{obj}} = 62$, respectively), while at higher protection levels there is again an increase of both indicators. However, the cost of resources emerges as the most impacting parameter on the energy strategy, and thus robust solutions are in general less dependent on volatile imported resources. As an example, the fully robust solution ($\Gamma_{\text{obj}} = |J_{\text{obj}}|$), features lower emissions (-20%), a lower consumption of fossils (-23%) and more installed capacity (+8%) compared to the deterministic case.

4.1. Uncertainty in the objective function

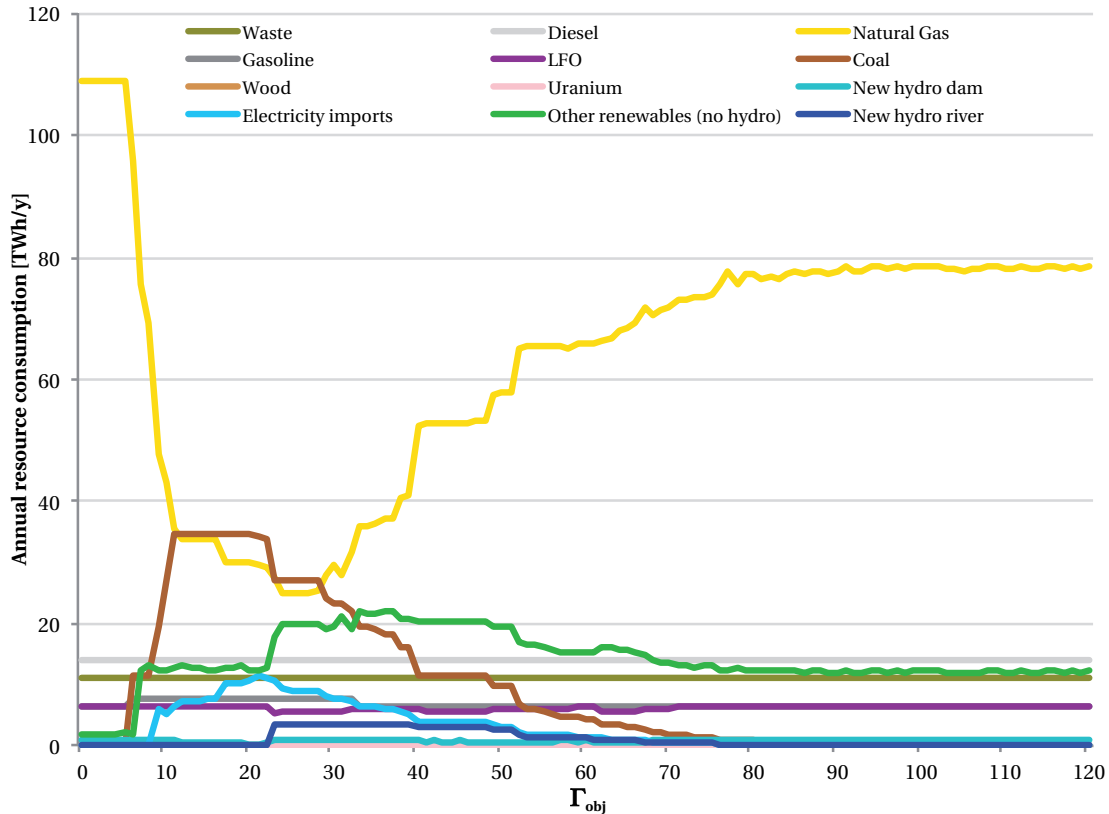


Figure 4.4 – Evolution of the energy system configuration vs. protection level Γ_{obj} : annual consumption of resources.

In the deterministic solution, the share of electricity production (Figure 4.6) not covered by hydro is entirely supplied by CCGT, with 3 GW_e of installed capacity. Wind is included in the mix at low protection levels ($\Gamma_{obj} \geq 7$), while for medium uncertainty budgets a diversified mix (including coal, electricity imports, PV, new hydro run-of-river and dams) is chosen; CHP installed capacity steadily increases when augmenting the protection level. With increasing protection levels, there is a tendency to shift towards renewables and more efficient technologies, i.e. towards higher investment-to-operating cost ratios. As an example, coal is first used in standard ultra-supercritical (U-S) power plants, and then in more efficient integrated gasification combined cycle (IGCC) plants; NG is initially burned in standard CCGT plants, and then in CHP units. Efficiency thus acts as an *uncertainty damper* as, by optimizing the conversion of resources, it reduces the exposure of the energy system to the volatility of fuel prices.

A similar trend is observed for heat supply (Figure 4.7). The deterministic solutions, mostly relying on the combustion of fossil fuels in boilers, are gradually replaced by HPs in the case of decentralized heat, and by CHP for centralized heat (DHN) and industry. The option of centralized heat supply (%_{Dhn}) is optimal for medium uncertainty budgets.

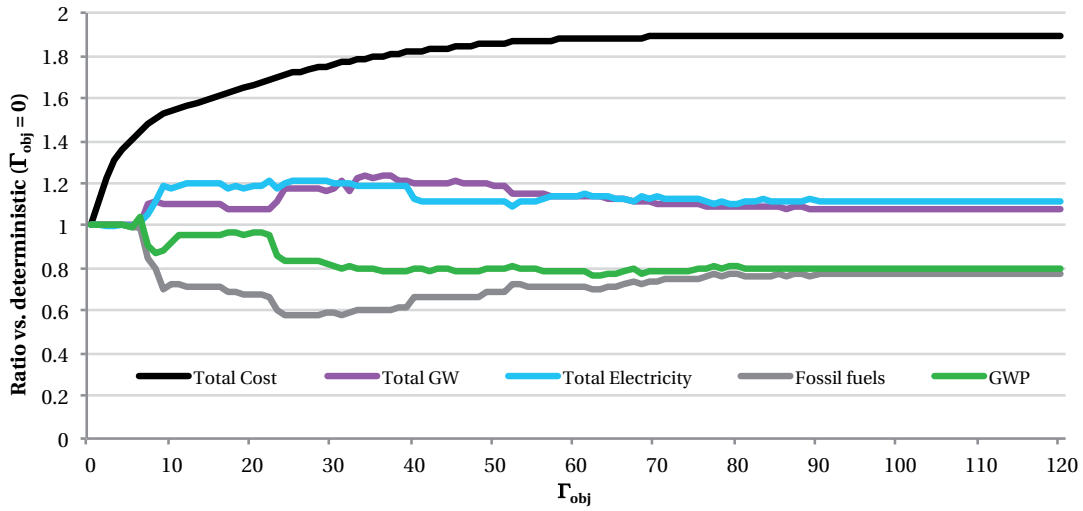


Figure 4.5 – Performance indicators (cost, GHG emissions, installed capacity, electricity in the system, consumption of fossil fuels.) vs. protection level Γ_{obj} : ratio vs. deterministic solution ($\Gamma_{obj} = 0$).

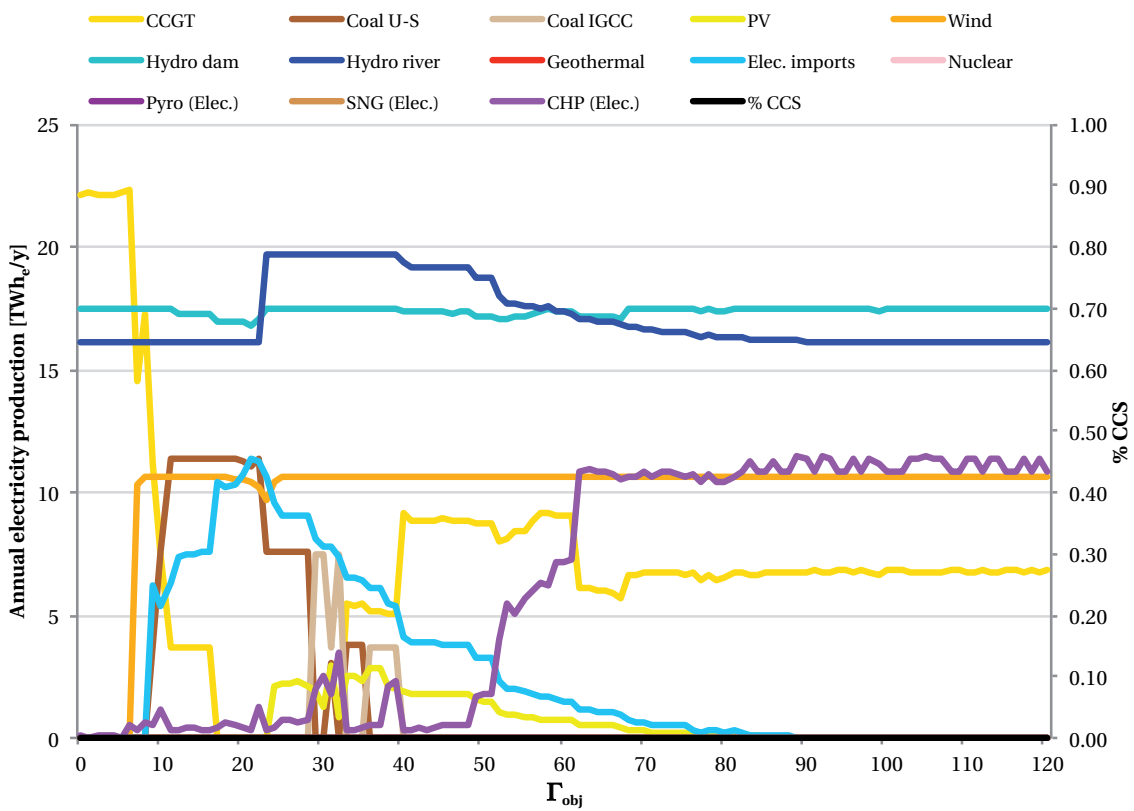


Figure 4.6 – Evolution of the energy system configuration vs. protection level Γ_{obj} : electricity production.

4.1. Uncertainty in the objective function

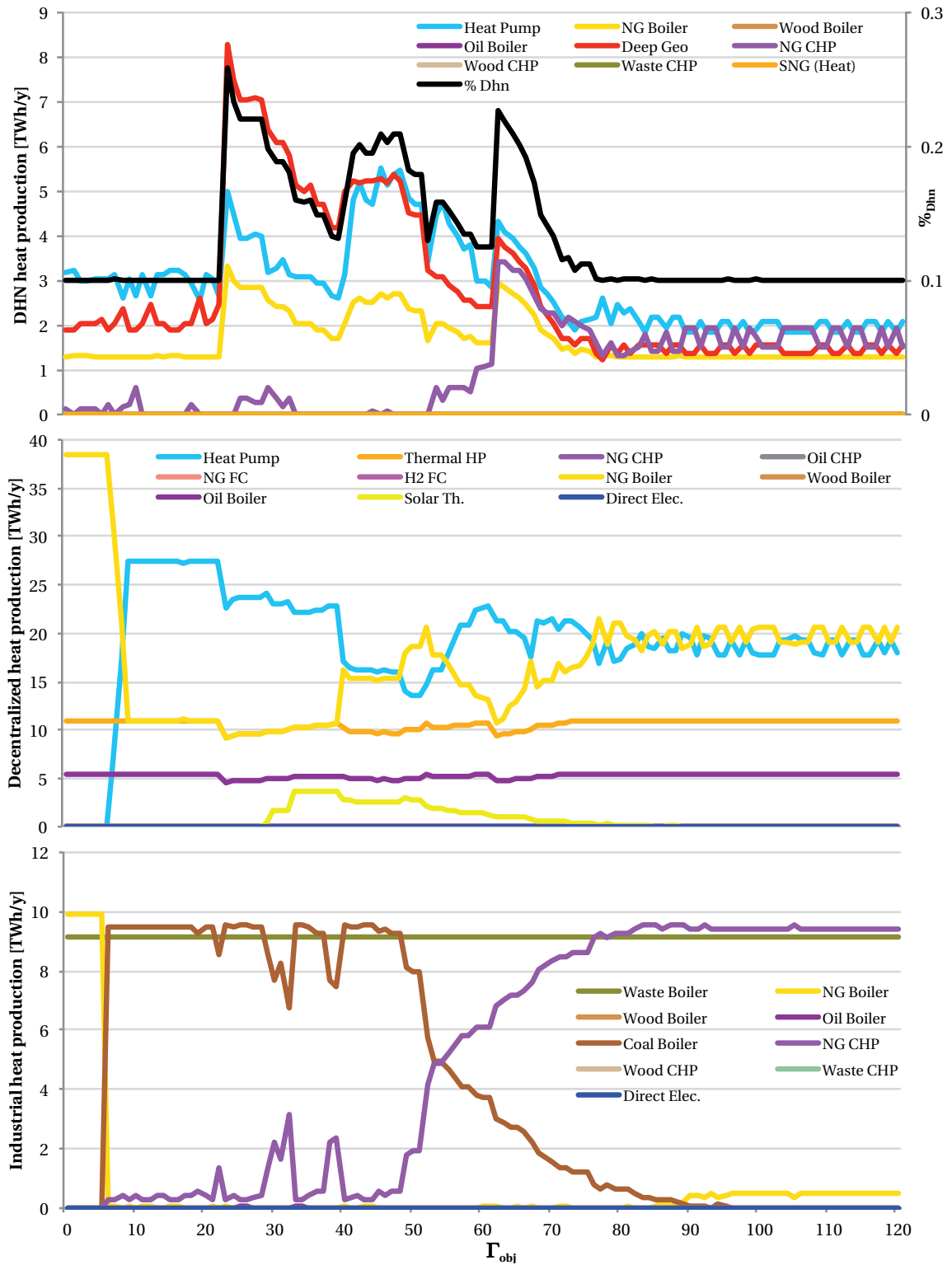


Figure 4.7 – Evolution of the energy system configuration vs. protection level Γ_{obj} : DHN (top), decentralized (middle) and industrial (bottom) heat production.

Overall, the results show the interest of the solutions obtained at medium protection levels, and thus of the approach by Bertsimas and Sim [62], which allows to identify them. In fact, various technologies and system configurations appear only at medium uncertainty budgets. In the standard robust optimization approach by Soyster [60], assuming all parameters at worst case, these solutions do not emerge.

4.1.4 Evaluation of the robust solutions

When robust optimization aims at ensuring feasibility against constraint violations (e.g. inability to meet the demand), robust solutions are normally compared based on the value of the objective, i.e. by measuring the difference in the cost of the robust solutions compared to the nominal case. In fact, by increasing protection against worst case, constraint violations are reduced at the price of a higher objective value. Bertsimas and Sim [62] define this trade-off as the *price of robustness*.

However, when uncertainty is considered for the cost coefficients in the objective, the use of this metric is discouraged. In fact, as discussed by Gorissen et al. [125], each value of Γ_{obj} corresponds to a different “scenario” for the uncertain parameters. Thus, the objectives at different values of Γ_{obj} are not directly comparable. In this case, they recommend comparing solutions via *simulation* studies.

To do this, 15 representative solutions are selected using the *k-medoids* algorithm [157], which clusters the obtained energy system configurations based on the total annual output of technologies and resources. These representative energy system configurations are characterized in Table 4.2.

Two sets of simulations are carried out to evaluate the performance of these configurations. In the first one, all the decision variables of the MILP problem are fixed to the values obtained in output of the robust optimization runs. This means that both the investment and the operation strategy of the system are fixed for all the simulations. The MILP model is run $n_{sample} = 10000$ times sampling the values of the uncertain parameters (i_{rate} , c_{inv} , c_{maint} , c_{op} , n) from uniform distributions over the entire uncertainty range (Table 2.1). For all the simulations, the fixed costs which are constant for all the solutions and which have a high impact on the objective - such as the investment cost of existing hydroelectric power plants, of the electricity grid and of energy efficiency measures - are set to zero. The results of the first set of simulations are displayed by the full lines in Figure 4.8. For all the representative solutions in Table 4.2, the mean (\bar{x}), standard deviation (σ) and the maximum value over the different runs are compared to the same statistics for the deterministic case ($\Gamma_{obj} = 0$). On the one hand, robust solutions have a higher average total cost than the nominal case ($\bar{x}_0 = 7786$ MCHF/y). On the other hand, the standard deviation of robust solutions is significantly lower, reaching almost half of the deterministic case standard deviation ($\sigma_0 = 1694$ MCHF/y) for $\Gamma_{obj} \in \{27; 30; 37\}$.

Table 4.2 – Characterization of the representative energy system configurations selected via *k-medoids* clustering.

Γ_{obj}	Electricity production										Other					Renewables ^a [TWh/y]
	CCGT [GW _e]	Coal [GW _e]	PV [GW _e]	Wind [GW _e]	New dams [GW _e]	New river [GW _e]	Imports [TWh _e /y]	Boilers [GW _{th}]	CHP [GW _{th}]	Elec HPs [GW _{th}]	Solar Th. [GW _{th}]	Deep Geo [GW _{th}]	%Dth [-]			
0	3	0	0	0	0.428	0	0	22.26	0.02	0.75	0	0.25	0.100	2.76		
6	3	0	0	0	0.440	0	0	22.29	0.08	0.73	0	0.25	0.100	2.79		
7	2	0	0	5.10	0.440	0	0	19.49	0.04	3.57	0	0.28	0.100	13.2		
8	2.5	0	0	5.30	0.440	0	0.01	15.34	0.1	7.57	0	0.35	0.100	13.9		
9	1.5	0.5	0	5.30	0.440	0	6.20	11.29	0.08	11.73	0	0.25	0.100	13.5		
14	0.5	1.5	0	5.30	0.352	0	7.51	11.27	0.06	11.75	0	0.28	0.100	13.4		
19	0	1.5	0	5.25	0.208	0	10.29	11.27	0.08	11.63	0	0.39	0.100	13.6		
27	0	1	2.30	5.30	0.440	0.850	9.09	13.18	0.12	10.54	0	1.17	0.221	24.5		
30	0	1 ^b	1.32	5.30	0.440	0.850	7.78	12.46	0.38	10.10	1.63	1.01	0.189	24.2		
37	1	0.5 ^c	2.91	5.30	0.440	0.850	6.12	12.02	0.08	9.69	3.64	0.78	0.149	26.4		
44	1.5	0	1.85	5.30	0.367	0.726	3.89	15.03	0.06	7.70	2.68	0.81	0.195	24.2		
56	1.5	0	0.85	5.30	0.349	0.334	1.79	13.40	0.86	8.71	1.59	0.37	0.142	18.0		
68	1	0	0.36	5.30	0.427	0.157	0.75	12.78	1.56	9.22	0.67	0.32	0.148	15.6		
91	1	0	0.02	5.30	0.440	0.006	0.03	14.12	1.56	7.67	0	0.21	0.100	13.2		
200	1	0	0	5.30	0.440	0	0	13.53	1.64	8.18	0	0.18	0.100	12.9		

^aIncluding PV, wind, new hydro dam and run-of-river plants, deep geothermal, solar thermal^bintegrated gasification combined cycle (IGCC)

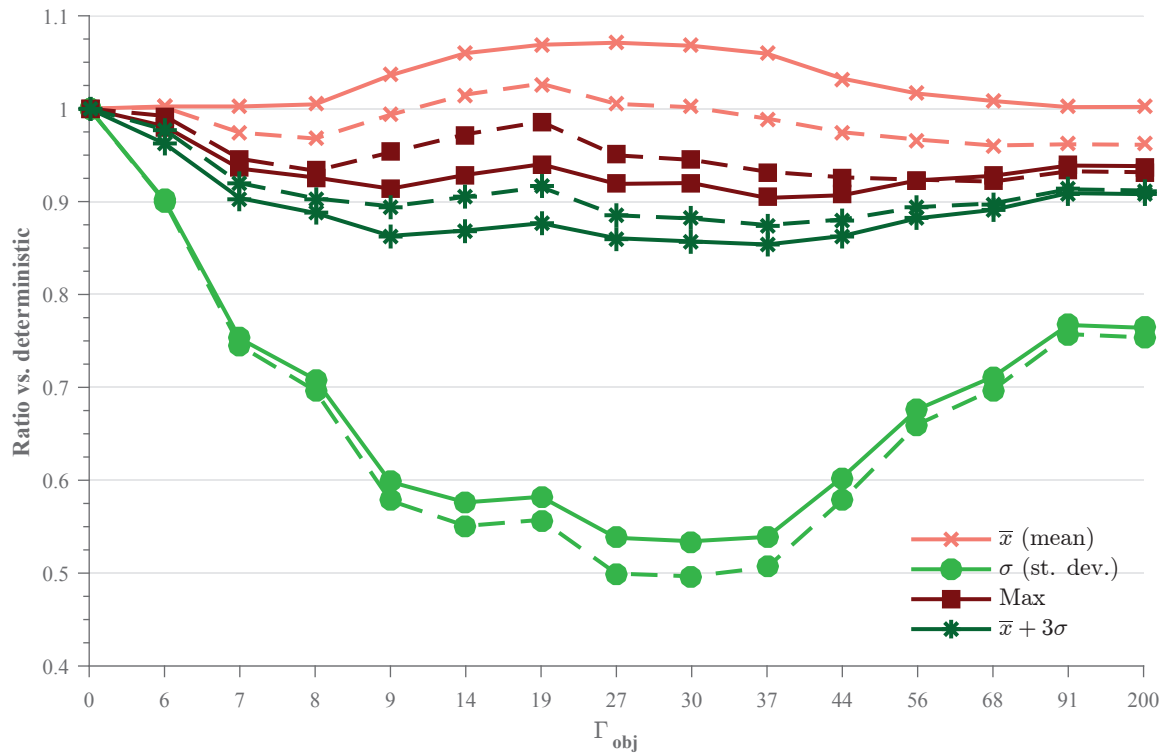


Figure 4.8 – Simulation results for the robust solutions in Table 4.2: mean (\bar{x}), standard deviation (σ), maximum value and $\bar{x} + 3\sigma$ for the objective value. First test (full lines): all decision variables fixed, uncertain parameters (i_{rate} , c_{inv} , c_{maint} , c_{op} , n) sampled from entire uncertainty range. Second test (dashed lines): only investment decisions are fixed (free resources), uncertain parameters (c_{op}) sampled from worst-case part of range.

Looking at the worst-case performance, the maximum objective value for all robust solutions is lower than in the deterministic case; also, evaluating the likelihood of being 3σ higher than the mean, it emerges that solutions obtained at medium uncertainty budgets (with a higher penetration of renewables) offer more stability and protection against unfavorable realizations of uncertainty. Similarly to the results presented in the previous section, the indicators in Figure 4.8 denote a sharp deviation away from the deterministic solution for low and medium protection levels, and then a convergence back in the direction of the deterministic solution for higher values of Γ_{obj} . Interestingly, a similar trend for the standard deviation is observed in the portfolio example application in Bertsimas and Sim [62].

The first set of simulations, in which both the investment and operation decision variables are fixed, offers precious insights on the behavior of the robust solutions compared with the deterministic case. However, in real energy systems applications, once the investment strategy is defined, the operating strategy of the system can be - at least partly - adapted based on the realization of the uncertain parameters. As Gorissen et al. [125] recommend, simulation “*should reflect the real-life situation*” and “*the uncertainty set that is used for optimization may be different than the set for*

evaluation". Thus, in the second set of simulations, investment-related decision variables (such as the installed capacity of technologies, \mathbf{F}) and parameters (such as i_{rate} , c_{inv} , c_{maint} , n) are fixed, while operating decision variables (such as \mathbf{F}_t) are left free, i.e. determined by the optimization, and uncertainty is considered only for the cost of resources. Thus, a difference is made in the simulations between *here-and-now* (present) uncertainties, which are known once the investment decision is taken, and *wait-and-see* (future) uncertainties. Also, to evaluate worst-case performance, only worst-case realizations of the operating cost are considered, i.e. c_{op} is drawn from a uniform distribution having as lower bound the nominal value, and as upper bound the maximum cost.

The results of the second set of simulations are displayed by the dashed lines in Figure 4.8. The main difference with the results obtained with the first set of simulations is that, in this case, most robust solutions feature both a lower average total cost and a lower standard deviation compared to the deterministic case ($\bar{x}_0 = 9970$ MCHF/y, $\sigma_0 = 1033$ MCHF/y). This means that, in real energy system applications, robust solutions can even *on average* perform better than the deterministic solution, when faced with adverse uncertainty.

Overall, the two sets of simulations further confirm the interest of the presented robust optimization approach, i.e. of generating solutions at low and medium protection levels. Also, the high standard deviations reveal that uncertainty strongly impacts the performance of a given solution. In fact, the coefficient of variation ($c_v = \frac{\sigma}{\bar{x}}$) of the different solutions is between [11%, 22%] in the first set of simulations, and [5%, 10%] in the second set. These values are generally higher than the difference among the average performance of the solutions (Figure 4.8). This suggests that, when accounting for uncertainty, the difference between the evaluated energy strategies is of the same order of magnitude of the variability of the individual solutions. Thus, a robust energy strategy with a higher penetration of renewables might be not significantly more costly than a deterministic, fossil-based, alternative.

4.2 Uncertainty in the constraints

Robust optimization works *constraint-wise*, i.e. the robust formulations are applied individually to the different constraints of an optimization model. In energy system cost minimization problems, most impacting uncertain parameters are often found in a "special" constraint, i.e. the objective function. This justifies the focus on uncertainty in the objective in most of the reviewed literature. However, as revealed by the GSA results in Table 3.3, various impacting parameters - such as the availability of resources (*avail*), the capacity factors ($c_{p,t}$), the demand (*endUses_{year}*) and the conversion efficiencies (η) - are also found in the other constraints.

In the reviewed literature, uncertainty in the constraints is seldom addressed. When it is addressed, uncertainty is normally considered only for an *a priori* selected subset of parameters, most often the demand (to ensure that demand is met for any realization of the uncertain parameters). This

is mainly due to two reasons: *i*) the fact that the same uncertain parameters appear in multiple constraints; *ii*) the fact that most constraints contain very few - and often only one - uncertain parameters.

The first issue, highlighted by Hajimiragha et al. [132] (“*given the limitation of the robust optimization techniques [...], uncertain parameters [...] which simultaneously appear in multiple constraints and the objective function cannot be handled by this methodology*”), can often be addressed by improving the model structure, aiming at obtaining concise and compact formulations. This constitutes both the motivation and the content of the first chapter of this thesis.

The second issue, discussed by Rager et al. [158], can be exemplified by a model with N constraints, each of them with only one uncertain parameter. Hence, if applying Bertsimas and Sim [62], $\Gamma_i \in [0, 1], \forall i = 1, \dots, N$. In this case, on the one hand the problem becomes trivial for the i -th constraint; on the other hand, the problem becomes combinatorial when considering all the N constraints, as there are N binary protection parameters Γ_i . Although this second issue can also be addressed (at least partly) by working on the model formulation, it constitutes nonetheless a rather typical and intrinsic characteristic of energy system models. Babonneau et al. [154] propose a method to deal with this problem. Thus, first the method by Babonneau et al. [154] is briefly introduced, and then it is applied to the MILP case study.

4.2.1 The robust formulation by Babonneau et al. [154]

The idea behind the approach proposed by Babonneau et al. [154] is to ensure global protection for a set of constraints, instead of protecting each constraint individually. In the context of an energy security problem, they propose a robust formulation to ensure that energy can be transferred among different regions through “channels”, which are subject to uncertain availability. In particular they consider the constraint in Eq. 4.28, in which **ACT** is the decision variable denoting the quantity of energy carried through a given channel $i = 1, \dots, N$, AF is the (uncertain) availability of the channel, and CAP is the channel capacity.

$$\mathbf{ACT}(i) - AF(i) \times CAP(i) \leq 0 \quad \forall i = 1, \dots, N \quad (4.28)$$

Instead of protecting each i -th constraint, a new “global” redundant constraint is added to the model formulation by summing over the constraint indices, as in Eq. 4.29.

$$\sum_{i=1}^N (\mathbf{ACT}(i) - AF(i) \times CAP(i)) \leq 0 \quad (4.29)$$

The robust formulation is then applied to Eq. 4.29. Summing over a given set implies that the

uncertainty budget is “shared” among the different components of the set. Using Bertsimas and Sim [62], this corresponds to having only one protection parameter $\Gamma \in [0, N]$, instead of N protection parameters $\Gamma_i \in [0, 1], \forall i = 1, \dots, N$, which has the advantage of replacing an intractable combinatorial problem with an easily manageable uncertainty set. As Babonneau et al. [154] comment, “*we are interested in protecting the total energy supply [...], not that of each channel separately*”. This means that, applying their method, the focus is moved from the individual component to the robustness of the entire system.

4.2.2 Application to the case study

The method proposed by Babonneau et al. [154] is applied to the MILP case study for the following parameters: $avail, c_{p,t}, endUses_{year}, \eta$. The application of the method is not automatic as, although mathematically possible, in a real situation not all elements of a set can share the same uncertainty budget. Thus, the implementation is separately discussed for the uncertain parameters of interest, which offer different representative examples.

Availability of resources

Resource availability (*avail*) is accounted for in Eq. 1.12, and it is considered limited only for the two local resources (wood and waste).

$$\sum_{t \in T} \mathbf{F}_t(i, t) t_{op}(t) \leq \mathit{avail}(i) \quad \forall i \in RES \quad (1.12)$$

Applying the method by Babonneau et al. [154], new robust constraints are added to the formulation as in Eqs. 4.30, in which $\Gamma_{\mathit{avail}} \in [0, 2]$ is the protection parameter, δ_{avail} is the maximum worst-case deviation from the nominal value of avail , $\mathbf{z}_{\mathit{avail}}$ and $\mathbf{p}_{\mathit{avail}}$ are the dual variables.

$$\sum_{i \in RES} \sum_{t \in T} \mathbf{F}_t(i, t) t_{op}(t) + \mathbf{z}_{\mathit{avail}} \Gamma_{\mathit{avail}} + \sum_{i \in RES} (\mathbf{p}_{\mathit{avail}}(i) - \mathit{avail}(i)) \leq 0 \quad (4.30)$$

$$\mathbf{z}_{\mathit{avail}} + \mathbf{p}_{\mathit{avail}}(i) \geq \delta_{\mathit{avail}}(i) \quad \forall i \in RES$$

$$\mathbf{z}_{\mathit{avail}}, \mathbf{p}_{\mathit{avail}} \in \mathbb{R}^+$$

Eq. 4.30 implies that the uncertainty budget can be shared between the two uncertain parameters, i.e. there is a total “unavailability budget” which can be shared between wood and waste. In the case study (Table A.22), the use of waste is always maximized, as waste is free of charge; wood, instead, has a high projected cost in 2035, i.e. its use is far from being cost optimal. Thus, changing the value of

Chapter 4. Robust optimization

the protection parameter Γ_{avail} in Eqs. 4.30 has no impact on the solution, as the uncertainty budget is always entirely attributed to the unused resource (wood). This means that, for this uncertain parameter, the application of the method by Babonneau et al. [154] brings no advantage over the standard formulation, which corresponds to separately considering the availability of wood and waste.

Period capacity factor

The capacity factor for the different periods ($c_{p,t}$) defines the maximum output of renewables in each period based on the installed capacity (Eq. 1.8). The parameter is defined - and uncertain - for the five modeled seasonal renewable energy technologies (new and existing hydroelectric dams and run-of-river plants, PV, wind, solar thermal) and for the 12 months, resulting in 60 instances of the uncertain parameter.

$$\mathbf{F}_t(j, t) \leq \mathbf{F}(j) c_{p,t}(j, t) \quad \forall j \in TECH, \forall t \in T \quad (1.8)$$

$c_{p,t}$ is indexed over the set of technologies ($TECH$) and the set of periods (T). Summing over $TECH$, i.e. sharing the uncertainty budget among the different technologies, can lead to a similar behavior to the one observed for *avail*, resulting in an attribution of the entire uncertainty budget to the most expensive technologies. Summing over T , instead, distributes the uncertainty budget over the different periods. This is enforced by the addition of Eqs. 4.31, in which $\Gamma_{c_{p,t}} \in [0, 12]$ is the protection parameter, $\delta_{c_{p,t}}$ is the maximum worst-case deviation from the nominal value of $c_{p,t}$, $\mathbf{z}_{c_{p,t}}$ and $\mathbf{p}_{c_{p,t}}$ are the dual variables.

$$\sum_{t \in T} (\mathbf{F}_t(j, t) - \mathbf{F}(j) c_{p,t}(j, t)) + \mathbf{z}_{c_{p,t}}(j) \Gamma_{c_{p,t}} + \sum_{t \in T} \mathbf{p}_{c_{p,t}}(j, t) \leq 0 \quad \forall j \in TECH \quad (4.31)$$

$$\mathbf{z}_{c_{p,t}}(j) + \mathbf{p}_{c_{p,t}}(j, t) \geq \delta_{c_{p,t}}(j) \mathbf{F}(j) \quad \forall j \in TECH, \forall t \in T$$

$$\mathbf{z}_{c_{p,t}}, \mathbf{p}_{c_{p,t}} \in \mathbb{R}^+$$

Formulation 4.31 groups equally the 60 uncertain parameters into 5 constraints, controlled by the protection parameter $\Gamma_{c_{p,t}}$. When $\Gamma_{c_{p,t}}$ is increased of a unitary step, for each technology the $c_{p,t}$ of an additional period assumes its worst-case realization. To ensure a realistic yearly distribution of $c_{p,t}$ in the uncertain domain, Eq. 4.32 additionally imposes that, if a given technology is installed, the maximum deviation from the nominal output in a given period be at maximum $\delta_{c_{p,t}}$.

$$\mathbf{F}_t(j, t) \geq \mathbf{F}(j) (c_{p,t}(j, t) - \delta_{c_{p,t}}(j)) \quad \forall j \in TECH, \forall t \in T | c_{p,t}(j, t) < 1 \quad (4.32)$$

Thus, the application of the method by Babonneau et al. [154] to the period capacity factor is effective as it offers a more manageable uncertainty set; however, it also highlights the need of carefully evaluating over which sets the method can be applied.

Efficiencies and energy demand

The conversion efficiency of technologies (η) and the yearly energy demand ($endUses_{year}$) are accounted for in the layer balance equation (Eq. 1.13). In total, 52 uncertain instances of η and 15 uncertain instances of $endUses_{year}$ are considered.

$$\underbrace{\sum_{i \in RES \cup TECH \setminus STO} f(i, l) \mathbf{F}_t(i, t) + \sum_{j \in STO} (\mathbf{Sto}_{out}(j, l, t) - \mathbf{Sto}_{in}(j, l, t)) - \mathbf{EndUses}(l, t)}_{\mathbf{LB}} = 0 \quad \forall l \in L, \forall t \in T \quad (1.13)$$

These parameters are present in different constraints: η is linked to the parameter f (see Section B.3), which enters as well in Eq. 1.18, while $endUses_{year}$ is linked to the decision variables $\mathbf{EndUses}$ via the equations in Figure 1.4. However, as all these are equality constraints, Eq. 1.13 can be rewritten in an extended form as in Eq. 4.33. The equation takes as an example the electricity layer, which is representative as it includes resources, technologies (producers and consumers), demand and losses.

$$\sum_{i \in RES \cup TECH \setminus STO} f(i, l) \mathbf{F}_t(i, t) + \sum_{j \in STO} (\mathbf{Sto}_{out}(j, l, t) - \mathbf{Sto}_{in}(j, l, t)) - \frac{\sum_{s \in S} endUses_{year}(l, s)}{\sum_{t \in T} t_{op}(t)} - \frac{\%lighting(t)}{t_{op}(t)} \sum_{s \in S} endUses_{year}(Lighting, s) - \left(\sum_{i \in RES \cup TECH \setminus STO | f(i, l) > 0} f(i, l) \mathbf{F}_t(i, t) \right) \%loss(l) = 0 \quad l = Elec., \forall t \in T \quad (4.33)$$

The possibility of including all the uncertain parameters in a single set of constraints simplifies - and, in some cases, makes possible - the development of the robust counterpart. To obtain the robust counterpart, the first step is the relaxation of the equality constraint Eq. 1.13 to an inequality constraint, i.e. $\mathbf{LB} \geq 0$. This does not pose problems as it simply implies allowing an excess of production in the energy system. As a matter of fact, transforming equalities into inequalities is quite common in robust optimization, “*since often [equality] constraints restrict the feasibility region drastically or even lead to infeasibility*” [125], as in this case. Second, the application of the method by Babonneau et al. [154] is considered by summing over the set L .

As defined in Section 1.1.2, layers are all the elements in the system that need to be balanced in each period, i.e. resources and end-uses demand. Summing over the set of layers is possible only if the summed layers are “compatible”, e.g. if an additional demand in one layer can be compensated by

Chapter 4. Robust optimization

an additional consumption in the other one. This is clearly not always possible, e.g. an additional transportation demand cannot be satisfied by the import of more uranium. In particular, resource layers need to remain separate. As a consequence, for resource layers the method by Babonneau et al. [154] cannot be meaningfully adopted, and thus the classical robust formulation by Bertsimas and Sim [62] applies (Eqs. 4.34)

$$\mathbf{LB} - \mathbf{z}_{\mathbf{lb}}(l, t)\Gamma_{lb} - \sum_{i \in \text{TECH} \setminus \text{STO}} \mathbf{p}_{\mathbf{f}}(i, l, t) \geq 0 \quad \forall l \in L \cap \text{RES}, \forall t \in T \quad (4.34)$$

$$\mathbf{z}_{\mathbf{lb}}(l, t) + \mathbf{p}_{\mathbf{f}}(i, l, t) \geq \delta_f(i, l)\mathbf{y}_{\mathbf{lb}}(i, t) \quad \forall i \in \text{TECH} \setminus \text{STO}, \forall l \in L \cap \text{RES}, \forall t \in T | f(i, l) < 0 \vee f(i, l) > 0 \wedge l \neq \text{Elec.}$$

$$\mathbf{z}_{\mathbf{lb}}(l, t) + \mathbf{p}_{\mathbf{f}}(i, l, t) \geq \delta_f(i, l)\mathbf{y}_{\mathbf{lb}}(i, t)(1 - \%_{\text{loss}}(l)) \quad \forall i \in \text{TECH} \setminus \text{STO}, \forall l \in L \cap \text{RES}, \forall t \in T | f(i, l) > 0 \wedge l = \text{Elec.}$$

$$\mathbf{F}_t(i, t) \leq \mathbf{y}_{\mathbf{lb}}(i, t) \quad \forall i \in \text{TECH} \setminus \text{STO}, \forall t \in T$$

$$\mathbf{z}_{\mathbf{lb}}, \mathbf{p}_{\mathbf{f}}, \mathbf{y}_{\mathbf{lb}} \in \mathbb{R}^+$$

In Eqs. 4.34 Γ_{lb} is the protection parameter, $\mathbf{z}_{\mathbf{lb}}$ and $\mathbf{p}_{\mathbf{f}}$ are the dual variables, δ_f is the maximum worst-case deviation from the nominal value of f , calculated as in Eq. 4.35, in which δ_η is the maximum worst-case deviation from the nominal efficiencies (η) of energy conversion technologies.

$$\delta_f = \begin{cases} \frac{1}{\eta} \frac{\delta_\eta}{\eta - \delta_\eta} = -f \frac{\delta_\eta}{\eta - \delta_\eta}, & \text{if } f < 0 \\ \delta_\eta = f \frac{\delta_\eta}{\eta}, & \text{otherwise} \end{cases} \quad (4.35)$$

Some types of end-use demand, instead, can be compatible. As an example, an additional mobility demand can be supplied by either public or private transportation technologies, or an additional low temperature heat demand can be satisfied by centralized or decentralized technologies. Thus, the method by Babonneau et al. [154] can be applied to these layers with Eqs. 4.36. The formulation, by an appropriate set definition, cancels out the decision variables $\%_{\text{Dhn}}$, $\%_{\text{Public}}$ and $\%_{\text{Rail}}$, avoiding possible multiplications among variables which would make the formulation nonlinear.

$$\sum_{l \in L | l \in \text{EUT OF EUC}(euc)} \mathbf{LB} - \mathbf{z}_{\mathbf{lb}}(l, t)\Gamma_{lb} - \sum_{i \in \text{TECH} \setminus \text{STO}} \mathbf{p}_{\mathbf{f}}(i, euc, t) - \sum_{eui \in \text{EUI OF EUC}(euc)} \sum_{s \in S} \mathbf{p}_{\text{dem}}(eui, s, t) \geq 0 \quad \forall euc \in \text{EUC}, \forall t \in T \quad (4.36)$$

$$\mathbf{z}_{\mathbf{lb}}(euc, t) + \mathbf{p}_{\text{dem}}(eui, s, t) \geq \delta_{\text{dem}}(eui, s) \frac{\%_{\text{lighting}}(t)}{t_{\text{op}}(t)}$$

$$\forall euc \in \text{EUC}, \forall eui \in \text{EUI OF EUC}(euc), \forall s \in S, \forall t \in T | eui = \text{Lighting}$$

$$\mathbf{z}_{lb}(euc, t) + \mathbf{p}_{dem}(eui, s, t) \geq \delta_{dem}(eui, s) \frac{\%_{sh}(t)}{t_{op}(t)}$$

$$\forall euc \in EUC, \forall eui \in EUI \text{ OF } EUC(euc), \forall s \in S, \forall t \in T | eui = \text{Heat LowT SH}$$

$$\mathbf{z}_{lb}(euc, t) + \mathbf{p}_{dem}(eui, s, t) \geq \frac{\delta_{dem}(eui, s)}{\sum_{t \in T} t_{op}(t)}$$

$$\forall euc \in EUC, \forall eui \in EUI \text{ OF } EUC(euc), \forall s \in S, \forall t \in T | eui \notin \{\text{Lighting, Heat LowT SH}\}$$

$$\mathbf{z}_{lb}, \mathbf{p}_{dem} \in \mathbb{R}^+$$

The sets of equations 4.34-4.36 define the robust counterpart of the layer balance constraint (Eq. 1.13), in which the protection parameter Γ_{lb} controls the uncertainty levels of f and $endUses_{year}$. By increasing Γ_{lb} of a unitary step, for each period an additional uncertain parameter takes its worst case realization, allowing to account for demand and efficiency uncertainties in the planning of the energy system. It has to be noted that, as the uncertain parameters are not indexed over T , the parameter which changes is not necessarily the same for all t .

The application of the method by Babonneau et al. [154] to Eq. 1.13 shows the advantages of concise model formulations for uncertainty studies. In fact, if the deterministic model is already rather complex, which is often the case in the energy field, obtaining the robust counterparts can be difficult - and lead to extremely intricate formulations - or, in some cases, practically impossible, as highlighted by Hajimiragha et al. [132]. Eq. 1.13 serves as representative example of this. Although the constraint offers various challenges, such as the presence of different uncertain parameters, some of them linked to other constraints, its robust counterpart is obtained with the addition of only two sets of additional constraint. This is made possible by the fact of using a MILP formulation developed for uncertainty, together with an appropriate definition of sets.

Overall, the application to the case study reveals the interest of the method by Babonneau et al. [154] for the robust optimization of strategic energy planning models, offering tractable uncertainty sets in the place of an otherwise intractable combinatorial problem. However, it also shows that the use of the method is not automatic, but it requires thorough case-by-case evaluation to make sure of its consistency.

4.2.3 Evaluation of the robust solutions

As previously discussed, uncertainty in the constraints is linked to feasibility: by increasing protection against worst case, constraint violations are reduced at the price of a higher objective value. For example, a robust energy system will normally be more expensive, but more likely to satisfy the demand. This trade-off is measured by the price of robustness (PoR), which is defined as the difference between the objective (cost) of a given robust solution and the objective of the deterministic

Chapter 4. Robust optimization

problem. Measuring the PoR “is useful if the objective is certain, since in that case PoR is the amount that has to be paid for being robust against constraint violations” [125]. Thus, the effect of robustness in the constraints is evaluated via simulation while keeping the deterministic objective function, i.e. $\Gamma_{obj} = 0$. As an example, the focus of the analysis is on the layer balance constraint (Γ_{lb}).

Equivalently to the tests performed in Section 4.1.4 for uncertainty in the objective, 10 different energy system configurations are obtained by gradually increasing the value of Γ_{lb} from the deterministic case ($\Gamma_{lb} = 0$) to the fully robust solution ($\Gamma_{lb} = |J_{lb}|$). Then, two sets of simulations are carried out. In the first one, all the decision variables of the MILP problem are fixed to the values obtained in output of the robust optimization runs. This means that both the investment and the operation strategy of the system are fixed in all the simulation runs. The MILP model is run $n_{sample} = 10000$ times sampling the values of the uncertain parameters (f , $endUses_{year}$) from uniform distributions over the entire uncertainty range (Table 2.1). In the second set of simulations, to better represent the reality of energy systems, only investment-related decision variables (such as the installed capacity of technologies, \mathbf{F}) are fixed, while operating decision variables (such as \mathbf{F}_t) are left free, i.e. determined by the optimization.

The results of both tests are reported in Table 4.3. To measure the magnitude of the constraint violations, a positive variable ξ is added to the robust constraints and also to the objective function with a high penalty cost. As expected, by increasing the protection level Γ_{lb} , constraint violations

Table 4.3 – Simulation results for uncertainty in the constraints: price of robustness (PoR) against statistics of constraint violations ξ (\bar{x} : mean, σ : standard deviation). First test: all decision variables fixed. Second test: only investment decisions are fixed (free resources). Uncertain parameters are the efficiencies (f) and the end-use demand ($endUses_{year}$), sampled from entire range.

Γ_{lb}	C_{tot}^a [MCHF/y]	PoR [MCHF/y]	Renewables ^b [TWh/y]	%viol [%]	Test 1			Test 2	
					\bar{x}_ξ [GW] ^c	σ_ξ [GW] ^c	%viol [%]	\bar{x}_ξ [GW] ^c	σ_ξ [GW] ^c
0	13834	0	2.96	99.9%	0.254	0.140	53.3%	0.093	0.078
1	14491	657	7.06	24.9%	0.064	0.061	1.05%	0.041	0.034
2	14633	799	1.42	8.50%	0.067	0.062	0.05%	0.011	0.009
3	14712	878	1.89	2.73%	0.063	0.056	0%	-	-
4	14769	935	10.97	0.81%	0.048	0.045	0%	-	-
5	14812	978	13.59	0.31%	0.042	0.033	0%	-	-
6	14849	1015	12.90	0.04%	0.019	0.009	0%	-	-
7	14873	1039	16.24	0%	-	-	0%	-	-
8	14888	1054	17.49	0.01%	0.009	0.000	0%	-	-
20	14904	1070	18.00	0%	-	-	0%	-	-

^a Including fixed costs for existing hydroelectric dams, existing electricity grid and efficiency measures.

^b Including PV, wind, new hydro dam and run-of-river plants, deep geothermal, solar thermal

^c [Mpkm/h] for passenger, [Mtkm/h] for freight mobility end-uses

are sharply reduced, both in terms of frequency, and in terms of mean (\bar{x}) and standard deviation (σ). The first test shows that constraint violations start to become negligible at low values of the protection parameter ($\Gamma_{lb} \geq 4$). Thus, to obtain good protection levels it is not needed to be fully robust, which further confirms the interest of the approach by Bertsimas and Sim [62]. The second test, in which the operation strategy of the system is left free to adapt to the realizations of the uncertainty, reveals that in a real situation the deterministic solution has still a high risk of infeasibility, and that this risk disappears as soon as uncertainty is taken into account. Also, similarly to what observed in the case of uncertainty in the objective, the increase of Γ_{lb} is associated to a higher penetration of renewables in the system.

Overall, the tests reveal that uncertainty in the constraints, which is seldom considered in the literature, can have a significant impact on the definition of the energy strategy. Also, the proposed robust formulation can identify appropriate trade-offs between the suboptimality of robust solutions and the risk of constraint violations. In fact, the results suggest that in real energy system applications, low levels of protection against uncertainty - and, thus, low additional costs - are sufficient to highly reduce the risk of infeasibilities (e.g. inability to satisfy the demand).

4.3 Decision-making for energy systems

The formulations and results presented in the previous sections of this chapter offer a complete framework to apply robust optimization to strategic energy planning models, as well as an insight on how the energy strategy changes when uncertainty is separately accounted for in the objective function and in the other constraints. However, these mathematical methods need to be linked to the energy planning practice. As an example, Grossmann et al. [36], reviewing the use of the method by Bertsimas and Sim [62] in the field of process system design, comment that “*it is not trivial*” for a user to adequately specify the uncertainty budget (Γ). In fact, if probabilistic results - as the ones presented in Bertsimas and Sim [62] - can help identifying appropriate bounds for the constraints, in the case of the objective the translation of robust optimization results into energy planning decisions is not obvious.

Thus, the purpose of this section is to evaluate how the presented methods can support the decision-making practice in the energy field. To do this, first, a different, target-oriented perspective, is offered to interpret robust optimization results. Second, a method is proposed to address uncertainty both in the objective function and in the other constraints. Third, robust energy strategies are compared with a realistic example, in which future modifications in the investment decisions are allowed as uncertainty unfolds over time. Fourth, robust solutions are compared to the investment strategy offered by the more “traditional” stochastic programming approach.

4.3.1 A target-oriented perspective on robust optimization

A *target-oriented* approach to robust optimization has been proposed by Sy [159] as a way to translate robust formulations into a language more familiar to decision-makers. The fundamental idea behind this approach, in the words of Brown and Sim [160], is that targets “*are often very natural for investors to specify, whereas traditional models based on risk measures or utility functions depend critically on tolerance parameters, which are often difficult for investors to intuitively grasp and even harder to appropriately assess.*”. In other words, it is easier to ask a decision-maker what is the maximum cost he/she can accept paying, than asking to quantify his/her aversion to risk in terms of probability (e.g. asking to define a good value of Γ).

In a target-oriented formulation, the MILP model is modified “*such that the objective function [...] maximizes the robustness index subject to achieving the [...] target*” [142]. This means that, considering uncertainty in the objective, the MILP formulation is rewritten as in Eq. 4.37, in which $\mathbf{C}_{\text{tot}}(\Gamma_{\text{obj}})$ is the robust formulation of the objective function (Eqs. 4.26) and $\mathbf{C}_{\text{tot}}^*$ is the target maximum cost defined by the decision-maker.

$$\begin{aligned} \max \quad & \Gamma_{\text{obj}} \\ \text{s.t.} \quad & \mathbf{C}_{\text{tot}}(\Gamma_{\text{obj}}) \leq \mathbf{C}_{\text{tot}}^* \end{aligned} \tag{4.37}$$

Problem 4.26 can be solved by binary search for any given value of $\mathbf{C}_{\text{tot}}^*$ [159]. As commented by Sy [159], “*maximizing Γ can be interpreted as maximizing the robustness of the system to uncertainty with regards to meeting the specified performance requirements*”, i.e. the higher the protection level Γ_{obj} , the more likely it is that the total cost of the system will not exceed the corresponding target set by the decision-maker.

The results of the target-oriented approach applied to the objective function of the MILP case study are illustrated in Figure 4.9, which is equivalent to Figure 4.4 but with \mathbf{C}_{tot} replacing the protection level (Γ_{obj}) on the x-axis. As also shown by the performance indicators in Figure 4.5, there is a sharp increase in the total cost for very low values of Γ_{obj} . Figure 4.9 reveals that, as this is due to the “activation” of the fixed costs of existing technologies, the energy strategy does not change. Interestingly, as soon as solutions start changing, the marginal growth of the protection level against an increase in total cost (i.e. the derivative of the black line) gets much higher, i.e. a small increase in the target total cost corresponds to a significant increase in the robustness of the solutions. Also, most solutions are concentrated in a relatively narrow variation of total cost. For the decision-maker, this means that shifting towards more renewables and efficient technologies ensures a significantly higher protection against worst-case at the price of a relatively small increase in the target total cost of the system.

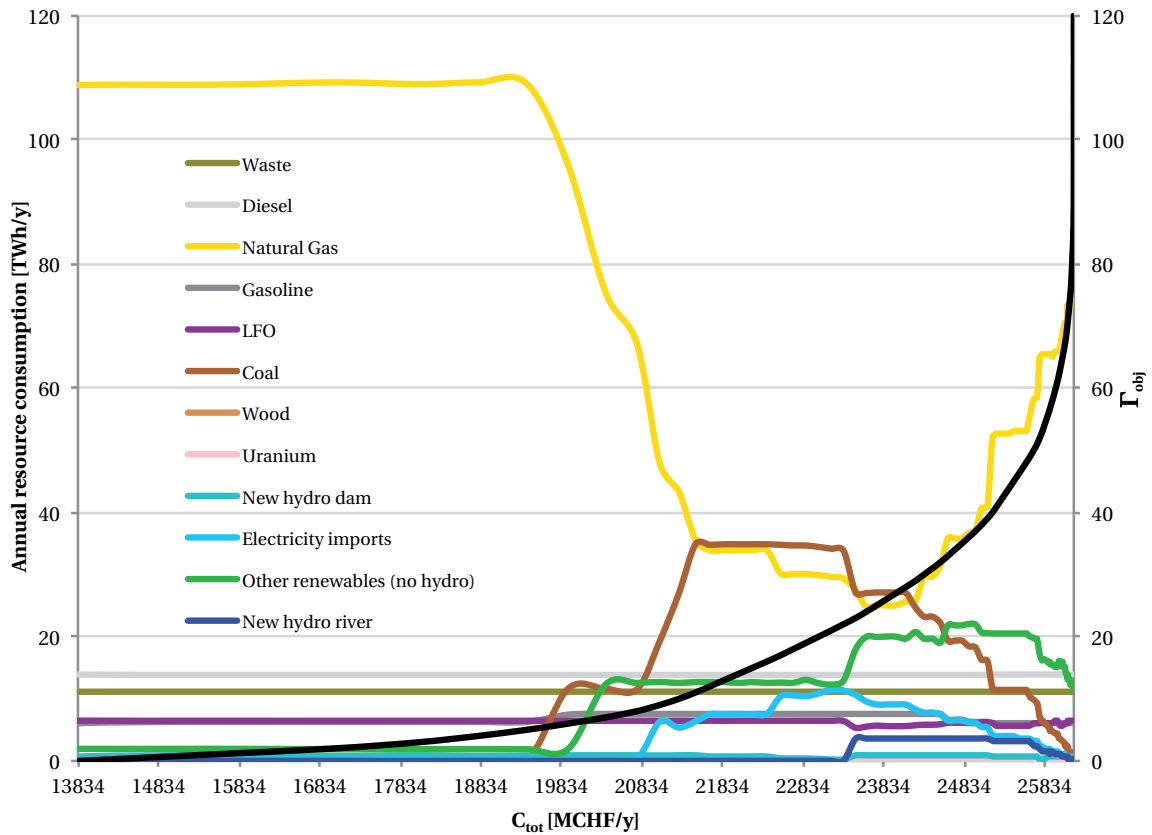


Figure 4.9 – Evolution of the energy system configuration vs. objective (C_{tot}): annual consumption of resources. The black line indicates the value of Γ_{obj} .

Overall, the target-oriented approach to robust optimization does not impact the problem formulation, but it offers a different perspective both in terms of interaction with the energy model, and of results analysis. This enables a more intuitive understanding of the impact of robustness in the definition of the energy strategy.

4.3.2 First feasibility, then optimality

Although the target-oriented approach offers an interesting perspective to interpret robust optimization results, simulation remains the most appropriate way of comparing different investment strategies to support decision-making [125]. In fact, if robust solutions are obtained considering worst-case realizations of uncertainty, simulation studies can challenge these solutions by using different uncertainty sets, which can better represent real-life conditions.

In the previous sections, uncertainty in the objective function and in the other constraints has been separately considered, as the two are fundamentally different: on the one hand, uncertainty in the

constraints linked to *feasibility*, and its evaluation (using PoR) is meaningful when the objective is certain; on the other hand, uncertainty in the objective is linked to *optimality*. However, energy planners are interested in solutions that are both feasible *and* cost-effective, which requires to simultaneously consider uncertainty in the objective function *and* in the other constraints. Thus, in this section, a method is proposed to consider both types of uncertainty, with the final aim of aiding decision-making.

The fundamental idea behind the proposed method can be summarized as: *first feasibility, then*

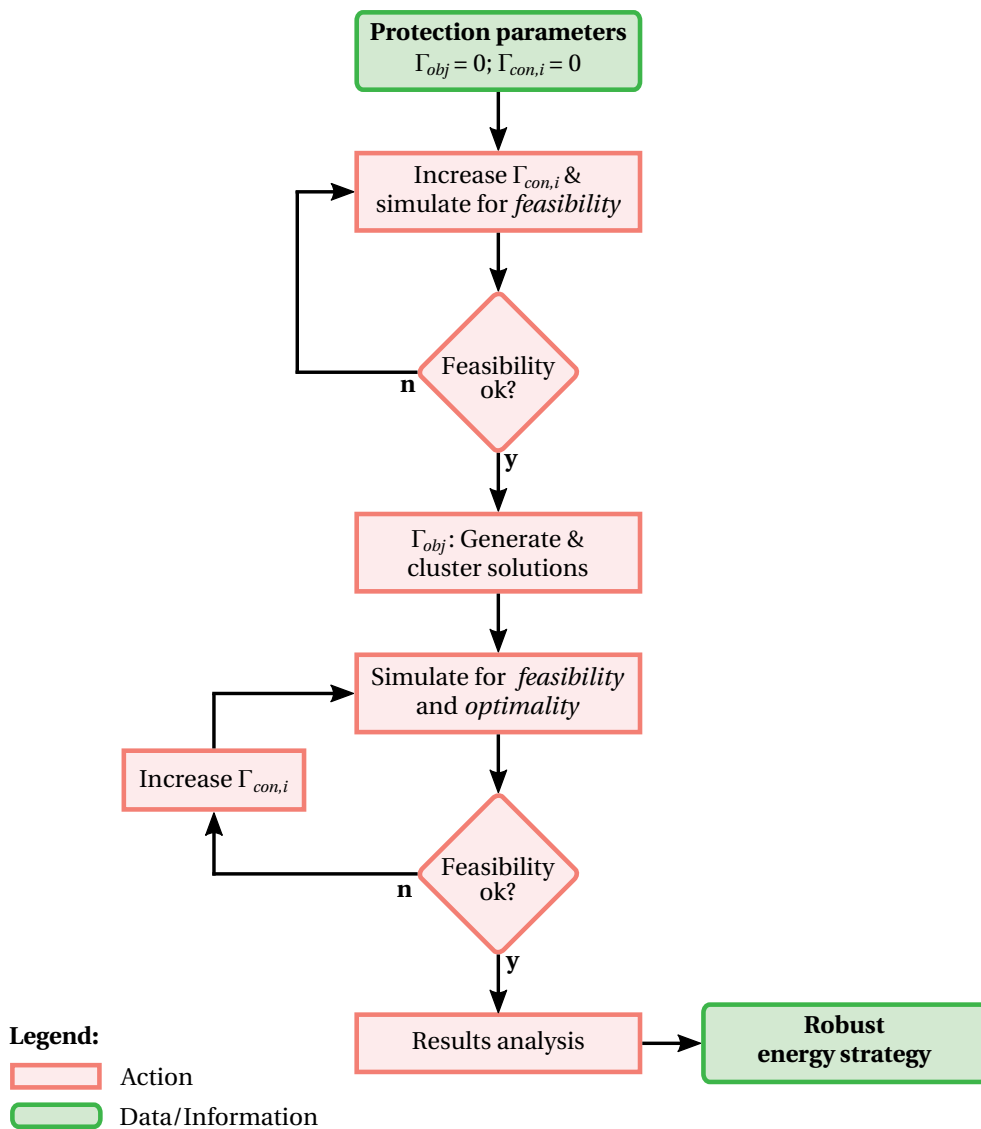


Figure 4.10 – Flowchart of the proposed decision-making method: uncertainty is first considered in the constraints to ensure feasibility, and then in the objective to evaluate optimality.

optimality. In other words, feasibility (e.g. ability to satisfy the demand) is a *condicio sine qua non*, i.e. it makes sense to evaluate optimality only for solutions which satisfy the desired feasibility criteria. This has also the advantage of limiting the number of solutions to simulate: in fact, if in the case of the objective it is relevant to evaluate solutions obtained at all protection levels (corresponding to different cost scenarios), in the case of the other constraints there is no interest in considering solutions at higher protection levels than the one ensuring the desired degree of feasibility.

The steps of the method are illustrated by the flowchart in Figure 4.10 considering a problem with uncertainty in the objective function (with protection parameter Γ_{obj}) and in N other constraints (with protection parameters $\Gamma_{con,i}, \forall i = 1, \dots, N$). Starting with the deterministic solution ($\Gamma_{obj} = 0, \Gamma_{con,i} = 0$), the protection level in the constraints is gradually increased until the desired level of feasibility is reached (keeping $\Gamma_{obj} = 0$). Feasibility is evaluated through simulations in which *all* the uncertain parameters in the constraints are made to vary. Once feasibility is ensured, the $\Gamma_{con,i}$ are kept fixed and different solutions are generated for uncertainty in the objective by varying Γ_{obj} . Out of the generated solutions, a representative set - selected, for example, using *k-medoids* clustering - is simulated accounting for uncertainty of *all* model parameters. Of course, as feasibility is initially assessed only in the case of $\Gamma_{obj} = 0$, the new solutions generated by considering uncertainty in the objective might introduce feasibility issues. In this case, $\Gamma_{con,i}$ can be further increased. Finally, statistical analysis on the simulation results leads to the selection of the final robust energy strategy.

The method is applied to the MILP Swiss energy system case study. Based on the developments presented earlier in this chapter, the model has one protection parameter for the objective (Γ_{obj} , accounting for the uncertainty of the cost-related parameters $i_{rate}, c_{inv}, c_{maint}, c_{op}, n$) and two protection parameters for the other constraints: $\Gamma_{c_{p,t}}$ (accounting for the uncertainty of $c_{p,t}$) and Γ_{lb} (accounting for the uncertainty of f and $endUses_{year}$). First, uncertainty in the constraints is evaluated. On the one hand, numerical tests reveal that $\Gamma_{c_{p,t}}$ does not significantly impact feasibility. On the other hand, the results in Table 4.3 reveal that Γ_{lb} has a strong influence: for a real energy system situation (test 2 in Table 4.3), feasibility is sharply improved already for $\Gamma_{lb} = 1$.

Thus, Γ_{lb} is fixed to 1, and uncertainty in the objective is evaluated. For consistency with the results presented in Figure 4.8 (in which $\Gamma_{lb} = 0$), the same values of Γ_{obj} are used to select the 15 representative solutions. The representative energy system configurations, listed in the upper part of Table 4.4, are simulated $n_{sample} = 10000$ times, sampling the values of the uncertain parameters (all uncertain parameters) from uniform distributions over the entire uncertainty range. To represent the reality of energy systems, only investment-related decision variables (such as the installed capacity of technologies, F) are fixed, while operating decision variables (such as F_t) are left free, i.e. determined by the optimization.

The results are shown in Figure 4.11, in which the different robust solutions are compared to the deterministic case ($\Gamma_{obj} = 0, \Gamma_{lb} = 0$). In terms of optimality, simulation results are in line with what observed in Figure 4.8: robust solutions are on average more expensive, but feature a lower

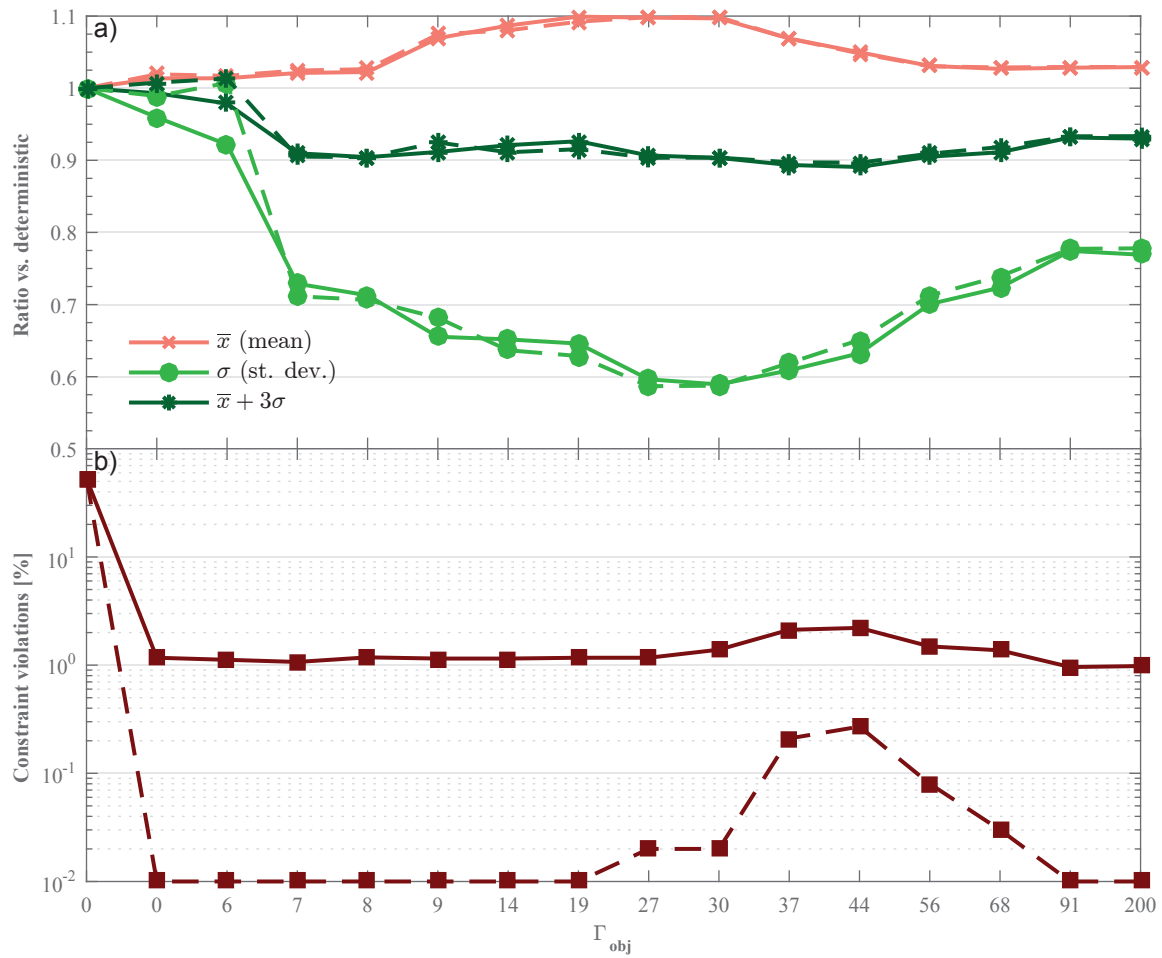


Figure 4.11 – Simulation results for the robust solutions with uncertainty in the objective and in the constraints: a) mean (\bar{x}), standard deviation (σ), $\bar{x} + 3\sigma$ and for the objective value and b) frequency of constraint violations. Reference (on the y axis) is the deterministic solution ($\Gamma_{obj} = 0$, $\Gamma_{lb} = 0$). Full lines: $\Gamma_{lb} = 1$. Dashed lines: $\Gamma_{lb} = 2$. Solutions are simulated on all uncertain parameters (sampled from entire uncertainty range) and only investment decisions are fixed (free resources).

variability and offer a better protection against worst-case. The main difference is in terms of feasibility: considering uncertainty in the constraints by fixing $\Gamma_{lb} = 1$ causes a dramatic reduction in constraint violations compared to the deterministic solution.

Interestingly, introducing uncertainty in the objective slightly increases the frequency of constraint violations of some solutions, reaching 2.21% for $\Gamma_{obj} = 37$. If this is above the feasibility threshold desired by the decision-maker, the protection level in the constraints can be further increased. As an example, by fixing $\Gamma_{lb} = 2$ (lower part of Table 4.4 and dashed lines in Figure 4.11), infeasibility is reduced to negligible values, while maintaining similar performance in terms of cost.

Table 4.4 – Characterization of the representative energy system configurations for $\Gamma_{lb} = 1$ and $\Gamma_{lb} = 2$.

Γ_{obj}	Γ_{lb}	Electricity production										Other					
		CCGT [GW _e]	Coal [GW _e]	PV [GW _e]	Wind [GW _e]	New dams [GW _e]	New river [GW _e]	Imports [TWh _e /y]	Boilers [GW _{th}]	CHP [GW _{th}]	Elec HPs [GW _{th}]	Solar Th. [GW _{th}]	Deep Geo [GW _{th}]	%Dnn ^a [-]	Renewables ^b [TWh/y]		
0	1	2	0	0	0	0	0	0	0	0	0	0	0	0	0.83	0.314	7.1
6	1	3	0	0	0	0	0	0	0	0	0	0	0	0	0.32	0.120	3.2
7	1	2	0	0	0	5.30	0	0	0	0	0	0	0	0	0.23	0.120	13.3
8	1	2	0	0	0	5.30	0	0	0	0	0	0	0	0	0.18	0.120	12.9
9	1	1.5	0.5	0	0	5.30	0	0	0	0	0	0	0	0	0.32	0.120	13.7
14	1	0.5	1	0	0	5.30	0	0	0	0	0	0	0	0	0.32	0.120	13.4
19	1	0	1.5 ^c	0	0	5.30	0	0	0	0	0	0	0	0	0.67	0.181	15.5
27	1	0	1	3.01	5.26	0.440	0.850	9.72	13.21	0.20	0.20	0.20	0	0	1.38	0.252	26.4
30	1	0	1 ^c	2.96	5.30	0.440	0.850	9.28	13.04	0.20	0.20	0.20	1.16	1.31	0.241	27.2	
37	1	1	0.5 ^c	1.89	5.30	0.440	0.850	5.46	11.23	0.58	0.58	0.58	3.72	0.83	0.151	25.7	
44	1	1.5	0	1.92	5.30	0.440	0.754	4.03	12.92	0.50	0.50	0.50	3.52	0.83	0.230	25.8	
56	1	1	0	0.83	5.30	0.413	0.327	1.74	13.17	1.62	1.62	1.62	1.54	0.74	0.293	20.7	
68	1	1	0	0.47	5.30	0.440	0.202	1.00	12.75	1.88	1.88	1.88	0.89	0.64	0.277	18.6	
91	1	1	0	0.02	5.30	0.425	0.007	0.04	10.39	2.22	2.22	2.22	0.03	0.23	0.121	13.3	
200	1	1	0	0	5.30	0.424	0	0	10.33	2.26	2.26	2.26	0	0.25	0.132	13.4	
0	2	1	0	0	0	0.440	0	0.01	21.73	2.40	2.27	2.40	0	0.07	0.322	1.42	
6	2	1.5	0	0	0	0.380	0	0	21.06	1.82	0.89	1.82	0	0	0.129	0.78	
7	2	2	0	0	5.30	0.440	0	0.12	11.88	1.18	10.65	1.18	0	0.25	0.158	13.4	
8	2	2	0	0	5.30	0.440	0	0	11.79	1.26	10.93	1.26	0	0.28	0.178	13.6	
9	2	1	0	0	5.30	0.000	0	15.90	12.63	0.20	11.53	0.20	0	0.64	0.231	15.4	
14	2	0.5	1 ^c	0	5.30	0.053	0	12.54	14.07	0.20	11.12	0.20	0	0.85	0.318	17.1	
19	2	0	1.5 ^c	0	5.30	0.275	0	12.21	14.08	0.18	10.78	0.18	0.00	1.20	0.318	19.3	
27	2	0	1 ^c	3.27	5.30	0.440	0.850	9.48	13.02	0.22	10.40	0.22	0.77	1.38	0.254	27.5	
30	2	0	1 ^c	3.20	5.30	0.440	0.850	9.44	13.00	0.22	10.38	0.22	0.77	1.40	0.253	27.5	
37	2	1	0.5 ^c	2.08	5.30	0.440	0.850	5.47	11.53	0.62	9.78	0.62	3.60	1.04	0.187	27.0	
44	2	1	0	1.90	5.30	0.429	0.748	4.01	12.76	0.98	9.22	0.98	3.54	0.83	0.243	25.9	
56	2	1	0	0.84	5.30	0.337	0.366	1.77	13.28	1.72	9.72	1.72	1.54	0.76	0.301	20.9	
68	2	1	0	0.44	5.30	0.349	0.194	0.93	13.17	2.10	10.19	2.10	0.83	0.60	0.322	17.9	
91	2	1	0	0.02	5.30	0.269	0.008	0.04	10.60	2.52	10.79	2.52	0.03	0.32	0.167	13.7	
200	2	1	0	0	5.30	0.278	0	0	10.57	2.52	10.80	2.52	0	0.32	0.165	13.6	

^a %Dnn \in [0.1,0.3]. The share of heat supplied by the DHN over 0.3 is the additional heat demand in the uncertain domain (Eq. 4.36).

^b Including PV, wind, new hydro dam and run-of-river plants, deep geothermal, solar thermal

^c At least one power plant is integrated gasification combined cycle (IGCC)

Thus, by considering uncertainty in both the objective and in the other constraints, the proposed method can offer solutions which are both feasible and cost-effective. Also, by first ensuring feasibility in the constraints and then evaluating cost-optimality, it limits the computational requirements and respects the conceptual difference between the two cases. Interestingly, the results show that relatively low protection levels in the constraints are sufficient to ensure the reliability of the system, at the price of a marginal loss in terms of average optimality. This additionally confirms the interest of a probabilistic approach to robust optimization, as interesting energy system configurations both in terms of feasibility and cost-effectiveness - and with a high penetration of renewables and efficient technologies (Table 4.4) - are obtained at medium protection levels both in the objective and in the other constraints.

4.3.3 Robust investment strategies and overcapacity in the electricity sector

In all the simulation studies performed in this chapter, the investment strategy - corresponding to the values of the decision variables \mathbf{F} - has been fixed to the values in output of the robust optimization runs (\mathbf{F}^*), i.e. $\mathbf{F}(j) = \mathbf{F}^*(j), \forall j \in TECH$. However, in the reality of national energy systems, it can happen that if a given technology is too expensive to operate, that technology is shut down and additional investments are made on other alternatives, thus generating an *overcapacity*. This is rather typical in the European electricity sector. For example, as mentioned in the Introduction, this is the case in the Netherlands, where past expectations of low NG prices led to substantial investments in new CCGT power plants that were then shut down because non-economically viable to operate. Another example is the Italian electricity sector, where 23.3 GW_e of additional fossil capacity have been installed in the years 2000-2011. This led to a total installed capacity of 122.3 GW_e in 2011 for a 56.5 GW_e peak demand in the same year [161], and to a consequent underutilization of the newly installed power plants in favor of competing technologies and of electricity imports. Even when investments are private, overcapacity can constitute a cost for the public if *capacity payment* policies are adopted [162]. Thus, this section answers the following research question: *Do robust investment strategies limit the risks of overcapacity in the energy system?*

The MILP model presented in Chapter 1 is a *one-stage* model, which does not consider the possibility of *recourse*, i.e. of “*reactive actions after the realization of the uncertainty*” [36], such as a change in the investment decision or in the operating strategy. In fact, although recent developments, such as adjustable robust optimization (ARO) [149] and linear decision rules (LDR) [148], allow to consider recourse in robust optimization, obtaining robust formulations for multi-stage problems is to date extremely difficult [59] and restricted to a set of tractable functions.

Thus, a simulation-based approach is used to answer this question, considering the possibility of modifications in the investment strategy as uncertainty unfolds. To do this, for all the solutions listed in Table 4.2, it is fixed that $\mathbf{F} \geq \mathbf{F}^*$ for electricity production technologies. This means that the investment decision in output of the robust optimization - $\mathbf{F}^*(j)$ - becomes the lower bound

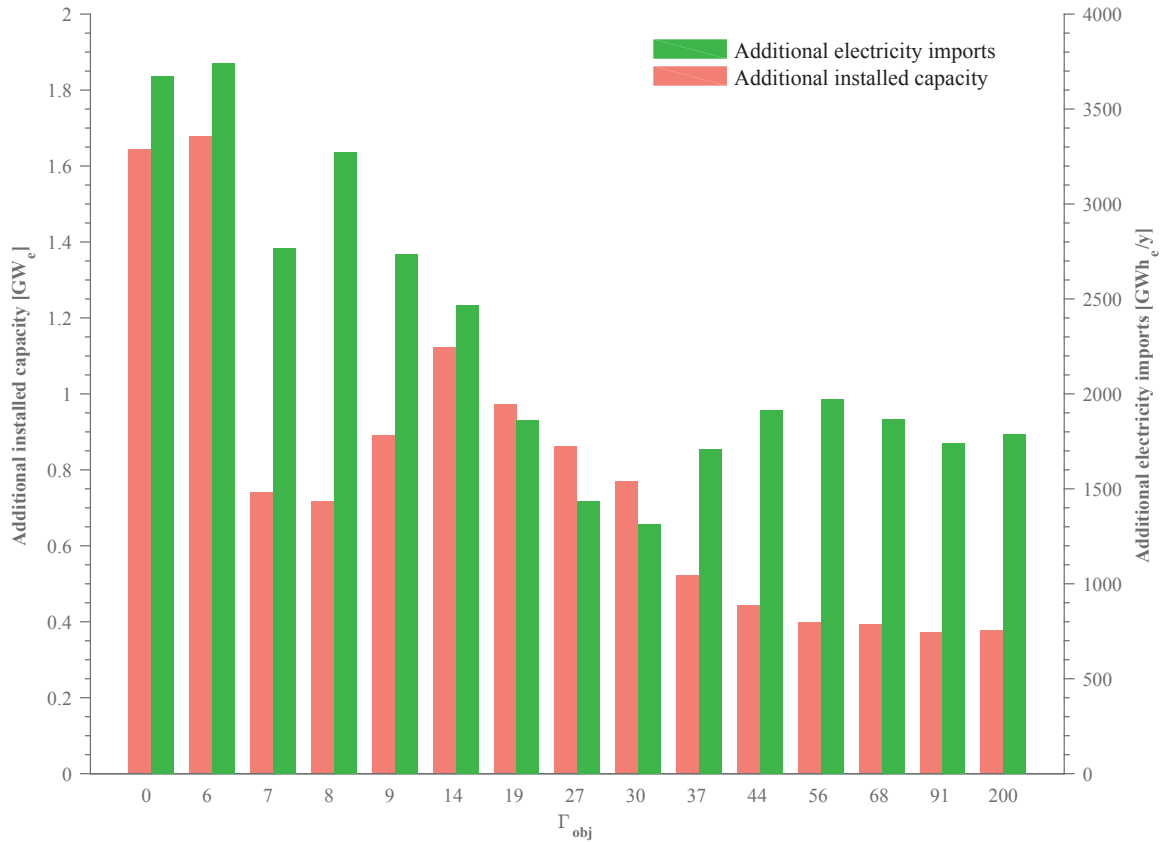


Figure 4.12 – Average additional installed capacity and electricity imports for the robust solutions obtained at different values of Γ_{obj} . Results of simulations with uncertain parameters c_{op} and $c_{p,t}$, sampled from uniform distributions over the entire range. Lower bound for size of electricity production technologies ($\mathbf{F} \geq \mathbf{F}^*$) and for electricity imports is fixed, while use resources and operating strategy are determined by the optimization.

for the installed capacity of the j -th technology. As a consequence, for each simulated vector of uncertain parameters, existing technologies can be left unused and be replaced by the installation of additional capacity. Furthermore, as the choice of relying on electricity imports is part of the energy strategy, also for electricity imports the lower bound is set to the amount imported in the robust solutions.

The 15 representative energy system configurations in Table 4.2 are run $n_{sample} = 10000$ times, considering uncertainty for the operation-related parameters (c_{op} for fossils and $c_{p,t}$ for renewables) sampled from uniform distributions over the entire uncertainty range. For each run, the additional installed capacity in the system and the additional electricity imports are measured.

Figure 4.12 plots the average additional installed capacity and the average additional imports of electricity for the 15 different energy system configurations over the 10000 simulations. The figure reveals that the deterministic investment decision ($\Gamma_{obj} = 0$), made without considering uncertainty,

is the most subject to the risk of overcapacity. As detailed in Table 4.2, this solution heavily relies on NG for electricity supply, and thus, in case of high NG prices, it is better to invest on other technologies than to operate the CCGT plants. On average, the additional installed capacity is in the order of magnitude of three large conventional power plants. Interestingly, this reproduces the dynamics which led to overcapacity in the previously mentioned European countries. Robust investment strategies - with a higher share of more efficient technologies, of renewables and a higher investment-to-operating cost ratio - are instead less likely to require major future modifications. This example is relevant for energy planners, as it shows that, when considering uncertainty, policies reducing the dependency on fossil fuels can also limit the risk of overcapacity, which would result in additional financial as well as environmental costs.

4.3.4 Comparison with stochastic programming

At last, it is relevant to compare robust solutions with the more “traditional” way of incorporating uncertainties in optimization models, i.e. *stochastic programming*. The basic idea of stochastic programming is to optimize the expected value of the objective over all the possible realizations of uncertainty, which are modeled as a *scenario tree*. Stochastic models are two- or multi-stage, meaning that at the nodes of the scenario tree recourse decisions can be made to adapt the solution as uncertainty unfolds. As commented by Grossmann et al. [36], its multi-stage nature makes stochastic programming “*appropriate for long-term [...] planning [...], since it does not fix all the decisions at the initial point of the planning horizon as it allows recourse decisions in future times to adapt in response to how the uncertainties are revealed*”.

According to Birge and Louveaux [57], who offer a thorough introduction to stochastic programming, a two-stage stochastic LP problem with fixed recourse is expressed in its general form by Eq. 4.38, in which \mathbf{x} are the first-stage decision variables; \mathbf{y} are the second-stage decision variables; $\omega \in \Omega$ are random events (scenarios) which can realize between the first and the second stage; ψ denotes the uncertain parameters; q , b and \mathcal{A} are the data of the first-stage problem; q , β and \mathcal{T} are the data of the second-stage problem, which are known for a given scenario ω .

$$\begin{aligned}
 \min \quad & c^T \mathbf{x} + \mathbb{E}_\psi [\min q(\omega)^T \mathbf{y}(\omega)] & (4.38) \\
 \text{s.t.} \quad & \mathcal{A} \mathbf{x} = b \\
 & \mathcal{T}(\omega) \mathbf{x} + \mathcal{W} \mathbf{y}(\omega) = \beta(\omega) \\
 & \mathbf{x}, \mathbf{y}(\omega) \in \mathbb{R}^+
 \end{aligned}$$

The objective function of Eq. 4.38 contains a deterministic term $c^T \mathbf{x}$ and the expected value (\mathbb{E}) of the second-stage objective $q(\omega)^T \mathbf{y}(\omega)$ taken over all realizations of the scenario ω . The distinction between the first-stage (*here-and-now*) and the second-stage (*wait-and-see*) can be represented the

example the scenario tree in Figure 4.13.

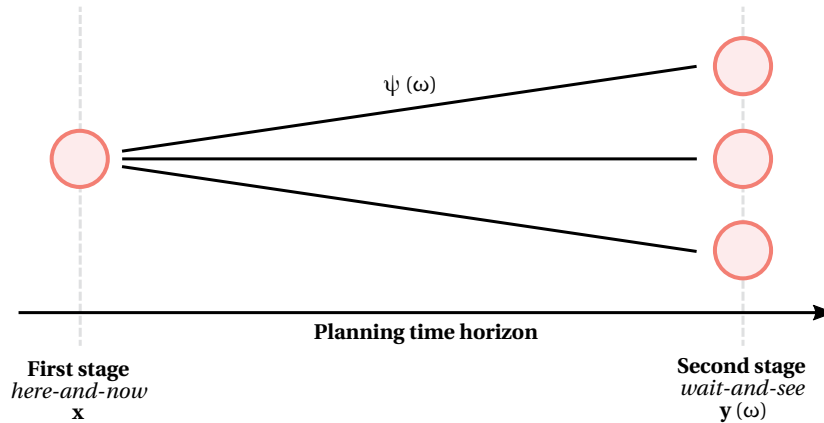


Figure 4.13 – Example of scenario tree for a two-stage stochastic programming problem

A stochastic version of the Swiss national MILP model is obtained using DET2STO, a handy software tool developed by Thénié et al. [163] to automatically generate the deterministic equivalent of stochastic programming problems. A natural choice is to consider investment-related decisions (such as \mathbf{F}) as first-stage decision variables, and operating decisions (such as \mathbf{F}_t , \mathbf{Sto}_{in} and \mathbf{Sto}_{out}) as second-stage decision variables. The scenarios are generated by permuting three values (low-nominal-high) for each uncertain parameter θ , which results in 3^θ scenarios. A first observation is that this exponential growth limits the number of parameters θ to be considered. In fact, the solving time is above 1h for $\theta = 5$, and over three days for $\theta = 6$ on a 2.4 Ghz 8-core machine, and even the LP relaxation of the problem overflows the 8 GB available RAM resources for $\theta \geq 8$. Thus, the scenarios are generated considering 7 uncertain parameters for the LP relaxation of the problem. In particular, the discount rate (i_{rate}) and the cost of imported resources (c_{op} of NG, electricity imports, light fuel oil (LFO), coal, gasoline and diesel) are selected based on the GSA results in Table 3.3.

The resulting problem, featuring 2.4 million linear variables, is solved to optimality in 3h. The obtained solution is reported in Table 4.5: electricity production is supplied by CCGT, wind and new hydro dams, while heat supply is dominated by fuel boilers.

A simulation study is carried out to compare this stochastic solution to the deterministic one and to three representative robust solutions. These five energy system configurations (Tables 4.2, 4.4 and Table 4.5) are simulated $n_{sample} = 10000$ times, sampling the values of the uncertain parameters (all uncertain parameters) from uniform distributions over the entire uncertainty range. Only investment-related decision variables are fixed, while operating decision variables are determined by the optimization.

The results, illustrated in Figure 4.14, reveal that the stochastic solution has an average performance

Table 4.5 – Optimal investment strategy of the stochastic programming problem.

	Technology	Installed size	Units
Electricity Production	CCGT	0.52	[GW _e]
	Coal	0	[GW _e]
	PV	0	[GW _e]
	Wind	5.30	[GW _e]
	New Dam	0.44	[GW _e]
	New River	0	[GW _e]
Heat Production	Boilers	22.0	[GW _{th}]
	CHP	1.31	[GW _{th}]
	Elec. HPs	2.18	[GW _{th}]
	Solar Th.	0	[GW _{th}]
	Deep Geo	0.77	[GW _{th}]
	%Dhn	0.3	[-]

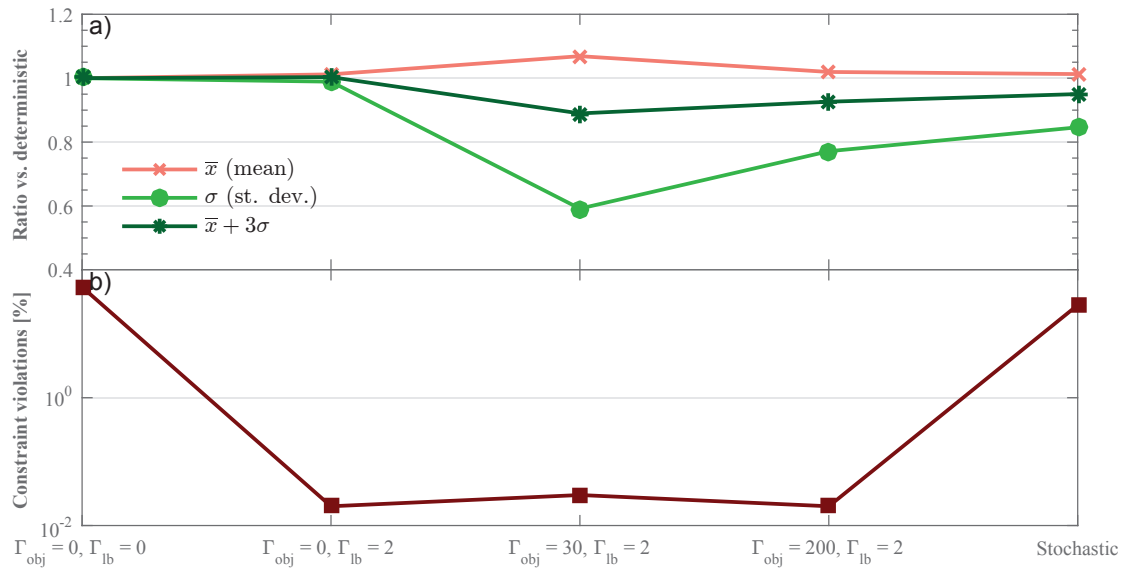


Figure 4.14 – Simulation results comparing stochastic vs. representative robust solutions: a) mean (\bar{x}), standard deviation (σ), $\bar{x} + 3\sigma$ and for the objective value and b) frequency of constraint violations. Reference (on the left y-axis) is the deterministic solution (Table 4.2). Representative robust solutions are detailed in Table 4.4. Stochastic solution (on the right y-axis) is detailed in Table 4.5. Solutions are simulated on all uncertain parameters (sampled from entire uncertainty range) and only investment decisions are fixed (free resources).

similar to the deterministic solution (+1.3%) and a lower standard deviation (−15%). Robust solutions are on average more expensive (reaching +6.9% compared to the deterministic case), but offer a better protection against worst-case and against the risk of constraint violations. The latter is due to the fact that in stochastic programming, due to the computational limits, the uncertainty of parameters linked to feasibility in the constraints is not accounted for.

Overall, the simplified comparison confirms that the advantage of robust optimization over stochastic programming primarily lies in its computational performance. Although the multi-stage nature of stochastic programming makes it the natural answer to strategic energy planning problems, computational barriers, along with the difficulty in appropriately defining PDFs and scenarios, can limit its practical applications. In these situations, robust optimization proves to be a good alternative, offering tractable formulations even when considering uncertainty for hundreds of parameters, and thus allowing to address issues related to both feasibility and optimality of energy systems.

Discussion

This chapter proposes a complete framework to incorporate uncertainty in strategic energy planning optimization models using the robust formulation by Bertsimas and Sim [62]. First, uncertainty in the objective function and in the other constraints is separately considered. On the one hand, for uncertainty in the objective, a novel robust formulation is proposed and demonstrated, extending Bertsimas and Sim [62] to consider the the case of multiplied uncertain parameters. On the other hand, the method proposed by Babonneau et al. [154] is adopted to systematically consider uncertainty in the other constraints; this additionally shows the advantages of using concise formulations when aiming at incorporating uncertainty in optimization models. Overall, the presented developments allow to consider uncertainty for *all* uncertain parameters in strategic energy planning models, which constitutes a novelty in the literature.

Then, the robust formulations for the constraints (related to feasibility) and for the objective (related to the optimality) are put together to propose a decision-making method for energy systems, with the goal of identifying solutions which are both reliable and cost-effective.

To answer the real-world research question posed at the beginning of the chapter, the presented formulations and methods are applied to the MILP Swiss national energy system model presented in Chapter 1. The results reveal that the deterministic energy strategy illustrated in Figure 4.2, heavily relying on fossil fuels, changes dramatically when uncertainty is accounted for. In general, robust solutions are characterized by a significantly higher penetration of renewables and efficient technologies. Simulation studies reveal that robust investment strategies are on average marginally more expensive than the deterministic solution, but offer more reliability (e.g. low risk of not meeting demand) and stability over time, due to a reduced dependency on highly volatile fossil fuel prices. The simulations additionally highlight the interest of generating robust solutions at intermediate

protection levels, which confirms the validity of probabilistic approaches to robust optimization, such as the one by Bertsimas and Sim [62].

Finally, the proposed approach is compared to stochastic programming, which is the “traditional” way of incorporating uncertainty in long-term planning problems. The comparison reveals that robust optimization can be a good alternative to stochastic programming. In fact, strategic energy planning problems are characterized by a large number of input parameters together with low availability of data to quantify their PDFs. In this context, the application of stochastic programming is limited by the curse of dimensionality and by the difficulty in defining scenarios. Robust optimization, instead, can handle large numbers of uncertain parameters and does not rely on the definition of PDFs, and thus can better support energy planners in identifying reliable and cost-effective energy strategies.

Conclusions

Overview

- Summary of the main results
- Recommendations and guidance to integrate uncertainty in energy models
- Future perspectives

The research question motivating this thesis covers two dimensions. The first dimension - *“how can we facilitate the integration of uncertainty in the energy modeling practice?”* - is methodological, as it concerns the presentation of methods to facilitate the integration of uncertainty in energy planning. The answer along this dimension is declined in four main contributions, ranging from energy modeling to uncertainty characterization, from global sensitivity analysis to robust optimization. The second dimension - *“how does uncertainty impact strategic energy planning?”* - is practical, as it concerns the application of these methods to a real energy planning problem. To do this, the presentation of the methods is systematically associated to their validation on the representative case study of the Swiss energy system. Overall, the thesis offers a complete framework covering all the phases of strategic energy planning, from the modeling of the energy system to its optimization under uncertainty. This framework, together with a full documentation of models, methods and data, can support decision-makers to integrate uncertainty in the energy planning process.

As the methods, contributions and results are detailed in the dedicated chapters, these concluding remarks summarize the main findings, provide recommendations and guidance to integrate uncertainty in energy models, and envision future perspectives.

Main results summary

The main finding of this work is that **uncertainty dramatically impacts strategic energy planning decisions**. In fact, the deterministic solution, i.e. the energy strategy defined without accounting for uncertainty, drastically changes as soon as uncertainty is considered. Uncertainty is seldom considered in the current energy planning practice, which normally relies on long-term forecasts

Conclusions

for important parameters or in which, as it emerges from discussions with industrial partners, long-term decisions are in some cases merely based on today's data. The results presented in this thesis show that forecasts, especially of fuel prices, are inevitably inaccurate, and that decisions made without considering uncertainty are likely to generate overcapacity in the future.

Second, **uncertainty characterization matters**. In fact, the quantification of input uncertainties in Chapter 2 reveals that uncertainty levels vary significantly for different parameters, and that the way in which uncertainty is characterized has a strong impact on the output results. In particular, economic parameters, such as the discount rate and the price of imported resources, emerge as the most impacting factors.

An additional result is the importance of **considering all uncertain parameters** in the analysis. In fact, the proposed sensitivity analysis and optimization under uncertainty methods allow to consider a large number of uncertain parameters, which are typically found in strategic energy planning models, at the price of reasonable computational expenses. This is a novelty compared to the literature in the field, in which uncertainty is often only considered for a limited subset of *a priori* selected parameters. The results of the application to the case study reveal that parameters which are commonly considered as fixed assumptions in energy models, and whose uncertainty is therefore seldom investigated, emerge as very impacting.

At last, the presented robust optimization framework allows to systematically integrate uncertainty in optimization-based energy planning models for decision support. In the case study, **robust energy strategies are characterized by a higher penetration of renewables and efficient technologies**, and thus by a higher investment-to-operating cost ratio compared to the deterministic solution. Simulation studies reveal that robust investment strategies can offer more reliability (e.g. low risk of not meeting demand) and stability over time, due to a reduced dependency on highly volatile fossil fuels, at the price of a marginally higher average cost. Also, due to the large uncertainty of cost parameters, solutions generally show a high variability (i.e. high standard deviations), which suggests that a robust energy strategy with a higher penetration of renewables might not be significantly more costly than a deterministic, fossil-based, alternative.

Recommendations and guidance

Based on the obtained results and the hours dedicated to the research work behind this thesis, some recommendations and guidance are provided to energy modelers aiming at integrating uncertainty in optimization models, and summarized in the following points:

- **A little uncertainty is better than no uncertainty at all.** In this thesis, various structured methods are presented and applied to consider uncertainty in energy modeling. Although the natural recommendation is to apply these methods to the case study of interest, a direct

application in the energy modelling and planning practice might not be possible for a variety of - often very practical - reasons (e.g. time constraints, project deadlines, etc.). In these cases, even a very basic consideration of uncertainty, such as a local sensitivity analysis, can already provide interesting insights on the results of the study.

- **Model for uncertainty.** Integrating uncertainty in energy planning models can pose difficulties both in terms of problem formulation and of computational burdens. In this thesis, it is shown that a concise model formulation and an efficient computational performance facilitate - and often make possible - the integration of uncertainty in energy models. This should be considered in the development of the deterministic formulations of optimization models. In fact, if solving the deterministic version of a model already poses computational challenges, the integration of uncertainty is likely to be practically infeasible, or to result in trivial applications.
- **Keep it simple.** Linked to the previous point, modelers have a natural tendency to increase the level of detail of models, most often in aspects closely related to their own expertise. As an example, an energy modeler with a strong background in thermodynamics is likely to focus on the accurate representation of the performance of technologies, and to simply assume a default value for an economic parameter as the interest rate. The results in this thesis suggest that sensitivity analysis studies can help defining priorities in modeling. Thus, it is good practice to begin integrating uncertainty in the early-stage development of a model, for both computational and time management reasons.
- **Challenge your assumptions.** The results obtained in this thesis reveal that modelers' assumptions can be very impacting. However, in the modeling practice, making assumptions is unavoidable. Considering *all* parameters means also considering assumed parameters as uncertain factors, which allows modelers to better evaluate - and, possibly, modify - their initial assumptions.
- **Fully document data sources.** A plague of the current scientific literature is the difficulty in reproducing published results [164]. This is due to the fact that a complete documentation of models and data is rarely provided, which can as well affect the credibility of the models [165]. Especially when dealing with uncertainty, a meticulous and structured documentation of the used data sources can facilitate reproducibility of the work, comparisons, and adaptation to other case studies.
- **Optimize for what is certain.** In this thesis, cost optimization is used for decision-making as economics are often the dominant driver in energy planning choices. However, economic parameters are also the inputs with the highest uncertainty. Other objectives, e.g. the CO₂ emissions associated to the combustion of fossil fuels or the energy efficiency, have much lower levels of uncertainty. Thus, decision-makers can decide to optimize for more "certain" objectives, and evaluate economic performance *a posteriori* via uncertainty analysis.
- **Uncertainty as a debugging tool.** When developing a model, making mistakes is unavoidable. Simulating the model in the uncertain domain is, in this case, a powerful way of finding errors.

In fact, by covering all the solution space, uncertainty exposes the model to combinations of input parameters which often make hidden mistakes come to light.

Future perspectives

Future improvements of the presented work are envisioned along five main research tracks.

First, from the modeling point of view, the comparison with stochastic programming has highlighted the interest of **multi-stage decision-making including recourse**. Although the inclusion of recourse in robust optimization is to date an open challenge, recent developments - such as linear decision rules (LDR) [148] and adjustable robust optimization (ARO) [149] - make it possible to include recourse in robust formulations.

Second, robust optimization has been here applied using the - rather successful - formulation by Bertsimas and Sim [62]. However, after the proposal of their milestone method, **robust optimization** has been constantly evolving, with **developments** proposing tighter bounds, as in the work by Guzman et al. [166], or entirely new approaches, such as distributionally robust optimization [151], a paradigm where the uncertain problem data are governed by a probability distribution that is itself subject to uncertainty. If information about the distribution of the data is available, this approach allows to make use of it in the decision process, whereas using the method by Bertsimas and Sim [62] this additional information would be discarded. Thus, there is an interest in investigating the application of these latest developments in robust optimization to the MILP formulation presented in Chapter 1.

Third, there is also an interest in **increasing the spatial and temporal granularity** of the case study. In fact, in this work, the Swiss energy system has been modeled in a rather simplified way, which does not allow to consider daily variations of the energy system, or its spatial dimensions. Spatial and temporal granularity can have a significant impact, especially with an increasing penetration of renewables; as an example, a more refined time resolution could capture the short-term intermittence of power generation by wind and solar. The model could as well be extended on the demand side by including investment options for energy efficiency measures. Of course, a wider resolution of the model is likely to increase its computational time, which requires the identification of an appropriate trade-off between computational requirements and model accuracy.

Fourth, due to time constraints, in Chapter 2 parameters have been divided in groups based on their similarity, and uncertainty has been characterized for one representative parameter per category. Future work envisions the **uncertainty quantification of the individual parameters**, which can increase the accuracy of the obtained results.

Last, but probably most importantly, in this thesis uncertainty has been considered for quantifiable elements in a model, mainly economic and technical parameters. However, in the reality of energy

planning there are also **other sources of uncertainty**, such as the enforcement of policies, the evolution of neighbouring energy systems, the social acceptance, the behavior of people and markets, the advent of breakthrough technologies, etc. These parameters are evidently more difficult to quantify, but at the same time possibly more likely to severely impact the energy strategy, and thus they should be additionally considered. This could result in decision-support frameworks in which quantitative methods are complemented by qualitative assessments, as advocated by van der Sluijs et al. [167].

Uncertainty is seldom considered in the current energy planning practice. This thesis contributes to a systematic consideration of uncertainty in energy models by identifying the fundamental research questions and by proposing methods to answer them. As the consideration of uncertainty is an emerging topic in the literature, the focus of the thesis is intentionally broad, not aiming at providing definitive answers to the research questions which motivate it. As a consequence, future research is envisioned along the three main research axes of this thesis, namely *i*) the development of energy models suitable for uncertainty, *ii*) the quantification of input uncertainties, and *iii*) the definition of methods to integrate them in decision-making.

As energy modeling is often inevitably problem specific, it is crucial that researchers working in this area fully document their models and data sources, in order to ensure reproducibility and adaptation to other case studies, and systematically compare their proposed methods to the state-of-the-art in the literature. In the long run, this will generate *i*) a set of available modeling frameworks at different scales (building, urban, national, etc.) with the appropriate level of detail to allow the consideration of uncertainty; *ii*) a structured collection of data to characterize the uncertainty of each uncertain parameter; *iii*) a set of specific methods to integrate the different types of uncertainty in decision-making. This can ultimately allow the translation of the methods presented in the literature into practical tools in the hands of decision-makers to shape the future of energy systems.

A Swiss energy system data

Overview

The appendix is complementary to Chapter 1 as it details the input data for the application of the MILP modeling framework to the case study of Switzerland in the years 2035 and 2011, the latter used for model validation.

The resources and technologies in Figure 1.2 are characterized in terms of energy and mass balances, cost (operating and investment), and environmental impact (global warming potential (GWP)).

For GHG emissions, LCA data are taken from the Ecoinvent database v3.2¹ [168] using the “allocation at the point of substitution” method. GWP is assessed with the “GWP100a - IPCC2013” indicator. For technologies, the GWP impact accounts for the technology construction; for resources, it accounts for extraction, transportation and combustion.

For the cost, the reported data are the nominal values for Switzerland in the year 2035. All costs are expressed in *real*² Swiss Francs for the year 2015 (CHF₂₀₁₅). All cost data used in the model originally expressed in other currencies or referring to another year are converted to CHF₂₀₁₅ to offer a coherent comparison. The method used for the conversion is illustrated by Eq. A.1.

$$c_{inv}[\text{CHF}_{2015}] = c_{inv}[C_y] \cdot \frac{\text{USD}_y}{C_y} \cdot \frac{\text{CEPCI}_{2015} [\text{USD}_{2015}]}{\text{CEPCI}_y [\text{USD}_y]} \cdot \frac{\text{CHF}_{2015}}{\text{USD}_{2015}} \quad (\text{A.1})$$

Where C and y are the currency and the year in which the original cost data are expressed, respectively, USD is the symbol of American Dollars and the Chemical Engineering's Plant Cost Index

¹ The database is consulted online: <http://www.ecoinvent.org>

² *Real* values are expressed at the net of inflation. They differ from *nominal* values, which are the actual prices in a given year, accounting for inflation.

Appendix A. Swiss energy system data

Table A.1 – CEPCI values [169]

Year	CEPCI
1982	285.8
1990	357.6
1991	362.3
1992	367.0
1993	371.7
1994	376.4
1995	381.1
1996	381.7
1997	386.5
1998	389.5
1999	390.6
2000	394.1
2001	394.3
2002	395.6
2003	402.0
2004	444.2
2005	468.2
2006	499.6
2007	525.4
2008	575.4
2009	521.9
2010	550.8
2011	585.7
2012	584.6
2013	567.3
2014	576.1
2015	556.3

(CEPCI) [169] is an index taking into account the evolution of the equipment cost (values reported in Table A.1). As an example, if the cost data are originally in EUR₂₀₁₀, they are first converted to USD₂₀₁₀, then brought to USD₂₀₁₅ taking into account the evolution of the equipment cost (by using the CEPCI), and finally converted to CHF₂₀₁₅. The intermediate conversion to USD is motivated by the fact that the CEPCI is expressed in *nominal* USD. Although this conversion method is originally defined for technology-related costs, in this thesis as a simplification it used also for the cost of resources.

A.1 Energy demand

The EUD for heating, electricity and mobility in 2035 is calculated from the data in [81] for the “Politisches Massnahmenpaket” (“PMF”, Political Measures of the Federal Council) scenario in the year 2035.

A.1.1 Heating

The EUD for SH in households is calculated as the product of the number of inhabitants in Switzerland, the *per capita* living space and the annual specific heating requirement (Table A.2).

The EUD for HW in households is the only heating requirement which is not calculated based on the “PMF” scenario. It is calculated assuming a *per capita* daily HW consumption of 50 L/day/inhabitant and a temperature increase of 40 °C [170].

Table A.2 – Data for the calculation of the end use energy demand in the households sector.

	“PMF” scenario in 2035 [81]
Population [10^6 people]	8.89
Living space [m^2/person]	67
Specific heating requirement [$\text{kWh}/\text{m}^2/\text{y}$]	49.5
HW consumption [$\text{L}/\text{day}/\text{person}$]	50 [170]
Temperature increase for HW production [$^{\circ}\text{C}$]	40

Table A.3 reports input data and calculated values for the heating EUD in the different sectors.

The calculation of the end-use heating demand in the industry and services sectors starts from the FEC data by type of heat usage, available in Table 9-18 and Table 9-23 in [81]. The FEC values reported in [81] are the sum of the fuel consumption in boilers, the electricity consumption for direct electric heating and for HPs, and the ambient heat used by the latter. The EUD for heating in the industry and service sectors accounts for the heat supplied by the HPs (equal to the sum of the ambient heat and their electricity consumption), the heat produced by direct electric heating systems (equal to their electricity consumption) and the heat supplied by boilers (which is estimated assuming a 90% efficiency).

For both sectors, first the FEC is shared among the different technologies, then it is proportionally divided among space heating, hot water and process heating. The ambient heat consumption is obtained from tables 9-21 and 9-27 in [81]. The electricity consumed by the heat pumps using the reported ambient heat is calculated using a coefficient of performance (COP) of 3.7. The COP is based on the ambient heat and electricity consumption of the heat pumps in the household sector in 2035 (table 9-7 and 9-10 in [81]). The electricity consumption for direct electric heating is computed as the sum of the electricity consumption for space heating, hot water and process heating (Tables 9-19 and 9-24 in [81]) minus the calculated electricity consumption of the heat pumps. The use

Appendix A. Swiss energy system data

of direct electric heating systems is divided between space heating, hot water and process heating proportionally to the FEC of each end-use type. It is assumed that heat pumps are not used for the high temperature EUD in the industry sector. Thus, the use of heat pumps is shared between space heating and hot water.

In the model, there is a repartition between low temperature and high temperature heating EUD. The first one includes EUD for space heating and hot water. The second one is the EUD for process heating. The services sector has only low temperature heating EUD, while the industry sector has both.

Table A.3 – FEC and EUD in the household, industry and service sectors.

“PMF” scenario in 2035 [81]					
	EUD type	Technology/Source	Households [GWh/y]	Industry [GWh/y]	Services [GWh/y]
FEC	Space heating			5361	15861
	Hot water			1389	3556
	Process heating			20722	0
FEC		Fuels ^a		22211	16361
		Ambient heat		244	1750
		Elec. heat pumps		92	653
		Elec. direct heating		4925	653
	Space heating	Fuels		4133	13365
		Ambient heat		194	1430
		Elec. heat pumps		73	533
		Elec. direct heating		961	533
FEC ^a	Hot water	Fuels		1071	2996
		Ambient heat		50	320
		Elec. heat pumps		19	120
		Elec. direct heating		249	120
	Process heating	Fuels		17007	0
		Ambient heat		0	0
		Elec. heat pumps		0	0
		Elec. direct heating		3715	0
EUD ^a	Space heating		29489	4948	14525
	Hot water		7538	1282	3256
	Process heating		0	19021	0
EUD ^a	Low temperature		37027	6230	17781
	High temperature		0	19021	0

^a Calculated values.

Process heating and HW demand are considered constant over the year, whereas SH demand is shared over the year according to $\%_{heating}$ (Table A.4).

Table A.4 – Monthly distribution factors for SH demand ($\%_{heating}$) and electricity demand for lighting ($\%_{lighting}$).

	Yearly share (adding up to 1) of space heating and lighting [-]											
	Jan.	Feb.	Mar.	Apr.	May	Jun.	Jul.	Aug.	Sep.	Oct.	Nov.	Dec.
$\%_{heating}^a$	0.198	0.165	0.142	0.032	0	0	0	0	0.015	0.090	0.138	0.219
$\%_{lighting}^b$	0.124	0.102	0.092	0.071	0.059	0.044	0.041	0.040	0.068	0.105	0.124	0.132

^a Calculated from the heating degree days for Pully, CH, for 2011.

^b Data from the “Eclairage 100” curve in figure 5-1 [171].

A.1.2 Electricity

The values in Table A.5 list the electricity demand that is not related to heating for the three sectors in 2035. The values are taken from tables 9-11, 9-13, 9-15, 9-19 and 9-24 in [81]. Lighting demand is shared over the year according to $\%_{lighting}$ (Table A.4), while the rest of the electricity demand is considered constant over the different months.

Table A.5 – Electricity demand not related to heating by sector.

“PMF” scenario in 2035 [81]		
	Lighting [GWh]	Others [GWh]
Households	425	10848
Industry	1264	10444
Services	3805	15026

A.1.3 Mobility

The annual passenger transport demand in Switzerland for 2035 is expected to be 146e09 pkms [81]. Passenger transport demand is divided between public and private transport. The lower ($\%_{public,min}$) and upper bounds ($\%_{public,max}$) for the use of public transport are 30% and 50% of the annual passenger transport demand, respectively.

The annual freight transport demand in Switzerland for 2035 is expected to be 40.0e09 tkms. It is shared between road (trucks) and rail (train) freight transport [81]. The lower ($\%_{rail,min}$) and upper bounds ($\%_{rail,max}$) for the use of freight trains are 40% and 60% of the annual freight transport demand, respectively.

A.2 Electricity production and storage

A.2.1 Renewables

Table A.6 – Renewable electricity production technologies

	f_{ref} [GW]	c_{inv} [CHF ₂₀₁₅ /kW _e]	c_{maint} [CHF ₂₀₁₅ /kW _e /y]	gwp_{constr} [kgCO ₂ -eq./kW _e]	Lifetime [y]	c_p [%]	f_{min} [GW]	f_{max} [GW]
Solar PV	3.00e-06	1000 ^a	15.9 ^a	2081 [168]	25 [172]	11.3 ^b	0	25 ^c
Wind Turbine	3.00e-03	1466 ^d	23.9 ^d	622.9 [168]	20 [176]	23.0 ^e	0	5.30 ^f
Existing Hydro Dam	8.08	4828 [181]	24.1 [181]	1693 [168]	40 [181]	23.4	8.08 [182]	8.08 [182]
New Hydro Dam ^g	1.00e-3	3437	2.89				0	0.44
Existing Hydro River	3.80	5387 [181]	53.9 [181]				3.80 [182]	3.80 [182]
New Hydro River ^g	1.00e-04	5919	76.3	1263 [168]	40 [181]	48.4	0	0.85
Geothermal ^h	7.6e-03	11464	465	2.493e01 [168]	30	86 [183]	0	0.70 ⁱ

^a Investment cost based on expert opinion (Christophe Ballif, EPFL, April 2017), O&M cost scaled proportionally based on IEA data. The IEA [106] indicates a c_{inv} of 1557 CHF₂₀₁₅/kW_e and a c_{maint} of 24.7 CHF₂₀₁₅/kW_e for a residential system in 2035.

^b Cumulated PV installed capacity in Switzerland reached about 0.44 GW in 2012, of which 0.226 GW deployed in the same year. In the same year the overall PV production has been 320.29 GWh [173]. Therefore, assuming a constant growth rate for the installed capacity, the average capacity factor is 0.113.

^c In Switzerland the available/adequate surface for solar panels deployment is estimated to be 140 km² for roofs and 55 km² for façades [174]. Assuming that 40% of this surface is used for the installation of PV panels with a 25% [175] electrical efficiency, then the photovoltaic potential is 25 TWh/y.

^d Onshore wind turbines in 2035 [106].

^e The actual capacity factor is approximately 0.19 in Switzerland [177]. The IEA states that “turbine design advancement in ten years allows for significant increase in capacity factors” [178]. The new low wind speed turbines are expected to have a capacity factor of 0.33 for an average annual wind speed of 5.5 m/s at 50 m height [178]. In Switzerland, there are several possible locations where average annual wind speed reaches 5.5 m/s [179]. Considering these factors and adopting a conservative approach, the selected value for 2035 is chosen to be 0.23.

^f The maximum electricity production potential is estimated to be 10.7 TWh/y (potential that can be accepted by the Swiss population) [180].

^g See the dedicated section.

^h Organic Rankine cycle (ORC) cycle at 6 km depth for electricity production (Appendix D.3.4).

ⁱ 4.4 TWh/y are estimated in [81] for the year 2050.

Data for the considered renewable electricity production technologies are listed in Table A.6. As described in Section 1.1.2, for seasonal renewables (Table A.7) the capacity factor $c_{p,t}$ is defined for each time period. In Table A.6, the yearly capacity factor (c_p) is reported. For these technologies, the relation between $c_{p,t}$ and c_p is expressed by Eq. A.2.

$$c_{p,t} = \frac{c_p \cdot 365 \cdot dist_t}{days_t} \quad (A.2)$$

In which $dist_t$ is the share of electricity production in period t (summing up to 1) and $days_t$ is the number of days in month t . The values are reported in Table A.7. For all the other electricity supply

technologies (renewable and non-renewable) with a uniform monthly distribution, $c_{p,t}$ is equal to the default value of 1.

Table A.7 – Monthly electricity production share from renewable energy sources.

	Monthly electricity production share ($dist_t$) [-]											
	Jan.	Feb.	Mar.	Apr.	May	Jun.	Jul.	Aug.	Sep.	Oct.	Nov.	Dec.
Solar PV ^a	0.040	0.064	0.090	0.111	0.117	0.114	0.123	0.117	0.093	0.066	0.038	0.027
Wind ^b	0.120	0.093	0.104	0.065	0.065	0.050	0.055	0.050	0.058	0.103	0.112	0.125
Hydro Dam ^c	0.091	0.083	0.068	0.056	0.077	0.098	0.097	0.094	0.101	0.077	0.076	0.082
Hydro River ^c	0.053	0.042	0.054	0.074	0.109	0.130	0.135	0.125	0.093	0.066	0.059	0.060

^a Production profile for photovoltaic electricity in the Mittenland (Switzerland) [184].

^b Data from real installation in Mont-Soleil and Mont-Crosin (Switzerland) [185]

^c Average monthly distribution factors in the years 2008-2011 [186]. These profiles are used for both existing and new hydroelectric plants. Part of the monthly electricity production can be “shifted” to other months if the height of the dams is increased (see the dedicated section for details).

Hydro power in Switzerland

The projected capacity factors for hydroelectric run-of-river plants and dams are calculated based on the data in Table A.8. A decrease in the electricity production is expected in the next years due to the application of the LEaux law [187]. The law defines the minimum flow rates for rivers. In order to respect them, during some periods of the year it may be necessary to stop the power plants, i.e. letting the water flow bypassing the turbines. This will have as a consequence a decrease in the annual electricity production. The decrease in electricity production is estimated to be 1400 GWh/y [187]. In the model, the LEaux production penalty is shared between run-of-river plans and dams proportionally to their net yearly electricity production. The net electricity production is the total electricity production minus the electricity consumed for the pumping in the dams.

Table A.8 – Data for the calculation of the future capacity factors for hydro run-of-river and dams.

	Hydro river	Hydro dam
Net electricity production (2012) [GWh] [182]	16981	17297
Installed power (2012) [GW] [182]	3.84	8.08
LEaux effect [GWh] [187]	-686	-714
c_p [%]	48.4	23.4

The Swiss Federal Office of Energy (SFOE) has evaluated the development potential for hydroelectricity [187]. The results of the study are presented in Table A.9.

Forecasts in [81] for the year 2050 are based on the development potential under optimized conditions in Table A.9. This potential is distributed between hydro river and hydro dam (Table A.10).

Appendix A. Swiss energy system data

Table A.9 – Development potential for hydroelectricity in Switzerland [187].

	Additional net electricity production	
	Current conditions [GWh/y]	Optimized conditions [GWh/y]
New big plants	770	1430
Small hydro	1290	1600
Transformation, extension	870	1530
Total potential	2930	4560

Table A.10 – Development potential for hydroelectricity in Switzerland by 2050 [81].

	Additional net electricity production [GWh/y]
Small hydro	1600
Hydro run-of-river	2000
Hydro dams	900
Total potential	4500

In the model, this additional potential is added to the 2012 net electricity production to obtain the electricity production potential of Swiss hydroelectric power plants in 2050 (Table A.11). The small hydro potential is attributed to the hydro run-of-river technology as additional capacity. The values in Table A.11 for 2050 already include the decrease in production caused by the LEaux law.

Table A.11 – Net hydroelectricity production and installed power in Switzerland in the years 2012 and 2050.

	2012 [182]		2050	
	Production [GWh/y]	Power^a [GW]	Production [GWh/y]	Power^a [GW]
Hydro river	16981	3.84	19895	4.69
Hydro dam	17297	8.08	17483	8.52

^a The capacity factors in Table A.8 are used to calculate the installed power in 2050.

For the cost calculations, it is necessary to consider the way in which the additional electricity is produced (new dams, new run-of-river plants, improvement and renovation of existing plants). Table A.12 estimates this repartition based on data from [81] and [187].

Increasing the heights of existing dam has two consequences: an additional net electricity production (Table A.12) and an additional storage capacity of 2400 GWh [188]. Currently in Switzerland there is an electricity deficit during winter and an electricity surplus during summer months. Hydro-

A.2. Electricity production and storage

Table A.12 – Development potential of hydroelectricity in Switzerland by 2050 [81, 187].

	Additional net electricity production	
	Hydro river [GWh/y]	Hydro dam [GWh/y]
Renovation	677	463
Dams height increase	0	330
New big plants	1324	108
New small plants	1600	0

electric dams help equilibrating the seasonal balance by storing a fraction of the water harvested during spring and summer, for additional electricity production in winter months. Nonetheless, this “shifting capacity” is limited, as dams are forced to turbine water during summer months (despite the excess of electricity production) to avoid the risk of dam overflow [186]. The additional storage capacity allows to shift electricity production from summer to winter, meaning that 2400 GWh can be subtracted from the summer production, and be delivered in winter. This modifies the monthly distribution factors for hydro dams in Table A.7. In the model, this behaviour is represented by the *StoHydro* technology, described in Section 1.2.1.

Table A.13 and Table A.14 contain the data used for the calculation of the specific investment and O&M costs reported in Table A.6. The capacity factors calculated in Table A.8 are used for the calculation of the installed power.

Table A.13 – Investment cost data for the new hydro power plants in Switzerland.

	Hydro river			Hydro dam		
	Power [GW]	c_{inv} [CHF ₂₀₁₅ /kW _e]	Total Inv. [10 ⁶ CHF ₂₀₁₅]	Power [GW]	c_{inv} [CHF ₂₀₁₅ /kW _e]	Total Inv. [10 ⁶ CHF ₂₀₁₅]
Renovation	0.16	4278 [189]	683	0.23	2849 [189]	643
Dam height increase	-	-	-	0.16	3807	612 ^a
New big plants [181]	0.31	5387	1681	0.05	4828	254
New small plants	0.38	7054 ^b	2660	-	-	-
Total	0.85	5919	5023	0.44	3437	1509

^a The investment cost for increasing the height of dams is proportional to the amount of extra electricity associated to the increased potential energy of the water: [0.8, 0.9] CHF₂₀₁₅/kWh [188]. The mean of the interval is used in the calculations.

^b Average between values in Table 2-4 and in Table 2-5 for new small plants in 2035 [189]

Appendix A. Swiss energy system data

Table A.14 – O&M cost data for the new hydroelectric power plants in Switzerland.

	Hydro river			Hydro dam		
	Power [GW]	c_{maint} [CHF ₂₀₁₅ /kW _e /y]	Total O&M [10 ⁶ CHF ₂₀₁₅]	Power [GW]	c_{maint} [CHF ₂₀₁₅ /kW _e /y]	Total O&M [10 ⁶ CHF ₂₀₁₅]
Renovation	0.16	-	-	0.23	-	-
Dam height increase	-	-	-	0.16	-	-
New big plants [181]	0.31	54 [181]	16.8	0.05	24 [181]	1.27
New small plants	0.38	127 ^a	47.9	-	-	-
Total	0.85	76.3	65.7	0.44	2.89	1.27

^a Average between values in table 2-4 and in table 2-5 for new small plants in 2035 [189]

A.2.2 Non-renewable electricity supply technologies

Data for the considered fossil electricity production technologies are listed in Table A.15. The maximum installed capacity (f_{max}) is set to a value high enough (10 GW_e) for each technology to potentially cover the entire demand. For CCS technologies, a 90% capture rate is assumed.

A.2.3 Seasonal storage

The modeled seasonal storage option consists in the production of synthetic methane from the excess of electricity. This synthetic methane is then used for producing electricity during periods of deficit in electricity supply. This procedure is also known as Power-to-NG-to-Power. The seasonal storage model is based on the liquified CH₄-CO₂ system (LM-C) presented by Al-musleh et al. [75]. It consists of a reversible FC which is used as electrolyzer to produce hydrogen when there is excess electricity in the grid. The hydrogen is sent to a methanation reactor where it is mixed with CO₂ to produce methane which is liquified (LNG) previous to storage. When there is a shortage of electricity, the methane is gasified and oxidized in the FC to produce electricity. The produced CO₂ is liquified and stored for being used as input of the methanation reaction; thus, this system is a carbon closed loop, as there is no emission of CO₂.

The elements considered for the calculation of the investment and O&M costs are the reversible FC, the liquefaction train and the tanks for storing CH₄ and CO₂. The data required for the cost calculation is available in Table A.16. It has been assumed that the O&M cost (c_{maint}) are 5% of the initial investment cost, and that the lifetime of the different components is 25 years.

A.2.4 Electricity grid

The replacement cost of the Swiss electricity grid is 58.6 billions CHF₂₀₁₅ [196] and its lifetime is 80 years [197]. The electricity grid will need additional investment depending on the penetration level

A.2. Electricity production and storage

Table A.15 – Non-renewable electricity supply technologies. Abbreviations: combined cycle gas turbine (CCGT), carbon capture and storage (CCS), ultra-supercritical (U-S), integrated gasification combined cycle (IGCC)

	f_{ref} [GW]	c_{inv} [CHF ₂₀₁₅ /kW _e]	c_{maint} [CHF ₂₀₁₅ /kW _e /y]	gwp_{constr} [kgCO ₂ -eq./kW _e]	Lifetime [y]	c_p [%]	η_e [%]
Nuclear	1	5175 ^a	110 [106]	707.9 [168]	60 [191]	84.9 ^b	37
CCGT	0.5	824 [106]	21.1 [106]		25 [192]	85.0	63 ^d
CCGT CCS	0.5	1273 [106]	30.2 [106]	183.8 ^c [168]	25 [192]	85.0	57 ^e
U-S Coal	0.5	2688 ^f	31.7 ^f		35 [192]	86.8 [192]	49 ^g
U-S Coal CCS	0.5	4327 ^h	67.6 ^h		35 [192]	86.8 [192]	42 ⁱ
IGCC	0.5	3466 ^j	52.3 ^j	331.6 ^c [168]	35 [192]	85.6 [192]	54 ^k
IGCC CCS	0.5	6045 ^l	73.9 ^l		35 [192]	85.6 [192]	48 ^m

^a Investment cost: 3664 CHF₂₀₁₅/kW_e [106] + dismantling cost in Switzerland: 1511 CHF₂₀₁₅/kW_e [190].

^b Data for the year 2012 [173]

^c In the lack of specific data, assuming same impact for standard and CCS power plants.

^d 0.4-0.5 GW_e CCGT in 2035 (realistic optimistic scenario) [192].

^e CCGT with post-combustion CCS in 2025 (very optimistic scenario) [192].

^f 1.3 GW_e advanced pulverized coal power plant [193]. c_{maint} is fixed cost (31.18 CHF₂₀₁₅/kW_e/y) + variable cost (0.54 CHF₂₀₁₅/kW_e/y assuming 7600 h/y).

^g Pulverized coal in 2025 (realistic optimistic scenario) [192].

^h 1.3 GW_e advanced pulverized coal power plant with CCS [193]. c_{maint} is fixed cost (66.43 CHF₂₀₁₅/kW_e/y) + variable cost (1.15 CHF₂₀₁₅/kW_e/y assuming 7600 h/y).

ⁱ Pulverized coal with post-combustion CCS in 2025 (realistic optimistic scenario) [192].

^j 1.2 GW_e IGCC power plant [193]. c_{maint} is fixed cost (51.39 CHF₂₀₁₅/kW_e/y) + variable cost (0.88 CHF₂₀₁₅/kW_e/y assuming 7500 h/y).

^k IGCC in 2025 (realistic optimistic scenario) [192].

^l 0.52 GW_e IGCC power plant with CCS [193]. c_{maint} is fixed cost (72.83 CHF₂₀₁₅/kW_e/y) + variable cost (1.03 CHF₂₀₁₅/kW_e/y assuming 7500 h/y).

^m IGCC with post-combustion CCS in 2025 (realistic optimistic scenario) [192].

Table A.16 – Data for the seasonal storage cost calculation.

	Parameter	Unit	Value
Technical data [75]	Lower Heating Value (LNG)	[MJ/kg]	50
		[MJ/m ³]	21882
	Roundtrip efficiency	[%]	56.1 ^a
	Storage requirement	[m ³ _{CH₄} /GWh _{e,out}]	232
		[m ³ _{CO₂} /GWh _{e,out}]	264
Specific investment cost (c_{inv})	Tank	[kCHF ₂₀₁₅ /GWh _{e,out}]	585 ^b
	Liquefaction plant	[CHF ₂₀₁₅ /kW _{LNG}]	233 ^c
	Reversible FC	[CHF ₂₀₁₅ /kW _e]	2934 ^d

^a Power-to-LNG efficiency is 79.2% and LNG-to-Power efficiency is 70.8% [75].

^b Accounting for the investment of the CO₂ and CH₄ tanks. Based on the average of the cost interval 94-283 MCHF₂₀₁₅ for a 160000 m³ tank in Hjortset et al. [194], i.e. 1180 CHF₂₀₁₅/m³.

^c Average of the points in [195] (Figure 17), excluding high cost locations.

^d Same specific investment as the advanced cogeneration technology (Table A.19).

Appendix A. Swiss energy system data

of the decentralized and stochastic electricity production technologies. The needed investments are expected to be 2.5 billions CHF₂₀₁₅ for the high voltage grid and 9.4 billions CHF₂₀₁₅ for the medium and low voltage grid. These values correspond to the scenario 3 in [196]. The lifetime of these additional investments is also assumed to be 80 years.

A.3 Heating and cogeneration technologies

Table A.17, Table A.18 and Table A.19 detail the data for the considered industrial, centralized and decentralized CHP technologies, respectively. In some cases, it is assumed that industrial (Table A.17) and centralized (Table A.18) technologies are the same.

f_{min} and f_{max} for heating and CHP technologies are 0 and 20 GW_{th}, respectively. The latter value is high enough for each technology to supply the entire heat demand in its layer. Thus, for heating and cogeneration technologies the maximum and minimum shares are controlled in the model by $f_{min,\%}$ and $f_{max,\%}$, respectively.

Table A.17 – Industrial heating and cogeneration technologies.

	f_{ref} [MW]	c_{inv} [CHF ₂₀₁₅ /kW _{th}]	c_{maint} [CHF ₂₀₁₅ /kW _{th} /y]	gwp_{constr} [kgCO ₂ -eq./kW _{th}]	Lifetime [y]	c_p [%]	η_e [%]	η_{th} [%]	$f_{min,\%}$ [%]	$f_{max,\%}$ [%]
CHP NG	20	1504 ^a	98.9 ^b	1024 [168]	20 [192]	85	44 ^c	46 ^c	0	50
CHP Wood ^d	20	1154 [106]	43.2 [106]	165.3 [168]	25 [198]	85	18 [106]	53 [106]	0	100
CHP Waste	20	3127 ^e	119 ^e	647.8 ^f	25 [198]	85	20 [198]	45 [198]	0	50
Boiler NG	10	62.9 ^g	1.26 ^g	12.3 ^h	17 [199]	95	0	92.7 ^g	0	60
Boiler Wood	10	123 ^g	2.46 ^g	28.9 [168]	17 [199]	90	0	86.4 ^g	0	100
Boiler Oil	10	58.6 ⁱ	1.26 ^j	12.3 [168]	17 [199]	95	0	87.3 ^g	0	50
Boiler Coal	1	123 ^k	2.46 ^k	48.2 [168]	17 [199]	90	0	82	0	50
Boiler Waste	1	123 ^k	2.46 ^k	28.9 ^l	17 [199]	90	0	82	0	100
Direct Elec.	0.1	355 ^m	1.61 ^m	1.47 [168]	15	95	0	100	0	20

^a Calculated as the average of investment costs for 50 kW_e and 100 kW_e internal combustion engine cogeneration systems [81].

^b Calculated as the average of investment costs for 50 kW_e and 100 kW_e internal combustion engine cogeneration systems [189].

^c 200 kW_e internal combustion engine cogeneration NG system, very optimistic scenario in 2035 [192].

^d Biomass cogeneration plant (medium size) in 2030-2035.

^e Biomass-waste-incineration CHP, 450 scenario in 2035 [106].

^f Impact of MSW incinerator in Appendix D.3.8, using efficiencies reported in the table.

^g Appendix D.3.5

^h Assuming same impact as industrial oil boiler.

ⁱ 925 kW_{th} oil boiler (GTU 530) [200]

^j Assumed to be equivalent to a NG boiler.

^k Assumed to be equivalent to a wood boiler.

^l Assuming same impact as industrial wood boiler.

^m Commercial/public small direct electric heating [201].

For the DHN, the investment for the network is also accounted for. The specific investment (c_{inv}) is 882 CHF₂₀₁₅/kW_{th}. This value is based on the mean value of all points in [103] (Figure 3.19), assuming a full load hours of 1535 per year (see table 4.25 in [103]). The lifetime of the DHN is

A.3. Heating and cogeneration technologies

Table A.18 – District heating technologies.

	f_{ref} [MW]	c_{inv} [CHF ₂₀₁₅ /kW _{th}]	c_{maint} [CHF ₂₀₁₅ /kW _{th} /y]	gwp_{constr} [kgCO ₂ -eq./kW _{th}]	Lifetime [y]	c_p [%]	η_e [%]	η_{th} [%]	$f_{min,\%}$ [%]	$f_{max,\%}$ [%]
HP	1	368 ^a	12.8 ^b	174.8 [168]	25	95	0	400	0	50
CHP NG	20	1340 ^c	40.1 ^c	490.9 ^d	25 [192]	85	50 ^e	40 ^e	0	50
CHP Wood ^f	20	1154 [106]	43.2	165.3	25 [198]	85	18 [106]	53 [106]	0	100
CHP Waste ^f	20	3127	119	647.8	25 [198]	85	20 [198]	45 [198]	0	50
Geothermal ^g	23	1620	60.1	808.8 [168]	30	85	0	100	0	50
Boiler NG ^f	10	62.9 ^h	1.26 ^h	12.3	17 [199]	95	0	92.7 ^h	20	80
Boiler Wood ^f	10	123 ^h	2.46 ^h	28.9	17 [199]	90	0	86.4 ^h	0	100
Boiler Oil ^f	10	58.6	1.26	12.3	17 [199]	95	0	87.3 ^h	0	50

^a Calculated with the equation: c_{inv} [EUR₂₀₁₁] = 3737.6 * $E^{0.9}$, where E is the electric power (kW_e) of the compressor, assumed to be 2150 kW_e. Equation from [202], taking only the cost of the technology (without installation factor).

^b Ground-water heat pump with 25 years lifetime [203].

^c CCGT with cogeneration [106].

^d Impact of NG CHP in Appendix D.3.6, using efficiencies reported in the table.

^e η_e and η_{th} at thermal peak load of a 200-250 MW_e CCGT plant, realistic optimistic scenario in 2035 [192].

^f Assumed same technology as for industrial heat and CHP (Table A.17)

^g Direct use of a geothermal well at 4.2 km depth (Appendix D.3.4).

^h Appendix D.3.5

expected to be 60 years. The lower ($\%_{dhn,min}$) and upper bounds ($\%_{dhn,max}$) for the use of DHN are 10% and 30% of the annual low temperature heat demand, respectively.

Table A.20 reports the monthly distribution factors which are used for the calculation of $c_{p,t}$ using equation A.2. For all the other heat supply technologies (renewable and non-renewable) $c_{p,t}$ is equal to the default value of 1.

Table A.20 – Monthly heat production share from decentralized solar thermal panels.

	Monthly heat production share ($dist_t$) [-]											
	Jan.	Feb.	Mar.	Apr.	May	Jun.	Jul.	Aug.	Sep.	Oct.	Nov.	Dec.
Solar Thermal ^a	0.048	0.062	0.090	0.089	0.106	0.110	0.121	0.112	0.098	0.076	0.049	0.041

^a The calculation of the monthly share for solar thermal is based on the SPF model [208] with radiation data from the village of Verbier, Switzerland. It has been assumed that the mean temperature of the water inside the panel is 40°C.

Appendix A. Swiss energy system data

Table A.19 – Decentralized heating and cogeneration technologies.

	f_{ref} [MW]	c_{inv} [CHF ₂₀₁₅ /kW _{th}]	c_{maint} [CHF ₂₀₁₅ /kW _{th} /y]	gwp_{constr} [kgCO ₂ -eq./kW _{th}]	Lifetime [y]	c_p [%]	η_e [%]	η_{th} [%]	$f_{min,\%}$ [%]	$f_{max,\%}$ [%]
HP	0.01	525 ^{ab}	22.5 ^c	164.9 [168]	18 ^c	28.5 ^d	0	300	0	50
Thermal HP	0.01	337 ^{eb}	10.1 ^f	381.9 [168]	20	28.5 ^d	0	150	0	20
CHP NG ^g	0.005	1504	98.9	1024	20 [192]	28.5 ^d	44	46	0	40
CHP Oil	0.01	1394 ^h	87.5 ⁱ	1024 ^j	20	28.5 ^d	39 ^k	43 ^k	0	40
FC NG	0.01	7734 ^l	155 ^m	2193 [168]	20 [207]	28.5 ^d	58 ⁿ	22 ⁿ	0	20
FC H ₂ ^o	0.01	7734	155	2193	20 [207]	28.5 ^d	58	22	0	20
Boiler NG	0.01	169 ^p	5.08 ^p	21.1 ^p	17 [199]	28.5 ^d	0	90 ^p	20	80
Boiler Wood	0.01	494 [70]	17.3 [70]	21.1 ^q	17 [199]	28.5 ^d	0	85 [70]	0	100
Boiler Oil	0.01	152 [200]	9.12 ^r	21.1 ^p	17 [199]	28.5 ^d	0	85 ^p	10	50
Solar Th.	0.01	768 ^s	8.64 ^t	221.2 [168]	20 [201]	11.3 ^u	0	-	0	40
Direct Elec.	0.01	42.7 ^v	0.19 ^w	1.47 [168]	15 [201]	28.5 ^d	0	100	0	20

^a 10.9 kW_{th} Belaria compact IR heat pump [204].

^b Catalog data divided by 2.89. 2.89 is the ratio between Swiss catalog prices and prices found in the literature. Calculated by dividing the average price of a decentralized NG boiler (489 CHF₂₀₁₅/kW_{th}) in Swiss catalogs [205] by the price for the equivalent technology found in literature (169 CHF₂₀₁₅/kW_{th}, Appendix D.3.5).

^c 6 kW_{th} air-water heat pump [201].

^d 2500 h/y of operation (assumption).

^e Specific investment cost for a 15.1 kW_{th} absorption heat pump (Vitosorp 200-F) [205]

^f 3% of c_{inv} (assumption).

^g Assumed same technology as for industrial CHP NG (Table A.17)

^h Assumed to be equivalent to a 100 kW_e internal combustion engine cogeneration NG system [81].

ⁱ Assumed to be equivalent to a 100 kW_e internal combustion engine cogeneration NG system [189].

^j Assuming same impact as decentralized NG CHP.

^k Efficiency data for a 200 kW_e diesel engine [168]

^l System cost (including markup) for a 5 kW_e solid-oxide FC system, assuming an annual production of 50000 units [206].

^m 2% of the investment cost [106].

ⁿ Solid-oxide FC coupled with a NG turbine, values for very optimistic scenario in 2025 [207].

^o Assumed to be equivalent to FC NG.

^p Appendix D.3.5

^q Assuming same impact as NG and oil decentralized boilers.

^r 6% of c_{inv} , based on ratio between investment and O&M cost of boiler of similar size in [199].

^s 504 CHF₂₀₁₅/m² for the UltraSol Vertical 1V Hoval system [204]. For conversion from CHF₂₀₁₅/m² to CHF₂₀₁₅/kW_{th}, it is assumed an annual heat production of 650 kWh/m² (average for the best oriented roofs in the town of Verbier, Switzerland [141]).

^t 1.1% of the investment cost, based on ratio investment-to-O&M cost in [201].

^u The calculation of the capacity factor for solar thermal is based on the SPF model [208] with radiation data from the village of Verbier, Switzerland. It has been assumed that the mean temperature of the water inside the panel is 40°C.

^v Resistance heaters with fan assisted air circulation in [199].

^w In the lack of specific data, same investment-to-O&M ratio as for direct electric heating in the industry sector (Table A.17).

A.4 Transport

In the model, for transport technologies only the operating cost (fuel consumption) is considered. Investment, O&M costs and emissions associated to the construction are not accounted for. The efficiencies for the passenger vehicles in 2035 (Table A.21) are calculated with a linear interpolation between the 2010 and 2050 values presented in Table 6 in Codina Gironès et al [71]. For private mobility, the average occupancy assumed in [71] is 1.6 passenger/vehicle (data for the year 2010 in Switzerland, from [80]).

Table A.21 – Fuel and electricity consumption for transport technologies in 2035 [71], and minimum/maximum shares allowed in the model.

Vehicle type	Fuel [kWh/pkm]	Electricity [kWh/pkm]	$f_{min, \%}$ [%]	$f_{max, \%}$ [%]
Gasoline car	0.430		20	100
Diesel car	0.387		20	100
NG car	0.483		0	50
Hybrid electric vehicle (HEV) ^a	0.247		0	30
Plug-in hybrid electric vehicle (PHEV) ^b	0.176	0.045	0	30
Battery electric vehicle (BEV)		0.107	0	30
FC car	0.179		0	20
Tram and Trolley Bus		0.165	0	30
Diesel Bus and Coach	0.265		0	30
Diesel HEV Bus and Coach	0.183		0	30
NG Bus and Coach	0.306		0	30
FC Bus and Coach	0.225		0	20
Train		0.092	0	80

^a Using gasoline as only fuel.

^b It is assumed that electricity is used to cover 40% of the total distance and petrol to cover the remaining 60%.

The technologies available for freight transport are trains and trucks. Trains are considered to be only electric. Their efficiency in 2035 is 0.069 kWh/tkm [71]. The efficiency for freight transport by truck is 0.51 kWh/tkm based on the weighted average of the efficiencies for the vehicle mix in [71].

A.5 Resources

The availability of all resources, except for wood and MSW, is set to a value high enough to allow unlimited use in the model. No import of hydrogen or biofuels is accounted for in the implementation. Wood availability is 12279 GWh/y [209] (“wet wood”, 50% humidity, $LHV_{wb} = 8.279 \text{ MJ/kg}_{wb}$, Table D.3), while MSW is limited to 11142 GWh. For the calculation of the MSW availability it is considered that the average *per capita* annual waste production is 730 kg (2014 data for Switzerland, from [210]), 50% of it is recycled [211] and the lower heating value (LHV) is 12.35 MJ/kg (Table D.3).

Appendix A. Swiss energy system data

The number of inhabitants in Switzerland in 2035 is expected to be 8.90 millions [81].

Table A.22 details the prices of resources (c_{op}) and the GHG emissions (gwp_{op}) associated to their production, transportation and combustion. c_{op} for imported biofuels is assumed to be equal to the price of the respective fossil equivalent. No cost is associated to the MSW, as it is assumed that it should be collected anyway. Export of electricity are possible, but they are associated to a zero selling price.

Table A.22 – Price and GHG emissions of resources.

Resources	c_{op} [CHF ₂₀₁₅ /MWh _{fuel}]	gwp_{op} [kgCO ₂ -eq./MWh _{fuel}]
Electricity Import	90.06 ^a	482 ^b
Gasoline	87.96 ^c	345 ^b
Diesel	85.16 ^d	315 ^b
LFO	60.59 ^e	311.5 ^b
NG	34.82 ^f	267 ^b
Wood	93.24 ^g	11.8 ^b
MSW	0	150 ^b
Coal	30.17 ^h	401 [168]
Uranium	4.140 ⁱ	3.9 [168]

^a Based on average market price in the year 2010 (50 EUR₂₀₁₀/MWh, from [212]). Projected from 2010 to 2035 using a multiplication factor of 1.36 [81].

^b Table D.3

^c Based on 1.49 CHF₂₀₁₅/L (average price in 2015 for gasoline 95) [213]. Taxes (0.86 CHF₂₀₁₅/L, [214]) are removed and the difference is projected from 2015 to 2035 using a multiplication factor of 1.24 [104].

^d Based on 1.55 CHF₂₀₁₅/L (average price in 2015) [213]. Taxes (0.87 CHF₂₀₁₅/L, [214]) are removed and the difference is projected from 2015 to 2035 using a multiplication factor of 1.24 [104].

^e Based on 0.705 CHF₂₀₁₅/L (average price in 2015 for consumptions above 20000 L/y) [215]. Taxes (0.22 CHF₂₀₁₅/L, [214]) are removed and the difference is projected from 2015 to 2035 using a multiplication factor of 1.24 [104].

^f Based on 24.95 CHF₂₀₁₅/MWh, average import price in the years 2015-2016 at the Swiss border. Projected from 2015 to 2035 using a multiplication factor of 1.40 [104]. Import price data received by e-mail from the Swiss Federal Office of Statistics (SFOS) [216], Feb. 2017.

^g It is based on 47.58 CHF₂₀₁₅/MWh (Table D.3), and projected from 2015 to 2035 using a multiplication factor of 1.96 [81].

^h It is based on 18.06 CHF₂₀₁₁/MWh [217], and projected from 2011 to 2035 using a multiplication factor of 1.46 [104].

ⁱ Average of the data points for 2035 in [218], accounting for the efficiency of nuclear power plants (Table A.15).

A.6 Other parameters

Hydrogen production

Three technologies are considered for hydrogen production: electrolysis, NG reforming and biomass gasification. The last two options include CCS systems for limiting the CO₂ emissions. Table A.23 contains the data for the hydrogen production technologies.

Table A.23 – Hydrogen production technologies.

	c_{inv} [CHF ₂₀₁₅ /kW _{H2}]	c_{maint} [CHF ₂₀₁₅ /kW _{H2} /y]	Lifetime [y]	c_p [-]	η_{H2} [%]
Electrolysis [219]	329	32.9 ^a	15	0.9	85
CH ₄ reforming [220]	728	68.8	25 ^b	0.86	73
Biomass gasification [220]	2697	209	25 ^b	0.86	43

^a Assumed to be 10% of c_{inv} , for coherence with the data in [220].

^b Assumption.

Biomass to synthetic fuels

Two technology options are considered for the conversion of woody biomass to synthetic fuels: pyrolysis and gasification. The main product of the pyrolysis process is bio-oil, which is considered equivalent to fossil LFO. The main product of the gasification process is SNG, which is considered equivalent to fossil NG. Data for the technologies are reported in Table A.24 (Appendix D.3.3). In the table, efficiencies are calculated with respect to the wood in input (50% humidity, on a wet basis LHV) and “fuel” stands for the main synthetic fuel in output.

Table A.24 – Woody biomass to synthetic fuels conversion technologies (Appendix D.3.3).

	c_{inv} [CHF ₂₀₁₅ /kW _{fuel}]	c_{maint} [CHF ₂₀₁₅ /kW _{fuel} /y]	Lifetime [y]	c_p [-]	η_{fuel} [%]	η_e [%]	η_{th} [%]
Pyrolysis	1435	71.8	25	0.85	66.6	1.58	-
Gasification	2930	149	25	0.85	74	3.15	9.01

Energy demand reduction cost

The energy efficiency cost is a cost difference between the “business as usual” scenario, which has the highest energy demand, and the “Political measures of the Federal Council” scenario in [81]. The cost is divided in two categories: private households and industry and services. The values are 806 MCHF₂₀₁₅/y and 1050 MCHF₂₀₁₅/y respectively [221]. As in the model only the “PMF” scenario is considered for the energy demand (Table A.3), the demand reduction is a fixed cost in the model.

Other

The real discount rate for the public investor i_{rate} is fixed to 3.215%, average of the range of values used to define the corresponding uncertainty range (see Section 2.2.2).

Losses ($\%_{loss}$) in the electricity grid are fixed to 7%. This is the ratio between the losses in the grid and the total annual electricity production in Switzerland in 2015 [222]. DHN losses are assumed to

Appendix A. Swiss energy system data

be 5%. $\%_{Peak_{DHN}}$ is assumed to be equal to 2.

The input and output efficiency of the storage ($\eta_{sto,in}$ and $\eta_{sto,out}$) are defined to allow the connection between the storage technologies (*StoHydro* and *Power2Gas*) and their respective layers (electricity and LNG, respectively). The efficiency is 1 in all cases as the *StoHydro* unit represents a “shift” in the monthly production of the dams, while the LNG storage tank is assumed to have no losses.

A.7 2011 data for model validation

This section details the data of the Swiss energy system in the year 2011 used to validate the MILP model in Section 1.2.2. The input data for the year 2011 used for the model validation are: *i*) the yearly EUD values in the different sectors ($endUses_{year}$); *ii*) the relative annual production shares of the different technologies for each type of EUD; *iii*) the share of public mobility ($\%_{Public}$), of train in freight ($\%_{Rail}$) and of centralized heat production ($\%_{Dhn}$); *iv*) the fuel efficiency of mobility technologies.

The FEC data for Switzerland in the year 2011 are available in [77, 81, 80]. The EUD is calculated based on the FEC using a similar procedure as the one described in Section A.1.1. The obtained input data for model validation are reported in Table A.25. $\%_{Public}$, $\%_{Rail}$ and $\%_{Dhn}$ are reported in Table A.26 with the corresponding sources.

Table A.25 – End-uses demand in Switzerland ($endUses_{year}$) in 2011, calculated from [77, 81, 80].

	Units	Households	Services	Industry	Transportation
Electricity (other)	[GWh]	10277.8	11166.7	13416.7	0.0
Lighting	[GWh]	1583.3	4138.9	1722.2	0.0
Heat high T	[GWh]	0.0	1146.4	22020.4	0.0
Heat low T (SH)	[GWh]	38861.1	15584.2	4982.7	0.0
Heat low T (HW)	[GWh]	8236.1	3153.0	839.9	0.0
Passenger mobility	[Mpkm]	0.0	0.0	0.0	121600.0
Freight mobility	[Mtkm]	0.0	0.0	0.0	27660.0

Table A.26 – $\%_{Public}$, $\%_{Rail}$ and $\%_{Dhn}$ for the Swiss energy system in the year 2011.

	Share [%]
$\%_{Public}$	20.0% [80]
$\%_{Rail}$	36.8% [81]
$\%_{Dhn}$	6.4% [77, 81]

The annual net electricity production shares for electricity production technologies is taken from [78]. The yearly shares of mobility and heating & CHP technologies per type of EUD (with respect to the

main output) are reported in Tables A.27-A.31.

For public mobility (Table A.27, [77, 78]), it is assumed that all biofuels and NG are used in public mobility, and that the electricity not used in freight is shared between trains and trolleybus with a 60%-40% share, respectively. For private mobility (Table A.28, [77, 80]) the repartition between the different types of vehicles is estimated based on the number of vehicles in Switzerland in 2012 (77% gasoline, 22% diesel, 1% hybrid) and their fuel efficiencies. For all mobility technologies, 2010 efficiencies from [71] are used in the model validation.

For low and high temperature heat production (Tables A.29, A.30 and A.31, [77, 78, 82, 81]), the electricity production from CHP plants is taken from [82], Table A.2), while the input fuel and the heat production are estimated based on the efficiencies assumed for 2035. In Section 1.2.2, for DHN it is assumed that all waste is used in CHP units, although in reality a share of waste is only used for electricity production.

Table A.27 – Yearly shares of public mobility technologies for the Swiss energy system in 2011.

	Share Mpkm [%]
Tram and Trolley Bus	12.8%
Diesel Bus and Coach	49.7%
Diesel HEV Bus and Coach	0.0%
NG Bus and Coach	3.0%
FC Bus and Coach	0.0%
Train/Metro	34.6%

Table A.28 – Yearly shares of private mobility technologies for the Swiss energy system in 2011.

	Share Mpkm [%]
Gasoline car	75.8%
Diesel car	22.5%
NG car	0.0%
HEV	1.7%
PHEV	0.0%
BEV	0.0%
FC car	0.0%

Appendix A. Swiss energy system data

Table A.29 – Yearly shares of decentralized low temperature heat & CHP technologies for the Swiss energy system in 2011.

Share heat [%]	
HP	6.0%
Thermal HP	0.0%
CHP NG	0.5%
CHP Oil	0.1%
FC NG	0.0%
FC H ₂	0.0%
Boiler NG	25.7%
Boiler Wood	8.2%
Boiler Oil	49.8%
Solar Th.	0.5%
Direct Elec.	9.2%

Table A.30 – Yearly shares of DHN low temperature heat & CHP technologies for the Swiss energy system in 2011.

Share heat [%]	
HP	4.8%
CHP NG	1.2%
CHP Wood	6.6%
CHP Waste	72.5%
Boiler NG	13.8%
Boiler Wood	0.0%
Boiler Oil	0.6%
Deep Geothermal	0.4%

Table A.31 – Yearly shares of industrial high temperature heat & CHP technologies for the Swiss energy system in 2011.

Share heat [%]	
CHP NG	2.4%
CHP Wood	0.8%
CHP Waste	1.8%
Boiler NG	24.3%
Boiler Wood	7.0%
Boiler Oil	25.6%
Boiler Coal	5.1%
Boiler Waste	5.6%
Direct Elec.	27.5%

B Uncertainty characterization data

Overview

The appendix is complementary to Section 2.2 as it further details the data used for the uncertainty characterization of the Swiss MILP model parameters. Additionally, it is shown how the obtained ranges are applied to the model parameters in cases in which it is not trivial.

B.1 Discount rate

The errors in forecasts in Goodhart and Lim [91] refer to the two-year time horizon errors for the New Zealand central bank (Table 8). The different estimates for long-term forecasts in the US are reported in [92], Table 1.

B.2 End-use energy demand

For households, services, and industry, the main data source for the range definition is a report commissioned by the Swiss confederation [81]. In this report, three scenarios are available: “BaU” (Business as Usual), “PMF” (Political Measures of the Federal Council) and “NEP” (New Energy Policies). In the example MILP model, the PMF scenario is used as source for the nominal values of the energy demand, whereas the NEP and the BaU can be used to define the lower and upper bounds, respectively. At an aggregated sector level, the ranges for 2035 end-use energy demand resulting by comparing the scenarios are [-13.5%, 11.0%] for households, [-12.7%, 9.8%] for services, and [-11.3%, 8.9%] for industry.

These ranges are compared with the error in past energy demand forecasts. The IEA has been forecasting energy demand for several decades. One of the first analyses of errors in these forecasts

Appendix B. Uncertainty characterization data

was performed by Linderoth [19] in the early 2000s. Errors were found to be as high as 40% over a 10-12 year time horizon, with higher errors in the industry sector. Liao et al. [94] studied errors in more recent IEA total energy supply forecasts over a 6-year time horizon, finding smaller errors: deviations from forecasts were within 2 percentage points for most countries, with the exception of China (5.68%). Due to good data availability, many works in the literature have focused on the errors in forecasts for the US. Bezdek and Wendling [20] reviewed 49 long term forecasts covering the period 1952-2000. Errors in predicting US total energy consumption for the year 2000 were as high as 50% over a 25-year time horizon. The US EIA publishes regularly a retrospective review on its own energy demand forecasts. EIA errors in forecasts have been analyzed by O'Neill and Desai [21], Fischer et al. [95], and at a sector level by Winebrake and Sakva [22]. Figure 1 analyzes the errors in the energy demand forecasts published yearly in the EIA AEO in the period 1994-2014 [23]. Each AEO report includes forecasts for the following 15-20 years. The average of errors in absolute values (full lines) and the minimum/maximum errors (dotted lines) in energy demand forecasts are calculated for the different sectors with respect to the forecast time horizon. The time horizon is the difference between the target year of the forecast and the year of publication of the AEO. As an example, the 10-year time horizon includes the errors calculated after 10 years from the publication of the reports (such as the forecast for 2003 published in the 1993 AEO, the forecast for 2004 published in the 1994 AEO, etc.). A positive error indicates an overestimation, i.e. the forecast is higher the actual value in a given year.

The figure shows that errors are increasing over time. Also, forecasts of energy demand in the industry sector show higher average errors, suggesting that the evolution of energy demand in this sector remains to date more difficult to predict. The maximum forecast errors are of 24.3% for households total energy demand, 24.7% for services, and 35.5% for industry. These errors are wider than the ranges proposed in [81]. Thus, for the calculation of the final ranges, $R_{\%}$ is taken as twice the maximum error in each sector, shared asymmetrically over the nominal value proportionally to the values in [81]. This leads to the final ranges for 2035 end-use energy demand: [-26.8%, 21.8%] for households, [-27.8%, 21.5%] for services, and [-39.9%, 31.2%] for industry.

For transportation, passenger mobility demand [pkm] is decomposed as the product of population and average mobility per person. [223] presents scenarios for the evolution of the Swiss population to 2060, indicating a lower bound of 7.79 million people, and an upper bound of 9.76 millions people. In the three scenarios in [81], it is estimated that the average mobility need in 2035 will be between 15416 pkm/ca and 16428 pkm/ca. The final range of [-14.5%, 14.5%] is obtained by multiplying the extreme values.

All the obtained ranges for 2035 are scaled using the factor calculated in Eq. 2.4. This means that a uniform distribution is assumed within the bounds of the range.

B.3 Technology efficiency

For mature technologies, uncertainty is characterized based on collection of current market data. Boilers are taken as representative technologies for the efficiency of mature, standard technologies ($\eta_{mature, standard}$). [96] offers an overview of the efficiency of today's state of the art technologies. Summing up all available measures to increase the energy efficiency of a boiler, a maximum improvement of 9% is obtained on average. Efficiency ranges are indicated for different types of boiler: coal boilers [75%, 85%], oil boilers [72%, 80%], NG boilers [70%, 75%], biomass boilers [60%, 70%]. The average of these ranges ($\pm 5.7\%$) is taken as final range for mature and standard technologies. Gasoline cars are taken as representative technologies for the efficiency of mature, customized technologies ($\eta_{mature, customized}$). The US Department of Energy publishes yearly a report and a dataset with the fuel efficiencies of the different vehicles in the US market [97]. The dataset is filtered in order to obtain the fuel efficiency of only front-wheel drive gasoline cars, with a 1.8 L to 2.2 L engine. The efficiency of these 108 vehicle models is between 22.9 miles-per-gallon (MPG) and 34.6 MPG. This range ($\pm 20.6\%$) is taken as final range for mature and customized technologies. PV panels are taken as representative technologies for the efficiency of new technologies. The range for the future efficiency is taken from the different available forecasts. The IEA forecasts the average efficiency of typical commercial flat-plate modules to be 25% in 2030. The target efficiencies are 25% for single-crystalline PV, 21% for multi-crystalline [224]. This means that the average modules available in the market are expected to have the same efficiencies that are reached today with the best research-cell prototypes (new data are regularly reported in [225]). From the IEA report, a range can be estimated for efficiencies in 2030. The lower bound for 2030 is a 20% efficiency, whereas the upper bound is fixed to 30% due to the possible appearance of emerging technologies and novel concepts. This range ($\pm 20\%$) is taken as range for new technologies. It is then combined with the ranges for mature technologies by applying Eq. 2.2 to obtain the final ranges for new, standard technologies ($\eta_{new, standard}$) and new, customized technologies ($\eta_{new, customized}$).

Application to the example MILP model

In the example MILP model, technology efficiencies are accounted for in the f parameter, the matrix defining for all technologies and resources outputs to (positive) and inputs from (negative) layers. As an example, a 90% efficient NG boiler takes $1.11 \text{ kW}_{\text{NG}}$ in input from the NG layer for each kW_{th} output to a heat demand layer. In this case f is the reciprocal of the efficiency η . Thus, Eq. 2.1 cannot be directly applied, as the uncertain parameter is at the denominator of the equation. Also, when using relative ranges, care needs to be taken not to violate the thermodynamic limit for efficiencies; and, in the context of a GSA, the uncertainty of technologies having more than one output (e.g. cogeneration) needs to be correctly accounted for. To address these three issues, the following rules are followed:

Appendix B. Uncertainty characterization data

- If $f < 0$ (input to technology), then $[R_{min}, R_{max}] = [\frac{R_0}{1+R\%,min}, \frac{R_0}{1+R\%,max}]$. Else, if $f > 0$ (output from technology), then Eq. 2.1 applies.
- When using relative ranges, it needs to be verified that technology efficiencies do not violate thermodynamic limits. As an example, electric heaters have a nominal efficiency of 100%. Values higher than 100% would violate the thermodynamic limit for the technology. In these cases, the thermodynamic limits are used instead of the bounds deriving from the application of the relative ranges.
- In the MILP model structure, $f(i, j) = 1$ if j is main output layer for technology/resource i . This unitary value is not uncertain as it is part of the model structure. Thus, if a technology has only one output, the uncertainty is accounted for in the input. As an example, heat is the only output for a NG boiler. Thus, the uncertainty is in the amount of NG in input for producing 1 unit of heat. If a technology has more than one output, a different approach is used. This is the case of cogeneration units, producing both heat (main output) and electricity. Cogeneration units have an electrical (η_e) and a thermal (η_{th}) efficiency. This is shown in Figure B.1.

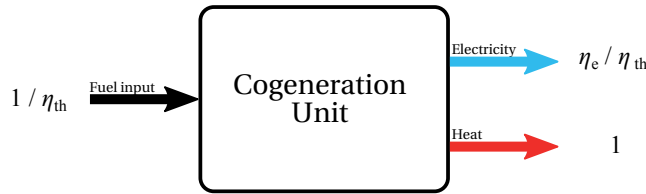


Figure B.1 – Implementation of a cogeneration unit in the example MILP model.

As the thermal output is fixed to 1, the uncertain parameters are the fuel input (reciprocal of η_{th}) and the electricity output ($\frac{\eta_e}{\eta_{th}}$). In the GSA, these two parameters are considered independent. To do this, first new values are drawn from distributions for both the fuel input ($\frac{1}{\eta_{th}}$)' and the electricity output ($\frac{\eta_e}{\eta_{th}}$)'. Then, the fuel input is set to $(\frac{1}{\eta_{th}})' \frac{1+(\eta_e/\eta_{th})'}{1+(\eta_e/\eta_{th})_0}$. In this way, the parameters are varied independently. As an example, the ratio between the efficiencies can be changed without impacting the total efficiency of the unit.

B.4 Resources availability and maximum capacity of technologies

For the availability of local resources, the maximum yearly potential of wood in Switzerland is assessed from various sources. The reviewed works are reported in Table B.1. The minimum (36 PJ/y) and the maximum (70 PJ/y) values are used in the definition of the range.

For the maximum installed size of renewable technologies, data for the potential of solar PV are

Table B.1 – Maximum yearly potential of woody biomass in Switzerland from different sources.

Source	Max. potential [PJ/y]
Oettli et al. [226]	59.1
Steubing et al. [209]	42.3
Thees et al. [227]	36
Thees et al. [228]	53.3
BIOSWEET vision [229]	70

used in the definition of the uncertainty range. In the wiki of the online calculator¹ presented in [74] the maximum potential for electricity production is 25 TWh_e/year, assuming to install panels on 40% of the well-oriented roofs and façades and a 25% efficiency. This is taken as the lower bound for the range. The upper bound is taken from the estimation reported in [230] of 32 TWh_e produced in 2050 with a 27.2 % efficiency. This value, scaled to a 25% efficiency, is taken as the upper bound, obtaining a final range of ± 24.1%.

B.5 Capacity factor

For the definition of the yearly capacity factor, Swiss nuclear power plants are taken as representative technologies. The Federal Office of Statistics provides historical data for the capacity factor of the 5 nuclear power plants in Switzerland in the period 1990-2014². The data are summarized in Table B.2.

Table B.2 – Analysis of yearly capacity factors (c_p) of Swiss nuclear power plants. 1990-2014 data from Swiss Federal Office of Statistics. 2015 data and installed capacity from [222].

Power plant	Capacity [MW _e]	c_p 1990-2015 [%]		
		Average	Min	Max
Beznau I	365	86.3	19.5	99.3
Beznau II	365	87.6	62.7	99.6
Mülheberg	373	88.8	76.0	94.8
Gösgen	1010	91.3	74.5	96.1
Leibstadt	1220	85.8	56.5	92.5
Total	3333	88.1	76.0	93.7

From the table it emerges that, although on average quite regular, capacity factors can have substantial drops. As an example, in 2015 the Beznau I and II plants suffered extended periods of extraordinary maintenance, which brought the global capacity factor of Swiss nuclear plants to the minimum value in recent history (76%). In the model the nominal value is taken for the year 2012 (84.9%). As in the model the c_p is the same for all nuclear power plants, the range is defined based

¹ Accessible at <http://www.swiss-energyscope.ch>

² Accessible at <https://www.pxweb.bfs.admin.ch>

Appendix B. Uncertainty characterization data

on the minimum (76%) and maximum (93.7%) total values.

Based on the grouping in Section 2.2.1, the distribution over the year of the period capacity factor ($c_{p,t}$) is assumed to be non-uncertain. Thus, for solar technologies the uncertainty is on the yearly global radiation, which is modeled to be the only factor determining the variation of $c_{p,t}$. Historical data of solar radiation for different locations worldwide can be found in [98]³. For certain locations, maximum deviations of 28.6% are found from the average. Thus, this variation is taken to define the uncertainty range of the parameter.

The obtained ranges for 2035 are scaled using the factor calculated in Eq. 2.3. This means that a uniform distribution is assumed within the bounds of the range.

B.6 Technologies investment cost

Table B.3 details the sources and the method used for the calculation of the specific investment cost uncertainty range. Decentralized NG boilers are considered representative for mature technologies. In the lack of data about the actual number of NG boilers installed for the different available sizes, uncertainty is calculated for a 10 kW_{th} boiler. As a simplification, this range is used to define the epistemic uncertainty of all technologies (with the exception of the DHN). PV panels are taken as representative for new technologies. The range for future residential rooftop PV investment costs is taken from the minimum/maximum values from the forecasts reported in Table B.4.

Table B.3 – Technologies specific investment cost: sources for the definition of the uncertainty range. Epistemic (ϵ) and aleatory (α) uncertainties are combined as in Eq. 2.2.

Technology	$R_{\%,\epsilon}$	$R_{\%,\alpha}$	$R_{\%}$
Decentralized NG Boiler	[-21.6%, 21.6%] ^a	-	[-21.6%, 21.6%]
PV	[-21.6%, 21.6%]	[-33.2%, 33.2%] ^b	[-39.6%, 39.6%]
Nuclear reactors	[-21.6%, 21.6%]	[0, 117.3%] ^c	[-21.6%, 119.3%]
Hydro Dams	[-21.6%, 21.6%]	[0, 70.6%] ^c	[-21.6%, 73.8%]
Thermal plants	[-21.6%, 21.6%]	[0, 12.6%] ^c	[-21.6%, 25.0%]
Wind farms	[-21.6%, 21.6%]	[0, 7.7%] ^c	[-21.6%, 22.9%]
DHN	-	[-39.3, 39.3%] ^d	[-39.3, 39.3%]
Geothermal	[-21.6%, 21.6%]	[-33.3, 58.2%] ^e	[-39.7, 62.1%]

^a Range of investment costs a 10 kW_{th} NG boiler from catalog data in Switzerland.

^b Range of investment costs for the year 2035 for rooftop PV. Calculated from forecasts (Table B.4). Since the range is applied to all new technologies, it does not include overrun costs reported in [100], also because they are negligible (1.3%).

^c Based on the mean cost overrun of projects calculated in [100].

^d Based on range between favourable and unfavourable conditions for a given DHN connection density, estimated from Figure 3.19 in [103].

^e Range calculated using Eq. 4 in [101] for a 4000 m well.

³ Available online at <http://bsrn.awi.de>. Data quality check performed by Anna Sophia Wallerand (EPFL).

Table B.4 – Projection for the investment cost of rooftop residential PV systems in 2035 from different sources.

Source	c_{inv} (PV) [CHF ₂₀₁₅ /kW _e]
IEA, 2014 (NPS scenario - Europe) [106]	1748
IEA, 2014 (450 scenario - Europe) [106]	1555
EU “energy roadmap 2050”, 2011 [104]	1952
AES, 2013 [175]	1868
Prognos AG, 2007 [218]	2479
Bloomberg, 2015 [231]	[1329, 2019]
ETIP PV, 2011 [172]	1272 ^a

^a Forecast for the year 2030.

B.7 Resources cost

The future price of wood is the representative parameter for local resources ($c_{op,local}$). The lower and upper bounds of the range are defined based on the values of the BaU and NEP scenarios in [81], respectively. The range is scaled based on Eq. 2.4, thus assuming uniform distributions with linearly increasing ranges.

The future price of NG is the representative parameter for imported resources ($c_{op,import}$). Errors in past EIA forecasts (analyzed in Figure 2) are studied to define its range. Using US market forecasts for Switzerland is motivated by the lack of data for past forecasts in the European market. NG price forecasts for the US electric power sector are published yearly in the AEOs. Forecasts are expressed in real currency, which differs for each AEO. Thus, to obtain a common basis of comparison, all forecasts are converted to USD₂₀₁₃ (using the GDP deflator from the U.S. Department of Commerce, Bureau of Economic Analysis [25]) and compared to the actual NG prices in the different years. In this way, the error factors e (defined in the Introduction), are calculated. Two indications are obtained from the analysis: *i*) there is no evidence that error factors are bigger in the long term than in the short term, and *ii*) error factors are symmetrically distributed. In fact, the analyzed data suggest that it is equally likely to have an overestimation by a given error factor or an underestimation by the same factor, e.g. it is equally likely that the predicted value for a given year is half of the actual value or twice the actual value. Of course, this symmetry in error factors leads to asymmetrical relative ranges. Applying symmetrically the maximum error factor ($e_{max} = 3.32$) results in a [-69.9%, 232%] range over the nominal value, as -69.9% corresponds to a possible overestimation by a factor 3.32, and +232% to a factor 3.32 underestimation. As uncertainty is constant over time, Eq. 2.3 is applied. This means assuming that, in each year of the planning horizon, error factors are uniformly distributed in $[-(e_{max} - 1), e_{max} - 1]$, where 0 represents a correct forecast, a positive value represents

Appendix B. Uncertainty characterization data

an underestimation, a negative value represents an overestimation. The scaled error factor is $e^* = 1.899$, corresponding to a final range of [-47.3%, 89.9%] for the category.

Application to the example MILP model

The first step of the GSA in Chapter 3, using the Morris method, assumes a uniform distribution for all the parameters within the defined range. The mean of a uniform PDF is the average between its lower and upper bounds. If the range is asymmetrical, this causes the mean to be different from the nominal value. This potential distortion is particularly impacting in the case of parameters belonging to the $c_{op,import}$ category, due to the wide and asymmetric uncertainty range. Thus, in the GSA, the value of the parameter in the uncertain domain ($c'_{op,import}$) is defined as in Eq. B.1.

$$c'_{op,import} = \begin{cases} c_{op,import,0} * (1 + e), & \text{if } e \geq 0 \\ \frac{c_{op,import,0}}{1 - e}, & \text{otherwise} \end{cases} \quad (\text{B.1})$$

Where e is the error factor drawn from the uniform distribution $[-(e^* - 1), e^* - 1]$. This allows to sample from a uniform distribution, which is mathematically convenient for the Morris method, while respecting the symmetry in the error factors emerged from the analysis.

B.8 Other parameters: technologies lifetime

Table B.5 lists the data and ranges for the lifetime of domestic boilers collected from different sources. Some source already propose ranges: the minimum range is 5 years, the maximum is 9 years. A range of 9 years over the nominal value (17 years) corresponds to a $\pm 26.5\%$ range.

Table B.5 – Lifetime (n) of boilers from different sources.

Source	$n(\text{Boilers})$ [y]
Lutz et al., 2006 [232]	[13,19] (NG); [12,19] (Oil)
Gas Research Institute, 1990 [233]	[13,22]; [25,30]; [20,25] (NG) ^a
Kattan and Ruble, 2012 [109]	20 (All fuels)
UK “2050 Calculator” [234] ^b	15 (All fuels)
NERA & AEA, 2009 [201]	15 (Biomass)
EU Commission, 2008 [199]	17 (All types)
Schulz et al., 2007 [108]	15 (Biomass)
e4tech, 2010 [235]	15

^a Comparison of estimates: first range is from first-owner use of product, second range is from ASHRAE 1984 handbook, third range is the final proposed range.

^b Cost assumptions available online at http://2050-calculator-tool-wiki.decc.gov.uk/cost_sources/1

C Urban energy modeling - Integration of deep geothermal energy and woody biomass conversion pathways in cities

Overview

This appendix is complementary to Chapter 1, as it proposes a MILP modeling framework for urban energy systems and applies it to the integration of geothermal and biomass resources. *This chapter has been published as Moret et al. [236].*

Urban systems account for about two-thirds of global primary energy consumption and energy-related greenhouse gas emissions, with a projected increasing trend. Deep geothermal energy and woody biomass can be used for the production of heat, electricity and biofuels, thus constituting a renewable alternative to fossil fuels for all end-uses in cities: heating, cooling, electricity and mobility. This chapter presents a methodology to assess the potential for integrating deep geothermal energy and woody biomass in an urban energy system. The city is modeled in its entirety as a multiperiod optimization problem with the total annual cost as an objective, assessing as well the environmental impact with a LCA approach. For geothermal energy, deep aquifers and enhanced geothermal system (EGS) are considered for stand-alone production of heat and electricity, and for cogeneration. For biomass, besides direct combustion and cogeneration, conversion to biofuels by a set of alternative processes (pyrolysis, Fischer-Tropsch (FT) synthesis and synthetic natural gas production) is studied. With a scenario-based approach, all pathways are first individually evaluated. Secondly, all possible combinations between geothermal and biomass options are systematically compared, taking into account the possibility of hybrid systems. Results show that integrating these two resources generates configurations featuring both lower costs and environmental impacts. In particular, synergies are found in innovative hybrid systems using excess geothermal heat to increase the efficiency of biomass conversion processes. The application to a case study demonstrates the advantages of using a system approach for the analysis over a stand-alone comparison between options.

As discussed in the Introduction, substitution of fossil fuels with renewable energy sources, such as geothermal and biomass, is one of the key actions to tackle climate change. In 2008, geothermal energy and bioenergy accounted for 0.1% and 10.2% of global primary energy supply, respectively. Within bioenergy, woody biomass had the largest share [4]. Based on 2003 data, the worldwide use of biomass has been estimated to be 38% of the global potential [237]. Bioenergy demand is expected to increase at least threefold by 2050 [4]. Geothermal energy is projected to cover 3.5% of the global electricity production and 3.9% of the final energy for heat in the same year [238].

As of 2014, 54% of the world population lived in urban areas, a figure expected to rise to 66% by 2050 [239]. Urban systems account for about two-thirds of global primary energy consumption and for 71 % of global energy-related GHG emissions [240]. Heating, cooling, electricity and mobility are the four components of urban systems final energy consumption. Deep geothermal energy¹ and woody biomass are widely available renewable resources and represent a promising alternative to fossil fuels to meet this demand. Although often only considered for electricity production [242], deep geothermal energy can provide baseload supply in heating dominated urban energy systems for low temperature heating requirements, which constitute the largest share of heat demand [243], whereas biomass can be used for higher temperatures and peaks. The high heat density in cities makes the deployment of DHNs more economically competitive [244]. DHNs are necessary in order to integrate large-scale renewables (such as deep geothermal wells) and cogeneration systems for heat supply [245].

In the literature, most studies focus on a stand-alone comparison of energy conversion pathways. The contextualization of technology assessment within urban energy systems presents the advantage of defining a reference state of the energy system, taking into account the structure and seasonal variation of the demand, and the existing and competing technologies. It also allows to capture the complexity deriving from the interaction between the different energy sectors, such as the penetration of electric technologies for heating and mobility end-uses [34]. In recent years, some authors have applied this approach to geothermal energy and biomass. Gerber et al. [246] used multi-objective optimization for the evaluation of deep geothermal and biomass (direct combustion and gasification) integration in an urban system taking into account total yearly cost and GWP with a LCA approach. The urban system is modeled in its entirety (only decentralized heating is excluded) and one year is broken down into a set of independent periods. It is highlighted that results strongly depend on the integration within urban systems. Alberg Østergaard et al. [247] applied the EnergyPLAN model [38] to design a 100% renewable scenario for a Danish city for the year 2050, mostly based on biomass, geothermal and wind power. Low-depth resources combined with absorption heat pumps are considered for geothermal, whereas the biomass is converted to biogas and SNG. In these works only a subset of the possible energy conversion pathways is considered,

¹“Deep geothermal energy” is here used for resources of depth greater than 1000 m and temperatures exceeding 60 °C [241].

and no possibility for heat integration between geothermal and biomass technologies is taken into account. Other studies focus only on one of the two resources. As an example, Sommer et al. [248] assessed the economics of geothermal district heating for a community in California. Vallios et al. [249] proposed a methodology for the design of biomass district heating systems, whereas Pantaleo et al. [70] developed an approach to design optimal biomass supply chains for heat and power generation in urban areas. The approach was then applied to a generic urban model [111].

Integration and hybridization with geothermal and solar resources have been identified as a strategic research priority for biomass in Europe [250]. Hybrid geothermal-biomass systems are here defined as energy conversion systems coupling the two resources. Hybridization has been applied to the production of electricity in ORCs, with geothermal heat used for biomass drying and preheating, and biomass supplying the remaining heat requirements at higher temperature. This is the case for an existing 35.5 MW_e installation in California, USA [251]. Borsukiewicz-Gozdur [252] proposed a hybrid ORC concept using two working fluids. Thain and DiPippo [253] recently explored different interesting configurations for hybrid geothermal-biomass power plants. These hybridization pathways focus on electricity production cycles, showing the possibility of achieving higher efficiencies by combining the two resources.

Integration of hybrid solutions in urban energy systems has been recently explored. Kilikis [254] proposed a hybrid lignite-geothermal plant for a district energy system and hydrogen production facility for a Turkish city. A wider energy system integration has been proposed for the Cornell University campus (USA) [255]: a hybrid geothermal-natural gas-biomass conversion system in which geothermal energy is used in combination with biomass for heat production, and excess geothermal heat is used for electricity production with an ORC during periods of low heating demand. In these works there is no hybridization at the level of the energy conversion processes, as the two resources contribute separately to the energy services supply in the district. The case study at Cornell was recently widened by Beckers et al. [256], including the hybrid option of using geothermal heat for biomass drying prior to gasification. Malik et al. [257] studied a multi-generation biomass-geothermal system to produce heating, cooling and electricity for cities, and liquified gas and drying for industrial processes. In a case study evaluating different options for the integration of geothermal energy in the urban system of Lausanne (Switzerland), Amblard [258] highlights that the availability of geothermal heat in summer surpasses the demand. A preliminary case study [259] has shown the interest of using this excess geothermal heat in summer for biomass drying. In this preliminary case study only a subset of options was considered and the LCA analysis was limited to the GWP indicator.

Thus, the main gaps identified in the literature are *i)* the consideration of only part of the urban system and *ii)* of a subset of energy conversion pathways for deep geothermal and biomass. This specificity implies that *iii)* optimization of the overall urban system is seldom performed. Furthermore *iv)* hybrid options are often evaluated stand-alone and not integrated in urban systems,

and *v*) LCA analysis is limited to the GWP impact assessment method. Consequently, we present a methodology for evaluating the potential benefits of deep geothermal and woody biomass integration in urban energy systems. To achieve this *i*) a model is developed for the entire urban energy system with the appropriate level of detail for the analysis. *ii*) Multiple options are considered for the resources: deep aquifers and EGS for deep geothermal; drying, combustion in boilers and cogeneration engines, pyrolysis, gasification, FT for woody biomass. *iii*) The model is formulated as a multi-period MILP problem and *iv*) the use of process integration [65] ensures accounting for hybridization possibilities. Furthermore, *v*) The LCA analysis is extended to include human health impact assessment methods along with global warming potential.

The developed methodology is illustrated by an application case study in the city of Lausanne (Switzerland, 140,421 inhabitants in 2015). The city has an existing DHN supplying a significant share of the heating final energy demand. The projected expansion of the DHN offers an opportunity for the integration of renewable energy. The case study is presented in detail in Section D.1.

First the methodology is presented, with the definition of the urban system MILP model, the performance indicators and the scenario-based approach (Section C.1). The options for deep geothermal and biomass are first individually assessed and then systematically combined in order to explore the possible synergies. Scenario results are analyzed with a particular focus on interesting synergies between the two renewable resources (Section C.2), with the goal of identifying the most promising strategies for urban systems planning.

C.1 Methodology

Figure C.1 offers an overview of the scenario-based methodology. First, the MILP urban energy system model is developed. The model represents the superstructure common to all scenarios, i.e. it is a general formulation including all the possible investigated pathways. Based on this general framework, a scenario is defined by a set of additional constraints fixing the use or the size of the corresponding resources or technologies. For each scenario, the optimal solution in terms of total cost is identified, and LCA indicators for GWP and human health are calculated.

The methodology is implemented in the OSMOSE calculation platform [260]. Extensive documentation of the methodology and of the technology models in Appendix D allows reproducibility and application to different case studies and technologies.

C.1.1 Urban energy system model

An urban energy system model has been defined as “*a formal system that represents the combined processes of acquiring and using energy to satisfy the energy service demands of a given urban area*” [34]. Thus, it is a simplified representation of an urban system accounting for the energy flows within its boundaries. The urban energy system model developed for this work is depicted in Figure C.2.

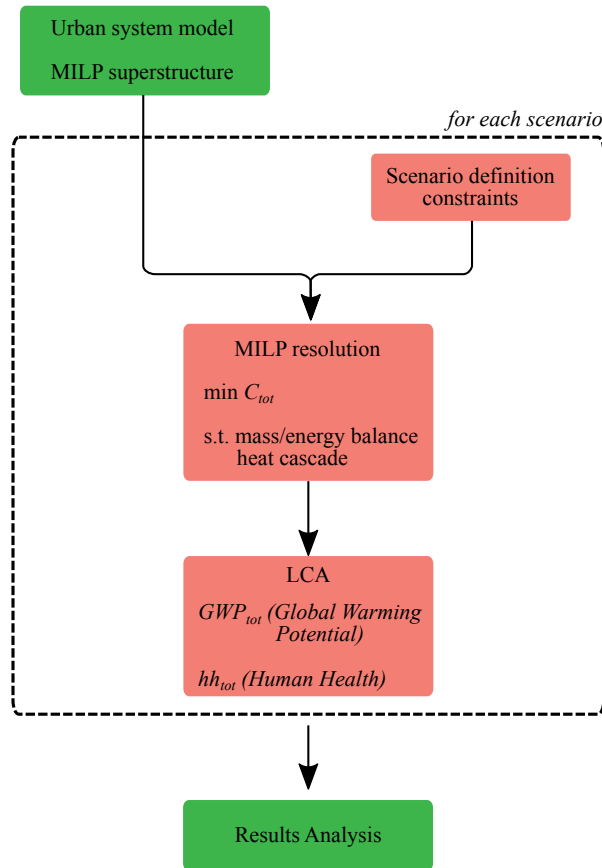


Figure C.1 – Overview of the scenario-based methodology

The urban energy system is modeled in its entirety. Imported and indigenous resources can be converted with energy conversion technologies to satisfy end-use demand in energy services: heat, mobility (private and public) and electricity. Cooling is not accounted for in this work. Heat production is separated into centralized and decentralized. Geothermal and biomass options are considered for centralized heat production together with existing technologies such as boilers, a waste-water treatment plant (WWTP) and a MSWI. A DHN delivers the produced heat to the consumers. A multiperiod formulation dividing the year in four periods (winter, mid-season, summer, peak) is adopted in order to account for seasonality. Storage across periods is allowed for certain resources. All the unit models and their adaptation to the Lausanne case study are described in detail in Section D.3.

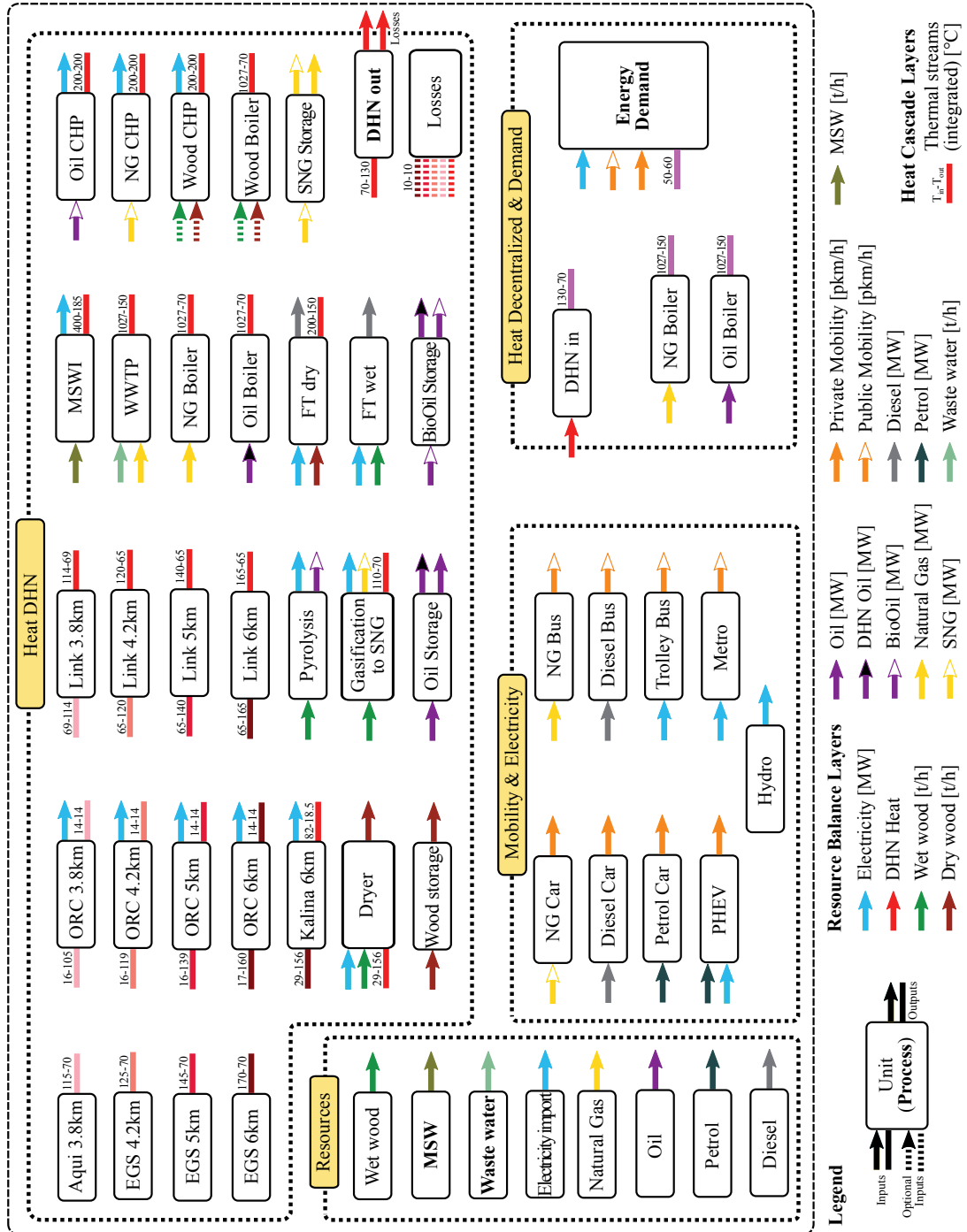


Figure C.2 – Urban energy system model.

Each resource or technology model corresponds to a *unit*. Each unit has inputs and outputs, which are associated with two types of layers: *resource balance* and *heat cascade*. Each layer of type *resource balance* corresponds to a mass flow or power balance in the entire system. As an example, all the diesel imported or produced by the Fischer-Tropsch units needs to be consumed by the units having this resource as an input. Thermal streams belong to the *heat cascade* layers. To simplify the representation, for units with multiple thermal streams only the net heating requirement or excess are shown in Figure C.2. Thermal streams can exchange only with other streams belonging to the same heat cascade layer, while “linking” units can be used to connect different heat cascade layers. In the case of geothermal, for example, the use of different heat cascades allows the option of either directly supplying the district heating network or producing electricity with an ORC or Kalina cogeneration cycle.

C.1.2 MILP model formulation

This section details the constraints of the MILP. The MILP formulation is based on the work by Maréchal and Kalitventzeff [65], later extended to include time-dependency [261] and mass balances [246]. The multiperiod storage formulation is a novelty of this work. Sets, parameters and variables of the MILP model with their relative indexes are reported in Section D.2. The model structure is conceptually equivalent to the modeling framework presented in Chapter 1; however, the level of detail is higher, as this formulation accounts for process integration - and thus for the temperature levels of the thermal streams - and for the fixed costs of technologies.

The objective is the minimization of the total annual cost of the energy system (C_{tot}), sum of the total annualized investment (C_{inv}) and of the yearly operating cost (C_{op}) of the units (Eq. C.1).

Unit sizing and costing

The binary variable \mathbf{Use}_t defines the use of a unit in a given period: if $\mathbf{Use}_t(u, t) = 0$ the unit u is not used in t , if $\mathbf{Use}_t(u, t) = 1$ the unit is used. The binary parameter use_f can be used to force the use of a unit in a given period (Eq. C.2). The operation of a unit in a given period is defined by the variable \mathbf{Mult}_t . Units inputs and outputs are defined for the default size of the unit ($\mathbf{Mult}_t(u, t) = 1$) and are proportionally scaled based on the value of this variable. The parameters f_{\min} and f_{\max} define the lower and upper bound for the unit operation, respectively (Eq. C.3). A unit is called *process* if $use_f(u, t) = f_{\min}(u) = f_{\max}(u) = 1$, otherwise it is called *utility*.

The variables \mathbf{Use} and \mathbf{Mult} are linked to the investment decision. They represent the binary decision of purchasing the unit (Eq. C.4) and the chosen size (Eq. C.5) with respect to the default size, respectively. The annualized investment cost of a unit is the sum of a fixed component $c_{\text{inv},\text{fix}}$ related to the unit purchase, and a variable part $c_{\text{inv},\text{var}}$ associated to the chosen size (Eq. C.6).

$$\begin{aligned}
 \min C_{\text{tot}} &= \sum_{u \in U} (C_{\text{inv}}(u) + \sum_{t \in T} C_{\text{op}}(u, t)) & (C.1) \\
 \text{s.t. } \mathbf{Use}_t(u, t) &\geq use_f(u, t) & (C.2) \\
 f_{\text{min}}(u) \mathbf{Use}_t(u, t) &\leq \mathbf{Mult}_t(u, t) \leq f_{\text{max}}(u) \mathbf{Use}_t(u, t) & (C.3) \\
 \mathbf{Use}_t(u, t) &\leq \mathbf{Use}(u) & (C.4) \\
 \mathbf{Mult}_t(u, t) &\leq \mathbf{Mult}(u) & (C.5) \\
 C_{\text{inv}}(u) &= c_{\text{inv}, \text{fix}}(u) \mathbf{Use}(u) + c_{\text{inv}, \text{var}}(u) \mathbf{Mult}(u) & (C.6) \\
 C_{\text{op}}(u, t) &= (c_{\text{op}, \text{fix}}(u) \mathbf{Use}_t(u, t) + c_{\text{op}, \text{var}}(u) \mathbf{Mult}_t(u, t)) t_{\text{op}}(t) & (C.7) \\
 \mathbf{Mult}_s(s, t) &= \mathbf{Mult}_t(u, t) & (C.8) \\
 \sum_{s \in S_{\text{HOR}}(l, t) | T_{\text{out}}^*(s, t) \geq T_{\text{int}}(l, t, k) + \delta} cp(s, t) \mathbf{Mult}_s(s, t) (T_{\text{in}}^*(s, t) - T_{\text{out}}^*(s, t)) &- \sum_{s \in S_{\text{COVD}}(l, t) | T_{\text{in}}^*(s, t) \geq T_{\text{int}}(l, t, k) + \delta} cp(s, t) \mathbf{Mult}_s(s, t) (T_{\text{out}}^*(s, t) - T_{\text{in}}^*(s, t)) + \\
 \sum_{s \in S_{\text{HOR}}(l, t) | T_{\text{out}}^*(s, t) \leq T_{\text{int}}(l, t, k) \wedge T_{\text{in}}^*(s, t) \geq T_{\text{int}}(l, t, k) + \delta} cp(s, t) \mathbf{Mult}_s(s, t) (T_{\text{in}}^*(s, t) - T_{\text{int}}(l, t, k)) &- \sum_{s \in S_{\text{COVD}}(l, t) | T_{\text{in}}^*(s, t) \leq T_{\text{int}}(l, t, k) \wedge T_{\text{out}}^*(s, t) \geq T_{\text{int}}(l, t, k) + \delta} cp(s, t) \mathbf{Mult}_s(s, t) (T_{\text{out}}^*(s, t) - T_{\text{int}}(l, t, k)) - \mathbf{R}(l, t, k) = 0 \\
 \mathbf{R}(l, t, k) &= 0 & (C.9) \\
 \mathbf{RB}_{\text{in}}(l, u, t) &= rb_{\text{in}}(l, u, t) \mathbf{Mult}_t(u, t) & (C.10) \\
 \mathbf{RB}_{\text{out}}(l, u, t) &= rb_{\text{out}}(l, u, t) \mathbf{Mult}_t(u, t) & (C.11) \\
 \sum_{u \in U_L(l)} (\mathbf{RB}_{\text{in}}(l, u, t) - \mathbf{RB}_{\text{out}}(l, u, t)) &= 0 & (C.12) \\
 \mathbf{RB}_{\text{out}}(l, u, t) - \sum_{(l, u, t) \in \text{RB}_{\text{links}}} \mathbf{RB}_{\text{in}}(l, u, t) &= \mathbf{RB}_{\text{in}}(l, u, t) - \sum_{(l, j, u, t) \in \text{RB}_{\text{links}}} \mathbf{RB}_{\text{flow}}(l, j, u, t) & (C.13) \\
 \mathbf{Mult}_t(u, t) &= \mathbf{Mult}_t(u, t - 1) + \left(\sum_{i \in \text{STO}_{\text{IN}}(u), i \in U_L(l)} \mathbf{RB}_{\text{in}}(l, i, t) \eta(i) - \sum_{j \in \text{STO}_{\text{OUT}}(u), j \in U_L(l)} \mathbf{RB}_{\text{out}}(l, j, t) / \eta(j) \right) t_{\text{op}}(t) & (C.14) \\
 \mathbf{RB}_{\text{flow}}(l, i, j, t) &= 0 & (C.15) \\
 \mathbf{RB}_{\text{flow}}(l, i, j, t) &= 0 & (C.16)
 \end{aligned}$$

Appendix C. Urban energy modeling

The hourly operating cost of a unit is the sum of a fixed component $c_{op,fix}$ related to the use of the unit, and a variable part $c_{op,var}$ associated to its operation. The hourly operating cost is multiplied by the period duration $t_{op}(t)$ in order to calculate the total operating cost in period t (Eq. C.7).

Heat Cascade

Process integration enforces feasibility of heat exchange according to the second principle of thermodynamics. The following equations apply the classical heat cascading constraints following the process integration terminology [262].

Thermal streams have the same multiplication factor (**Mult_s**) of the unit they belong to (Eq. C.8). They are described by their thermodynamic properties: corrected input/output temperature (T_{in}^* , T_{out}^*), enthalpy (H_{in} , H_{out}) and heat capacity flowrate (cp). *Hot streams* are streams whose output enthalpy level is lower than the input one (heat sources), whereas *cold streams* have output enthalpy higher than input enthalpy (heat sinks). Streams belong to heat cascade layers. Each heat cascade layer is divided into temperature intervals defined by their lower temperature T_{int} . **R** is the amount of heat that is transferred from each temperature interval k to the lower ones. It is equal to the heat cascaded from higher temperature intervals, resulting from the difference of heat provided by hot streams and heat needed by cold streams, to which the net heat available in k (Eq. C.9) is added.

T_{min} and T_{max} are the lowest and the highest temperature intervals of each heat cascade, respectively. Eq. C.10 ensures that no heat is cascaded above T_{max} and below T_{min} .

Resource Balance

Resource balance constraints ensure mass flow and power balance in the system.

rb_{in} is the default input value from a resource balance layer to a unit, whereas rb_{out} is the default output from a unit to a resource balance layer. Each unit can have multiple inputs and outputs associated to different layers, but it can only have one input or output in the same layer. Inputs and outputs are scaled according to the operation of the unit in order to get the total input (**RB_{in}**, Eq. C.11) and output (**RB_{out}**, Eq. C.12) in each period. Eq. C.13 enforces that each layer is balanced in each period, i.e. the sum of the outputs of all units in a given layer equals the sum of the inputs.

RB_{flow} defines connections between units belonging to the same resource balance layer. As units can be only “producers” or “consumers” with respect to a given layer, Eq. C.14 ensures all the resource output of units is consumed by other units having the same resource as an input. This variable is needed, for example, if the exchange between specific units needs to be forbidden or restricted.

Storage

Storage units allow storage of resources across periods. Each storage unit can be thought of as a “tank”. The level of the tank, i.e. the amount of energy or resource stored, is represented by the **Mult_t**

of this unit.

Each storage unit can have multiple inputs and outputs. In the optimization model each input or output corresponds to an “auxiliary” unit linked to the main storage. Input units close the balance of a given layer by storing a certain amount of the resource, increasing in this way the level of the main storage unit. On the other hand, output units can decrease the level of the storage by inputting the resource to the corresponding layer. Inputs and outputs to the storage can be associated with an efficiency η . The level of the storage unit at the end of each period is equal to the level at the end of the previous period plus inputs minus outputs by the auxiliary units. This circular balance of the storage unit is ensured by Eq. C.15. Eq. C.16 enforces that no loop exists between output and input of a given storage unit.

C.1.3 Performance Indicators

Scenarios for biomass and geothermal technologies are evaluated based on economic and environmental performance indicators (PIs).

Total annual cost

The total annual cost of the energy system (C_{tot} , Eq. C.1) is chosen as objective of the optimization model under the assumption that for a given pathway the sizing and operation of the energy system is determined by economic criteria.

The total annual cost results from the sum of the total annualized investment and maintenance cost of technologies, and the yearly operating cost of resources. For technologies and resources within the city boundaries (in terms of ownership) investment and O&M costs are accounted for, while a purchasing price is attributed to all imported resources. As an example, if natural gas is imported by a public service provider, only the cost paid at the import is accounted for. The profit made by the public service provider when selling the resource to private consumers is not accounted for in the total cost as it constitutes just a transfer of money within the system. This global approach to urban energy systems cost calculation has two main advantages: *i*) it avoids the need of assuming prices for produced fuels and exchanges within the urban system boundaries and *ii*) it allows the definition of only one indicator representing the global cost for the public.

Technologies investment costs are annualized based on their economic lifetime. In this framework, annualized investment cost of existing technologies is also accounted for. This is coherent with the fact that at the end of their lifetime these technologies need to be replaced. In this way, the cost of technologies is spread over their whole lifetime, whereas financial depreciation would only attribute this cost to their early years of operation, leaving an upfront investment cost to future generations. As detailed in Appendix A, a real discount rate is adopted and cost values are expressed in real 2015 currency in order to provide a common basis for comparison.

LCA environmental impact indicators

As shown in Figure C.1, environmental impact indicators are calculated for each scenario after the optimization phase. Environmental impact is calculated following a LCA approach, i.e. taking into account emissions of technologies and resources *from cradle to grave*. The reference database for impact assessment is ecoinvent [168]. Data used in the model are reported in Appendix D. The impact categories of interest in this work are the GWP and the impact on human health, the latter included in order to account for the impact of biomass combustion. A different calculation approach is followed for these two categories.

For GWP calculation the “IPCC 2013 - GWP 100a” impact assessment method [263] is selected. The global annual emissions GWP_{tot} , expressed in ktCO₂-eq./year, are calculated with an approach symmetrical to the one used for the cost calculation (Eq. C.17). They are defined as the sum of the emissions related to the construction (C) and end-of-life (E) of the energy conversion technologies ($TECH$), allocated to one year based on the technology lifetime n , and the emissions related to resources (RES). The latter are the emissions associated to fuels (from cradle to combustion) and imports of electricity. For resources, the construction phase corresponds to the extraction, processing and transportation whereas operation (O) corresponds to fuel combustion. Operating emissions of technologies, mainly corresponding to auxiliary materials and maintenance, are accounted for only if they are non-negligible.

The conceptual separation between technologies and resources for GWP calculation allows the integration of biofuels without increasing the model complexity. As an example, Figure C.2 shows that when SNG is produced it can be input in the natural gas layer, thus replacing its fossil equivalent. As a consequence, the total GWP emissions are reduced as the utilization of the fossil natural gas resource is lower. If emissions related to combustion were allocated to technologies, instead, unit models would need to be duplicated in order to account for the different emissions of fossil resources and their biogenic alternatives.

$$GWP_{tot} = \sum_{j \in TECH} \left(\frac{GWP_{C,E}(j)}{n(j)} + GWP_O(j) \right) + \sum_{i \in RES} GWP_{C,O}(i) \quad (C.17)$$

On the other hand, human health emissions are technology-dependent. In this case, combustion emissions can not be allocated to the resources as the combustion processes vary based on the technology. Thus, for this category the operating emissions of technologies (*human health* (hh)_O) include the resource combustion as well. Extraction, processing and transportation remain allocated to the resources (Eq. C.18).

$$hh_{tot} = \sum_{j \in TECH} \left(\frac{hh_{C,E}(j)}{n(j)} + hh_O(i) \right) + \sum_{i \in RES} hh_C(i) \quad (C.18)$$

Since there is no consensus on an impact assessment method for the human health indicator, two methods are chosen to address different aspects. The “impact 2002+” method [264], which includes an endpoint indicator for the human health, is widely used by the scientific community. It integrates a wide range of pollutants and health effects, such as respiratory effects, ionizing radiation or human toxicity. The Swiss Eco-factors 2013 [265], based on the method of the ecological scarcity (“ecoscarcity 2013”), provide a wide range of midpoint indicators related to specific environmental issues, and are based on the scientifically supported goals of the Swiss environmental policy. For this method, the category “main air pollutants and PM” has been chosen as another indicator representative of the human health. This indicator is more focused on air emissions, which are of particular concern in the case of wood combustion.

C.1.4 Scenarios

In the scenario definition phase, pathways for geothermal and biomass conversion technologies are enforced in order to explore the solution space.

Individual scenarios

Table C.1 lists the 20 *individual* scenarios, i.e. scenarios in which geothermal and biomass options are separately assessed.

Scenario 0 is the base case reference scenario, with no wood use and no geothermal installation. Scenarios 1-9 evaluate different options for geothermal alone, i.e. no wood is used in the system. Each one of the options envisions the drilling of one well at different depths (aquifer at 3.8 km, EGS at 4.2 km, 5 km and 6 km). In all these scenarios the heat available from the geothermal resource can directly supply the DHN. In the “direct use” case this is the only possible use of geothermal heat. In the “ORC” and “Kalina” scenarios the respective electricity production or cogeneration cycles are also available. The cycles installed capacity is fixed based on the associated resource. As cycles are designed for this size [266], from the operation point of view they can either be used at their respective nominal capacity, or be left unused. The latter case would be motivated by a higher profitability of directly using the heat.

In scenarios 10-20 the different wood conversion pathways are assessed in the absence of geothermal. The consumption of the total wet wood availability in the urban system (100 kt/y) is common to all scenarios. “Wet wood” ($\Phi = 50\%$) can be processed in a dryer to obtain “dry wood” ($\Phi = 15\%$). In the cases of direct combustion of wood in boilers or cogeneration and of biochemical conversion with the FT process, wet wood and dry wood are considered as optional inputs. Under the assumption that the drying process is equivalent for all the modeled biofuel production processes, the comparison between wet and dry wood input in the FT case is considered representative for the

Appendix C. Urban energy modeling

Table C.1 – List of individual scenarios

#	Biomass	Geothermal
0	-	-
1	-	3.8 km Direct use
2	-	3.8 km ORC
3	-	4.2 km Direct use
4	-	4.2 km ORC
5	-	5 km Direct use
6	-	5 km ORC
7	-	6 km Direct use
8	-	6 km ORC
9	-	6 km Kalina
10	Wet wood boiler	-
11	Dry wood boiler	-
12	Wet wood CHP	-
13	Dry wood CHP	-
14	Pyrolysis boiler	-
15	Pyrolysis CHP	-
16	Wet Wood FT	-
17	Dry Wood FT	-
18	SNG in NG	-
19	SNG CHP	-
20	SNG Mobility	-

SNG and pyrolysis cases. In the case of fuel production, all the different uses of the produced biofuels are accounted for. As an example, the default option for SNG is the replacement of fossil natural gas (NG) without impacting the technology mix (scenario 18). SNG could be also used in more efficient ways such as CHP (scenario 19) and in private mobility (scenario 20). As these technologies are not available in the reference scenario, this causes a change in the technology and fuel mix (e.g. SNG cars replacing diesel cars in mobility). Thus, these scenarios link the production of SNG to the deployment of CHP and cars using the biofuel as an input. Without a wider deployment of these technologies compared to the reference case, biofuels would simply replace their respective fossil equivalents.

A different approach is adopted for the scenarios involving electricity production technologies. In these scenarios electricity can be produced by ORC and CHP units. This electricity could be used in various ways, with significant differences in terms of environmental impact. This is shown in Table C.2: the impact on GHG is low when replacing a low-carbon electricity mix (such as the Swiss one), and high when used in heat pumps (replacing NG used in boilers) or electric vehicles (replacing diesel used in cars). Taking into account separately all these options would lead to an intractable number of scenarios. Thus, the assumption is that the produced electricity always replaces the

Table C.2 – Avoided GWP emissions (resources only) associated to the different uses of 1 kWh of electricity. Based on data as in Appendix D, unless otherwise specified.

Use type	Avoided GWP100a ^a [kgCO ₂ -eq./kWh _e]
Substitution Swiss el. mix	0.110
Substitution UCTE el. mix	0.482
Heat pump ^b	0.961
Electric car ^c	1.052

^a Only accounting for emissions related to resources. Emissions related to the production of the kWh of electricity not accounted for

^b Assuming COP = 3.5 and substitution of DHN NG boilers

^c Assuming 0.199 kWh_e/km [168] and substitution of diesel cars

current Union for the Co-ordination of Transmission of Electricity (UCTE) European electricity mix, which is chosen as a representative average between the possible available pathways. This mix has also a high human health impact. The choice is mainly motivated by the need of keeping the number of scenarios within a tractable number. The importance of linking the production of biofuels to a wider deployment of efficient technologies is discussed in [267].

Combined scenarios

The 9 individual scenarios for geothermal and 11 individual scenarios for biomass are systematically combined in order to investigate the interest of combining the two resources, with a particular focus on hybrid solutions. The 99 resulting scenarios are called *combined* scenarios.

C.2 Results

C.2.1 Individual scenarios: geothermal and biomass alone

The 20 individual scenarios listed in Table C.1 are the scenarios for which geothermal and biomass options are separately assessed. Performance indicators for the individual scenarios are reported in Figure C.4: the subplots depict hh_{tot}^2 (a) and GWP_{tot} (b) against the total annual cost C_{tot} , respectively. The lower the value of the indicators, the better the scenario performance. Geothermal and biomass options are compared to the reference (scenario 0), which represents the default state of the urban energy system without any use of wood or geothermal. The reference scenario is characterized by a total annual cost of 544.6 MCHF, and annual emissions of 777.7 ktCO₂-eq. and 62.9 kpts, respectively. Resources are responsible for 31.9% of the total cost and for 92.0% of the global GHG emissions. In

² The figure depicts only the “impact2002+” indicator. Results related to the “ecoscarcity 2013” indicator are reported in Section D.4.

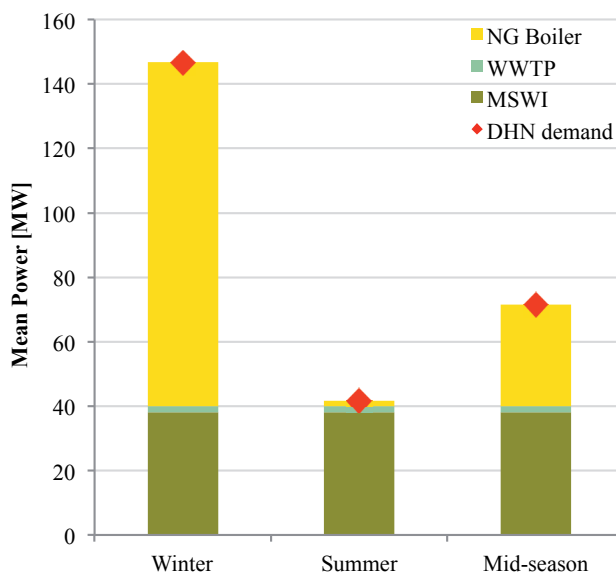


Figure C.3 – DHN heat supply and demand in the reference scenario (scenario 0).

the reference scenario, the heat provided by the WWTP and MSWI can almost entirely satisfy the DHN heat demand during the summer period, with a very low share left to natural gas during this season (Figure C.3).

Geothermal options

Scenarios 1-9 individually assess geothermal solutions at different depths, with the additional options of electricity production and cogeneration.

All EGS options (at 4.2 km, 5 km and 6 km) allow a reduction of both the total cost and the environmental impact indicators compared to the reference scenario. For the total cost, this reduction is due to the fact that the savings generated by the reduction of natural gas imports for DHN heat production are greater than the annualized investment cost of the wells. The benefit is even higher for the environmental impact, as the emissions related to the drilling are substantially lower than the avoided emissions from fossil fuels combustion.

When direct use of geothermal heat is the only available option, there is an excess of heat in summer as the DHN heat demand is already almost entirely satisfied by the MSWI and the WWTP. In the scenarios in which the installation of an ORC or Kalina cycle is forced in the system (scenarios 4, 6, 8, 9), this otherwise “waste” geothermal heat is converted to electricity. Results show that in all these scenarios the cycles are operated only during the summer period, whereas in the other seasons the “direct use” of geothermal heat is the optimal solution for the urban system. Thus, when there is a demand of heat in the system it is better to fully exploit the available geothermal heat to replace

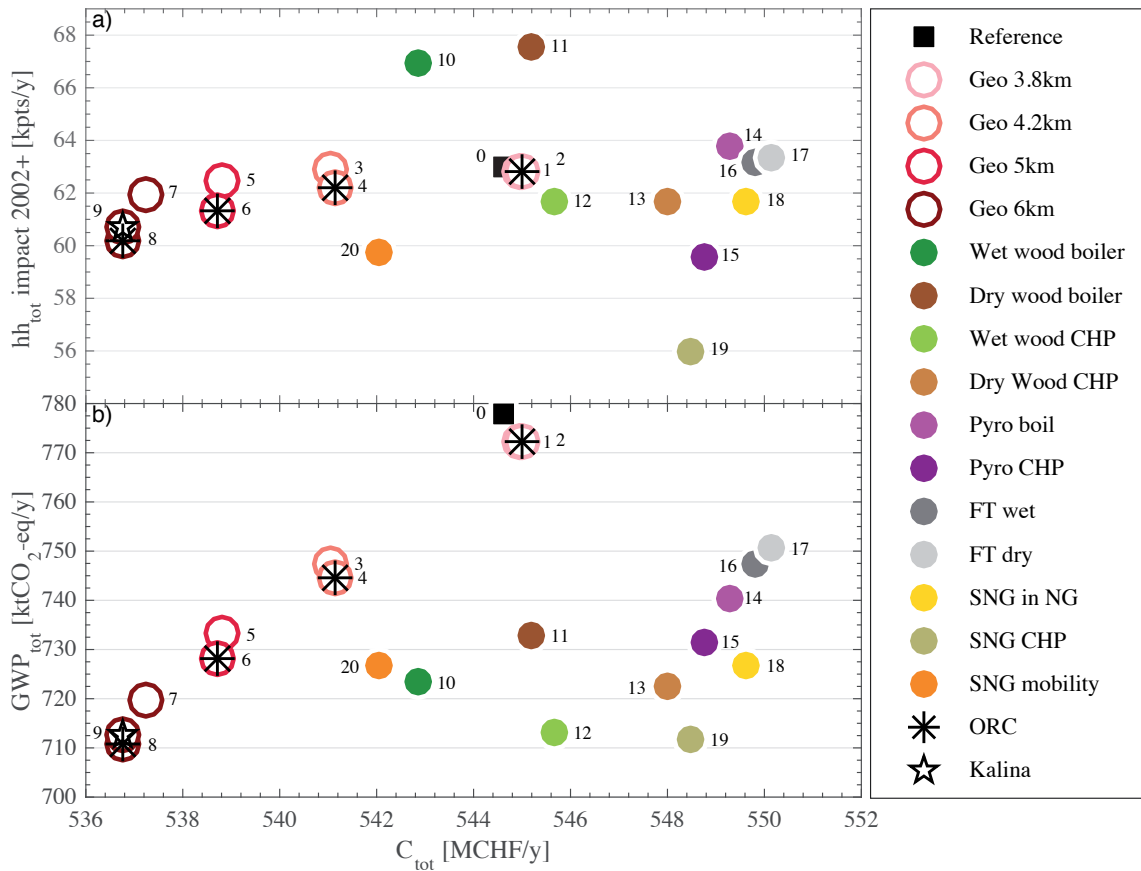


Figure C.4 – Results of the individual scenarios listed in Table C.1: individual assessment of geothermal and biomass options.

natural gas, instead of converting it to electricity at substantially lower efficiencies.

The benefits of EGS solutions increase with the depth of the installation, as the power-to-investment cost ratio gets higher. The best option for geothermal is therefore the 6 km well with ORC (scenario 8), which allows yearly savings of 7.83 MCHF, 67.0 ktCO₂-eq. and 2.75 kpts compared to the reference scenario. The ORC is preferred to the Kalina cycle as cogeneration of heat and power is not an interesting option in summer. In winter the cogeneration option is not optimal due to the high temperature of the DHN, which strongly limits the share of useful heat that can be recovered from the cogeneration power plant.

On the other hand, the aquifer option at 3.8 km (scenario 1) is of little interest. Compared to the EGS alternatives, it features a comparable investment cost but with a much lower expected mass flow rate. This leads to a higher total cost of the system, as the annualized investment for the well is higher than the savings in natural gas imports. When the corresponding ORC is added in the system (scenario 2) it is never economical to use it.

Biomass options

Scenarios 10-20 individually assess different pathways for the conversion and use of the entire woody biomass potential (100 kt/y).

The scenarios with direct combustion of wood in boilers or cogeneration power plants (scenarios 10-13) generally perform better in terms of total cost. In scenario 10, involving the combustion of wet wood in a boiler, the total annual cost of the system is reduced (-1.77 MCHF/y). In fact, in this scenario the savings generated by the reduced natural gas imports are higher than the cost of wood harvesting and of wood boiler technologies. The best results in terms of GHG emissions reduction from direct wood combustion are obtained in the case of wet wood-based cogeneration. Compared to the boiler case, the lower savings associated with heat production are compensated by the avoided emissions of electricity imports. For both total costs and GWP, drying the wood externally prior to combustion is a suboptimal solution (scenarios 11 and 13). Dry wood combustion is advantageous compared to wet wood combustion as the efficiency is higher and there is less water in the wood to be evaporated. Nonetheless, as no excess heat is available in these scenarios, external wood drying requires an additional natural gas consumption in the system. This additional consumption is higher than the benefits generated by the combustion of dry wood. Thus, in absence of excess heat in the system, it is more efficient to directly burn wet wood instead of externally drying it prior to combustion. This is mainly due to the fact that the external drying evaporates the water contained in the wood at a lower efficiency (52%) compared to the evaporation during the combustion process. The positive impacts on GHG emissions reduction, due to the lower NG consumption, are in trade-off with the negative impacts of wood combustion on human health. These negative impacts are mainly caused by the direct emissions of wood combustion. In the case of combustion in boilers, this leads to an overall increase of the human health impact compared to the reference scenario. This is more pronounced in the case of dry wood (+4.58 kpts/y compared to the reference) due to the electricity and natural gas emissions associated to the external dryer. In the case of cogeneration, these emissions are compensated by the avoided electricity imports. The strong reduction is due to the high impact on human health of the UCTE electricity import mix.

Scenarios 14-20 assess the pathways for the chemical conversion of woody biomass to biofuels. Scenarios 18-20, which assess the conversion of wood to SNG, result in the highest reduction of GHG emissions, with global values which are comparable to the combustion pathways. This is due to the high efficiency of the SNG process (74% fuel production with respect to wood input, on a wet basis). Scenario 18 is the default case, in which SNG replaces fossil NG. Scenario 19 (SNG CHP) offers the best results in terms of both GWP and human health, with a reduction of 66.0 ktCO₂-eq. and 6.96 kpts/y, respectively. In terms of GHG emissions reduction, wet wood CHP is suboptimal compared to SNG CHP. The higher electrical efficiency of the latter, in fact, compensates the losses of the wood-to-SNG conversion. The use of SNG in mobility (scenario 20), linked to a corresponding deployment of SNG cars, offers the best performance in terms of cost. This is due to the high cost

of diesel, which is partly substituted by SNG. This scenario has a similar performance in terms of GWP compared to scenario 18 due to the lower efficiency of SNG cars compared to diesel cars, which is in trade-off with the higher emissions of diesel compared to natural gas. The pyrolysis pathways (scenarios 14 and 15) present similar results but are limited with respect to GWP by a lower conversion efficiency (66.6% fuel production with respect to wood input, on a wet basis), and with respect to human health by the direct emissions associated to the combustion of pyrolysis oil [268]. On the other hand, they present the advantage of lower initial investment costs. The production of Fischer-Tropsch fuels to substitute diesel mobility (scenarios 16-17) is the least interesting option, as it is characterized by a lower conversion efficiency (49.8% fuel production with respect to wet wood input, on a wet basis) and very high investment costs³, which strongly reduce the high savings in operating cost due to reduced diesel consumption. Scenario 17 is the scenario with the highest total cost (+5.53 MCHF/y).

Unlike the case of direct combustion, the comparison between internal and external drying of wood shows that the two options are basically equivalent for biofuel production processes. This is due to the fact that when the drying is performed within the process (“FT wet”, scenario 16) using the available excess heat generated by the process itself, the efficiency is 62%, which is comparable to the one of the external dryer. Hence, when the drying is performed externally (“FT dry”, scenario 17) the additional natural gas consumption required by the drying process is almost equal to the reduction of natural gas imports caused by the supply of the excess process heat to the DHN. Thus, unlike for the case of direct combustion, in the case of biochemical conversion of woody biomass to biofuels and if no excess heat is available in the system, there is an equivalency between performing the drying externally or within the process. As mentioned in section C.1.4, the results for the FT case can be extended to the pyrolysis and SNG processes as the drying process is the same for all these pathways.

C.2.2 Combined scenarios: combination of biomass and geothermal options

Biomass and geothermal options are systematically combined in order to evaluate possible synergies offered by the integration of the two resources. 99 additional scenarios are generated by combining the 9 individual scenarios for geothermal and the 11 individual scenarios for biomass listed in Table C.1.

The performance of a given scenario with respect to the reference (scenario 0) and to each indicator is defined as in Eq. C.19:

$$\delta PI_x = PI_x - PI_0 \tag{C.19}$$

³ The FT model is based on [269], in which it is optimized for a bigger size compared to the one considered in this work.

Appendix C. Urban energy modeling

in which PI_x is the value of a performance indicator (C_{tot} , GWP_{tot} or hh_{tot}) for the scenario x . For the individual scenarios, x is the scenario number as listed in Table C.1. For the scenarios in which geothermal and biomass options are combined, $x = (i, j)$, with i being the scenario option for geothermal, and j the scenario option for biomass, again numbered as in Table C.1. As an example, scenario (1,10) is the combination of the 3.8 km aquifer for geothermal (scenario 1) with the wet wood boiler for biomass (scenario 10). The lower the value of δPI_x , the better the performance of scenario x compared to the reference case (scenario 0).

In order to evaluate the interest of the combined scenarios, a new indicator is defined as in Eq. C.20:

$$\Delta PI_{(i,j)} = \delta PI_{(i,j)} - (\delta PI_i + \delta PI_j) \quad (C.20)$$

$\Delta PI_{(i,j)}$ compares the performance of a given combined scenario ($\delta PI_{(i,j)}$) to the sum of the performance of the two corresponding individual scenarios ($\delta PI_i + \delta PI_j$). If $\Delta PI_{(i,j)} = 0$, the combination of the options i and j is equal to the sum of the benefits provided by scenarios i and j alone. If $\Delta PI_{(i,j)} < 0$, the combination generates a “positive synergy”, i.e. combining options i and j generates more savings than the sum of the savings provided by scenarios i and j alone. If $\Delta PI_{(i,j)} > 0$ instead, the combination generates a “negative synergy”, i.e. combining options i and j generates less savings than the sum of the savings provided by scenarios i and j alone.

Figure C.5 plots the values of ΔC_{tot} and ΔGWP_{tot} for the 99 combined scenarios. The use of symbols to refer to the scenarios in this figure is consistent with the convention used in Figure C.4. The dotted red lines highlight the points for which $\Delta PI_{(i,j)} = 0$. Out of the 99 scenarios, 37 lie at the intersection of these red lines. For these scenarios, both in terms of cost and of GWP, the combination between geothermal and biomass options has no advantage or disadvantage compared to the sum of the same options alone. Thus, these scenarios are not further discussed here as their performance is the sum of the benefits of the corresponding individual scenarios highlighted in Figure C.4.

Combined scenarios: negative synergies

Scenarios presenting negative synergies are shown in the upper right quadrant of Figure C.5, delimited by the dotted red lines. Out of the 35 scenarios showing a non-zero variation in terms of total cost, 21 show also a non-zero variation in terms of GWP (some points are exactly overlapping in the graph).

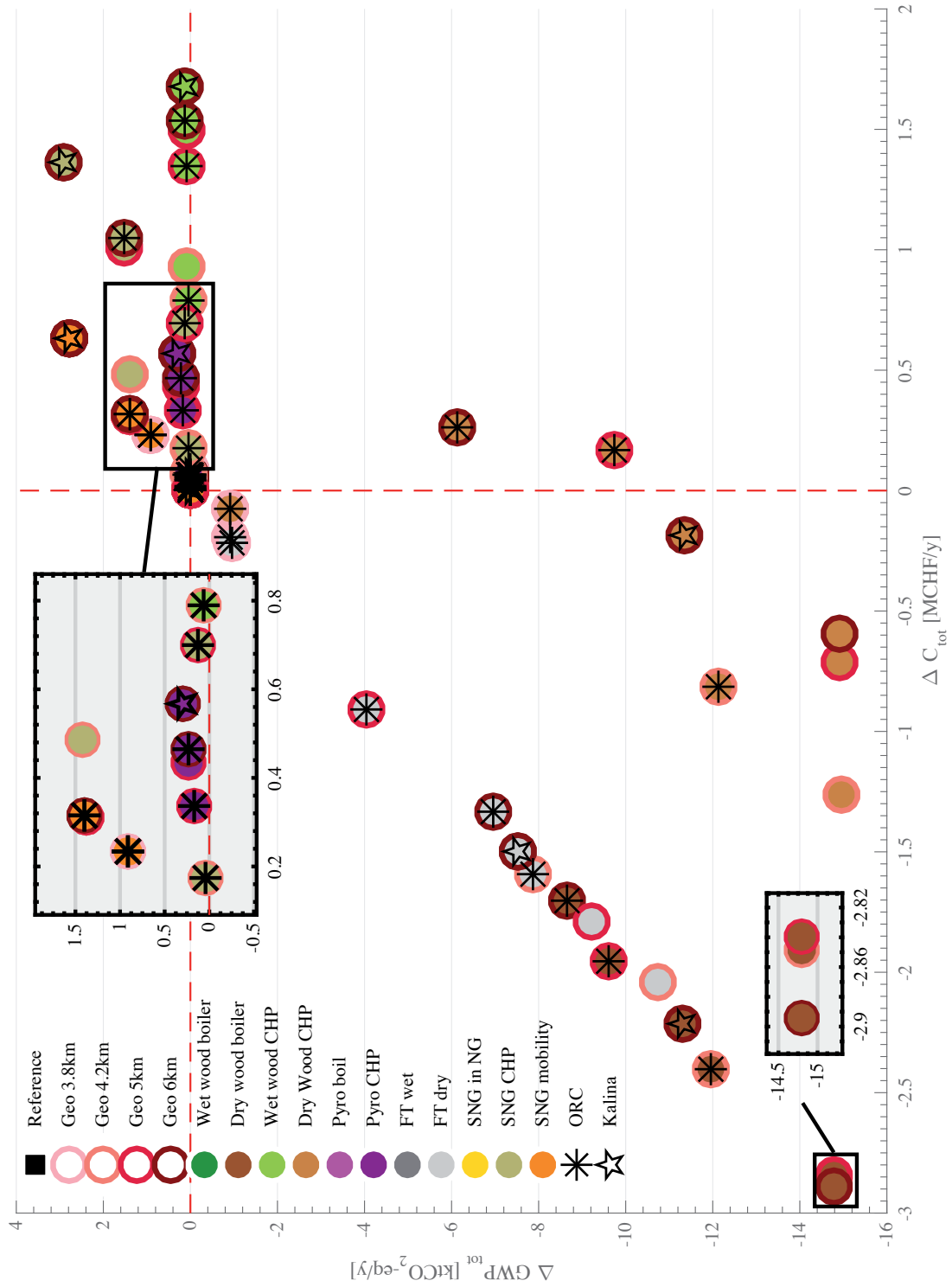


Figure C.5 – ΔC_{tot} and ΔGWP_{tot} for the geothermal-biomass combined scenarios.

Appendix C. Urban energy modeling

For the combined scenarios having a negative effect only on the total cost indicator ($\Delta GWP_{tot} = 0$), the difference derives by the sizing of the biomass energy conversion technologies. Among these scenarios, the ones combining wet wood based cogeneration with the EGS geothermal options show the worst performance in this regard. The reason is that in the individual scenario for wet-wood based cogeneration (scenario 12) the available wood is burned partly in winter and partly during the mid-season. When the EGS resources are added, it is economically optimal to burn the entire wood during winter, and therefore a bigger CHP unit is needed. The same applies to the scenarios combining pyrolysis CHP with the EGS options at 5 km and 6 km. In this case, this happens only with the geothermal options at higher depth because these two options can satisfy (fully in the case of the 6 km) the heat requirements of the DHN during the mid-season period.

The 21 scenarios showing a negative synergy also for the GWP indicator are those that include SNG production, with the exclusion of the ones coupled to 4.2 km and 5 km ORC options. For all these scenarios, the negative synergy for the GWP indicator is motivated by the slightly increased consumption of fossil natural gas in the system. In fact, in the individual scenarios involving SNG production (scenarios 18-20) the extra heat available in the SNG process is sufficient to replace the natural gas needed during the summer period to satisfy the small DHN heat requirement not provided by the MSWI and the WWTP. As this advantage of the SNG process is already included in the individual scenarios, the combined scenarios with the EGS options cannot benefit from this reduction. This additional natural gas consumption could be avoided by not operating the SNG process during the summer period, though this would lead to a substantial increase in the investment costs.

In general, the negative synergies associated to the integration are not significant and motivated by the choice of the total cost as objective of the MILP problem.

Combined scenarios: positive synergies

Scenarios presenting positive synergies with respect to GWP are shown in the lower part of Figure C.5, delimited by the horizontal dotted red line. This group of 27 scenarios consists of the combination of the three scenarios with external drying of wood (scenarios 11, 13 and 17) with all the 9 options for geothermal. Out of these 27 scenarios, 25 show also a positive synergy in terms of total cost (lower left quadrant of the figure). As discussed in section C.2.1 in the individual scenarios there is no interest for external drying of wood, especially in the case of wood combustion, where the suboptimality of external drying is greater. This is due to the fact that in the absence of excess heat in the system, external drying requires an additional consumption of fossil natural gas. As the MSWI and the WWTP supply the quasi-entirety of the heat needed in summer, when geothermal options are added in the combined scenarios, geothermal heat in summer represents instead an excess in the system. The positive synergy of these combined scenarios derives from the integration of excess geothermal heat in the biomass drying process, which leads to a global increase in the conversion

efficiency.

The six combined scenarios integrating the 3.8 km aquifer resources are of least interest. This is due to the low thermal output of the aquifer well. On the other hand, the integration of the three EGS direct use options for dry wood combustion (boilers and CHP) shows the highest improvement compared to the individual scenarios in terms of GHG emissions. This reduction is motivated by the substitution of fossil natural gas with geothermal heat for wood drying. In terms of total cost, the savings in natural gas imports are greater than the increased investment costs for wood boilers, CHP and storage units. In the case of cogeneration, as highlighted in the previous paragraph, the need of entirely burning the wood in winter causes higher investment costs for the cogeneration unit.

In the case of direct use of EGS integrated with combustion of dry wood, the maximum synergies are already obtained with the resource at 4.2 km depth. This is due to the fact that the excess heat in summer available from the 4.2 km well summed to the heat production from the MSWI is enough to dry the entire wet wood available, while at the same time satisfying the heat demand of the DHN. Thus, the 5 km and 6 km EGS options do not offer additional advantages in terms of synergy between the two resources.

The “FT dry” process has an excess heat available, corresponding to the amount of heat used in the “FT wet” option for wood drying. This excess heat is used for DHN heat supply. When combined with the direct use EGS options, differently from the case with dry wood combustion, the best performance is achieved with the 4.2 km EGS option. The reason is that the options at 5 km and 6 km can satisfy (fully in the 6 km case) the DHN heat requirements in the mid-season, so in this season the extra heat available from the “FT dry” process is in excess. In the case of integration with the 4.2 km well, this excess heat is also fully exploited during that period of the year, leading to better system integration and lower fossil natural gas consumption.

In the “direct use” individual scenarios the excess geothermal heat is almost entirely wasted. In the ORC and Kalina individual scenarios the cycles already partially exploit the excess geothermal heat in summer by converting it to electricity. This explains why in this figure the direct use EGS options show higher reductions than the options with ORC or Kalina cycles at 4.2 km and 5 km. In other words, a more efficient use of the excess geothermal heat in the individual scenarios reduces the benefits brought by the integration with the biomass drying processes. This is highlighted in Figure C.5 for the points in which wood dry options are integrated with ORCs at different depths: the positive synergy is lower for the 5 km compared to the 4.2 km EGS, as the 5 km option features a higher production of electricity in the corresponding individual scenario. In these combined scenarios, the cycles are not operated during summer as the heat is used for wood drying. An exception is represented by the combination between the dry wood conversion processes and the EGS options at 6 km with ORCs. In these combined scenarios, it is economically optimal to operate the cycles during the summer period due to the higher electrical efficiency of the supercritical cycle. This means that the wood is also partly dried during winter, causing a higher fossil natural gas

consumption in the system. This increase is more pronounced in the case of dry wood combustion compared to the FT due to the lower global efficiency of the external wood drying.

In general, the integration between biomass and geothermal options offers opportunities for strong positive synergies, identifying the interest of hybrid solutions in which the excess geothermal heat in summer is integrated in the wood drying process.

The $\Delta PI_{(i,j)}$ indicator, adopted in Figure C.5, is a relative indicator, ranking geothermal-biomass combinations relatively to the corresponding individual scenarios. A good performance of a combined scenario (low value of $\Delta PI_{(i,j)}$) can also be due to a suboptimal condition in the corresponding individual scenarios, and *vice-versa*. In other words, an efficient (inefficient) use of a resource in the individual scenarios can decrease (increase) the positive synergy of a combined scenario. An example is the highlighted negative synergy case of the SNG process, which is due to the fact that the corresponding individual scenarios are already benefiting from a reduced fossil natural gas consumption in periods of low DHN heat demand.

C.2.3 Evaluation of hybrid processes

Thus, to complete the analysis performed in the previous section, the 27 hybrid solutions need to be compared in absolute values. To do this, a new indicator is defined, comparing the corresponding geothermal-biomass combinations with and without external drying (Eq. C.21):

$$\Delta_{Hybrid}PI_{(i,k)} = PI_{(i,j)} - PI_{(i,j-1)} \quad (C.21)$$

in which k is a biomass conversion process for which the external drying option is defined (FT, wood boiler and wood CHP), j is the corresponding individual scenario with external drying ($j = 11, 13$ and 17 , respectively) and $j - 1$ is the corresponding individual scenario fuelled with wet wood. The indicator is calculated for all geothermal options $i \in [0; 9]$. Individual scenarios are numbered as in Table C.1. $\Delta_{Hybrid}PI$ is the difference between the biomass conversion process having dry wood as an input (external drying) and the same process fuelled with wet wood, with respect to a given performance indicator. As an example, $\Delta_{Hybrid}GWP_{tot,(1,FT)}$ is the difference between the “FT dry” ($j = 17$) and the “FT wet” processes ($j - 1 = 16$), both integrated with the 3.8 km aquifer for geothermal ($i = 1$), with respect to the GWP_{tot} performance indicator.

Results of the analysis are depicted in Figure C.6, plotting the Δ_{Hybrid} indicator for the total cost and the GHG emissions. The dotted red lines indicate the points for which $\Delta_{Hybrid}PI_{(i,k)} = 0$. For points lying on these lines the wet process is equivalent to the process with external drying, i.e. no advantage or disadvantage is associated with the external drying process. If $\Delta_{Hybrid}PI_{(i,k)} > 0$ then the wet process performs better than the dry option. In these cases, there is no interest for external

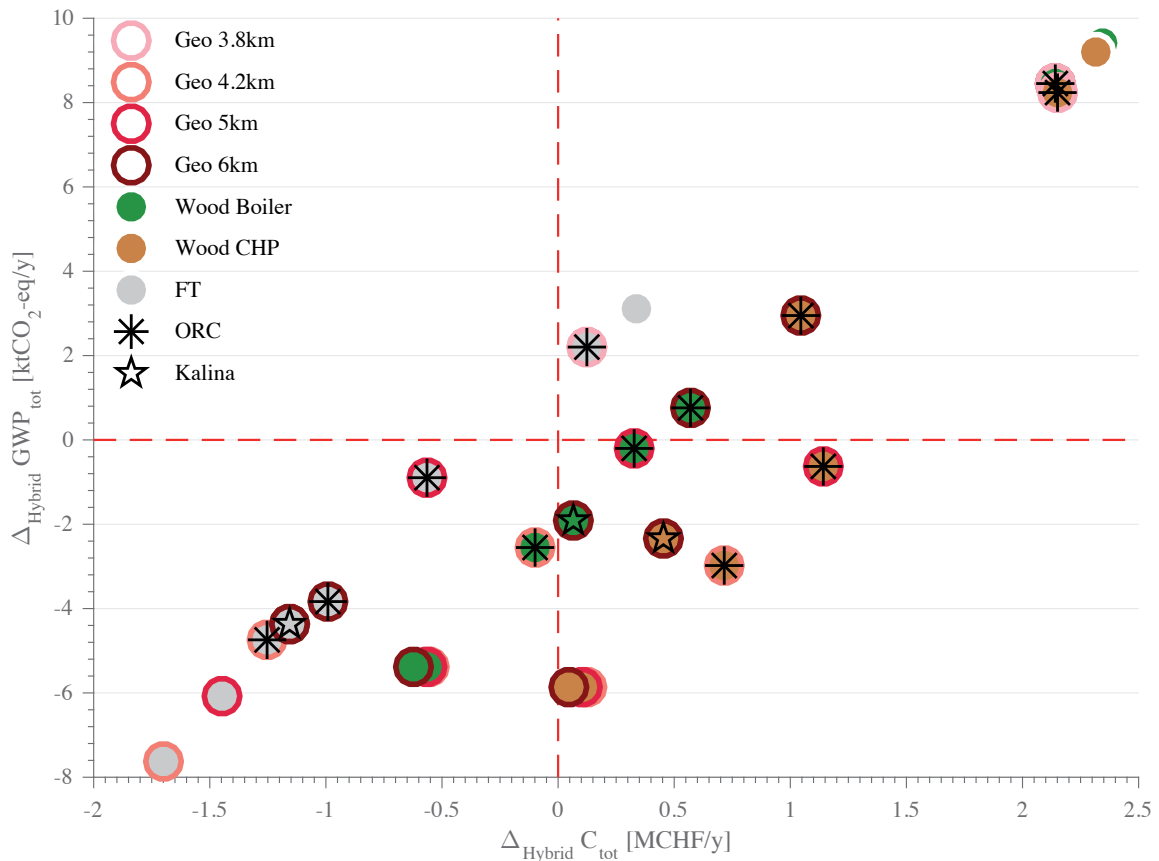


Figure C.6 – $\Delta_{\text{Hybrid}}C_{\text{tot}}$ and $\Delta_{\text{Hybrid}}GWP_{\text{tot}}$ for the hybrid biomass-geothermal processes.

drying. If $\Delta_{\text{Hybrid}}PI_{(i,k)} < 0$ then the option with external drying has a better performance than the wet wood fuelled option. Thus, the lower left quadrant of the graph highlights and ranks the hybrid solutions of interest. The lower the $\Delta_{\text{Hybrid}}PI_{(i,k)}$, the greater the interest of the geothermal-biomass hybrid system.

As a reference, the graph shows as well the Δ_{Hybrid} indicator for the individual scenarios, in which no geothermal option is activated. As expected, the individual scenarios are in the upper right quadrant of the figure. As discussed in section C.2.1, external wood drying is not an interesting option for the individual scenarios, as it leads to an overall increase of fossil natural gas consumption in the system. For these options, the wet wood fuelled process is more efficient than the dry wood process with external drying. The reason lies in the lower efficiency of external drying in evaporating the water contained in the wood. The suboptimality is greater in the case of processes with wood combustion, whereas for the biofuel production processes the difference in efficiency is lower. This explains the lower suboptimality of the FT process highlighted in the graph.

Scenarios with $\Delta_{\text{Hybrid}}PI_{(i,k)} > 0$, in the upper right quadrant of the figure, feature an overall increase

of NG consumption in the system in the “dry” case compared to the “wet” option. All the biomass processes combined with the 3.8km aquifer do not show an interest for external drying. In fact, the heat potential of the aquifer can supply only a small part of the heat needed to dry the entire wood available. Thus, in these cases the savings of natural gas due to the integration with geothermal heat in the drying process are lower than the additional natural gas consumption needed to dry the rest of the wood. The same applies to the combustion of dry wood coupled with the EGS 6 km ORC option. As previously discussed, operating the ORC cycles during summer has for consequence a higher NG consumption for wood drying in the other seasons.

Concerning the scenarios with negative Δ_{Hybrid} values, the best scenario for both indicator is the combination of the “FT dry” process with the EGS at 4.2km. As previously discussed, this is due to the fact that in this scenario the best balance in the system is achieved, allowing to fully exploit the geothermal heat in summer and the additional heat available from the FT process in the other seasons. Reaching higher depths for the geothermal wells would lead to lower benefits in terms of integration with the biomass chemical conversion processes, as there would be an excess of heat in the mid-season.

The comparison in absolute values of the hybrid geothermal-biomass options allows the identification of an optimal solution, maximizing the integration between the two resources. Due to the equivalence of the drying process, the results obtained for the FT can be extended to the pyrolysis and SNG processes.

C.2.4 Discussion

The scenario-based methodology offers a systematic evaluation of all the available options for deep geothermal and woody biomass. Performance indicators are the total annual cost of the energy system, objective of the MILP, and environmental impact indicators (GWP and human health).

First, geothermal and biomass options are separately evaluated. For geothermal, aquifer and EGS options are considered. Compared to the reference scenario, which features no wood use and no geothermal installation, all the EGS options allow a reduction of both the total cost and the environmental impact indicators. The direct use of geothermal heat in the district heating network of the city is the best option for geothermal energy. In periods of low heating demand, the MSWI and WWTP can almost entirely supply the district heating network. Thus, geothermal heat is in excess during these periods. The conversion of this excess heat to electricity with ORC allows to further improve the environmental performance indicators. The option of cogeneration is limited by the high temperature of the DHN.

For woody biomass, the best results are offered by the conversion of wood to SNG. The substitution of diesel cars with SNG cars offers the best performance in terms of cost, whereas GHG emissions and human health impacts are minimized by the combustion of SNG in CHP units. Pyrolysis scenarios

are limited by a lower conversion efficiency and by the impact on human health associated to BioOil combustion. Wood combustion pathways show good performances in terms of GHG emissions and have the advantage of lower investment costs. The option of direct combustion of wood is penalized by a negative impact on human health.

In the individual scenarios for woody biomass, wet ($\Phi = 50\%$) and dry ($\Phi = 15\%$) wood are evaluated as optional inputs. When no excess heat is available in the system, there is no interest for external wood drying, as the heat requirement of the dryer leads to an overall increase of fossil natural gas consumption in the system. On the other hand, when the combination of geothermal and biomass options is evaluated, the excess geothermal heat in summer can be integrated in the wood drying process. These hybrid systems can achieve higher savings in terms of total annual costs and GHG emissions than the corresponding geothermal and biomass options alone. The identification of hybrid geothermal-biomass processes for wood drying emerges as an efficient way of storing excess heat in summer in urban energy systems, leading to an increase in the global efficiency.

The chemical biomass conversion pathways benefit more from the hybridization than the wood combustion processes. This can be considered a general result as it depends on the efficiencies of the involved processes. On the other hand, the identification of the 4.2 km EGS option as the optimal one for the hybrid system is determined by the integration in the urban system. The seasonal variations of the demand in energy services and the constraints given by the presence of other energy conversion technologies strongly impact the evaluation of the different options

Overall, in this chapter a methodology to model urban energy systems for the integration of deep geothermal energy and woody biomass resources is developed and demonstrated by an application case study. A multiperiod MILP formulation for urban energy system modeling is proposed. The formulation includes process integration in order to account for potential hybrid solutions leading to positive synergies between the considered resources. The methodology is applied to the urban system of Lausanne, Switzerland. Results show that integrating these two resources generates configurations featuring both lower costs and environmental impacts. In particular, synergies are found in innovative hybrid systems using excess geothermal heat to increase the efficiency of biomass conversion processes.

In a stand-alone comparison of the technologies, it is often assumed that a demand exists for the produced energy services. This limit is overcome by contextualizing the comparison within urban energy systems. The application to the case study shows that taking into account the seasonal variations of the demand in energy services and the constraints given by the presence other energy conversion technologies strongly impacts the results.

D Urban energy modeling - data

Overview

The appendix is complementary to Appendix C as it details the input data for the application of the MILP urban energy system modeling framework to the case study of Lausanne (Switzerland).

This chapter has been published as Supplementary Information of Moret et al. [236].

D.1 Lausanne case study

The European urban system of Lausanne (Switzerland, 140,421 inhabitants in 2015) is taken as an example case study in this work. Figure D.1 shows the energy flow Sankey diagram of the city for the year 2012, taken as reference in this study. The final energy consumption is broken down into its three main components: heating (59.9%, including industry), electricity (22.9%, including industry) and transportation (17.2%). Cooling is negligible and thus not accounted for in this study. Industry has a small impact on the total final energy consumption (3.7%) of the urban system. Fossil fuels (oil and natural gas) account for 59.0% of the urban system's primary energy consumption, covering the largest share of the demand in the heating and in the transportation sectors.

A DHN, covering 20.6% of heating final energy consumption, is supplied by fossil fuel boilers (mainly running on natural gas), a WWTP and a MSWI cogeneration power plant. Electricity demand is mainly satisfied by hydroelectricity (80.9%), followed by nuclear (7.3%), and smaller contributions from other renewable resources (biomass, solar and wind).

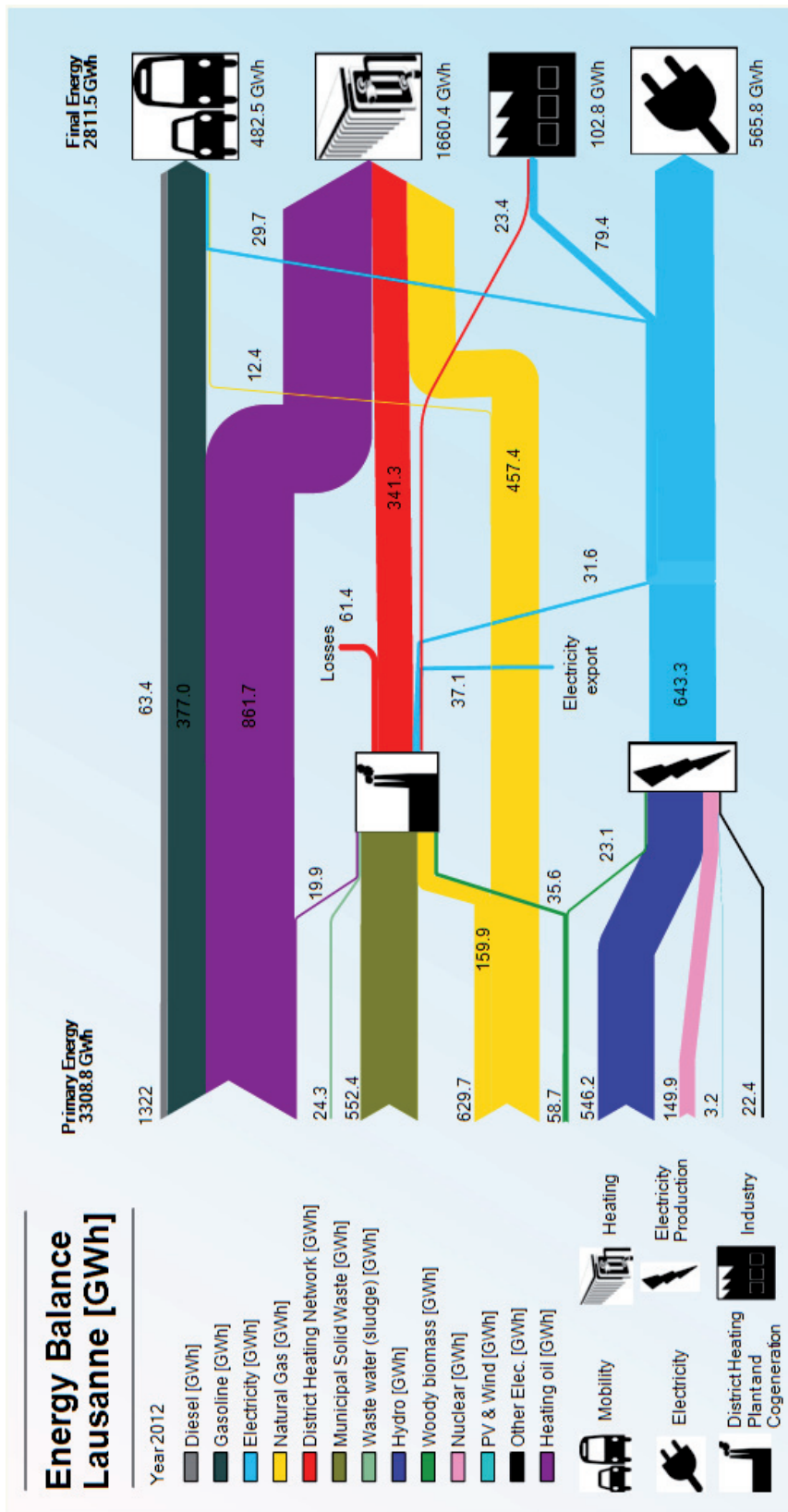


Figure D.1 – Energy flow Sankey diagram of the city of Lausanne (Switzerland) for the year 2012 (adapted from [258])

There is currently no deployment of deep geothermal technologies, while biomass (woody biomass and dry sludge from waste water) accounts for 2.5% of the primary energy consumption, with 15.4 kt (1 kt = 10^6 kg) of local woody biomass burned in the MSWI in the year 2012 out of a total potential estimated in the range of 50-100 kt/y¹.

The planned expansion of the DHN as well as the phasing out of nuclear power plants in Switzerland [64] present opportunities for a wider deployment of these two renewable resources as fossil fuel substitutes. The share of centralised heat production has a yearly growth rate of about 2%. The DHN is forecast to satisfy about 45% of the projected total heat demand by the year 2035.

D.1.1 Excess heat from the MSWI

The MSWI of the city (“TRIDEL”) is a cogeneration power plant, burning in 2012 161 kt of MSW and 15.4 kt of wet wood. In the same year, the total output of the power plant was 85.1 GWh_e of electricity and 261.6 GWh_{th} of heat. Out of the total production, 25.6% of the electricity and 1.2% of the heat are used to satisfy the internal energy requirements of the power plant [270].

As described in section D.3.8, the waste is burned in a boiler. The produced steam is expanded in a 20 MW_e turbine and then drawn-off (175 °C) for high temperature industrial applications and district heating. As the waste input is rather constant over the year, the potential heat production in summer is higher than the urban heat demand. Thus, in summer the steam is expanded until ambient temperature to increase the electricity output.

A simplified flowsheeting model of the MSWI power plant has been developed by Amblard [258] assuming constant waste input over the year. The goal of this modeling effort was to reproduce the seasonal behavior of the power plant, thus evaluating the marginal efficiency of electricity production in periods of low heating demand. Marginal efficiency is here defined as the ratio between the increase in electricity production in summer over the reduction in heat supply in the same period. Results show that the marginal efficiency of electricity production is 14.7%.

The thermal and electrical production of the MSWI are compared in Figure D.2 with the total DHN demand of Lausanne for the year 2012. The figure shows the mean monthly net power production compared to the DHN demand (in green). The black dotted line is the net mean thermal power output in the winter period. The area in red represents the thermal power that could theoretically be produced in periods of low heating demand if the power plant was operated all the year in the winter operating configuration, i.e. without expansion down to ambient temperature. This “excess heat” corresponds to approximately 97 GWh_{th} at a temperature above 175 °C. It is used today in the second stage of the condensing turbine of the MSWI to produce electricity with a very low efficiency. This is due to the low heat demand of the DHN in summer.

¹ Sustainable potential of wood in the area of Lausanne, personal communication from the Services Industriels de Lausanne (SiL)

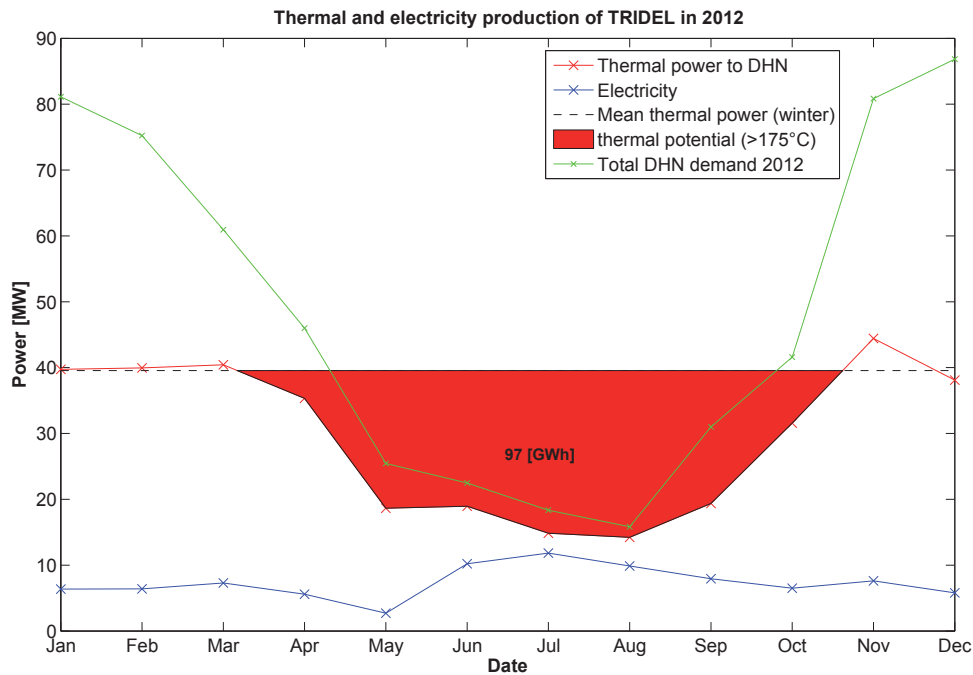


Figure D.2 – Lausanne MSWI thermal and electricity production compared to the DHN demand in the year 2012 [258]. The figure shows the high thermal potential available in summer, which is today converted to electricity at a low marginal efficiency.

In view of the planned future expansion of the DHN this heat could be used to supply the increased heat demand. Thus, in this work the winter mean operation conditions (38.65 MW thermal and 8.61 MW electric) are assumed for the whole year in the prospective scenarios. The auto consumption of the MSWI is accounted for in the model and is assumed constant over the year. In [259] it is shown that this heat would be sufficient to satisfy the projected DHN heat demand in the year 2035. When this is the case, the integration of geothermal resources generates an excess of heat in summer which can be integrated in biomass conversion processes.

D.1.2 Evolution of the energy system to 2035

The energy model used in this work takes the situation in the year 2012 as a reference. Nonetheless, as the integration of biomass and geothermal technologies represents a long term strategy of the city linked to the extension of the DHN, the evolution of the energy system to the year 2035 is considered. Some simplifying assumptions are made about the evolution of the Lausanne energy system between 2012 and 2035:

- Population growth: a 0.7% yearly rate is assumed for the demographic growth, increasing the urban system population from 137,000 inhabitants in 2012 to 161,000 in 2035.
- Demand in energy services: the specific demand per capita in energy services for electricity and transportation is assumed to remain constant, with the share of M_{pkm} provided by public transportation increased to 28.5% in 2035 and share repartition as in section D.3.9. The total heating demand is assumed to remain constant due to the balanced effects of population growth and building efficiency. The DHN is assumed to cover 45% of the heating end-uses, with an increased length of 170 km in 2035.
- Electricity production: the installation of a new 31 MW_e Kaplan turbine is considered.
- For decentralized boilers, an increased share of the heat demand is satisfied by natural gas boilers (60 %), with 40 % satisfied by oil boilers.

D.2 MILP model

Section C.1.2 illustrates the constraints of the optimization model. This section is complementary to it, as it details the sets, variables and parameters of the model in order to ensure reproducibility.

D.2.1 Sets

Figure D.3 shows the sets and subsets of the MILP formulation. The indices adopted in the figure are consistently used throughout Appendix C.

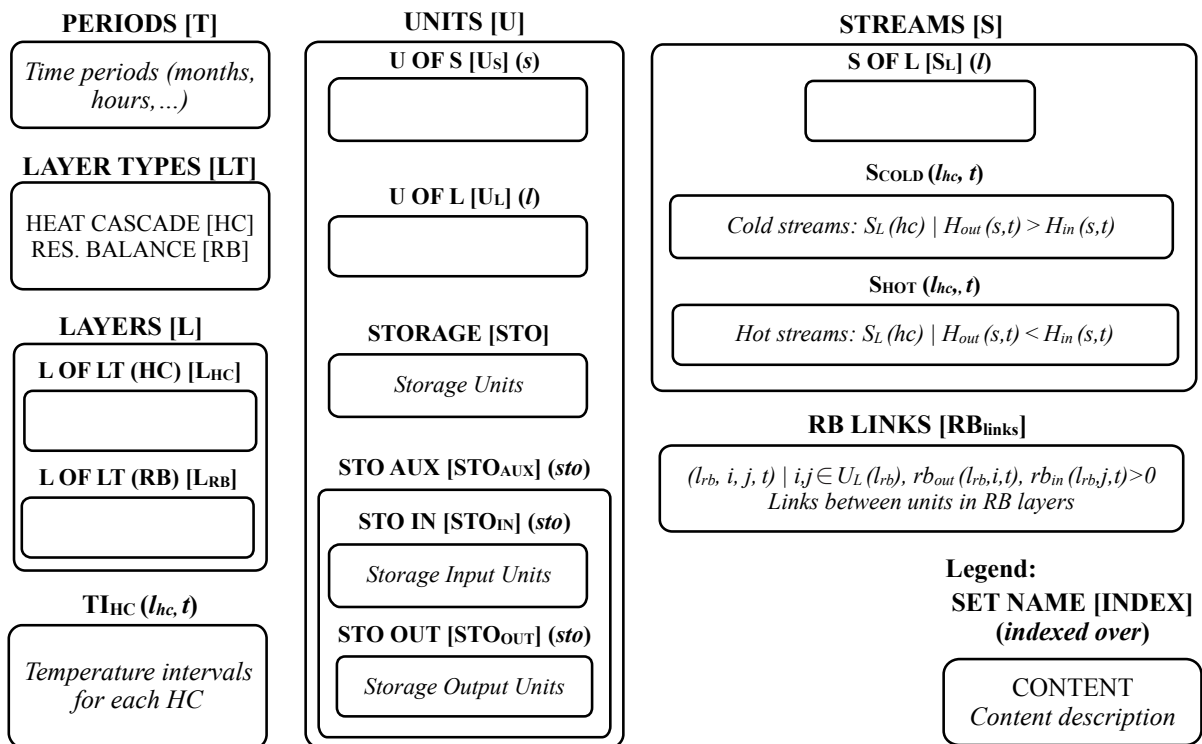


Figure D.3 – Sets of the MILP model with the corresponding indices

D.2.2 Parameters

Table D.1 lists the model parameters, specifying their units and description.

D.2.3 Variables

Table D.2 lists the model variables, specifying their units and description.

Table D.1 – Parameter list with description. Set indices as in Figure D.3

Parameter	Units	Description
$t_{op}(t)$	[h]	Time periods duration
$f_{min}, f_{max}(u)$	[-]	Min/max $Mult_t(u, t)$ if u is used
$use_f(u, t) \in \{0, 1\}$	[-]	Force use: If 1 then u must be used
$c_{inv,fix}(u)$	[MCHF/y]	Unit annualized fixed investment cost
$c_{inv,var}(u)$	[MCHF/y]	Unit ann. var. inv. cost if $Mult(u) = 1$
$c_{op,fix}(u)$	[MCHF/h]	Unit fixed operating cost
$c_{op,var}(u)$	[MCHF/h]	Unit var. op. cost if $Mult_t(u, t) = 1$
$T_{in}^*, T_{out}^*(s, t)^a$	[K]	Streams input/output temperature
$H_{in}, H_{out}(s, t)$	[MW]	Streams input/output enthaply
$cp(s, t)$	[MW/K]	Heat capacity flowrate := $\Delta H / \Delta T$
$T_{int}(l_{hc}, t, ti_{hc}(l_{hc}, t))$	[K]	Lower T of each temperature interval
$T_{max}(l_{hc}, t)$	[K]	:= $\max_{ti_{hc}(l_{hc}, t)}(T_{int}(l_{hc}, t, ti_{hc}(l_{hc}, t)))$
$T_{min}(l_{hc}, t)$	[K]	:= $\min_{ti_{hc}(l_{hc}, t)}(T_{int}(l_{hc}, t, ti_{hc}(l_{hc}, t)))$
δ	[K]	1e-5, used in heat cascade constraints
$rb_{in}(l_{rb}, u_l(l_{rb}), t)$	[MW] ^c	RB input for units if $Mult_t(u, t) = 1$
$rb_{out}(l_{rb}, u_l(l_{rb}), t)$	[MW] ^c	RB output for units if $Mult_t(u, t) = 1$
$\eta(sto_{aux})$	[-]	Efficiency [0;1] of storage input/output

^a Corrected temperatures: $T^* = T \pm \Delta T_{min}/2$ (+ if $s \in S_{COLD}$, - if $s \in S_{HOT}$)

Table D.2 – Variable list with description. All variables are continuous and non-negative, unless otherwise indicated.

Variable	Units	Description
Mult (u)	[-]	Unit size multiplication factor
Mult _t (u, t)	[-] ^b	Unit operation in each period
Use (u) $\in \{0, 1\}$	[-]	Unit use. If 0 unit is not purchased
Use _t (u, t) $\in \{0, 1\}$	[-]	Unit use in each period
C_{op} (u, t)	[MCHF]	Unit operating cost in each period
C_{inv} (u)	[MCHF/y]	Unit annualized investment cost
Mult _s (s, t)	[-]	Stream multiplication factor
R ($l_{hc}, t, ti_{hc}(l_{hc}, t)$)	[MW]	Heat cascaded from ti to lower ones
RB_{in} ($l_{rb}, u_l(l_{rb}), t$)	[MW] ^c	Total RB input for units
RB_{out} ($l_{rb}, u_l(l_{rb}), t$)	[MW] ^c	Total RB output for units
RB_{flow} (rb_{links})	[MW] ^c	Total RB flow between units

^b If $u \in STO$ it represents the level of the storage in energy or mass units

^c Units as in corresponding layer: [t/h] if layer is in mass, [pkm/h] for mobility

D.3 Unit models

This section details models and data used in the Lausanne case study. The unit models represented in Figure C.2 are characterized in terms of energy and mass balances, cost (operating and investment), and environmental impact (GWP and human health). Repartition of cost and LCA data between resources and technologies follows the methodology presented in Section C.1.3. For the cost data, expressed in real CHF₂₀₁₅, and for LCA data, the calculation approach detailed at the beginning of Appendix A is used. Additionally, the impact on human health is assessed with the “impact2002+ - human health” (expressed in points “pts”) and “ecoscarcity 2013 - main air pollutants and PM” (expressed in ecopoints “UBP” - *Umweltbelastungspunkte*) indicators.

Prices of resources and technologies are taken for the year 2015, under the assumption that the entire energy system is “rebuilt” in this year, and it will be operating in the same conditions in the future year taken as reference (2035). No future evolution of the investment cost of technologies and resources is accounted for. In the next sections, the total investment cost of the technologies is reported. In the MILP model, these investment costs are annualized based on the lifetime of the technologies by multiplying the total investment by the factor τ , calculated as in Eq. 1.2.

The lifetime of technologies (n) is assumed to be 25 years unless other data are found in the literature. As for the Swiss national energy system, the discount rate for the public investor is fixed at 3.215% (see Section A.6).

In this framework, annualized investment cost of existing technologies is also accounted for. This is coherent with the fact that at the end of their lifetime these technologies need to be replaced. In this way, the cost of technologies is spread over their whole lifetime, whereas financial depreciation would only attribute this cost to their early years of operation, leaving an upfront investment cost to future generations.

Most data reported in this section for the case study of Lausanne are coherent - in terms both of values and of calculation methodology - with the data reported in Appendix A for the Swiss energy system. However, there are (few) cases in which they differ, due to the different scales of the two applications or to the use of different sources. Cross-references are provided and sources are fully documented to clarify these cases.

D.3.1 Resources

Resources and their properties are listed in Table D.3.

Cost data refer to average values for Switzerland for the year 2015. For imported resources, such as heating oil, diesel, NG and electricity, the cost is taken at the city border, i.e. profit made by intermediate public service providers is not taken into consideration. MSW and dry sludge from waste-water treatment (WWT) are considered free of charge as they would need to be collected

anyway. The 2015 UCTE production mix LCA data are assumed for the electricity imports. For GWP, the impact associated to the resources includes the emissions related to their production, transport and use, under the simplifying assumption that, for fuels, the GWP of use is well represented by the emissions related to combustion and thus it is independent of the technology used. For human health and air quality this simplifying assumption is not suitable as these emissions are technology-dependent. Thus, for this category processing and transportation remain allocated to the resources, whereas combustion emissions are allocated to the technologies.

Woody biomass

Particular attention is given to the representation of biomass which refers here only to lignocellulosic biomass in the form of wood chips. The resource is represented by “wet wood” chips ($\Phi = 50\%$). The humidity (Φ), also called moisture content (MC) on a *wet basis* (wb), corresponds the mass of water [kg_{H_2O}] contained in 1 kg of wood [kg_{wb}]. As an example, 1 kg of wet wood (1 kg_{wb}) at $\Phi = 50\%$ contains 0.5 kg_{H_2O} and 0.5 kg of oven dry² wood [kg_{db}] ($\Phi = 0\%$). The reference LHV on a *db* ($\Phi = 0\%$) is 19 MJ/kg [271], and the corresponding LHV on a *wb* is calculated using Eq. D.1.

$$LHV_{wb} = LHV_{db} \cdot (1 - \Phi) - \Delta H_{vap} \cdot \Phi \quad \left[\frac{\text{MJ}}{\text{kg}_{wb}} \right] \quad (\text{D.1})$$

Where ΔH_{vap} is enthalpy of vaporization of water, equal to 2.443 MJ/kg [271]. In this work, when wood is represented in terms of power or energy equivalent, the *wb* representation is adopted unless otherwise stated.

The LHV_{db} is calculated from the higher heating value (HHV) by subtracting the energy of the water generated in the combustion reaction, as the LHV takes into account that this water is not condensed when leaving the system. Thus, the latent heat of condensation is not recovered as useful energy from the combustion process (Eq. D.2).

$$LHV_{db} = HHV - \frac{c_H}{2} \cdot \Delta H_{vap} \cdot M_{H_2O} \quad \left[\frac{\text{MJ}}{\text{kg}_{db}} \right] \quad (\text{D.2})$$

Where c_H is the mass fraction of hydrogen in the biomass composition, and M is the molar mass.

² As a simplification, “dry wood” refers to wood at $\Phi = 15\%$, “wet wood” to wood at $\Phi = 50\%$. Here the term “oven dry” is adopted to refer to wood at $\Phi = 0\%$. “Dry basis (*db*)” always indicates $\Phi = 0\%$.

Table D.3 – Resources properties

Resource	LHV [MJ/kg]	Density [kg/m ³]	Price [CHF ₂₀₁₅ /MWh]	GWP100a - IPCC2013 ^a [kgCO ₂ -eq./MWh]	hh - Impact2002+ ^b [pts/MWh]	ES2013 ^b [UBP/MWh]
Heating oil	42.90 [107]	843.1 [272]	86.55 ^c	311	7.48e-03	1.76e+04
Diesel	43.00 [107]	832.0 [273]	157.0 ^d	315	8.48e-03	1.94e+04
Petrol	42.60 [107]	745.0 [273]	173.6 ^e	345	1.07e-02	2.48e+04
NG	47.76 [107]	0.760 [168]	60.20 ^f	267	7.11e-03	1.57e+04
Electricity			105.6 ^g	482	8.21e-02	8.23e+04
Wet wood (Φ= 50%)	8.279 ^h	324.5 ⁱ	47.58 ^j	11.8 ^k	1.22e-03	2.95e+03
MSW	12.35 [277]	-	0	150 ^l	0	0
Dry sludge - WW	2.966 [277]	-	0	0 ^m	0	0

^a Impact associated to production, transport and combustion.

^b Impact associated to production, transport.

^c Average heating oil price for Jan-Nov 2015 for 800-1500 l consumers, corresponding to 0.8696 CHF₂₀₁₅/L [215].

^d Average Diesel price for Jan-Nov 2015, corresponding to 1.56 CHF₂₀₁₅/L [274].

^e Average 95 & 98 petrol price for Jan-Nov 2015, corresponding to 1.53 CHF₂₀₁₅/L [274].

^f It is assumed that the price for the City of Lausanne is twice the average import price Jan-Oct 2015 at the Swiss border (estimate based on personal communication from GazNat, May 2015. Import price data received by e-mail from the SFOS [216], Nov. 2015)

^g Import and production price index data for a big industry >20 GWh/y; average for Jan-Oct 2015 (data received by e-mail from the SFOS [216], Nov. 2015).

^h LHV on a wet basis (*wb*) calculated as in Eq. D.1.

ⁱ Density calculated as the average of wet (Φ = 45-55%) hardwood and softwood woodchips bulk density [271].

^j Price calculated as the average of wet (Φ = 45-55%) hardwood and softwood woodchips prices in Switzerland for the years 2014-2015 [275]. Does not include value-added tax (VAT).

^k In the IPCC 2013 GWP indicator implementation in Ecoinvent, non-fossil CO and CH₄ are assigned positive emission coefficients as detailed in [276]. Thus, wood combustion has non-zero emissions in the model. Emissions associated to combustion are 3.67 kgCO₂-eq./MWh. These emissions are allocated to the resource, under the assumption that all wood is burned at some stage in all the conversion pathways, including the ones involving production of biofuels.

^l GWP impact related to the treatment of MSW in an incineration plant, including auxiliary emissions due to the operation of the plant but not including its construction. This is not consistent with the other data presented in the table, however the incineration plant is the only technology treating MSW therefore associating the auxiliary emissions to the resource does not affect the results. Emissions related to production and transport of MSW are not accounted for.

^m Emissions related to production, transport and combustion of dry sludge are not accounted for.

D.3.2 Energy demand

The energy demand of the city is divided into heating, electricity and mobility. Cooling demand is negligible in the studied urban system. Table D.4 shows the values of the end-uses in energy services assumed for the City of Lausanne in 2035. As described in Section D.1.2, the energy demand in 2035 is calculated based on the 2012 situation, assuming a constant total demand for heating and a constant *per capita* demand for mobility and electricity. For electricity and heating, average power values are considered for the different periods in order to account for the seasonal variation in energy demand. Mobility is assumed to be constant over the different periods.

Table D.4 – Characterization of end-uses in energy services for the city of Lausanne in 2035.

Period	Duration [h]	Heating [MW]		Mobility [Mpkm/y]		Electricity [MW]
		DHN	Decentralized	Public	Private	
Summer	2928	35.33	43.18			69.87
Winter	3624	124.6	152.3	354.9	890.4	97.57
Mid-season	2208	60.82	74.34			90.64
Peak	1e-04	211.9 ^a	304.5 ^b			146.5 ^c

^a Ratio between peak and winter demand as in [258]. Calculated based on DHN hourly production profile.

^b Ratio between peak and winter demand assumed to be 2, as in [258].

^c Ratio between peak and winter demand assumed to be 1.5, as in [258].

The annual consumption for heating and electricity is calculated based on data provided by the Services Industriels de Lausanne (SiL), the public energy service provider of the city. The seasonal repartition of the heating demand, assumed equal for centralized and decentralized heating, is calculated based on the DHN hourly production profile. The share of the heat demand satisfied by the DHN is 45%.

Mobility is expressed in pkms. Based on the data from SiL and Transport Lausannois (TL), Amblard [258] has calculated a specific mobility of 7735 pkm/ca. for the city in 2012, with a 19.5% share of public mobility. In the year 2035, this share is assumed increased to 28.5%. The specific mobility is lower than the national value as the latter includes as well walking, biking, trains and flights, which are not accounted for in this model.

D.3.3 Biomass technologies

Wood dryer

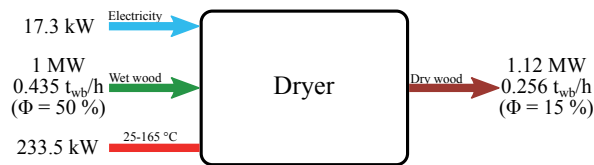


Figure D.4 – Wood dryer unit model.

The air wood dryer (Figure D.4) has wood at $\Phi = 50\%$ as an input, and wood at $\Phi = 15\%$ (LHV = 15.7835 MJ/kg_{wb}) as an output. The flowsheet model is originally developed in Belsim ValiTM by Gassner and Maréchal [278], while the cost functions are based on data from producers elaborated by Peduzzi [269]. Cost and emissions data are reported in Table D.5.

In Appendix C the concept of drying “efficiency” is adopted. This is defined as the theoretical heat needed to evaporate the water contained in the wood (\dot{m}_{H_2O}) over the actual heat needed for the drying process (\dot{Q}_{drying}^+). Eq. D.3 calculates the efficiency for the dryer as in Figure D.4.

$$\eta_{drying} = \frac{\dot{m}_{H_2O} \cdot \Delta H_{vap}}{\dot{Q}_{drying}^+} = \frac{(\dot{m}_{wood_{in}} - \dot{m}_{wood_{out}}) \cdot \Delta H_{vap}}{\dot{Q}_{drying}^+} = 0.52 \quad (D.3)$$

Where the amount of water evaporated is equal to the weight difference between input and output wood mass flow rate (kg_{wb}/s). Biomass chemical conversion processes with “wet” wood as an input ($\Phi = 50\%$) are modeled using the same dryer. The higher efficiency in that case (62%) is due to the fact that, when used in biomass chemical conversion processes, the dryer can reach a higher temperature (200 °C). In the model the external dryer is limited to 165 °C to achieve better integration with the available geothermal heat.

Table D.5 – Wood dryer parameters

	Value	Units	References
Reference size	3-18	MW _{in}	
c _{inv,fix} ^a	1.710e5	CHF ₂₀₁₅	[269]
c _{inv,var} ^a	6.457e4	CHF ₂₀₁₅ /MW _{in}	[269]
c _{op,fix} ^b	0.976	CHF ₂₀₁₅ /h	
c _{op,var} ^b	0.369	CHF ₂₀₁₅ /MWh _{in}	
Lifetime	50	y	[168]
GWP100a _{C,E} ^c	7.455e3	kgCO ₂ -eq./MW _{in}	
Impact2002+ _{C,E} ^c	3.699	pts/MW _{in}	
ES2013 _{C,E} ^c	7.313e6	UBP/MW _{in}	

^a Investment cost regression between 2.4 and 18.4 MW_{in} based on the WyssmontTM dryer cost reported in [269]. In the model, the regression is assumed valid in a larger range as the maximum size of the drying process is 79 MW which is obtained when all the wood is dried in the summer.

^b O&M assumed as 5% of c_{inv} over 8760 hours.

^c Calculated according to the size estimate reported by [269], considering steel as a construction material from [168]. Impacts only related to construction of the dryer. Operation impacts are not accounted for.

Fast pyrolysis for bio-oil production

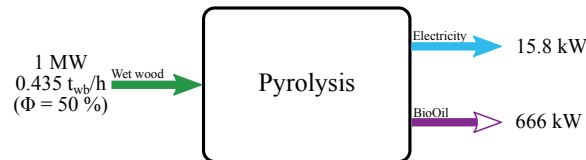


Figure D.5 – Pyrolysis unit model.

This model is adapted from the work by Shemfe et al. [279], presenting the performance analysis of a biomass fast pyrolysis biofuel production unit with electric power generation. In order to report the data coherently, the data in [279] are scaled under the simplifying assumption that the power input on a *wb* at $\Phi = 25\%$ (LHV = 13.050 MJ/kg_{wb}), as considered in [279], is equivalent to the power input on a *wb* at $\Phi = 50\%$, as considered in this study. The LHV of the bio-oil is calculated according to Boie's correlation [280] and the compositions reported by [281] (mass fraction of carbon, hydrogen and oxygen on a *dry basis (db)* of 0.56, 0.06 and 0.38, respectively), yielding 15.247 MJ/kg on a *wb*. Cost data are also adapted from the work by Shemfe et al. [279] according to the procedure described at the beginning of Appendix C, whereas O&M costs are assumed to be 5% of the investment. As further detailed in Section D.3.5, when bio-oil is used in combustion processes, human health emissions are considered as an average between LFO and Heavy fuel oil (HFO) (on an energy basis).

Appendix D. Urban energy modeling - data

This simplifying assumption is based on the study by Lehto et al. [268]. Cost and emissions data are reported in Table D.6. The possibility of using char to displace synthetic fertilizers is not considered in this study as in the model it is considered that the solid char is burnt in a combustion unit.

Table D.6 – Fast pyrolysis parameters

	Value	Units	References
Reference size	10	MW _{in}	[279]
c _{inv,fix}	-	CHF ₂₀₁₅	
c _{inv,var}	9.559e5	CHF ₂₀₁₅ /MW _{in}	adapted from [279]
c _{op,fix}	-	CHF ₂₀₁₅ /h	
c _{op,var} ^a	5.46	CHF ₂₀₁₅ /MWh _{in}	
Lifetime	25	y	
GWP100a _{C,E} ^b	1.080e4	kgCO ₂ -eq./MW _{in}	
Impact2002+ _{C,E} ^b	4.089	pts/MW _{in}	
ES2013 _{C,E} ^b	8.084e6	UBP/MW _{in}	

^a O&M assumed as 5% of c_{inv} over 8760 hours.

^b Calculated according to the size estimate reported by [269] for a dryer, considering steel as a construction material from [168]. Impacts only related to construction of the pyrolysis reactor. Operation impacts are not accounted for.

Fischer-Tropsch synthesis from biomass gasification

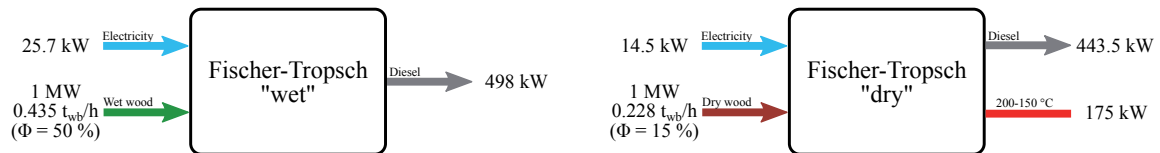


Figure D.6 – Fischer-Tropsch unit models for wet and dry wood input.

The Biomass to liquids (BtL) models considered in this study consist in the synthesis of FT fuels from lignocellulosic biomass and are described in detail in [269]. The main process considered in the present study is a base case process using entrained flow gasification. The first step is the pretreatment where raw biomass (50% or 15% Φ) is dried, torrefied, and ground into fine particles. The biomass particles are then gasified in a pressurized (30 bar) steam-oxygen blown entrained flow gasifier. The synthesis gas produced, consisting mainly of H₂, CO, CO₂ is cooled by a water quench and cleaned by a scrubber. A water gas shift reactor is used to adjust the H₂-to-CO ratio and CO₂ is removed by amine scrubbing in order to satisfy the requirements of the FT synthesis where the liquid hydrocarbon fuels are produced. Process integration allows heat recovery and the

co-production of electricity which is used to partly satisfy the requirement of the process. In the model, it is assumed that the produced FT fuels have the same properties as diesel. This model is adapted for this study and used to represent two different configurations. The first process, represented on the left in Figure D.6 and Table D.7, has wet wood ($\Phi = 50\%$) as an input. The second process, represented on the right in Figure D.6 and Table D.7, uses biomass which is delivered at the conversion facility at $\Phi = 15\%$ by an external dryer. The amount of heat used for wood drying in the first process (“FT wet”) is made available to supply the DHN in the second configuration (“FT dry”).

Table D.7 – Fischer-Tropsch synthesis from biomass gasification parameters

	Value		Units	References
	FT wet ($\Phi = 50\%$)	FT dry ($\Phi = 15\%$)		
Reference size	15-45		MW _{db,in}	
$c_{inv,fix}^a$	4.143e7	3.997e7	CHF ₂₀₁₅	[269]
$c_{inv,var}^a$	2.360e6	1.955e6	CHF ₂₀₁₅ /MW _{in}	[269]
$c_{op,fix}^a$	217.8	212.5	CHF ₂₀₁₅ /h	[269]
$c_{op,var}^a$	15.7	13.5	CHF ₂₀₁₅ /MWh _{in}	[269]
Lifetime	25		y	
GWP100 _{a_{C,E}} ^b	4.016e4	3.581e4	kgCO ₂ -eq./MW _{in}	
Impact2002 _{+_{C,E}} ^b	16.96	15.12	pts/MW _{in}	
ES2013 _{_{C,E}} ^b	3.353e7	2.990e7	UBP/MW _{in}	
GWP100 _{a_O} ^c	6.940e-1		kgCO ₂ -eq./MWh _{db,in}	
Impact2002 _{+_O} ^c	1.495e-3		pts/MWh _{db,in}	
ES2013 _{_O} ^c	4.806e3		UBP/MWh _{db,in}	

^a Linear regression of cost data in [269], where they are obtained for a 200-400 MW_{in} production plant.

^b Emissions associated to technology construction and end-of-life. Due to lack of data for a full LCA, emissions are assumed equal to the gasification to SNG process.

^c Emissions associated to technology operation, excluding combustion for GWP (allocated to the resource). Due to lack of data for a full LCA, emissions are assumed equal to the gasification to SNG process.

In both cases cost data is obtained by a linear regression of the costs of plants between 15 and 45 MW input of biomass (on a LHV_{db}). It should be underlined that these processes are very small compared to similar processes reported in the literature, generally ranging between 200 and 400 MW_{in} and also reaching over 1000 MW_{in} to benefit from economies of scale [282]. The small capacity is considered here according to the biomass availability for the city of Lausanne to study the interest of the implementation of a reduced size facility, if such an option will be feasible in the future. As for the technologies presented in the previous sections, the data is normalized to a biomass input of 1 MW (LHV_{wb}). The comparison of the two processes shows that the “FT dry” process using biomass at $\Phi = 15\%$, with the same input of 1000 kW (LHV_{wb}) as the “FT wet” process (using $\Phi = 50\%$ biomass), is actually processing less biomass in terms of mass on a *db*. This is the reason why the

Appendix D. Urban energy modeling - data

conversion to the FT fuel, on an *wb* energy basis, is smaller. The conversion on a *db* is the same. In the case of the “FT dry” process, the lower electricity requirement is due to the removal of the dryer unit.

Synthetic Natural Gas production from biomass gasification

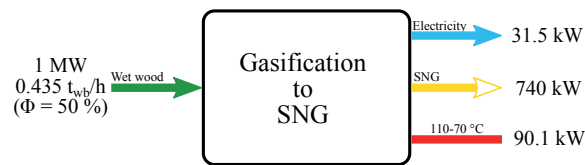


Figure D.7 – Gasification to SNG unit model.

The model of SNG production from woody biomass gasification (Figure D.7) is adapted from [235]. In this process, biomass is dried and gasified to produce syngas, a gas mixture mostly made of hydrogen (H₂), carbon monoxide (CO), carbon dioxide (CO₂), and methane (CH₄). The syngas is cooled and cleaned of tars and other contaminants. This gas is then compressed and catalytically reacted in a methanation reactor to produce a gas mixture composed primarily of methane and carbon dioxide. Finally, the gas is purified and the carbon dioxide removed, in order to produce SNG that matches the requirements for injection into the natural gas (NG) network. Thus, in the model it is assumed that the produced SNG fuel has the same properties as fossil NG.

In [235] data for two SNG production plants are reported. The size of these installations is 40.5 MW_{in} (“Gazobois” project) and 135 MW_{in} (input biomass at Φ = 50%), respectively. Mass and energy balances are taken from these installations. The temperature level of the excess useful heat is assumed to be high enough to partially supply the city’s DHN. Investment cost data are extrapolated from with data for a 20MW_{in} size with an exponential relation. Cost and emissions data are reported in Table D.8.

Table D.8 – Gasification to SNG parameters

	Value	Units	References
Reference size	20	MW _{in}	
C _{inv,fix}	-	CHF ₂₀₁₅	
C _{inv,var} ^a	2.168e6	CHF ₂₀₁₅ /MW _{in}	[235]
C _{op,fix}	-	CHF ₂₀₁₅ /h	
C _{op,var} ^b	12.62	CHF ₂₀₁₅ /MWh _{in}	[235]
Lifetime	25	y	
GWP100a _{C,E} ^c	4.016e4	kgCO ₂ -eq./MW _{in}	
Impact2002 _{+C,E} ^c	16.96	pts/MW _{in}	
ES2013 _{C,E} ^c	3.353e7	UBP/MW _{in}	
GWP100a _O ^d	6.940e-1	kgCO ₂ -eq./MWh _{db,in}	[246]
Impact2002 _{+O} ^d	1.495e-3	pts/MWh _{db,in}	[246]
ES2013 _O ^d	4.806e3	UBP/MWh _{db,in}	[246]

^a Exponential extrapolation of cost data in [235].

^b O&M are 5.1% of the total investment cost per year, over 8760 h.

^c Emissions associated to technology construction and end-of-life. Due to lack of data for a full LCA, assuming sum of emissions of a dryer unit, a pyrolysis unit for pre-treatment, and a gasifier. Multiplied by a factor 2 to account for emissions of other parts of equipment (cleaning, methanation, purification).

^d Emissions associated to technology operation, excluding combustion for GWP (allocated to the resource). Calculated using the impact of gasification, plus adding the operation impacts of gas cleaning, methanation and purification (RME, catalysts (ZnO, Ni, Al₂O₃), limestone and gypsum) as in [246].

D.3.4 Geothermal resources and technologies

Geothermal resources

The City of Lausanne does not present particularly favorable geological characteristics in terms of geothermal resources (Figure D.8). The geothermal gradient in the area is 0.03 °C/m [283]. In this work, deep aquifers and EGSs are considered. For aquifers, the Muschelkalk aquifer (3.8 km depth, [284] is considered). The Malm aquifer (2 km depth) is not included in this case study as its temperature level is too low in comparison to the temperature of the city's DHN. For EGS three different depths are considered: 4.2 km (upper limit of the crystalline *stratum*), 5 km and 6 km. Table D.10 characterizes the considered resources at different depths in terms of total heat extracted, pumping power, water expected mass flow rate, well temperature (T_{well}), total investment cost (including stimulation, exploration, fluid distribution and drilling), and cost for O&M. Technical parameters for the wells are average values over the lifetime calculated with the software environment GEOPHIRES [112], unless otherwise specified. The same software environment is also used for cost data estimation. The lifetime of the wells is assumed to be 30 years, the reinjection temperature is 70 °C, the pump efficiency is 80% and the capacity factor is 90%. It is assumed that 2 wells are needed for an aquifer and 3 wells are needed for an EGS.

Emissions related to drilling and operation of the wells are calculated in the post-computation phase according to the LCA methodology presented in [246] (Table D.9).

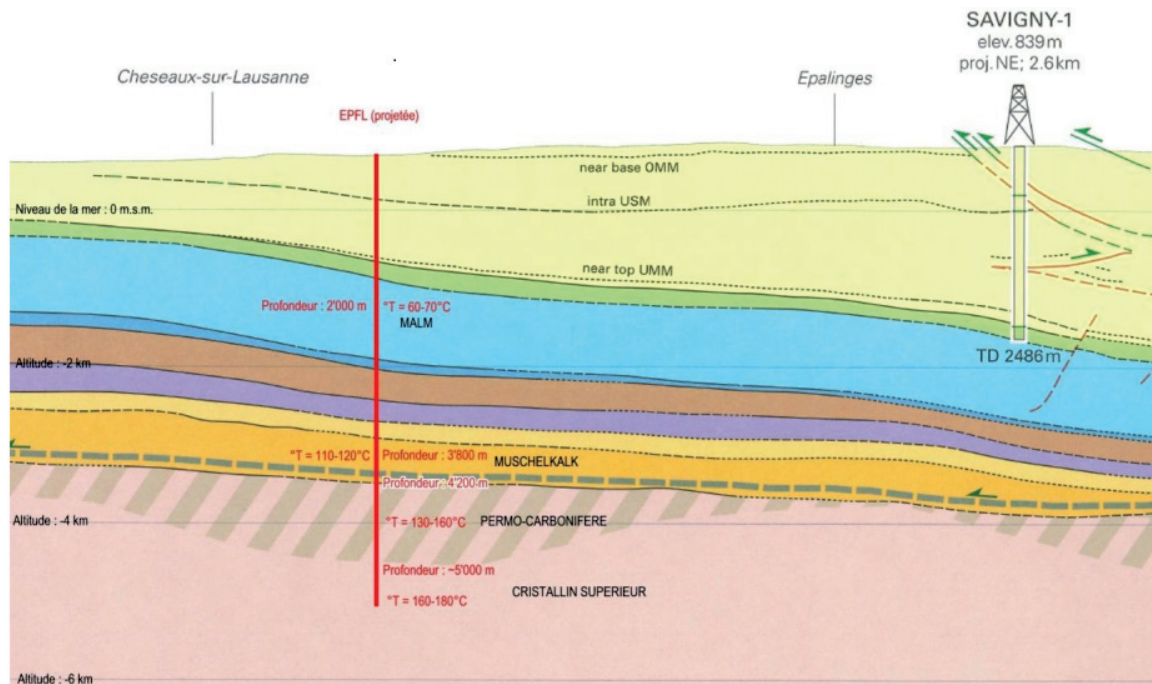


Figure D.8 – Geological profile of the city of Lausanne [283].

Table D.9 – Geothermal resources and energy conversion cycles emission parameters, calculated based on the LCA methodology presented in [246].

	LCA (C,E) ^a			LCA (O) ^b		
	GWP100a [kgCO ₂ -eq./u]	Impact2002+ [pts/u]	ES2013 [UBP/u]	GWP100a [kgCO ₂ -eq./h]	Impact2002+ [pts/h]	ES2013 [UBP/h]
Resources						
Aquifer 3.8 km	2.003e6	5.781e2	1.187e9	2.304e-4	9.657e-8	1.860e-1
EGS 4.2 km	6.069e6	1.760e3	3.650e9	1.184e1	3.440e-3	7.421e3
EGS 5 km	6.875e6	1.993e3	4.131e9	1.210e1	3.419e-3	7.381e3
EGS 6 km	7.871e6	2.279e3	4.724e9	1.166e1	3.366e-3	7.278e3
Cycles						
ORC 3.8 km	1.205e5	2.499e1	5.141e7	1.510	1.553e-4	3.222e2
ORC 4.2 km	4.773e5	6.905e1	1.383e8	9.027	4.126e-4	8.463e2
ORC 5 km	6.184e5	8.592e1	1.713e8	1.210e1	5.105e-4	1.044e3
ORC 6 km	8.711e5	1.275e2	2.520e8	1.704e1	7.603e-4	1.538e3
Kalina 6 km	2.944e5	7.904e1	1.653e8	1.862	4.999e-4	1.042e3

^a Emissions related to construction and end-of-life of one unit (u). For resources a unit is a well, for cycles it is one cycle.

^b Operating impact per one unit, over 7884 h (90% capacity factor).

Table D.10 – Geothermal resources parameters.

	Heat ^a [kW _{th}]	Pumping [kW _e]	Flow rate [kg/s]	T _{well} [°C]	C _{inv,fix} [CHF ₂₀₁₅ /u]	C _{op,var} [CHF ₂₀₁₅ /h] ^b
Aquifer 3.8 km	2544	3.50 [112]	13.5 [283]	115 [283]	2.143e7 [112]	4.964e1 [112]
EGS 4.2 km	23029	1231 [112]	100 [266]	125 [112]	3.731e7 [112]	1.756e2 [112]
EGS 5 km	31403	1180 [112]	100 [266]	145 [112]	4.836e7 [112]	2.287e2 [112]
EGS 6 km	41870	1053 [112]	100 [266]	170 [112]	6.370e7 [112]	3.001e2 [112]

^a Calculated based on T_{well} and reinjection temperature of 70 °C.

^b O&M cost per one well, over 7884 h (90% capacity factor).

Energy conversion cycles

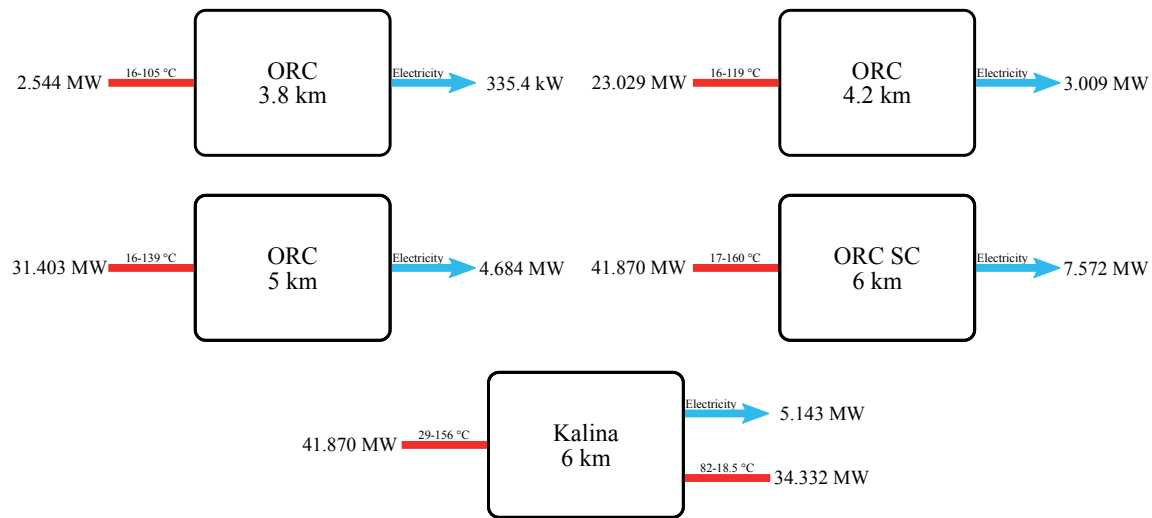


Figure D.9 – Simplified input-output representation of the geothermal ORC and Kalina cycles models.

The energy conversion cycles associated with the geothermal resources (Figure D.9) are taken from the optimal configurations presented in [266]. For electricity production, Organic Rankine cycles (ORCs) are considered for the resources shallower than 5 km with a single-loop configuration, while a supercritical (SC) cycle is chosen for the 6 km EGS. The high temperature of the city’s DHN makes cogeneration with geothermal resources an unoptimal solution. For this reason, only a Kalina cogeneration cycle at 6 km is chosen, being the only one with temperature levels able to partially satisfy the network demand. ORCs use R134a as working fluid, whereas Kalina cycles use a H₂O/NH₃ mixture. The cycles are originally modeled with the flowsheeting software Belsim VALI™ and optimized for each individual geothermal resource. The thermal streams corresponding to the optimal configurations are included in the MILP model. Figure D.9 offers a simplified input-output representation of the cycles, taking into account only the net heat requirement/surplus for the thermal streams. To calculate the efficiency, the power available from the corresponding geothermal resources is taken as input. ORCs are not used in cogeneration, so the excess low-temperature heat is rejected to the environment. For the Kalina cycle, the thermal production shown in the figure corresponds to the condensation stream.

Investment costs are calculated based on a recent report for Switzerland [102], indicating a reference investment cost of 3000 USD₂₀₁₀/kW_e (2891 CHF₂₀₁₅/kW_e) for a 13 MW_e ORC installation. The investment cost has been scaled for the different cycles in this work using an exponential relation with an exponent of 0.9, as indicated in the report. In the lack of better data, the same scaling has been applied also for the Kalina cycle. Due to the lower electrical efficiency of the latter, this leads to

higher specific investment cost for this cycle, as reported in [102]. The report indicates a lifetime of 30 years for the cycles. O&M costs are conservatively assumed to be 5% of the total investment cost per year, based on [285][106][112]. Emissions related to drilling and operation of the wells are calculated in the post-computation phase according to the LCA methodology presented in [246] (Table D.9).

D.3.5 Boilers

Centralized and decentralized NG boilers

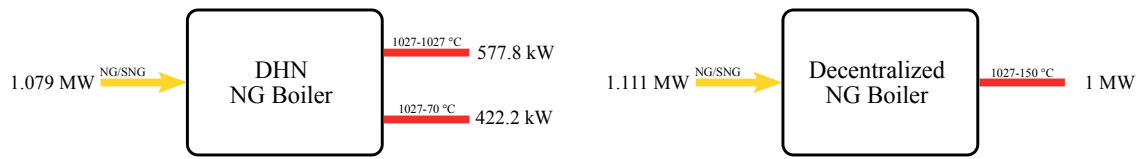


Figure D.10 – Centralized and decentralized NG boiler unit models.

Table D.11 – NG-SNG DHN and decentralized boilers parameters

	Value		Units	References
	DHN	Decentralized		
Reference size	5-20	0.01-0.03	MW _{th}	
$C_{inv,fix}$		-	CHF ₂₀₁₅	
$C_{inv,var}^a$	6.289e4	1.693e5	CHF ₂₀₁₅ /MW _{th}	[111]
$C_{op,fix}$		-	CHF ₂₀₁₅ /h	
$C_{op,var}^b$	3.145e-1	1.270	CHF ₂₀₁₅ /MWh _{th}	[111]
Lifetime	25	20	y	
GWP100 _{a,C,E}	2.590e3 ^c	2.109e4 ^d	kgCO ₂ -eq./MW _{th}	
Impact2002 _{+C,E}	8.401e-1 ^c	6.625 ^d	pts/MW _{th}	
ES2013 _{C,E}	1.884e6 ^c	1.285e7 ^d	UBP/MW _{th}	
GWP100 _{a,O} ^e		-	kgCO ₂ -eq./MWh _{in}	
Impact2002 _{+O} ^e		7.060e-4	pts/MWh _{in}	
ES2013 _O ^e		1.835e3	UBP/MWh _{in}	

^a Based on logarithmic regression on cost data in the range 0.02-10 MW_{th}.

^b For DHN O&M are 2% of investment cost, for decentralized 3% of investment cost. 4000 h/y of operation.

^c Assumed equal to DHN wood boiler (Table D.13).

^d Assumed equal to decentralized oil boiler (Table D.12).

^e Operation impacts for a decentralized NG boiler.

Appendix D. Urban energy modeling - data

These boiler unit models (Figure D.10) can have both fossil NG and SNG as inputs, which are assumed to have the same performance in terms of efficiency and the same emissions (GWP combustion emissions are allocated to the resources). The boilers electricity consumption is neglected. The DHN boiler is modeled in Belsim VALITM. The ideal efficiency on a LHV basis is 97.6% and 5% losses are assumed. The fumes reach an output temperature of 70 °C, and a distinction is made between the radiative and convective component of the heat production. For the decentralized boiler an overall efficiency of 90% is assumed. In the model, the share of decentralized NG boilers is fixed in order to supply 60% of the decentralized heat demand. Cost data are taken from [111] by logarithmic regression in the range 0.02-10 MW_{th}. Cost and emission data are reported in Table D.11.

Centralized and decentralized Oil-BioOil boilers

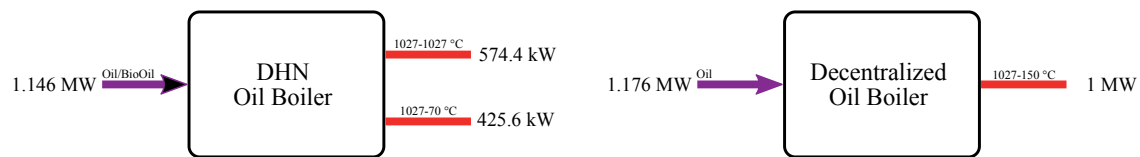


Figure D.11 – Centralized and decentralized Oil-BioOil boiler unit models.

The DHN boiler can have both fossil LFO and BioOil as inputs, which are assumed to have the same performance in terms of efficiency. The DHN boiler is modeled in Belsim VALITM. The ideal efficiency on a LHV basis is 96.95% for BioOil assuming the composition as in Section D.3.3, and 10% losses are assumed. The fumes reach an output temperature of 70 °C, and a distinction is made between the radiative and convective component of the heat production. The decentralized boiler model has only fossil oil as input. For the decentralized boiler an overall efficiency of 85% is assumed. The boilers electricity consumption is neglected. Cost data are assumed equal to the NG boilers (Table D.11). Human health operating emissions are different for fossil oil and BioOil combustion. For the latter, human health emissions are considered as an average between LFO and HFO (based on the same input energy basis). This simplifying assumption is based on the study by Lehto et al. [268]. Cost and emission data are reported in Table D.12.

Table D.12 – Oil and decentralized boilers parameters

	Value			Units	References
	DHN LFO	BioOil	Decentralized		
Reference size	5-20		0.01-0.03	MW _{th}	
$c_{inv,fix}$	-		-	CHF ₂₀₁₅	
$c_{inv,var}^a$	6.289e4		1.693e5	CHF ₂₀₁₅ /MW _{th}	[111]
$c_{op,fix}$	-		-	CHF ₂₀₁₅ /h	
$c_{op,var}^a$	3.145e-1		1.270	CHF ₂₀₁₅ /MWh _{th}	[111]
Lifetime	25		20	y	
GWP100a _{C,E}	2.590e3 ^b		2.109e4 ^c	kgCO ₂ -eq./MW _{th}	
Impact2002+ _{C,E}	8.401e-1 ^b		6.625 ^c	pts/MW _{th}	
ES2013 _{C,E}	1.884e6 ^b		1.285e7 ^c	UBP/MW _{th}	
GWP100a _O	-		-	kgCO ₂ -eq./MWh _{in}	
Impact2002+ _O	3.070e-3 ^d	1.298e-2 ^e	3.592e-3 ^f	pts/MWh _{in}	
ES2013 _O	8.262e3 ^d	3.096e4 ^e	9.196e3 ^f	UBP/MWh _{in}	

^a Assumed equal to NG boilers (Table D.11).

^b Assumed equal to DHN wood boiler (Table D.13).

^c Linear regression between impact data in the range 10-100 kW_{th} from [168].

^d Operation impact data for a 100 kW_{th} LFO boiler.

^e Average impact between 100 kW_{th} LFO and 1 MW_{th} HFO boilers from [168]. Simplifying assumption based on [268].

^f Operation impact data for a 10 kW_{th} LFO boiler.

Centralized wet and dry wood boilers

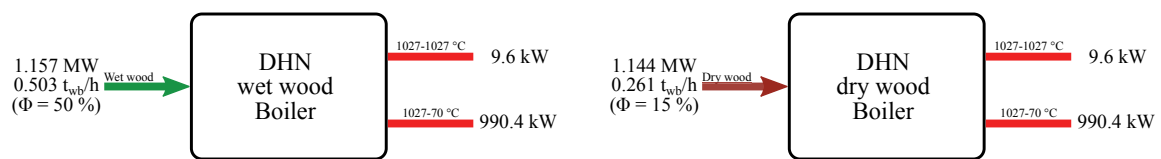


Figure D.12 – Centralized wet and dry wood boiler unit models.

The DHN wood boiler (Figure D.12) is modeled to be powered with either wet wood ($\Phi = 50\%$) or dry wood ($\Phi = 15\%$). The model, realized with the flowsheeting software Belsim VALITM, is used in order to calculate the variation of efficiency between the combustion of wet wood and dry wood, considering a stack temperature of 70 °C. Losses are considered as 10% of the heat output and the boilers electricity consumption is neglected. A distinction is made between the radiative and

Appendix D. Urban energy modeling - data

convective components of the heat production. The ideal efficiency on a LHV *wb* is 96.05% in the case of wet wood, and 97.11% in the case of dry wood. Cost data are taken from [111] by logarithmic regression on cost data in the range 0.02-20 MW_{th}. Operating emission data are taken from [168] for a state-of-the-art 1 MW_{th} boiler burning wood chips at $\Phi = 44.4\%$. Due to lack of emission data allowing to differentiate between wet and dry wood combustion, the same values on a *db* are assumed for the two cases. Cost and emission data are reported in Table D.13.

Table D.13 – Centralized wet and dry wood boilers parameters

	Value	Units	References
Reference size	5-20	MW _{th}	
$c_{inv,fix}$	-	CHF ₂₀₁₅	
$c_{inv,var}^a$	1.230e5	CHF ₂₀₁₅ /MW _{th}	[111]
$c_{op,fix}$	-	CHF ₂₀₁₅ /h	
$c_{op,var}^b$	6.150e-1	CHF ₂₀₁₅ /MWh _{th}	[111]
Lifetime	25	y	
GWP100 _{a_{C,E}} ^c	2.590e3	kgCO ₂ -eq./MW _{th}	
Impact2002 _{+_{C,E}} ^c	8.401e-1	pts/MW _{th}	
ES2013 _{C,E} ^c	1.884e6	UBP/MW _{th}	
GWP100 _{a_O}	-	kgCO ₂ -eq./MWh _{db,in}	
Impact2002 _{+_O}	1.615e-2	pts/MWh _{db,in}	
ES2013 _O	1.848e4	UBP/MWh _{db,in}	

^a Based on logarithmic regression on cost data in the range 0.02-20 MW_{th}.

^b O&M are 2% of investment cost over 4000 h/y of operation.

^c Based on data for 300 kW_{th} and 1 MW_{th} wood chips boilers. Extrapolated by exponential regression.

D.3.6 Electricity production & Cogeneration (CHP)

Hydroelectricity

In 2012, hydroelectricity supplied 79.9% of the total urban system electricity demand. The largest share of electricity production comes from the run-of-river power plant located in Lavey. It currently consists of three Kaplan turbines, each with a plate capacity of 31 MW_e, producing about 400 GWh_e/y. By 2035, a new unit will be installed and an increase of 75 GWh_e/y in production is expected. The power plant is modeled by Amblard [258] based on the information available in [286], estimating as well the seasonal variations. In the model it is assumed that hydroelectricity has priority over the other technologies, therefore the average production is fixed in each period to the values reported in Table D.14. Cost and emission data are reported in Table D.15.

Table D.14 – Fixed hydroelectricity power production in each period.

Period	Hydroelectricity production [MW _e]
Summer	56.82
Winter	45.85
Mid-season	75.33
Peak	124.0 ^a

^a Assuming that the new turbine has as well a 31 MW_e plate capacity.

Table D.15 – Hydroelectricity parameters

	Value	Units	References
C _{inv,fix}	-	CHF ₂₀₁₅	
C _{inv,var}	5.351e6	CHF ₂₀₁₅ /MW _e	[181]
C _{op,fix}	-	CHF ₂₀₁₅ /h	
C _{op,var} ^a	6.108	CHF ₂₀₁₅ /MWh _e	[181]
Lifetime	40	y	[181]
GWP100a ^b	4.699	kgCO ₂ -eq./MWh _e	
Impact2002+ ^b	1.070e-3	pts/MWh _e	
ES2013 ^b	3.486e3	UBP/MWh _e	

^a O&M assumed as 1% of c_{inv} based on [181], over 8760 h.

^b Emissions for construction, operation and end-of-life.

Natural Gas CHP

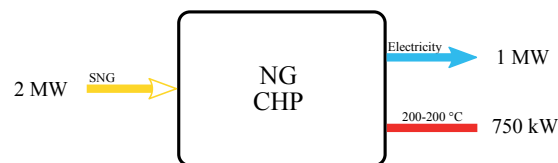


Figure D.13 – Natural gas CHP unit model.

The CHP unit (Figure D.13) in the model has SNG as an input, which is assumed equivalent to fossil NG. It is modeled as a CCGT, a cycle configuration combining a gas turbine with a bottoming steam cycle to achieve high electrical efficiencies. Efficiency data are taken from [192] for a typical 200-250 MW_e installation in 2035. As a simplification, the output temperature level is chosen high enough

Appendix D. Urban energy modeling - data

to satisfy the heat demand in the model. As CCGT plants in Switzerland are smaller (34-55 MW_e), cost data are taken from [287] for typical installations in Switzerland. Cost and emission data are reported in Table D.16.

Table D.16 – Natural Gas CHP parameters.

	Value	Units	References
Reference size	34-55	MW _e	[287]
c _{inv,fix}	-	CHF ₂₀₁₅	
c _{inv,var}	1.453e6	CHF ₂₀₁₅ /MW _e	[287]
c _{op,fix}	-	CHF ₂₀₁₅ /h	
c _{op,var}	9.684	CHF ₂₀₁₅ /MWh _e	[287]
Lifetime	25	y	[192]
GWP100a _{C,E}	3.927e5	kgCO ₂ -eq./MW _e	
Impact2002 _{C,E}	79.69	pts/MW _e	
ES2013 _{C,E}	1.519e8	UBP/MW _e	
GWP100a _O	-	kgCO ₂ -eq./MWh _{in}	
Impact2002 _O	3.570e-3	pts/MWh _{in}	
ES2013 _O	1.129e4	UBP/MWh _{in}	

Oil and BioOil CHP

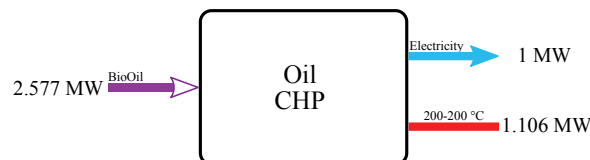


Figure D.14 – BioOil CHP unit model.

The CHP unit in the model has BioOil as an input (Figure D.14). For comparison, also the fossil oil option is reported here. LFO and BioOil are assumed to have the same performance in terms of efficiency. Due to lack of specific data for the technology, efficiency data are taken for a typical 200 kW_e diesel CHP engine [168]. As a simplification, the output temperature level is chosen high enough to satisfy the heat demand in the model. Cost data are taken from [192] for a 2 MW_e NG CHP with the same electrical efficiency as the diesel reference model. Coherently with what written in Section D.3.3, different human health emissions are considered for combustion of fossil LFO and

BioOil, due to the higher emissions of the latter. Cost and emission data are reported in Table D.17.

Table D.17 – Oil-BioOil CHP parameters

	Value		Units	References
	LFO	BioOil		
Reference size	0.2-2		MW _e	
C _{inv,fix}	-		CHF ₂₀₁₅	
C _{inv,var} ^a	1.107e6		CHF ₂₀₁₅ /MW _e	[192]
C _{op,fix}	-		CHF ₂₀₁₅ /h	
C _{op,var} ^a	11.55 ^b		CHF ₂₀₁₅ /MWh _e	[192]
Lifetime	20		y	[192]
GWP100a _{C,E} ^c	8.319e5		kgCO ₂ -eq./MW _e	
Impact2002+ _{C,E} ^c	1.780e2		pts/MW _e	
ES2013 _{C,E} ^c	3.530e8		UBP/MW _e	
GWP100a _O	-	-	kgCO ₂ -eq./MWh _{in}	
Impact2002+ _O	6.619e-3 ^c	1.298e-2 ^d	pts/MWh _{in}	
ES2013 _O	2.026e4 ^c	3.096e4 ^d	UBP/MWh _{in}	

^a Data for a 2 MW_e NG CHP.

^b Assuming 4000 h/y of operation.

^c Due to lack of technology-specific data, calculated based on data for 200 kW_e diesel CHP engine in [168].

^d Due to lack of LCA data for BioOil combustion, operation assumed equal to combustion in boiler (Table D.12).

Wet and dry wood CHP

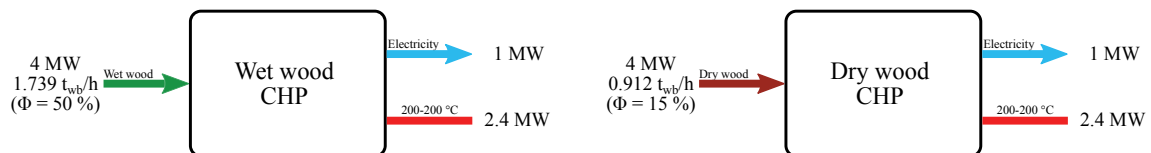


Figure D.15 – Wet and dry wood CHP unit model.

The wood CHP unit (Figure D.15) in the model can have wet ($\Phi = 50\%$) and dry ($\Phi = 15\%$) wood as inputs. The same performance in terms of *wb* efficiency is assumed in the two cases. As a simplification, the output temperature level is chosen high enough to satisfy the heat demand in the model. Efficiency and cost data are taken from [111] for a 5 MW_{th} (2.08 MW_e) biomass CHP-ORC system. Emission data are taken from [168] for a state-of-the-art 6.67 MW_{in} CHP burning wet wood ($\Phi = 52\%$). Due to lack of emission data allowing to differentiate between wet and dry wood

Appendix D. Urban energy modeling - data

combustion, the same values on a *db* are assumed for the two cases. Cost and emission data are reported in Table D.18.

Table D.18 – Wet and dry wood CHP parameters

	Value	Units	References
Reference size	2.08	MW _e	[111]
$c_{inv,fix}$	-	CHF ₂₀₁₅	
$c_{inv,var}$	4.651e6	CHF ₂₀₁₅ /MW _e	[111]
$c_{op,fix}$	-	CHF ₂₀₁₅ /h	
$c_{op,var}^a$	46.51	CHF ₂₀₁₅ /MWh _e	[111]
Lifetime	25	y	
GWP100 _{a_{C,E}}	4.868e5	kgCO ₂ -eq./MW _e	
Impact2002 _{+_{C,E}}	1.014e2	pts/MW _e	
ES2013 _{_{C,E}}	2.084e8	UBP/MW _e	
GWP100 _{a_O}	-	kgCO ₂ -eq./MWh _{db,in}	
Impact2002 _{+_O}	1.615e-2	pts/MWh _{db,in}	
ES2013 _{_O}	1.848e4	UBP/MWh _{db,in}	

^a O&M costs are 4% of the investment cost over 4000 h/y of operation.

D.3.7 Storage

The modeling of storage is detailed Section C.1.2. Storage units can have multiple inputs and outputs. This is also exploited in the case study to force scenarios. No LCA analysis is performed for the storage units.

SNG storage

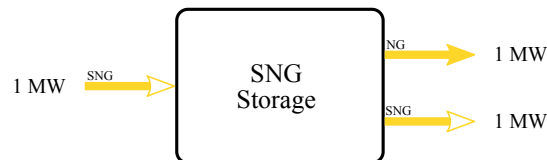


Figure D.16 – SNG storage unit model.

The SNG storage unit is used in the model to force the replacement of NG with SNG. In the model, in

fact, it is assumed that SNG is equivalent to fossil NG. Thus, it can be injected into the NG grid. No cost is associated to this storage unit, as it is assumed that the produced SNG can replace imports of fossil NG in Switzerland all-year-round using the existing grid infrastructure.

As shown in Figure D.16, the unit has an input (SNG layer) and two outputs (SNG and NG layers). This allows to force scenarios. On the one hand, when SNG replaces fossil NG in the model, only the NG output is activated. On the other hand, when SNG is used for CHP or mobility, only the SNG output is activated together with the corresponding cogeneration and mobility unit models.

Oil and BioOil storage

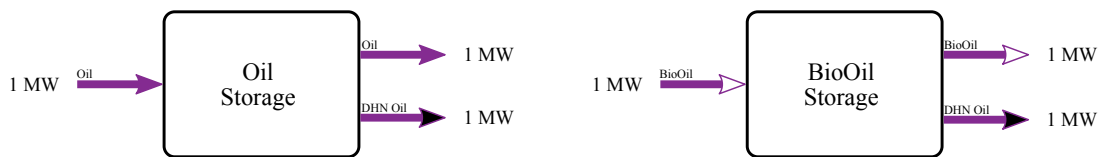


Figure D.17 – Oil and BioOil storage unit models.

In the model it is assumed that BioOil from fast pyrolysis can only be used in DHN technologies (boiler and CHP). Fossil oil can be used in DHN technologies and also for decentralized heat supply. As shown in Figure D.17, the BioOil storage unit has an input (BioOil layer) and two outputs (BioOil and DHN Oil layers). This allows to force scenarios. When the CHP oil unit is used in the system, the DHN oil output is deactivated in order to ensure that all the BioOil is consumed by the CHP unit. Cost data are taken from [288], who report an estimate from producers data for a 9375 m³ BioOil storage tank. The data are adapted for fossil oil storage accounting for the different physical properties of the two fuels. Cost data are summarized in Table D.19.

Table D.19 – Oil and BioOil storage tanks parameters

	Value		Units	References
	LFO	BioOil ^a		
Reference size	9.419e4	4.765e4	MWh _{fuel} ^b	
C _{inv,fix}	-	-	CHF ₂₀₁₅	
C _{inv,var}	1.204e1	2.380e1	CHF ₂₀₁₅ /MWh _{fuel}	[288]
C _{op,fix}	-	-	CHF ₂₀₁₅ /h	
C _{op,var} ^c	5.497e-5	1.087e-4	CHF ₂₀₁₅ /MWh _{fuel} /h	
Lifetime		50	y	

^a Assuming LHV = 15.247 MJ/kg (Section D.3.3) and density of 1200 kg/m³ as in [288].

^b Energy equivalent of the amount of fuel stored.

^c Assuming O&M as 4% of investment as for wood storage (Table D.20), over 8760 h.

Wood storage

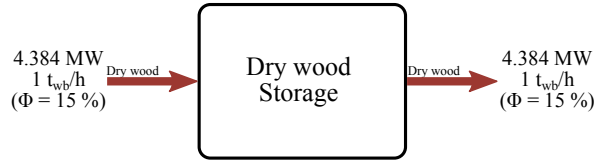


Figure D.18 – Dry wood storage unit model.

The dry biomass storage model (Figure D.18) is based on the “covered storage facility of a pole-frame structure having a metal roof without any infrastructure for biomass drying” presented in [289]. This storage has a maximum height of 6 m. [289] indicates that material losses are 0.5%/month. Thus, the output storage efficiency is set as $\eta(sto_{out}) = 99.5\%$. Cost data are summarized in Table D.20.

Table D.20 – Dry wood storage parameters

	Value ^a	Units	References
Reference size	-	MWh _{fuel} ^b	
c _{inv,fix}	-	CHF ₂₀₁₅	
c _{inv,var}	2.414e1	CHF ₂₀₁₅ /MWh _{fuel}	[289]
c _{op,fix}	-	CHF ₂₀₁₅ /h	
c _{op,var} ^c	1.102e-4	CHF ₂₀₁₅ /MWh _{fuel} /h	[289]
Lifetime	50	y	

^a Dry wood density is 235 kg/m³ for wood chips at Φ = 15% [271].

^b Energy equivalent of the amount of fuel stored.

^c O&M costs are 4% of investment over 8760 h.

D.3.8 Waste treatment and District Heating Network

Municipal Solid Waste Incinerator (MSWI)

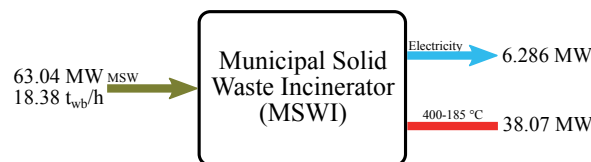


Figure D.19 – MSWI unit model.

A general description of the municipal solid waste incinerator (MSWI) of the city of Lausanne (“TRIDEL”) is offered in Section D.1.1. The MSWI is here represented in a simplified way based on the work by Amblard [258]. As of 2015, the power plant burns both municipal solid waste (MSW) and wet wood to produce steam, which is first expanded in a steam turbine down to 175 °C, and then used for DHN heat supply. In summer, the excess heat is expanded to ambient temperature in a second turbine.

In the model the winter operating mode is assumed for the whole year and no wet wood is burned in the plant. The winter efficiency is calculated based on 2012 data [270] and scaled in order to have only MSW as an input. The waste input is constant all over the year. In the model this is forced by setting the MSW resource as a process. The first principle efficiency is 74.98%, leading to a total heat production of 38.65 MW_{th} and a total electricity production of 8.61 MW_e. The share of thermal and electrical production for auto-consumption of the plant are 1.52% and 27%, respectively. Cost and emission data are reported in Table D.21.

Table D.21 – MSWI parameters

	Value	Units	References
Reference size	20/60	MW _e /MW _{th}	[270]
C _{inv,fix}	1.394e8/1.324e8 ^a	CHF ₂₀₁₅	[270]
C _{inv,var}	-	CHF ₂₀₁₅ /MW	
C _{op,fix}	-	CHF ₂₀₁₅ /h	
C _{op,var}	5.809 ^b	CHF ₂₀₁₅ /MWh	[270]
Lifetime	30/17.5 ^a	y	[270]
GWP100a _{C,E} ^c	1.838e7	kgCO ₂ -eq.	
Impact2002+ _{C,E} ^c	2.866e3	pts	
ES2013 _{C,E} ^c	6.939e9	UBP	
GWP100a _O ^d	-	kgCO ₂ -eq./MWh _{in}	
Impact2002+ _O	4.295e-3	pts/MWh _{in}	
ES2013 _O	4.810e3	UBP/MWh _{in}	

^a First value is for the power plant, second value for the electromechanical installation (turbines).

^b Includes O&M and salaries. Calculated over the total output, adding thermal and electrical production.

^c Total emissions for construction and end-of-life of a typical MSWI in Switzerland.

^d GWP impact related to the treatment of MSW in an incineration plant, including auxiliary emissions due to the operation of the plant, are attributed to the MSW resource (Table D.3).

Waste Water Treatment Plant (WWTP)

In the WWTP of Lausanne (“STEP”), the dry sludge obtained from the treatment of waste water is burned in a 4 MW_{th} boiler supplying heat to the DHN. Only the boiler is modeled in this work. NG

Appendix D. Urban energy modeling - data

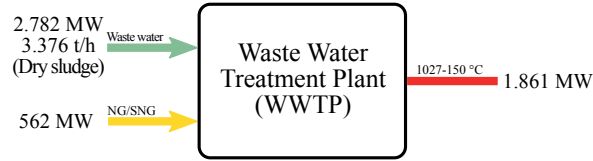


Figure D.20 – WWTP unit model.

Table D.22 – WWTP parameters

	Value	Units	References
Reference size	4	MW _{th}	[258]
$c_{inv,fix}$	$9.009e6^a$	CHF ₂₀₁₅	[291]
$c_{inv,var}$	-	CHF ₂₀₁₅ /MW _{th}	
$c_{op,fix}$	-	CHF ₂₀₁₅ /h	
$c_{op,var}$	$4.030e1$	CHF ₂₀₁₅ /MWh _{th}	Personal communication, SIL
Lifetime	25	y	
$GWP100a_{C,E}^b$	$5.947e7$	kgCO ₂ -eq.	
$Impact2002+_{C,E}^b$	$1.062e4$	pts	
$ES2013_{C,E}^b$	$2.374e10$	UBP	

^a Calculated based on the annual amortization value.

^b Total emissions for construction and end-of-life of a typical WWTP in Switzerland.

is also needed in the combustion process. The model represented in Figure D.20 is based on data for the power plant operation in 2012 [290]. In that year, the boiler processed 29.58 kt of dry sludge and delivered 16.3 GWh_{th} to the DHN as baseload. This is the net heat production, accounting for the share of heat needed for autoconsumption (4.95%). The global first principle efficiency was 58.6% and the capacity factor 84.7% (309 days of operation). In the work by Amblard [258] seasonal variations are accounted for in the WWTP model. As these variations are not significant, it is here assumed for simplicity that the power plant works with a constant input over the whole year. In the model this is forced by setting the waste water resource as a process. Operating emissions are not accounted for. Cost and emission data are reported in Table D.22.

District Heating Network (DHN)

The DHN unit in the model is used to transfer the heat produced by the centralized technologies to the heat demand units. The network is modeled based on the data available for Lausanne for the year 2012. In that year, the total length of the network was 101 km, delivering 364.7 GWh_{th}/y with 14.4% losses [258]. An increase of 3 km/y is assumed, leading to a total length of 170 km in 2035. As

detailed in Section D.1.2, it is projected that the share of heat demand supplied by the DHN in 2035 is 45%. The temperature of Lausanne's DHN is quite high (130-70 °C) and losses are fixed at 15% all-year-round. Emissions related to construction are based on the impact of needed materials (steel, foamed poliuretane, cement, concrete, diesel), which are taken from [292]. Operating emissions are not accounted for. Cost and emission data are reported in Table D.23.

Table D.23 – DHN parameters

	Value	Units	References
Reference size	170	km	[258]
$c_{inv,fix}$	5.100e8	CHF ₂₀₁₅	Personal communication, SiL
$c_{inv,var}$	-	CHF ₂₀₁₅ /MW	
$c_{op,fix}$	1.553e2 ^a	CHF ₂₀₁₅ /h	Personal communication, SiL
$c_{op,var}$	-	CHF ₂₀₁₅ /MWh	
Lifetime	50	y	Personal communication, SiL
GWP100 _{a_{C,E}} ^b	3.994e5	kgCO ₂ -eq.	[292]
Impact2002 _{+_{C,E}} ^b	5.448e1	pts	[292]
ES2013 _{_{C,E}} ^b	1.256e8	UBP	[292]

^a 8 CHF/m/y, over 8760 h.

^b Total emissions for the construction and end-of-life of the network, based on the needed materials (steel, foamed poliuretane, cement, concrete, diesel) from [292].

D.3.9 Mobility

This section covers the unit models for private and public mobility. The main difference with the other models is that the lifetime of the technologies is here expressed in terms of total covered distance. Thus, investment costs are annualized by fixing this parameter, without the need of assuming a lifetime in terms of time duration. Mobility demand is defined in Section D.3.2.

Private mobility

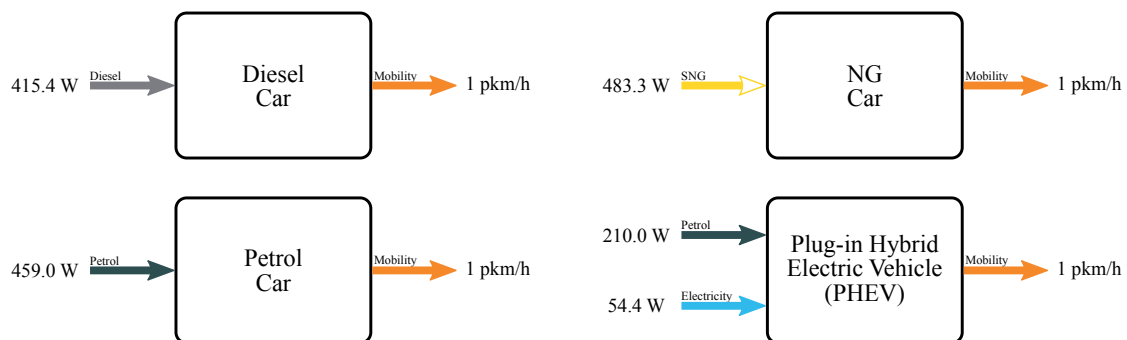


Figure D.21 – Private mobility unit models.

Figure D.21 shows the four types of vehicles modeled in this work: NG cars, diesel cars, petrol cars, PHEVs. The conversion efficiencies reported in the figure are taken for “EURO 5” vehicles from [168], with the exception of the PHEV, which is based on data for a typical 2015 vehicle from [293]. For the PHEV, in the model it is assumed that electricity is used to cover 40 % of the total distance and petrol to cover the remaining 60 %. If running only on electricity the PHEV consumes 135.9 Wh/pkm, whereas if running only on petrol the consumption is 349.9 Wh/pkm. The lifetime of all vehicles is 150000 km [294] and the average occupancy is 1.6 passenger/vehicle (data for the year 2010 in Switzerland, from [80]).

In the model it is assumed that 50% of the private mobility demand is supplied by PHEVs, with the remaining share being supplied by diesel cars. The NG car can have only SNG as an input, assuming the same performance in terms of efficiency, cost and emissions (for GWP emissions related to combustion are allocated to the resources). In the scenarios in which SNG is used in mobility, NG cars replace part of the diesel share.

Cost data are estimated from [295] for typical vehicles in Switzerland. The investment cost for a diesel car is 35000 CHF₂₀₁₅. The petrol car is assumed to be 5% cheaper, while the NG and PHEV car assumed to be 10% and 20% more expensive than the diesel car, respectively. O&M costs are 0.212 CHF₂₀₁₅/km for all vehicles. Emission data are summarized in Table D.25.

Public mobility

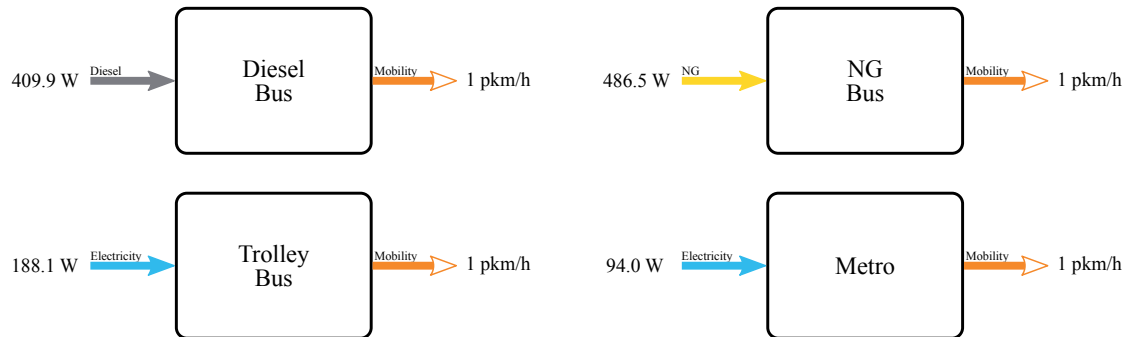


Figure D.22 – Public mobility unit models.

Figure D.22 shows the four means of public transport modeled in this work: NG buses, diesel buses, trolley buses (electric), metro. The conversion efficiencies reported in the figure are calculated from Amblard [258] based on the energy consumption of the Lausanne fleet in the year 2012 [296]. As there are no NG buses in Lausanne, the NG bus consumption is determined based on the diesel bus consumption multiplied by the ratio between the fuel economies of the correspondent private mobility models.

Data for cost, occupancy and lifetime are reported in Table D.24, together with the share of public pkm covered by each technology (fixed in the model). Emission data are summarized in Table D.25.

Table D.24 – Public mobility model parameters.

Technology	Share [%]	Occupancy [p/v]	$C_{inv,var}$ [CHF ₂₀₁₅ /v]	$C_{op,var}$ [CHF ₂₀₁₅ /km]	Lifetime [km]
Diesel Bus	5	16 [294]	5.250e5 [297]	6.057e-1 [297]	1.00e6 [294]
NG bus ^a	5	16 [294]	5.775e5	6.057e-1	1.00e6
Trolley bus	35	26 [294]	1.171e6 [297]	1.040 [297]	1.42e6 [294]
Metro	55	63 [258] ^b	4.758e6 [298]	1.040 ^c	1.12e6 [294] ^d

^a Due to lack of data for NG bus, investment cost assumed 10% higher than diesel bus. O&M costs and emissions assumed equal to diesel bus.

^b Based on 2012 data for Lausanne from [296].

^c Assumed equal to diesel bus. Does not include the cost for the needed infrastructure.

^d Data for a tram.

Table D.25 – Private and public mobility model emission parameters.

Technology	LCA (C,E) ^a			LCA (O)		
	GWP100a [kgCO ₂ -eq./v]	Impact2002+ [pts/v]	ES2013 [UBP/v]	GWP100a ^b [kgCO ₂ -eq./MWh _{in}]	Impact2002+ ^c [pts/MWh _{in}]	ES2013 ^c [UBP/MWh _{in}]
Private						
Diesel car ^d	1.157e4	2.842	4.978e6	3.254e1	3.361e-2	6.420e4
Petrol car ^d	1.146e4	2.794	4.919e6	2.955e1	1.934e-2	2.542e4
NG car ^d	1.146e4	2.794	4.919e6	3.183e1	1.811e-2	2.229e4
PHEV ^e	9.883e3	3.158	4.781e6	6.307e1	2.534e-2	6.207e4
Public						
Diesel Bus	3.993e4	9.426	1.832e7	3.990e1	5.977e-2	1.625e5
NG bus ^f	3.993e4	9.426	1.832e7	3.030e1	1.799e-2	2.214e4
Trolley bus	3.993e4	9.426	1.832e7	9.331e1	2.554e-2	6.329e4
Metro ^g	6.652e5	1.756e2	3.414e8	7.217e1	1.559e-2	4.166e4

^a Emissions related to construction and end-of-life of one vehicle (v).

^b Operating impact per MWh of input fuel, excluding fuel combustion and electricity consumption (allocated to resources).

^c Operating impact per MWh of input fuel, including fuel combustion, excluding electricity.

^d Construction emissions for a 1600 kg vehicle from [168].

^e Construction emissions for a 918 kg electric vehicle plus a 262 kg battery. Battery is replaced after 100000 km [168]. For the PHEV a 60% / 40% petrol/electricity share is assumed. Operating emissions in the table are per MWh_e (electricity only mode). For emissions when running on petrol, petrol car values are used.

^f As no data are available for NG buses emissions, construction emissions are assumed equal to Diesel bus. Operating impacts are calculated assuming same impact of NG cars (per pkm) and scaled according to the bus fuel economy.

^g Data for a regional passenger train in Switzerland [168]

D.4 Additional results

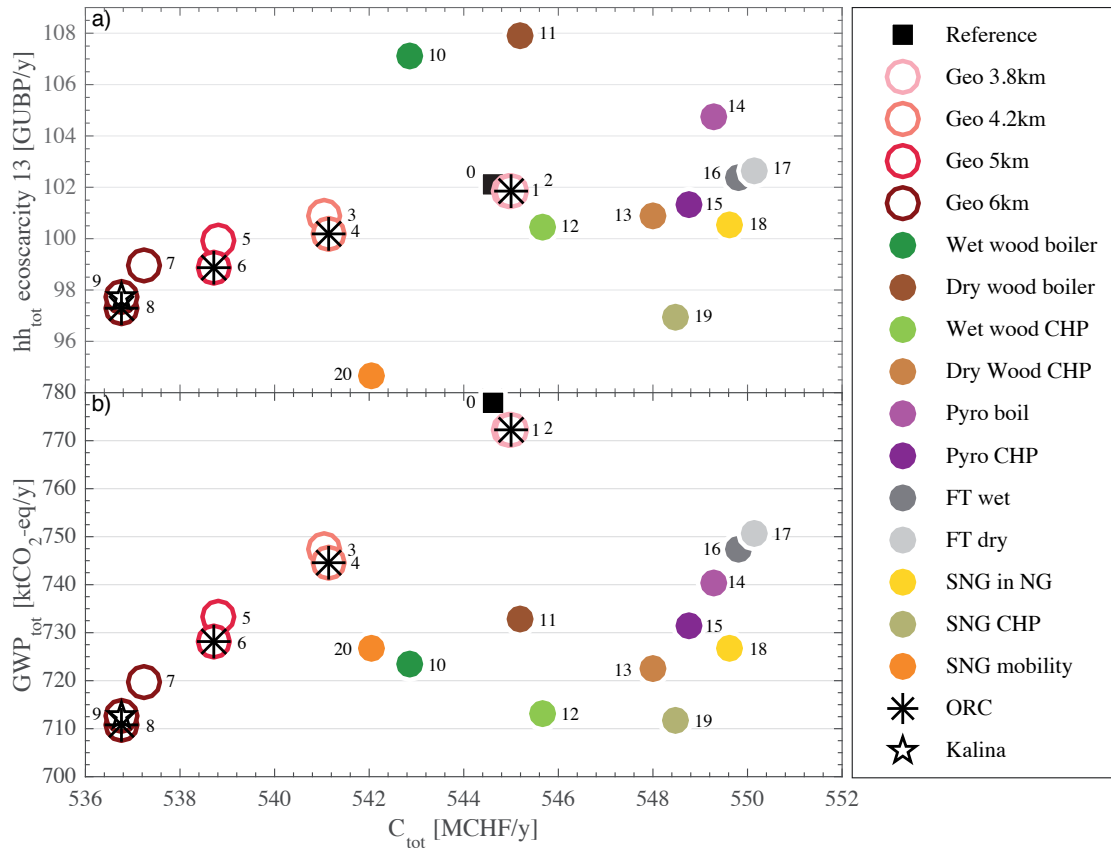


Figure D.23 – Results of the individual scenarios listed in Table C.1: individual assessment of geothermal and biomass options (1 GUPB = 1e9 UBP). The subplots depict hh_{tot} (a) and GWP_{tot} (b) against the total annual cost C_{tot} , respectively.

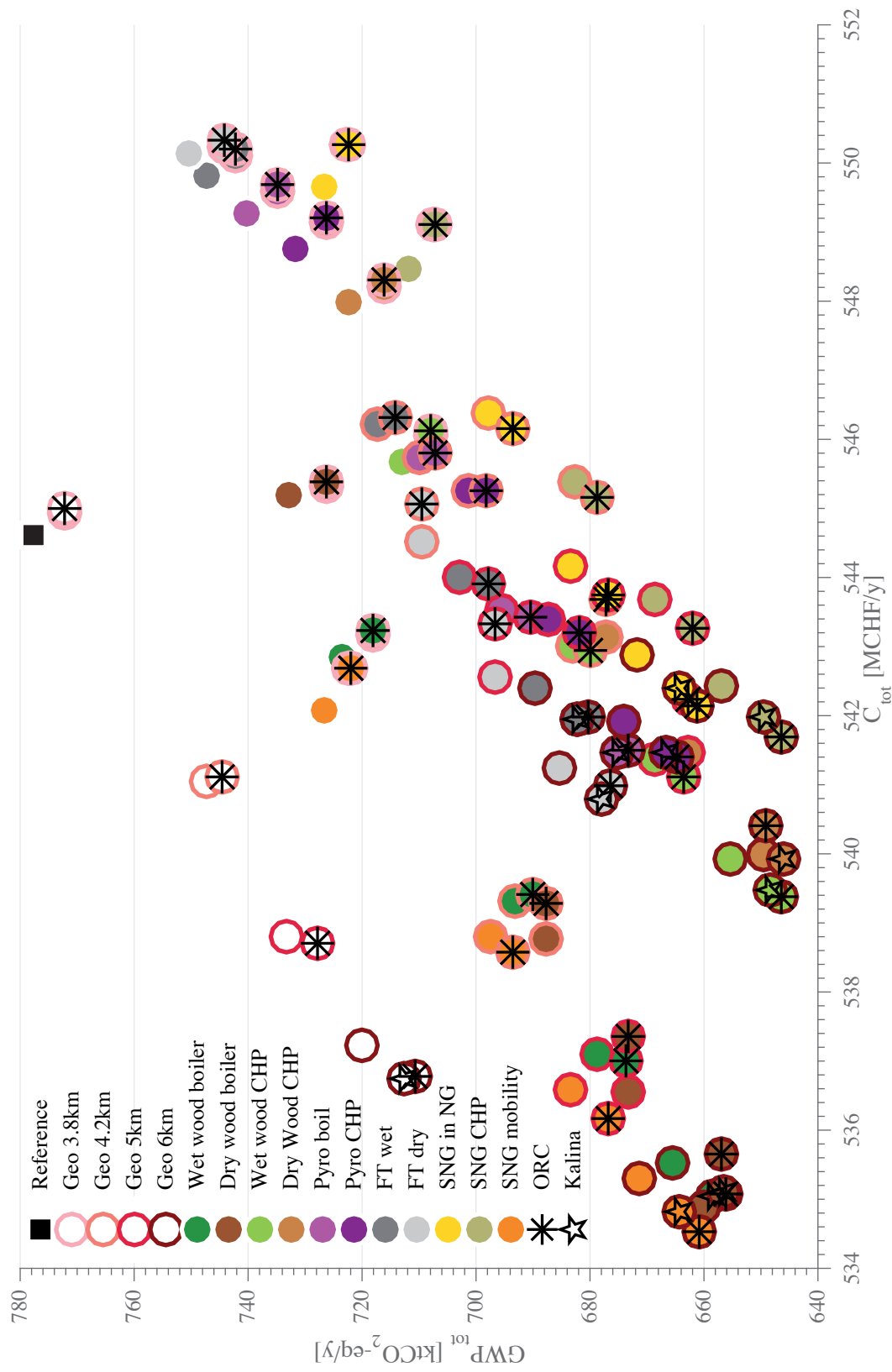


Figure D.24 – Results for all scenarios: Total annual cost vs GWP emissions.

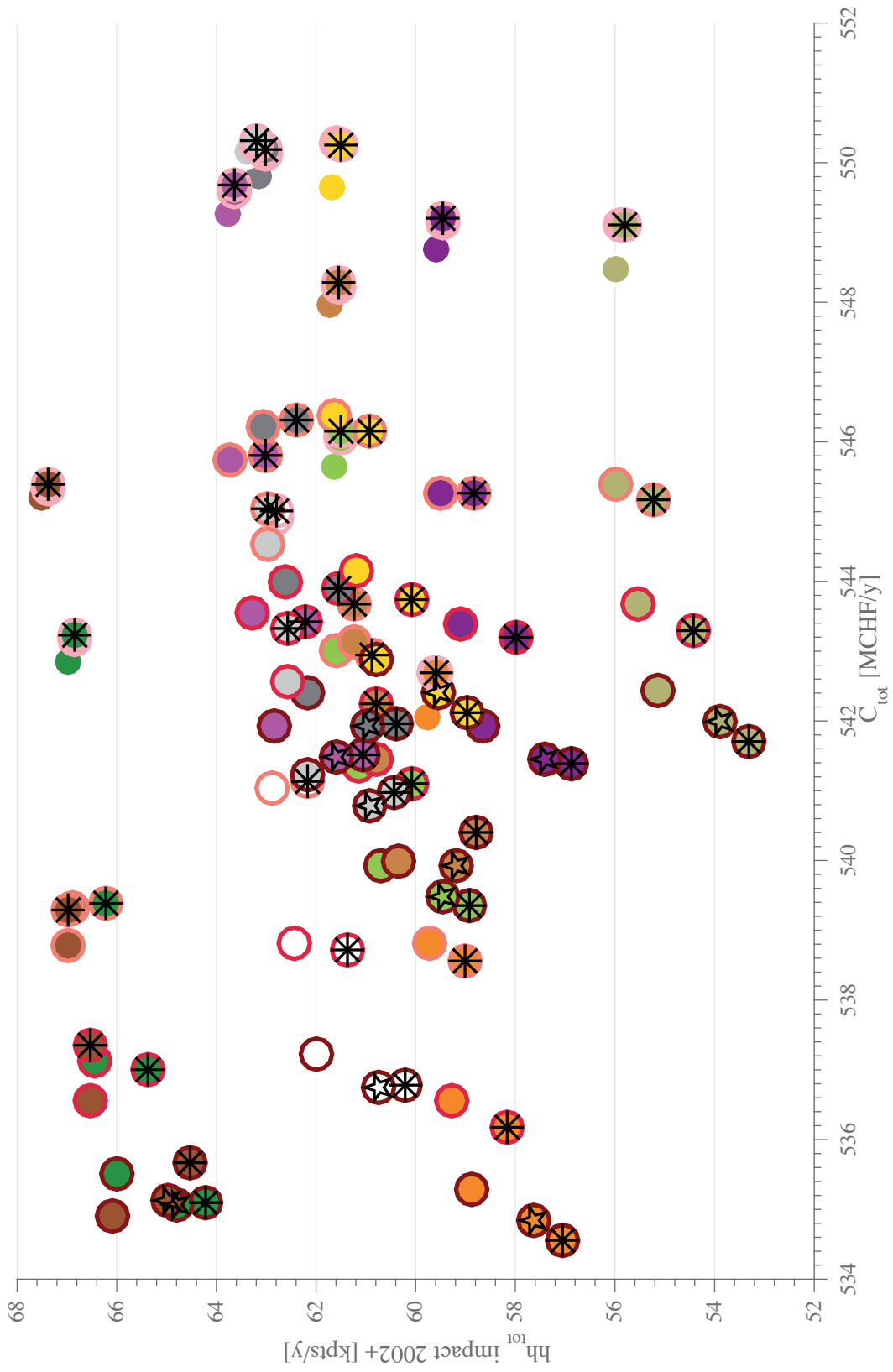


Figure D.25 – Results for all scenarios: Total annual cost vs human health emissions (for legend see Figure D.24).

Appendix D. Urban energy modeling - data

Table D.26 – δPI calculated for each performance indicator (Eq. C.19). Performance of each with respect to the reference (scenario 0).

#	Biomass	Geothermal	δC_{tot}	δGWP_{tot}	δhh_{tot}	δhh_{tot}
			[MCHF/y]	[ktCO ₂ -eq./y]	Imp2002+	ES2013
					[kpts/y]	[GUPB/y]
0	-	-	0	0	0	0
1	-	3.8 km Direct use	0.31	-5.38	-0.14	-0.32
2	-	3.8 km ORC	0.39	-5.38	-0.14	-0.32
3	-	4.2 km Direct use	-3.58	-30.4	-0.08	-1.29
4	-	4.2 km ORC	-3.50	-33.2	-0.76	-1.92
5	-	5 km Direct use	-5.80	-44.6	-0.52	-2.24
6	-	5 km ORC	-5.90	-49.8	-1.60	-3.27
7	-	6 km Direct use	-7.40	-57.8	-0.97	-3.15
8	-	6 km ORC	-7.83	-67.0	-2.75	-4.87
9	-	6 km Kalina	-7.86	-65.0	-2.20	-4.38
10	Wet wood boiler	-	-1.77	-54.4	4.03	4.96
11	Dry wood boiler	-	0.58	-45.0	4.58	5.78
12	Wet wood CHP	-	1.04	-64.5	-1.30	-1.72
13	Dry wood CHP	-	3.36	-55.4	-1.24	-1.28
14	Pyrolysis boiler	-	4.66	-37.5	0.84	2.59
15	Pyrolysis CHP	-	4.14	-46.2	-3.38	-0.84
16	Wet Wood FT	-	5.19	-30.3	0.21	0.24
17	Dry Wood FT	-	5.53	-27.1	0.42	0.54
18	SNG in NG	-	5.03	-51.0	-1.26	-1.62
19	SNG CHP	-	3.86	-66.0	-6.96	-5.23
20	SNG Mobility	-	-2.55	-51.2	-3.20	-7.47
(1,10)	Wet wood boiler	3.8 km Direct use	-1.44	-59.8	3.89	4.64
(2,10)	Wet wood boiler	3.8 km ORC	-1.37	-59.8	3.89	4.64
(3,10)	Wet wood boiler	4.2 km Direct use	-5.29	-84.7	3.96	3.67
(4,10)	Wet wood boiler	4.2 km ORC	-5.22	-87.6	3.28	3.04
(5,10)	Wet wood boiler	5 km Direct use	-7.50	-99.0	3.51	2.72
(6,10)	Wet wood boiler	5 km ORC	-7.60	-104.2	2.43	1.69
(7,10)	Wet wood boiler	6 km Direct use	-9.10	-112.2	3.06	1.81
(8,10)	Wet wood boiler	6 km ORC	-9.53	-121.4	1.29	0.09
(9,10)	Wet wood boiler	6 km Kalina	-9.56	-119.4	1.83	0.58
(1,11)	Dry wood boiler	3.8 km Direct use	0.70	-51.3	4.41	5.40
(2,11)	Dry wood boiler	3.8 km ORC	0.77	-51.3	4.41	5.40
(3,11)	Dry wood boiler	4.2 km Direct use	-5.85	-90.1	4.04	3.48

D.4. Additional results

Table D.26 – δPI calculated for each performance indicator (Eq. C.19). Performance of each with respect to the reference (scenario 0).

#	Biomass	Geothermal	δC_{tot}	δGWP_{tot}	δhh_{tot}	δhh_{tot}
			[MCHF/y]	[ktCO ₂ -eq./y]	Imp2002+	ES2013
					[kpts/y]	[GUPB/y]
(4,11)	Dry wood boiler	4.2 km ORC	-5.32	-90.1	4.05	3.48
(5,11)	Dry wood boiler	5 km Direct use	-8.06	-104.4	3.60	2.53
(6,11)	Dry wood boiler	5 km ORC	-7.28	-104.4	3.60	2.54
(7,11)	Dry wood boiler	6 km Direct use	-9.72	-117.6	3.15	1.62
(8,11)	Dry wood boiler	6 km ORC	-8.96	-120.6	1.57	0.33
(9,11)	Dry wood boiler	6 km Kalina	-9.50	-121.3	2.03	0.63
(1,12)	Wet wood CHP	3.8 km Direct use	1.45	-69.9	-1.44	-2.03
(2,12)	Wet wood CHP	3.8 km ORC	1.52	-69.9	-1.44	-2.03
(3,12)	Wet wood CHP	4.2 km Direct use	-1.60	-94.8	-1.37	-2.98
(4,12)	Wet wood CHP	4.2 km ORC	-1.66	-97.7	-2.05	-3.61
(5,12)	Wet wood CHP	5 km Direct use	-3.26	-109.0	-1.80	-3.91
(6,12)	Wet wood CHP	5 km ORC	-3.50	-114.2	-2.88	-4.94
(7,12)	Wet wood CHP	6 km Direct use	-4.68	-122.2	-2.25	-4.81
(8,12)	Wet wood CHP	6 km ORC	-5.25	-131.4	-4.03	-6.54
(9,12)	Wet wood CHP	6 km Kalina	-5.14	-129.5	-3.48	-6.04
(1,13)	Dry wood CHP	3.8 km Direct use	3.60	-61.7	-1.41	-1.65
(2,13)	Dry wood CHP	3.8 km ORC	3.68	-61.7	-1.41	-1.65
(3,13)	Dry wood CHP	4.2 km Direct use	-1.48	-100.7	-1.73	-3.51
(4,13)	Dry wood CHP	4.2 km ORC	-0.95	-100.7	-1.73	-3.50
(5,13)	Dry wood CHP	5 km Direct use	-3.15	-114.9	-2.17	-4.44
(6,13)	Dry wood CHP	5 km ORC	-2.37	-114.9	-2.16	-4.43
(7,13)	Dry wood CHP	6 km Direct use	-4.63	-128.1	-2.62	-5.34
(8,13)	Dry wood CHP	6 km ORC	-4.21	-128.5	-4.15	-6.51
(9,13)	Dry wood CHP	6 km Kalina	-4.69	-131.8	-3.75	-6.35
(1,14)	Pyrolysis boiler	3.8 km Direct use	4.98	-42.9	0.71	2.27
(2,14)	Pyrolysis boiler	3.8 km ORC	5.06	-42.9	0.71	2.27
(3,14)	Pyrolysis boiler	4.2 km Direct use	1.11	-67.8	0.77	1.30
(4,14)	Pyrolysis boiler	4.2 km ORC	1.18	-70.7	0.09	0.67
(5,14)	Pyrolysis boiler	5 km Direct use	-1.08	-82.1	0.33	0.35
(6,14)	Pyrolysis boiler	5 km ORC	-1.19	-87.3	-0.76	-0.68
(7,14)	Pyrolysis boiler	6 km Direct use	-2.67	-95.3	-0.13	-0.56
(8,14)	Pyrolysis boiler	6 km ORC	-3.11	-104.5	-1.90	-2.28
(9,14)	Pyrolysis boiler	6 km Kalina	-3.14	-102.5	-1.36	-1.79

Appendix D. Urban energy modeling - data

Table D.26 – δPI calculated for each performance indicator (Eq. C.19). Performance of each with respect to the reference (scenario 0).

#	Biomass	Geothermal	δC_{tot}	δGWP_{tot}	δhh_{tot}	δhh_{tot}
			[MCHF/y]	[ktCO ₂ -eq./y]	Imp2002+	ES2013
					[kpts/y]	[GUPB/y]
(1,15)	Pyrolysis CHP	3.8 km Direct use	4.52	-51.5	-3.51	-1.15
(2,15)	Pyrolysis CHP	3.8 km ORC	4.60	-51.5	-3.51	-1.15
(3,15)	Pyrolysis CHP	4.2 km Direct use	0.64	-76.5	-3.45	-2.12
(4,15)	Pyrolysis CHP	4.2 km ORC	0.65	-79.4	-4.13	-2.76
(5,15)	Pyrolysis CHP	5 km Direct use	-1.22	-90.6	-3.85	-2.99
(6,15)	Pyrolysis CHP	5 km ORC	-1.42	-95.8	-4.94	-4.04
(7,15)	Pyrolysis CHP	6 km Direct use	-2.69	-103.7	-4.29	-3.87
(8,15)	Pyrolysis CHP	6 km ORC	-3.22	-113.0	-6.07	-5.61
(9,15)	Pyrolysis CHP	6 km Kalina	-3.16	-110.9	-5.52	-5.10
(1,16)	Wet Wood FT	3.8 km Direct use	5.50	-35.6	0.07	-0.08
(2,16)	Wet Wood FT	3.8 km ORC	5.58	-35.6	0.07	-0.08
(3,16)	Wet Wood FT	4.2 km Direct use	1.61	-60.6	0.13	-1.05
(4,16)	Wet Wood FT	4.2 km ORC	1.69	-63.4	-0.55	-1.68
(5,16)	Wet Wood FT	5 km Direct use	-0.61	-74.9	-0.31	-2.00
(6,16)	Wet Wood FT	5 km ORC	-0.71	-80.1	-1.39	-3.03
(7,16)	Wet Wood FT	6 km Direct use	-2.21	-88.1	-0.77	-2.91
(8,16)	Wet Wood FT	6 km ORC	-2.64	-97.3	-2.54	-4.63
(9,16)	Wet Wood FT	6 km Kalina	-2.67	-95.3	-2.00	-4.14
(1,17)	Dry Wood FT	3.8 km Direct use	5.63	-33.5	0.26	0.16
(2,17)	Dry Wood FT	3.8 km ORC	5.70	-33.5	0.26	0.16
(3,17)	Dry Wood FT	4.2 km Direct use	-0.09	-68.2	0.03	-1.46
(4,17)	Dry Wood FT	4.2 km ORC	0.44	-68.2	0.03	-1.45
(5,17)	Dry Wood FT	5 km Direct use	-2.06	-81.0	-0.37	-2.31
(6,17)	Dry Wood FT	5 km ORC	-1.28	-81.0	-0.36	-2.30
(7,17)	Dry Wood FT	6 km Direct use	-3.37	-92.4	-0.77	-3.10
(8,17)	Dry Wood FT	6 km ORC	-3.63	-101.1	-2.53	-4.79
(9,17)	Dry Wood FT	6 km Kalina	-3.83	-99.7	-2.00	-4.33
(1,18)	SNG in NG	3.8 km Direct use	5.65	-55.0	-1.36	-1.85
(2,18)	SNG in NG	3.8 km ORC	5.65	-55.4	-1.44	-1.93
(3,18)	SNG in NG	4.2 km Direct use	1.76	-79.9	-1.30	-2.82
(4,18)	SNG in NG	4.2 km ORC	1.53	-84.2	-2.02	-3.54
(5,18)	SNG in NG	5 km Direct use	-0.46	-94.2	-1.74	-3.77
(6,18)	SNG in NG	5 km ORC	-0.87	-100.8	-2.86	-4.89

D.4. Additional results

Table D.26 – δPI calculated for each performance indicator (Eq. C.19). Performance of each with respect to the reference (scenario 0).

#	Biomass	Geothermal	δC_{tot}	δGWP_{tot}	δhh_{tot}	δhh_{tot}
			[MCHF/y]	[ktCO ₂ -eq./y]	Imp2002+	ES2013
					[kpts/y]	[GUPB/y]
(7,18)	SNG in NG	6 km Direct use	-1.75	-106.0	-2.15	-4.59
(8,18)	SNG in NG	6 km ORC	-2.49	-116.6	-3.96	-6.40
(9,18)	SNG in NG	6 km Kalina	-2.21	-113.2	-3.38	-5.82
(1,19)	SNG CHP	3.8 km Direct use	4.49	-70.0	-7.05	-5.46
(2,19)	SNG CHP	3.8 km ORC	4.48	-70.4	-7.13	-5.53
(3,19)	SNG CHP	4.2 km Direct use	0.77	-94.9	-6.99	-6.41
(4,19)	SNG CHP	4.2 km ORC	0.54	-99.1	-7.71	-7.13
(5,19)	SNG CHP	5 km Direct use	-0.93	-109.1	-7.41	-7.32
(6,19)	SNG CHP	5 km ORC	-1.34	-115.6	-8.53	-8.44
(7,19)	SNG CHP	6 km Direct use	-2.18	-120.9	-7.82	-8.14
(8,19)	SNG CHP	6 km ORC	-2.92	-131.5	-9.63	-9.95
(9,19)	SNG CHP	6 km Kalina	-2.64	-128.1	-9.05	-9.37
(1,20)	SNG Mobility	3.8 km Direct use	-1.93	-55.2	-3.29	-7.70
(2,20)	SNG Mobility	3.8 km ORC	-1.94	-55.6	-3.37	-7.78
(3,20)	SNG Mobility	4.2 km Direct use	-5.82	-80.1	-3.23	-8.67
(4,20)	SNG Mobility	4.2 km ORC	-6.05	-84.3	-3.95	-9.39
(5,20)	SNG Mobility	5 km Direct use	-8.04	-94.4	-3.67	-9.62
(6,20)	SNG Mobility	5 km ORC	-8.45	-101.0	-4.80	-10.74
(7,20)	SNG Mobility	6 km Direct use	-9.33	-106.2	-4.09	-10.44
(8,20)	SNG Mobility	6 km ORC	-10.07	-116.8	-5.90	-12.25
(9,20)	SNG Mobility	6 km Kalina	-9.79	-113.4	-5.32	-11.67

Bibliography

- [1] The World Bank. *Energy Use (Kg of Oil Equivalent per Capita) | Data*. <http://data.worldbank.org/indicator/EG.USE.PCAP.KG.OE>. (Visited on 05/26/2017).
- [2] European Commission - Eurostat. *Glossary: Kilograms of Oil Equivalent (Kgoe) - Statistics Explained*. [http://ec.europa.eu/eurostat/statistics-explained/index.php/Glossary:Kilograms_of_oil_equivalent_\(kgoe\)](http://ec.europa.eu/eurostat/statistics-explained/index.php/Glossary:Kilograms_of_oil_equivalent_(kgoe)). (Visited on 05/26/2017).
- [3] IEA - International Energy Agency. *Key World Energy Statistics 2016*. Tech. rep. IEA - International Energy Agency, 2016.
- [4] Intergovernmental Panel on Climate Change (IPCC). *Special Report on Renewable Energy Sources and Climate Change Mitigation*. Ed. by O. Edenhofer et al. United Kingdom and New York, NY, USA: Cambridge University Press, 2011.
- [5] IEA - International Energy Agency. *Energy Technology Perspectives 2014*. Tech. rep. IEA - International Energy Agency, 2014.
- [6] IEA - International Energy Agency. *Energy Technology Perspectives 2016*. Tech. rep. IEA - International Energy Agency, 2016.
- [7] Y. Zeng et al. “A Review on Optimization Modeling of Energy Systems Planning and GHG Emission Mitigation under Uncertainty”. en. In: *Energies* 4.10 (Oct. 2011), pp. 1624–1656. DOI: 10.3390/en4101624. (Visited on 10/23/2015).
- [8] Energy Information Administration, Office of Integrated Analysis and Forecasting. *NEMS. The National Energy Modeling System: An Overview 2003*. Tech. rep. Washington, DC: U.S. Department of Energy, 2003.
- [9] L. G. Fishbone and H. Abilock. “Markal, a Linear-Programming Model for Energy Systems Analysis: Technical Description of the Bnl Version”. en. In: *International Journal of Energy Research* 5.4 (Jan. 1981), pp. 353–375. ISSN: 1099-114X. DOI: 10.1002/er.4440050406. (Visited on 11/28/2014).
- [10] S. Messner and M. Strubegger. *User's Guide for MESSAGE III*. en. <http://pure.iiasa.ac.at/4527/>. Monograph. July 1995. (Visited on 04/06/2017).

Bibliography

- [11] A. D. Lamont. “Assessing the Long-Term System Value of Intermittent Electric Generation Technologies”. In: *Energy Economics* 30.3 (May 2008), pp. 1208–1231. ISSN: 0140-9883. DOI: 10.1016/j.eneco.2007.02.007. (Visited on 11/28/2014).
- [12] W. B. Powell et al. “SMART: A Stochastic Multiscale Model for the Analysis of Energy Resources, Technology, and Policy”. en. In: *INFORMS Journal on Computing* 24.4 (Sept. 2012), pp. 665–682. ISSN: 1091-9856, 1526-5528. DOI: 10.1287/ijoc.1110.0470. (Visited on 07/25/2013).
- [13] J. Koomey et al. “Improving Long-Range Energy Modeling: A Plea for Historical Retrospectives”. In: *The Energy Journal* 24.4 (2003), pp. 75–91.
- [14] P. Krugman. “Gambling with Civilization”. In: *The New York Review of Books* (Nov. 2013). ISSN: 0028-7504. (Visited on 11/15/2013).
- [15] W. D. Nordhaus. “The Allocation of Energy Resources”. In: *Brookings Papers on Economic Activity* 4.3 (1973), pp. 529–576. (Visited on 11/15/2013).
- [16] J. S. Hodges and J. A. Dewar. *Is It You or Your Model Talking? A Framework for Model Validation*. Tech. rep. RAND Corporation, 1992.
- [17] P. P. Craig, A. Gadgil, and J. G. Koomey. “What Can History Teach Us? A Retrospective Examination of Long-Term Energy Forecasts for the United States”. In: *Annual Review of Energy and the Environment* 27.1 (2002), pp. 83–118. DOI: 10.1146/annurev.energy.27.1.22001.083425. (Visited on 07/22/2016).
- [18] I. Sohn. “Long-Term Energy Projections: What Lessons Have We Learned?” In: *Energy Policy* 35.9 (Sept. 2007), pp. 4574–4584. ISSN: 0301-4215. DOI: 10.1016/j.enpol.2007.03.021. (Visited on 10/21/2014).
- [19] H. Linderoth. “Forecast Errors in IEA-Countries’ Energy Consumption”. In: *Energy Policy* 30.1 (Jan. 2002), pp. 53–61. ISSN: 0301-4215. DOI: 10.1016/S0301-4215(01)00059-3. (Visited on 08/01/2016).
- [20] R. H. Bezdek and R. M. Wendling. “A Half Century of Long-Range Energy Forecasts: Errors Made, Lessons Learned, and Implications for Forecasting”. en. In: *Journal of Fusion Energy* 21.3-4 (2002), pp. 155–172. ISSN: 0164-0313, 1572-9591. DOI: 10.1023/A:1026208113925. (Visited on 08/01/2016).
- [21] B. C. O’Neill and M. Desai. “Accuracy of Past Projections of US Energy Consumption”. In: *Energy Policy* 33.8 (May 2005), pp. 979–993. ISSN: 0301-4215. DOI: 10.1016/j.enpol.2003.10.020. (Visited on 07/22/2016).
- [22] J. J. Winebrake and D. Sakva. “An Evaluation of Errors in US Energy Forecasts: 1982–2003”. In: *Energy Policy* 34.18 (Dec. 2006), pp. 3475–3483. ISSN: 0301-4215. DOI: 10.1016/j.enpol.2005.07.018. (Visited on 10/21/2014).

-
- [23] U.S. EIA - Energy Information Administration. *Annual Energy Outlook Retrospective Review: Evaluation of 2014 and Prior Reference Case Projections*. Tech. rep. U.S. Department of Energy, 2015.
- [24] C. Baumeister and L. Kilian. *Forty Years of Oil Price Fluctuations: Why the Price of Oil May Still Surprise Us*. SSRN Scholarly Paper ID 2714319. Rochester, NY: Social Science Research Network, Jan. 2016. (Visited on 04/18/2016).
- [25] U.S. Department of Commerce - Bureau of Economic Analysis (BEA). *Current-Dollar and Real GDP*. <http://www.bea.gov/national/index.htm#gdp>. (Visited on 02/12/2016).
- [26] R. Wiser and M. Bolinger. *An Overview of Alternative Fossil Fuel Price and Carbon Regulation Scenarios*. Tech. rep. LBNL-56403. Ernest Orlando Lawrence Berkeley National Laboratory, 2004.
- [27] A. S. Siddiqui and C. Marnay. *Addressing an Uncertain Future Using Scenario Analysis*. Tech. rep. LBNL-62313. Ernest Orlando Lawrence Berkeley National Laboratory, 2006.
- [28] COGEN Europe. *IPCC Confirms Role of CHP in Long-Term CO2 Reduction*. http://www.cogeneurope.eu/ipcc-confirms-role-of-chp-in-long-term-co-reduction_623.html. Apr. 2014.
- [29] De Volkskrant. “Essent Legt Grote Centrale Stil - Archief - Voor Nieuws, Achtergronden En Columns”. In: *De Volkskrant* (Feb. 2014). (Visited on 04/06/2017).
- [30] E. Hirst and M. Schweitzer. “Uncertainty: A Critical Element of Integrated Resource Planning”. In: *The Electricity Journal* 2.6 (July 1989), pp. 16–27. ISSN: 1040-6190. DOI: 10.1016/1040-6190(89)90022-5. (Visited on 04/06/2017).
- [31] B.-M. S. Hodge et al. “A Multi-Paradigm Modeling Framework for Energy Systems Simulation and Analysis”. In: *Computers & Chemical Engineering*. Energy Systems Engineering 35.9 (Sept. 2011), pp. 1725–1737. ISSN: 0098-1354. DOI: 10.1016/j.compchemeng.2011.05.005. (Visited on 04/06/2017).
- [32] A. Mirakyan and R. De Guio. “Modelling and Uncertainties in Integrated Energy Planning”. In: *Renewable and Sustainable Energy Reviews* 46 (June 2015), pp. 62–69. ISSN: 1364-0321. DOI: 10.1016/j.rser.2015.02.028. (Visited on 01/31/2016).
- [33] J. DeCarolis et al. “Formalizing Best Practice for Energy System Optimization Modelling”. In: *Applied Energy* 194 (May 2017), pp. 184–198. ISSN: 0306-2619. DOI: 10.1016/j.apenergy.2017.03.001. (Visited on 04/06/2017).
- [34] J. Keirstead, M. Jennings, and A. Sivakumar. “A Review of Urban Energy System Models: Approaches, Challenges and Opportunities”. In: *Renewable and Sustainable Energy Reviews* 16.6 (Aug. 2012), pp. 3847–3866. ISSN: 13640321. DOI: 10.1016/j.rser.2012.02.047. (Visited on 07/22/2013).

Bibliography

- [35] V. Goel and I. E. Grossmann. “A Stochastic Programming Approach to Planning of Offshore Gas Field Developments under Uncertainty in Reserves”. In: *Computers & Chemical Engineering* 28.8 (July 2004), pp. 1409–1429. ISSN: 0098-1354. DOI: 10.1016/j.compchemeng.2003.10.005. (Visited on 06/10/2015).
- [36] I. E. Grossmann et al. “Recent Advances in Mathematical Programming Techniques for the Optimization of Process Systems under Uncertainty”. In: *Computer Aided Chemical Engineering*. Ed. by J. K. H. Krist V. Gernaey and R. Gani. Vol. 37. 12th International Symposium on Process Systems Engineering and 25th European Symposium on Computer Aided Process Engineering. Elsevier, 2015, pp. 1–14. (Visited on 06/19/2015).
- [37] D. Connolly et al. “A Review of Computer Tools for Analysing the Integration of Renewable Energy into Various Energy Systems”. In: *Applied Energy* 87.4 (Apr. 2010), pp. 1059–1082. ISSN: 0306-2619. DOI: 10.1016/j.apenergy.2009.09.026. (Visited on 04/07/2017).
- [38] H Lund and E Münster. “Modelling of Energy Systems with a High Percentage of CHP and Wind Power”. In: *Renewable Energy* 28.14 (Nov. 2003), pp. 2179–2193. ISSN: 0960-1481. DOI: 10.1016/S0960-1481(03)00125-3. (Visited on 01/08/2015).
- [39] W. Usher and N. Strachan. “Critical Mid-Term Uncertainties in Long-Term Decarbonisation Pathways”. In: *Energy Policy*. Modeling Transport (Energy) Demand and Policies 41 (Feb. 2012), pp. 433–444. ISSN: 0301-4215. DOI: 10.1016/j.enpol.2011.11.004. (Visited on 08/26/2015).
- [40] P. Zhou, B. W. Ang, and K. L. Poh. “Decision Analysis in Energy and Environmental Modeling: An Update”. English. In: *Energy* 31.14 (Nov. 2006). WOS:000241524100006, pp. 2604–2622. ISSN: 0360-5442. DOI: 10.1016/j.energy.2005.10.023.
- [41] N. Koltsaklis et al. “A Spatial Multi-Period Long-Term Energy Planning Model: A Case Study of the Greek Power System”. In: *Applied Energy* 115 (Feb. 2014), pp. 456–482. ISSN: 0306-2619. DOI: 10.1016/j.apenergy.2013.10.042. (Visited on 03/25/2015).
- [42] M. Wierzbowski, W. Lyzwa, and I. Musial. “MILP Model for Long-Term Energy Mix Planning with Consideration of Power System Reserves”. In: *Applied Energy* 169 (May 2016), pp. 93–111. ISSN: 0306-2619. DOI: 10.1016/j.apenergy.2016.02.003. (Visited on 05/09/2017).
- [43] D. H. Loughlin. “Using MARKAL Model to Evaluate Factors Influencing Low Carbon Power Generation”. In: Cincinnati, Ohio (USA), 2009.
- [44] T. L. Johnson et al. *MARKAL Scenario Analyses of Technology Options for the Electric Sector*. Tech. rep. Washington, DC: U.S. Environmental Protection Agency, 2006.
- [45] S. Messner, A. Golodnikov, and A. Gritsevskii. “A Stochastic Version of the Dynamic Linear Programming Model MESSAGE III”. In: *Energy* 21.9 (Sept. 1996), pp. 775–784. ISSN: 0360-5442. DOI: 10.1016/0360-5442(96)00025-4. (Visited on 04/07/2017).

-
- [46] U.S. EIA - Energy Information Administration. *Annual Energy Outlook (AEO) 2017*. https://www.eia.gov/outlooks/aeo/info_nems_archive.cfm. 2017. (Visited on 04/07/2017).
- [47] S. Pye, N. Sabio, and N. Strachan. “An Integrated Systematic Analysis of Uncertainties in UK Energy Transition Pathways”. In: *Energy Policy* 87 (Dec. 2015), pp. 673–684. ISSN: 0301-4215. DOI: 10.1016/j.enpol.2014.12.031. (Visited on 09/07/2016).
- [48] M. Dubuis. “Energy System Design under Uncertainty”. Doctoral Thesis. EPFL Lausanne, 2012.
- [49] L. Tock and F. Maréchal. “Decision Support for Ranking Pareto Optimal Process Designs under Uncertain Market Conditions”. In: *Computers & Chemical Engineering*. 24th European Symposium on Computer Aided Process Engineering (ESCAPE) 83 (Dec. 2015), pp. 165–175. ISSN: 0098-1354. DOI: 10.1016/j.compchemeng.2015.06.009. (Visited on 09/07/2016).
- [50] J. Kim, S. M. Sen, and C. T. Maravelias. “An Optimization-Based Assessment Framework for Biomass-to-Fuel Conversion Strategies”. en. In: *Energy & Environmental Science* 6.4 (Mar. 2013), pp. 1093–1104. ISSN: 1754-5706. DOI: 10.1039/C3EE24243A. (Visited on 06/10/2015).
- [51] G. Sin et al. “Uncertainty Analysis in WWTP Model Applications: A Critical Discussion Using an Example from Design”. In: *Water Research* 43.11 (June 2009), pp. 2894–2906. ISSN: 0043-1354. DOI: 10.1016/j.watres.2009.03.048. (Visited on 09/07/2016).
- [52] E. Carpaneto et al. “Cogeneration Planning under Uncertainty: Part I: Multiple Time Frame Approach”. In: *Applied Energy* 88.4 (Apr. 2011), pp. 1059–1067. ISSN: 0306-2619. DOI: 10.1016/j.apenergy.2010.10.014. (Visited on 09/07/2016).
- [53] C. Lythcke-Jørgensen, F. Haglind, and L. R. Clausen. “Exergy Analysis of a Combined Heat and Power Plant with Integrated Lignocellulosic Ethanol Production”. In: *Energy Conversion and Management* 85 (Sept. 2014), pp. 817–827. ISSN: 0196-8904. DOI: 10.1016/j.enconman.2014.01.018. (Visited on 08/30/2014).
- [54] A. Saltelli et al. *Global Sensitivity Analysis: The Primer*. en. John Wiley & Sons, Feb. 2008. ISBN: 978-0-470-72517-7.
- [55] A. Saltelli et al. “Sensitivity Analysis Practices: Strategies for Model-Based Inference”. In: *Reliability Engineering & System Safety*. The Fourth International Conference on Sensitivity Analysis of Model Output (SAMO 2004) SAMO 2004 The Fourth International Conference on Sensitivity Analysis of Model Output (SAMO 2004) 91.10–11 (Oct. 2006), pp. 1109–1125. ISSN: 0951-8320. DOI: 10.1016/j.ress.2005.11.014.
- [56] A. Soroudi and T. Amraee. “Decision Making under Uncertainty in Energy Systems: State of the Art”. In: *Renewable and Sustainable Energy Reviews* 28 (Dec. 2013), pp. 376–384. ISSN: 1364-0321. DOI: 10.1016/j.rser.2013.08.039. (Visited on 09/13/2013).

Bibliography

- [57] J. R. Birge and F. Louveaux. *Introduction to Stochastic Programming*. Springer Series in Operations Research and Financial Engineering. Springer New York, 2011. ISBN: 978-1-4614-0236-7 978-1-4614-0237-4.
- [58] G. B. Dantzig. “Linear Programming under Uncertainty”. In: *Management Science* 1.3/4 (Apr. 1955). ArticleType: research-article / Full publication date: Apr. - Jul., 1955 / Copyright © 1955 INFORMS, pp. 197–206. ISSN: 0025-1909. DOI: 10.2307/2627159. (Visited on 09/18/2013).
- [59] F. Babonneau, J.-P. Vial, and R. Apparigliato. “Robust Optimization for Environmental and Energy Planning”. en. In: *Uncertainty and Environmental Decision Making*. Ed. by J. A. Filar and A. Haurie. International Series in Operations Research & Management Science 138. Springer US, Jan. 2010, pp. 79–126. ISBN: 978-1-4419-1128-5 978-1-4419-1129-2. (Visited on 10/23/2014).
- [60] A. L. Soyster. “Convex Programming with Set-Inclusive Constraints and Applications to Inexact Linear Programming”. In: *Operations Research* 21.5 (Sept. 1973). ArticleType: research-article / Full publication date: Sep. - Oct., 1973 / Copyright © 1973 INFORMS, pp. 1154–1157. ISSN: 0030-364X. DOI: 10.2307/168933. (Visited on 09/18/2013).
- [61] A. Ben-Tal and A. Nemirovski. “Robust Solutions of Uncertain Linear Programs”. In: *Operations Research Letters* 25.1 (Aug. 1999), pp. 1–13. ISSN: 0167-6377. DOI: 10.1016/S0167-6377(99)00016-4.
- [62] D. Bertsimas and M. Sim. “The Price of Robustness”. In: *Operations Research* 52.1 (Feb. 2004), pp. 35–53. ISSN: 0030-364X, 1526-5463. DOI: 10.1287/opre.1030.0065. (Visited on 11/27/2013).
- [63] F. Campolongo, S. Tarantola, and A. Saltelli. “Tackling Quantitatively Large Dimensionality Problems”. In: *Computer Physics Communications* 117.1 (Mar. 1999), pp. 75–85. ISSN: 0010-4655. DOI: 10.1016/S0010-4655(98)00165-9. (Visited on 08/22/2016).
- [64] Swiss Federal Council. *Perspectives Énergétiques 2050 - Analyse Des Variantes d'offre d'électricité Du Conseil Fédéral*. May 2011.
- [65] F. Maréchal and B. Kalitventzeff. “Process Integration: Selection of the Optimal Utility System”. In: *Computers & Chemical Engineering*. European Symposium on Computer Aided Process Engineering-8 22, Supplement 1 (Mar. 1998), S149–S156. ISSN: 0098-1354. DOI: 10.1016/S0098-1354(98)00049-0. (Visited on 01/09/2015).
- [66] R. Fourer, D. Gay, and B. Kernighan. *AMPL: A Modeling Language for Mathematical Programming*. Duxbury Press, Nov. 2002. ISBN: 0-534-38809-4. (Visited on 01/09/2014).
- [67] S. Moret, M. Bierlaire, and F. Maréchal. “Strategic Energy Planning under Uncertainty: A Mixed-Integer Linear Programming Modeling Framework for Large-Scale Energy Systems”. In: *Computer Aided Chemical Engineering*. Ed. by Z. K. Bogataj and Miloš. Vol. 38. 26th

- European Symposium on Computer Aided Process Engineering. Elsevier, 2016, pp. 1899–1904. DOI: 10.1016/B978-0-444-63428-3.50321-0. (Visited on 02/14/2017).
- [68] W. W. Hogan. “Energy Policy Models for Project Independence”. In: *Computers & Operations Research* 2.3 (Dec. 1975), pp. 251–271. ISSN: 0305-0548. DOI: 10.1016/0305-0548(75)90008-8. (Visited on 05/09/2017).
- [69] J. Keirstead et al. “Evaluating Biomass Energy Strategies for a UK Eco-Town with an MILP Optimization Model”. In: *Biomass and Bioenergy*. Biorefinery 39 (Apr. 2012), pp. 306–316. ISSN: 0961-9534. DOI: 10.1016/j.biombioe.2012.01.022. (Visited on 05/09/2017).
- [70] A. M. Pantaleo et al. “Integration of Biomass into Urban Energy Systems for Heat and Power. Part I: An MILP Based Spatial Optimization Methodology”. In: *Energy Conversion and Management* 83 (2014), pp. 347–361. ISSN: 0196-8904. DOI: <http://dx.doi.org/10.1016/j.enconman.2014.03.050>.
- [71] V. Codina Gironès et al. “Strategic Energy Planning for Large-Scale Energy Systems: A Modelling Framework to Aid Decision-Making”. In: *Energy* 90, Part 1 (Oct. 2015), pp. 173–186. ISSN: 0360-5442. DOI: 10.1016/j.energy.2015.06.008. (Visited on 10/28/2015).
- [72] European Commission - Eurostat. *Glossary: Final Energy Consumption*. http://ec.europa.eu/eurostat/statistics-explained/index.php/Glossary:Final_energy_consumption. (Visited on 05/12/2017).
- [73] Y. Y. Haimes, L. S. Lasdon, and D. A. Wismer. “On a Bicriterion Formulation of the Problems of Integrated System Identification and System Optimization”. In: *IEEE Transactions on Systems, Man, and Cybernetics* SMC-1.3 (July 1971), pp. 296–297. ISSN: 0018-9472. DOI: 10.1109/TSMC.1971.4308298.
- [74] S. Moret et al. “Swiss-EnergyScope.Ch: A Platform to Widely Spread Energy Literacy and Aid Decision-Making”. In: *Chemical Engineering Transactions* 39 (2014), pp. 877–882.
- [75] E. I. Al-musleh, D. S. Mallapragada, and R. Agrawal. “Continuous Power Supply from a Baseload Renewable Power Plant”. In: *Applied Energy* 122 (June 2014), pp. 83–93. ISSN: 0306-2619. DOI: 10.1016/j.apenergy.2014.02.015. (Visited on 11/25/2014).
- [76] V. Codina Gironès et al. “Optimal Use of Biomass in Large-Scale Energy Systems: Insights for Energy Policy”. In: *Energy* (2017). ISSN: 0360-5442. DOI: 10.1016/j.energy.2017.05.027.
- [77] Swiss Federal Office of Energy (SFOE). *Overall energy statistics 2011*. DE/FR. Tech. rep. 2012.
- [78] Swiss Federal Office of Energy (SFOE). *Swiss electricity statistics 2011*. DE/FR. Tech. rep. Bern, Switzerland, 2012.
- [79] Swiss Federal Office of Energy (SFOE). *Swiss electricity statistics 2012*. DE/FR. Tech. rep. Bern, Switzerland, 2013.
- [80] Swiss Federal Office of Statistics (SFOS). *Statistique de la Suisse - Mobilité et transports 2013*. French. Tech. rep. Swiss Federal Office of Statistics (SFOS), 2013.

Bibliography

- [81] Prognos AG. *Die Energieperspektiven für die Schweiz bis 2050*. German. Dec. 2012.
- [82] Swiss Federal Office of Energy (SFOE). *Thermische Stromproduktion inklusive Wärmekraftkopplung (WKK) in der Schweiz - Ausgabe 2011*. German. Tech. rep. Nov. 2012.
- [83] Swiss Federal Office of Energy (SFOE). *Emissions d'après La Loi Sur Le CO2 et d'après Le Protocole de Kyoto*. Tech. rep. 2013.
- [84] S. Moret et al. "Characterization of Input Uncertainties in Strategic Energy Planning Models". In: *Applied Energy* 202 (Sept. 2017), pp. 597–617. ISSN: 0306-2619. DOI: 10.1016/j.apenergy.2017.05.106.
- [85] C. Lythcke-Jørgensen et al. "A Methodology for Designing Flexible Multi-Generation Systems". In: *Energy*. Special issue on Smart Energy Systems and 4th Generation District Heating 110 (Sept. 2016), pp. 34–54. ISSN: 0360-5442. DOI: 10.1016/j.energy.2016.01.084. (Visited on 11/17/2016).
- [86] D. E. Majewski et al. "TRusT: A Two-Stage Robustness Trade-off Approach for the Design of Decentralized Energy Supply Systems". In: *Energy* 118 (2017), pp. 590–599. ISSN: 0360-5442. DOI: 10.1016/j.energy.2016.10.065.
- [87] D. Lauinger et al. "A Linear Programming Approach to the Optimization of Residential Energy Systems". In: *Journal of Energy Storage* 7 (Aug. 2016), pp. 24–37. ISSN: 2352-152X. DOI: 10.1016/j.est.2016.04.009.
- [88] W. E. Walker et al. "Defining Uncertainty: A Conceptual Basis for Uncertainty Management in Model-Based Decision Support". In: *Integrated Assessment* 4.1 (Mar. 2003), pp. 5–17. ISSN: 1389-5176. DOI: 10.1076/iaij.4.1.5.16466.
- [89] M. G. Morgan et al. *CCSP, 2009: Best Practice Approaches for Characterizing, Communicating and Incorporating Scientific Uncertainty in Climate Decision Making*. en. Tech. rep. SAP 5.2. Washington D.C., USA: National Oceanic and Atmospheric Administration, Jan. 2009.
- [90] A. Der Kiureghian and O. Ditlevsen. "Aleatory or Epistemic? Does It Matter?" In: *Structural Safety*. Risk Acceptance and Risk Communication Risk Acceptance and Risk Communication 31.2 (Mar. 2009), pp. 105–112. ISSN: 0167-4730. DOI: 10.1016/j.strusafe.2008.06.020. (Visited on 08/27/2016).
- [91] C. A. E. Goodhart and W. B. Lim. "Interest Rate Forecasts: A Pathology". In: *International Journal of Central Banking (IJCB)* (2011). (Visited on 11/21/2016).
- [92] Council of Economic Advisers - Executive Office of the President of the United States. *Long-Term Interest Rates: A Survey*. Tech. rep. Executive Office of the President of the United States, 2015.
- [93] Swiss Federal Office of Energy (SFOE). *Explications relatives au calcul du taux d'intérêt calculé conformément à l'art. 13, al. 3, let. b, de l'ordonnance sur l'approvisionnement en électricité (OApEl) pour l'année tarifaire 2015*. French. 2014.

- [94] H. Liao et al. “Why Did the Historical Energy Forecasting Succeed or Fail? A Case Study on IEA’s Projection”. In: *Technological Forecasting and Social Change* (). ISSN: 0040-1625. DOI: 10.1016/j.techfore.2016.03.026. (Visited on 04/13/2016).
- [95] C. Fischer, E. Herrnstadt, and R. Morgenstern. “Understanding Errors in EIA Projections of Energy Demand”. In: *Resource and Energy Economics* 31.3 (Aug. 2009), pp. 198–209. ISSN: 0928-7655. DOI: 10.1016/j.reseneeco.2009.04.003. (Visited on 11/22/2016).
- [96] K. Vatopoulos et al. *Study on the State of Play of Energy Efficiency of Heat and Electricity Production Technologies*. Tech. rep. European Commission - Joint Research Center (JRC), 2012.
- [97] U.S. Department of Energy (DOE) and U.S. Environmental Protection Agency (EPA). *Fuel Economy Guide - Model Year 2016*. Tech. rep. 2016.
- [98] A. Ohmura et al. “Baseline Surface Radiation Network (BSRN/WCRP): New Precision Radiometry for Climate Research”. In: *Bulletin of the American Meteorological Society* 79.10 (1998), pp. 2115–2136.
- [99] E. W. Merrow, K. E. Phillips, and C. W. Myers. *Understanding Cost Growth and Performance Shortfalls in Pioneer Process Plants*. Tech. rep. RAND Corporation, 1981.
- [100] B. K. Sovacool, A. Gilbert, and D. Nugent. “Risk, Innovation, Electricity Infrastructure and Construction Cost Overruns: Testing Six Hypotheses”. In: *Energy* 74 (Sept. 2014), pp. 906–917. ISSN: 0360-5442. DOI: 10.1016/j.energy.2014.07.070. (Visited on 08/05/2016).
- [101] M. Z. Lukawski, R. L. Silverman, and J. W. Tester. “Uncertainty Analysis of Geothermal Well Drilling and Completion Costs”. In: *Geothermics* 64 (Nov. 2016), pp. 382–391. ISSN: 0375-6505. DOI: 10.1016/j.geothermics.2016.06.017. (Visited on 08/05/2016).
- [102] S. Hirschberg, S. Wiemer, and P. Burgherr. *Energy from the Earth. Deep Geothermal as a Resource for the Future?* Tech. rep. Zurich: ETH Zurich, 2015.
- [103] S. Thalmann et al. *Analyse Und Optimierung von Fernwärmenetzen*. Tech. rep. Zürich: Swiss Federal Office of Energy (SFOE), Nov. 2013.
- [104] European Commission. *Energy Roadmap 2050, Impact Assessment and Scenario Analysis*. Tech. rep. Brussels, Belgium: European Commission, Dec. 2011.
- [105] U.S. EIA - Energy Information Administration. *Annual Energy Outlook (AEO) 2015*. Tech. rep. U.S. Department of Energy, 2015.
- [106] IEA - International Energy Agency. *IEA World Energy Investment Outlook 2014 - Power Generation in the New Policies and 450 Scenarios*. English. 2014. (Visited on 07/20/2016).
- [107] Swiss Federal Office of Energy (SFOE). *Overall Energy Statistics 2014*. Tech. rep. 2015.
- [108] T. F. Schulz et al. “Assessing Wood-Based Synthetic Natural Gas Technologies Using the SWISS-MARKAL Model”. In: *Energy* 32.10 (Oct. 2007), pp. 1948–1959. ISSN: 0360-5442. DOI: 10.1016/j.energy.2007.03.006. (Visited on 11/30/2016).

Bibliography

- [109] P. Kattan and I. Ruble. “An Economic Assessment of Four Different Boilers for Residential Heating in Lebanon”. In: *Energy and Buildings* 50 (July 2012), pp. 282–289. ISSN: 0378-7788. DOI: 10.1016/j.enbuild.2012.02.057. (Visited on 11/30/2016).
- [110] K. Siler-Evans, M. G. Morgan, and I. L. Azevedo. “Distributed Cogeneration for Commercial Buildings: Can We Make the Economics Work?” In: *Energy Policy* 42 (Mar. 2012), pp. 580–590. ISSN: 0301-4215. DOI: 10.1016/j.enpol.2011.12.028. (Visited on 11/27/2013).
- [111] A. M. Pantaleo et al. “Integration of Biomass into Urban Energy Systems for Heat and Power. Part II: Sensitivity Assessment of Main Techno-Economic Factors”. In: *Energy Conversion and Management* 83 (July 2014), pp. 362–376. ISSN: 0196-8904. DOI: 10.1016/j.enconman.2014.03.051. (Visited on 08/23/2016).
- [112] K. F. Beckers et al. “Levelized Costs of Electricity and Direct-Use Heat from Enhanced Geothermal Systems”. In: *Journal of Renewable and Sustainable Energy* 6.1 (Jan. 2014), p. 013141. ISSN: 1941-7012. DOI: 10.1063/1.4865575. (Visited on 11/30/2014).
- [113] S. Fazlollahi. “Decomposition Optimization Strategy for the Design and Operation of District Energy Systems”. PhD thesis. EPFL, Lausanne, 2014. (Visited on 05/24/2017).
- [114] M. Pernet. “Smart Heat Design - Urban Energy System Design under Uncertainty”. Master thesis. EPFL Lausanne, 2014.
- [115] J. Han et al. “A Lignocellulosic Ethanol Strategy via Nonenzymatic Sugar Production: Process Synthesis and Analysis”. In: *Bioresource Technology* 182 (Apr. 2015), pp. 258–266. ISSN: 0960-8524. DOI: 10.1016/j.biortech.2015.01.135. (Visited on 02/12/2016).
- [116] A. Mian. “Optimal Design Methods Applied to Solar-Assisted Hydrothermal Gasification Plants”. PhD thesis. EPFL, Lausanne, 2016.
- [117] J. Morio. “Global and Local Sensitivity Analysis Methods for a Physical System”. en. In: *European Journal of Physics* 32.6 (2011), p. 1577. ISSN: 0143-0807. DOI: 10.1088/0143-0807/32/6/011.
- [118] X. Zhou, H. Lin, and H. Lin. “Global Sensitivity Analysis”. en. In: *Encyclopedia of GIS*. Springer US, 2008, pp. 408–409. ISBN: 978-0-387-30858-6 978-0-387-35973-1. DOI: 10.1007/978-0-387-35973-1_538. (Visited on 05/25/2017).
- [119] A. Saltelli and R. Bolado. “An Alternative Way to Compute Fourier Amplitude Sensitivity Test (FAST)”. In: *Computational Statistics & Data Analysis* 26.4 (Feb. 1998), pp. 445–460. ISSN: 0167-9473. DOI: 10.1016/S0167-9473(97)00043-1.
- [120] M. D. Morris. “Factorial Sampling Plans for Preliminary Computational Experiments”. In: *Technometrics* 33.2 (May 1991), pp. 161–174. ISSN: 0040-1706. DOI: 10.1080/00401706.1991.10484804. (Visited on 10/23/2014).

- [121] G. Sin and K. V. Gernaey. “Improving the Morris Method for Sensitivity Analysis by Scaling the Elementary Effects”. In: *Computer Aided Chemical Engineering*. Ed. by J. J. Thullie and Jan. Vol. 26. 19th European Symposium on Computer Aided Process Engineering. Elsevier, 2009, pp. 925–930. (Visited on 06/06/2016).
- [122] A. Saltelli et al. “Variance Based Sensitivity Analysis of Model Output. Design and Estimator for the Total Sensitivity Index”. In: *Computer Physics Communications* 181.2 (Feb. 2010), pp. 259–270. ISSN: 0010-4655. DOI: 10.1016/j.cpc.2009.09.018. (Visited on 11/17/2016).
- [123] S. Moret, M. Bierlaire, and F. Maréchal. “Robust Optimization for Strategic Energy Planning”. In: *Informatica* 27.3 (Nov. 2016), pp. 625–648. ISSN: 0868-4952. (Visited on 12/12/2016).
- [124] S. W. Wallace. “Decision Making Under Uncertainty: Is Sensitivity Analysis of Any Use?” In: *Operations Research* 48.1 (Feb. 2000), pp. 20–25. ISSN: 0030-364X. DOI: 10.1287/opre.48.1.20.12441.
- [125] B. L. Gorissen, I. Yanıkoğlu, and D. den Hertog. “A Practical Guide to Robust Optimization”. In: *Omega* 53 (June 2015), pp. 124–137. ISSN: 0305-0483. DOI: 10.1016/j.omega.2014.12.006.
- [126] E. Svensson, T. Berntsson, and A.-B. Strömberg. “Benefits of Using an Optimization Methodology for Identifying Robust Process Integration Investments under Uncertainty—A Pulp Mill Example”. In: *Energy Policy* 37.3 (Mar. 2009), pp. 813–824. ISSN: 0301-4215. DOI: 10.1016/j.enpol.2008.10.024.
- [127] A. Ben-Tal and A. Nemirovski. “Robust Solutions of Linear Programming Problems Contaminated with Uncertain Data”. en. In: *Mathematical Programming* 88.3 (Sept. 2000), pp. 411–424. ISSN: 0025-5610, 1436-4646. DOI: 10.1007/PL00011380. (Visited on 04/09/2017).
- [128] J. M. Mulvey, R. J. Vanderbei, and S. A. Zenios. “Robust Optimization of Large-Scale Systems”. In: *Operations Research* 43.2 (Apr. 1995), pp. 264–281. ISSN: 0030-364X. DOI: 10.1287/opre.43.2.264.
- [129] S. L. Janak, X. Lin, and C. A. Floudas. “A New Robust Optimization Approach for Scheduling under Uncertainty: II. Uncertainty with Known Probability Distribution”. In: *Computers & Chemical Engineering* 31.3 (Jan. 2007), pp. 171–195. ISSN: 0098-1354. DOI: 10.1016/j.compchemeng.2006.05.035. (Visited on 06/20/2016).
- [130] G. P. Ribas, S. Hamacher, and A. Street. “Optimization under Uncertainty of the Integrated Oil Supply Chain Using Stochastic and Robust Programming”. en. In: *International Transactions in Operational Research* 17.6 (Nov. 2010), pp. 777–796. ISSN: 1475-3995. DOI: 10.1111/j.1475-3995.2009.00756.x.
- [131] P. Kouvelis and G. Yu. *Robust Discrete Optimization and Its Applications* | Panos Kouvelis | Springer. 1997. ISBN: 978-1-4419-4764-2. (Visited on 06/01/2017).

Bibliography

- [132] A. Hajimiragha et al. "A Robust Optimization Approach for Planning the Transition to Plug-in Hybrid Electric Vehicles". In: *IEEE Transactions on Power Systems* 26.4 (Nov. 2011), pp. 2264–2274. ISSN: 0885-8950. DOI: 10.1109/TPWRS.2011.2108322.
- [133] J. Koo, K. Han, and E. S. Yoon. "Integration of CCS, Emissions Trading and Volatilities of Fuel Prices into Sustainable Energy Planning, and Its Robust Optimization". In: *Renewable and Sustainable Energy Reviews* 15.1 (Jan. 2011), pp. 665–672. ISSN: 1364-0321. DOI: 10.1016/j.rser.2010.07.050.
- [134] C.-S. Yu and H.-L. Li. "A Robust Optimization Model for Stochastic Logistic Problems". In: *International Journal of Production Economics* 64.1–3 (Mar. 2000), pp. 385–397. ISSN: 0925-5273. DOI: 10.1016/S0925-5273(99)00074-2.
- [135] R. Jiang, J. Wang, and Y. Guan. "Robust Unit Commitment With Wind Power and Pumped Storage Hydro". In: *IEEE Transactions on Power Systems* 27.2 (May 2012), pp. 800–810. ISSN: 0885-8950. DOI: 10.1109/TPWRS.2011.2169817.
- [136] A. Parisio, C. Del Vecchio, and A. Vaccaro. "A Robust Optimization Approach to Energy Hub Management". In: *International Journal of Electrical Power & Energy Systems* 42.1 (Nov. 2012), pp. 98–104. ISSN: 0142-0615. DOI: 10.1016/j.ijepes.2012.03.015.
- [137] L. Zhao and B. Zeng. "Robust Unit Commitment Problem with Demand Response and Wind Energy". In: *2012 IEEE Power and Energy Society General Meeting*. July 2012, pp. 1–8. DOI: 10.1109/PESGM.2012.6344860.
- [138] C. Dong et al. "Robust Planning of Energy Management Systems with Environmental and Constraint-Conservative Considerations under Multiple Uncertainties". In: *Energy Conversion and Management*. Global Conference on Renewable energy and Energy Efficiency for Desert Regions 2011 "GCREEDER 2011" 65 (Jan. 2013), pp. 471–486. ISSN: 0196-8904. DOI: 10.1016/j.enconman.2012.09.001.
- [139] A. Street, A. Moreira, and J. M. Arroyo. "Energy and Reserve Scheduling Under a Joint Generation and Transmission Security Criterion: An Adjustable Robust Optimization Approach". In: *IEEE Transactions on Power Systems* 29.1 (Jan. 2014), pp. 3–14. ISSN: 0885-8950. DOI: 10.1109/TPWRS.2013.2278700.
- [140] K. Akbari et al. "Optimal Investment and Unit Sizing of Distributed Energy Systems under Uncertainty: A Robust Optimization Approach". In: *Energy and Buildings* 85 (Dec. 2014), pp. 275–286. ISSN: 0378-7788. DOI: 10.1016/j.enbuild.2014.09.009.
- [141] J. M. F. Rager. "Urban Energy System Design from the Heat Perspective Using Mathematical Programming Including Thermal Storage". PhD thesis. Lausanne: EPFL, 2015.

- [142] C. L. Sy et al. “Target-Oriented Robust Optimization of Polygeneration Systems under Uncertainty”. In: *Energy*. Green Strategy for Energy Generation and Saving towards Sustainable Development 116, Part 2 (Dec. 2016), pp. 1334–1347. ISSN: 0360-5442. DOI: 10.1016/j.energy.2016.06.057.
- [143] T. S. Ng and C. Sy. “An Affine Adjustable Robust Model for Generation and Transmission Network Planning”. In: *International Journal of Electrical Power & Energy Systems* 60 (Sept. 2014), pp. 141–152. ISSN: 0142-0615. DOI: 10.1016/j.ijepes.2014.02.026.
- [144] C. Nicolas. *Robust Energy and Climate Modeling for Policy Assessment*. Paris 10, June 2016. (Visited on 05/31/2017).
- [145] J. Gong, D. J. Garcia, and F. You. “Unraveling Optimal Biomass Processing Routes from Bioconversion Product and Process Networks under Uncertainty: An Adaptive Robust Optimization Approach”. In: *ACS Sustainable Chemistry & Engineering* 4.6 (June 2016), pp. 3160–3173. DOI: 10.1021/acssuschemeng.6b00188.
- [146] D. E. Majewski et al. “Robust Multi-Objective Optimization for Sustainable Design of Distributed Energy Supply Systems”. In: *Computers & Chemical Engineering* (2016). ISSN: 0098-1354. DOI: 10.1016/j.compchemeng.2016.11.038. (Visited on 01/26/2017).
- [147] V. Gabrel, C. Murat, and A. Thiele. “Recent Advances in Robust Optimization: An Overview”. In: *European Journal of Operational Research* 235.3 (June 2014), pp. 471–483. ISSN: 0377-2217. DOI: 10.1016/j.ejor.2013.09.036.
- [148] D. Kuhn, W. Wiesemann, and A. Georghiou. “Primal and Dual Linear Decision Rules in Stochastic and Robust Optimization”. en. In: *Mathematical Programming* 130.1 (Nov. 2011), pp. 177–209. ISSN: 0025-5610, 1436-4646. DOI: 10.1007/s10107-009-0331-4. (Visited on 05/26/2017).
- [149] A. Ben-Tal, L. El Ghaoui, and A. Nemirovski. *Robust Optimization*. Princeton University Press, 2009.
- [150] X. Chen, M. Sim, and P. Sun. “A Robust Optimization Perspective on Stochastic Programming”. In: *Operations Research* 55.6 (2007), pp. 1058–1071. ISSN: 0030-364X.
- [151] W. Wiesemann, D. Kuhn, and M. Sim. “Distributionally Robust Convex Optimization”. In: *Operations Research* 62.6 (Oct. 2014), pp. 1358–1376. ISSN: 0030-364X. DOI: 10.1287/opre.2014.1314.
- [152] E. Svensson et al. “An Optimization Methodology for Identifying Robust Process Integration Investments under Uncertainty”. In: *Energy Policy* 37.2 (Feb. 2009), pp. 680–685. ISSN: 0301-4215. DOI: 10.1016/j.enpol.2008.10.023. (Visited on 02/07/2014).
- [153] C. Kwon, T. Lee, and P. Berglund. “Robust Shortest Path Problems with Two Uncertain Multiplicative Cost Coefficients”. en. In: *Naval Research Logistics (NRL)* 60.5 (Aug. 2013), pp. 375–394. ISSN: 1520-6750. DOI: 10.1002/nav.21540. (Visited on 01/09/2017).

Bibliography

- [154] F. Babonneau et al. “Energy Security: A Robust Optimization Approach to Design a Robust European Energy Supply via TIAM-WORLD”. en. In: *Environmental Modeling & Assessment* 17.1-2 (Apr. 2012), pp. 19–37. ISSN: 1420-2026, 1573-2967. DOI: 10.1007/s10666-011-9273-3. (Visited on 06/04/2017).
- [155] A. Schrijver. *Theory of Linear and Integer Programming*. en. Google-Books-ID: zEzW5mhppB8C. John Wiley & Sons, July 1998. ISBN: 978-0-471-98232-6.
- [156] A. Ghouila-Houri. “Caractérisation Des Matrices Totalement Unimodulaires”. In: *Comptes Rendus Hebdomadaires des Séances de l’Académie des Science* 254 (1962), pp. 1192–1194.
- [157] L. Kaufman and P. Rousseeuw. *Clustering by Means of Medoids*. North-Holland, 1987.
- [158] J. Rager et al. “Integrating Uncertainty into Urban Energy System Design”. In: *Computer Aided Chemical Engineering*. 26th European Symposium on Computer Aided Process Engineering 38 (Jan. 2016), pp. 1641–1646. ISSN: 1570-7946. DOI: 10.1016/B978-0-444-63428-3.50278-2.
- [159] C. L. Sy. “A Target-Oriented Robust Optimization Approach to Production and Logistics Planning Systems”. en. Thesis. Jan. 2013. (Visited on 06/30/2017).
- [160] D. B. Brown and M. Sim. “Satisficing Measures for Analysis of Risky Positions”. In: *Management Science* 55.1 (Oct. 2008), pp. 71–84. ISSN: 0025-1909. DOI: 10.1287/mnsc.1080.0929.
- [161] TERNA. *Dati Statistici Sull’energia Elettrica in Italia - Anno 2011*.
- [162] D. Hach and S. Spinler. “Capacity Payment Impact on Gas-Fired Generation Investments under Rising Renewable Feed-in — A Real Options Analysis”. In: *Energy Economics*. Energy Markets 53 (Jan. 2016), pp. 270–280. ISSN: 0140-9883. DOI: 10.1016/j.eneco.2014.04.022.
- [163] J. Thénié, C. van Delft, and J.-P. Vial. “Automatic Formulation of Stochastic Programs Via an Algebraic Modeling Language”. en. In: *Computational Management Science* 4.1 (Jan. 2007), pp. 17–40. ISSN: 1619-697X, 1619-6988. DOI: 10.1007/s10287-006-0022-z. (Visited on 07/05/2017).
- [164] A. Saltelli and S. Funtowicz. “What Is Science’s Crisis Really about?” In: *Futures* (May 2017). ISSN: 0016-3287. DOI: 10.1016/j.futures.2017.05.010.
- [165] J. P. van der Sluijs. “A Way out of the Credibility Crisis of Models Used in Integrated Environmental Assessment”. In: *Futures* 34.2 (Mar. 2002), pp. 133–146. ISSN: 0016-3287. DOI: 10.1016/S0016-3287(01)00051-9.
- [166] Y. A. Guzman, L. R. Matthews, and C. A. Floudas. “New a Priori and a Posteriori Probabilistic Bounds for Robust Counterpart Optimization: I. Unknown Probability Distributions”. In: *Computers & Chemical Engineering* 84 (Jan. 2016), pp. 568–598. ISSN: 0098-1354. DOI: 10.1016/j.compchemeng.2015.09.014. (Visited on 06/20/2016).

- [167] J. P. van der Sluijs et al. "Combining Quantitative and Qualitative Measures of Uncertainty in Model-Based Environmental Assessment: The NUSAP System". eng. In: *Risk Analysis: An Official Publication of the Society for Risk Analysis* 25.2 (Apr. 2005), pp. 481–492. ISSN: 0272-4332. DOI: 10.1111/j.1539-6924.2005.00604.x.
- [168] B. Weidema et al. *The Ecoinvent Database: Overview and Methodology, Data Quality Guideline for the Ecoinvent Database Version 3*. 2013. (Visited on 02/01/2015).
- [169] Chemical Engineering. *Chemical Engineering's Plant Cost Index*. <http://www.chemengonline.com/pci-home>. May 2016.
- [170] Groupement professionnel suisse pour les pompes à chaleur (GSP). *Production d'eau Chaude Sanitaire*. <http://www.fws.ch/production-d-eau-chaude-sanitaire.html>. (Visited on 10/08/2016).
- [171] T. Grieder and A. Huser. *Neue Ansätze Zur Verbrauchsabschätzung von Lampen in Privathaushalten*. Tech. rep. Swiss Federal Office of Energy (SFOE), 2008.
- [172] European Photovoltaic Technology Platform, ed. *A Strategic Research Agenda for Photovoltaic Solar Energy Technology*. 2nd ed. Luxembourg: Publications Office of the European Union, 2011. ISBN: 978-92-79-20172-1.
- [173] Swiss Federal Office of Energy (SFOE). *Swiss Electricity Statistics 2013*. Tech. rep. 2014.
- [174] IEA - International Energy Agency. *Potential for Building Integrated Photovoltaics*. Tech. rep. 2002.
- [175] Association des entreprises électriques suisses (AES). *Électricité photovoltaïque et solaire thermique*. French. Dec. 2013.
- [176] Association des entreprises électriques suisses (AES). *Energie Éolienne*. 2013.
- [177] Swiss Federal Office of Energy (SFOE). *Schweizerische Statistik Der Erneuerbaren Energien. Ausgabe 2014*. Tech. rep. Bern, Switzerland, June 2015.
- [178] IEA - International Energy Agency. *Technology Roadmap. Wind Energy*. Tech. rep. Paris, 2013.
- [179] SuisseÉole. *Windenergie-Daten Der Schweiz*. <http://wind-data.ch/>. (Visited on 10/02/2016).
- [180] Swiss Federal Office for the Environment. *Energiestrategie 2050. Berechnung Der Energiepotenziale Für Wind Und Sonnenenergie*. Tech. rep. Bern, Switzerland, Sept. 2012.
- [181] Association des entreprises électriques suisses (AES). *Grande hydraulique*. French. Tech. rep. 2014.
- [182] Swiss Federal Office of Energy (SFOE). *Statistique Des Aménagements Hydroélectriques de La Suisse - Etat Au 01.01.2013*. Tech. rep. 2013.
- [183] Association des entreprises électriques suisses (AES). *Électricité géothermique*. French. Tech. rep. 2012.

Bibliography

- [184] R. Nordmann and J. Remund. *L'évolution Des Besoins de Stockage Au Fur et à Mesure de La Sortie Du Nucléaire, Dans l'hypothèse Où l'on Remplace 70 % Du Nucléaire Par Du Photo-voltaïque*. 2012.
- [185] Juvent AG. *Centrale Éolienne Juvent*. <http://www.juvent.ch/accueil.html>.
- [186] Swiss Federal Office of Energy (SFOE). *Production et Consommation Totales d'énergie Élec-trique En Suisse 2008*. Tech. rep. 2009.
- [187] Swiss Federal Office of Energy (SFOE). *Le Potentiel Hydroélectrique de La Suisse. Potentiel de Développement de La Force Hydraulique Au Titre de La Stratégie Énergétique 2050*. Tech. rep. Bern, Switzerland, June 2012.
- [188] A. Schleiss. "Talsperreerhöhungen in Der Schweiz : Energiewirtschaftliche Bedeutung Und Randbedingungen". In: *Wasser Energie Luft* 104.3 (2012), pp. 199–203. (Visited on 02/10/2017).
- [189] V. Rits and A. Kirchner. *Die Energieperspektiven 2035 - Band 5 Analyse und Bewertung des Elektrizitätsangebotes*. German. Tech. rep. Basel: Prognos AG, June 2007, p. 607.
- [190] Swissnuclear. *Financement - Energienucléaire.Ch*. https://www.kernenergie.ch/fr/financement-_content---1--1306.html. (Visited on 02/10/2017).
- [191] Association des entreprises électriques suisses. *Energie Nucléaire*. Mar. 2014.
- [192] C. Bauer et al. *New Energy Externalities Developments for Sustainability (NEEDS) - Deliv-erable N° 7.2 - RS 1a: Final Report on Technical Data, Costs, and Life Cycle Inventories of Advanced Fossil Power Generation Systems*. English. Tech. rep. Mar. 2008.
- [193] U.S. EIA - Energy Information Administration. *Updated Capital Cost Estimates for Utility Scale Electricity Generating Plants*. English. Tech. rep. Washington, Apr. 2013.
- [194] K. Hjortset et al. "Development of Large-Scale Precast, Prestressed Concrete Liquefied Natural Gas Storage Tanks". In: (2013).
- [195] B. Songhurst. *LNG Plant Cost Escalation*. Tech. rep. Oxford, UK: The Oxford Institute for Energy Studies, Feb. 2014.
- [196] Association des entreprises électriques suisses (AES). *Scénarios Pour l'approvisionnement Électrique Du Futur. Rapport Global*. Tech. rep. 2012.
- [197] D. Stump. *Swiss parliament - 10.3348 - Sécuriser notre réseau de transmission et de distribu-tion d'électricité*. French. 2010. (Visited on 02/10/2017).
- [198] Ove Arup and Partners Ltd. *Review of the Generation Costs and Deployment Potential of Renewable Electricity Technologies in the UK*. Study Report. London: Department of Energy and Climate Change, Oct. 2011.
- [199] European Commission. *Energy Sources, Production Costs and Performance of Technologies for Power Generation, Heating and Transport*. 2008.

- [200] Walter Meier AG. *Listes de Prix Walter Meier. Prix Valables Dès Avril 2011*. 2011.
- [201] NERA Economic Consulting and AEA. *The UK Supply Curve for Renewable Heat. Study for the Department of Energy and Climate Change*. English. Tech. rep. London, UK, July 2009.
- [202] H. C. Becker. “Methodology and Thermo-Economic Optimization for Integration of Industrial Heat Pumps”. In: (2012). DOI: 10.5075/epfl-thesis-5341, \%0020urn:nbn:ch:bel-epfl-thesis5341-9. (Visited on 07/22/2016).
- [203] IEA - International Energy Agency. *Renewables for Heating and Cooling. Untapped Potential*. Tech. rep. Paris, 2007.
- [204] Hoval SA. *Catalogue Des Produits Hoval. Production de Chaleur et Génie Climatique*. Apr. 2016.
- [205] Viessman. *Viessman Products Catalogue*. 2016.
- [206] Battelle. *Manufacturing Cost Analysis of 1 kW and 5 kW Solid Oxide Fuel Cell (SOFC) for Auxilliary Power Applications*. Tech. rep. Feb. 2014.
- [207] R. Gerboni et al. *Final Report on Technical Data, Costs and Life Cycle Inventories of Fuel Cells*. Tech. rep. 2008.
- [208] J. A. Duffie and W. A. Beckman. *Solar Engineering of Thermal Processes, 4th Edition*. May 2013. ISBN: 978-0-470-87366-3.
- [209] B. Steubing et al. “Bioenergy in Switzerland: Assessing the Domestic Sustainable Biomass Potential”. In: *Renewable and Sustainable Energy Reviews* 14.8 (Oct. 2010), pp. 2256–2265. ISSN: 1364-0321. DOI: 10.1016/j.rser.2010.03.036. (Visited on 11/24/2016).
- [210] Eurostat. *Municipal Waste Statistics*. http://ec.europa.eu/eurostat/statistics-explained/index.php/Municipal_waste_statistics. (Visited on 02/13/2017).
- [211] M. Herczeg. *Municipal Waste Management in Switzerland*. Tech. rep. EEA - European Environmental Agency, Feb. 2013.
- [212] Epex spot. *Swissix Market Data Chart - Year 2010*. <https://www.epexspot.com/>. (Visited on 02/13/2017).
- [213] Swiss Federal Office of Statistics (SFOS). *IPC, Prix Moyens de l'énergie et Des Carburants*. 2016.
- [214] V. Beuret. *Evolution Des Marchés Des Énergies Fossiles 4 / 2015*. Tech. rep. Bern, Switzerland: Swiss Federal Office of Energy (SFOE), Mar. 2016.
- [215] Swiss Federal Office of Statistics (SFOS). *Indice Des Prix à La Consommation, Prix Moyens Mensuels Pour 100 l de Mazout Pour Des Quantités Types*. 2016.
- [216] Swiss Federal Office of Statistics (SFOS). *Indice Des Prix à La Production et à l'importation*. Tech. rep. 2015.

Bibliography

- [217] Association des entreprises électriques suisses (AES). *Centrale au charbon*. French. Tech. rep. 2012.
- [218] F. Ess, A. Kirchner, and V. Rits. *Kosten Neuer Kernkraftwerke*. Tech. rep. Basel, Switzerland: Prognos AG, Feb. 2011.
- [219] M. Gassner and F. Maréchal. “Thermo-Economic Optimisation of the Integration of Electrolysis in Synthetic Natural Gas Production from Wood”. In: *Energy*. 19th International Conference on Efficiency, Cost, Optimization, Simulation and Environmental Impact of Energy Systems ECOS 2006 33.2 (Feb. 2008), pp. 189–198. ISSN: 0360-5442. DOI: 10.1016/j.energy.2007.09.010. (Visited on 02/13/2017).
- [220] L. Tock. “Thermo-Environomic Optimisation of Fuel Decarbonisation Alternative Processes for Hydrogen and Power Production”. Doctoral Thesis. EPFL Lausanne, 2013.
- [221] *Perspectives Énergétiques 2050. Annexes Au Résumé*. Tech. rep. Bern, Switzerland: Office fédéral de l’énergie (OFEN), Oct. 2013.
- [222] Swiss Federal Office of Energy (SFOE). *Swiss Electricity Statistics 2015*. Tech. rep. 2016.
- [223] OFS - Office Fédéral de la Statistique. *Les Scénarios de l’évolution de La Population de La Suisse 2010-2060*. Tech. rep. 2010.
- [224] IEA - International Energy Agency. *Technology Roadmap - Solar Photovoltaic Energy*. Tech. rep. 2010.
- [225] U.S. National Renewable Energy Laboratory (NREL). *Best Research-Cell Efficiencies Chart*. http://www.nrel.gov/pv/assets/images/efficiency_chart.jpg. (Visited on 11/23/2016).
- [226] B Oetli et al. *Potentiale Zur Energetischen Nutzung von Biomasse in Der Schweiz*. Tech. rep. Swiss Federal Office of Energy (SFOE), 2004.
- [227] O. Thees et al. *Energieholzpotenziale Im Schweizer Wald Und Ihre Bereitstellungskosten*. Tech. rep. 2013.
- [228] O Thees et al. “Potenziale, Chancen Und Risiken Der Energieholznutzung Zur Rolle Des Holzes Im Schweizer Energiesystem”. In: 2014, pp. 29–42.
- [229] Swiss Competence Center for Energy Research (SCCER). *Biomass for Swiss Energy Future (BIOSWEET)*. <http://www.sccer-biosweet.ch>. (Visited on 11/24/2016).
- [230] D. Assouline, N. Mohajeri, and J.-L. Scartezzini. *Solar Photovoltaic Electricity Potential for Switzerland*. <http://www.sccer-feebd.ch/solar-photovoltaic-electricity-potential-for-switzerland/>. (Visited on 07/26/2016).
- [231] Bloomberg New Energy Finance. *H1 2015 North American PV Outlook*. Tech. rep. Jan. 2015.
- [232] J. Lutz et al. “Life-Cycle Cost Analysis of Energy Efficiency Design Options for Residential Furnaces and Boilers”. In: *Energy* 31.2–3 (Feb. 2006), pp. 311–329. ISSN: 0360-5442. DOI: 10.1016/j.energy.2005.02.002. (Visited on 11/30/2016).

- [233] J. Lewis and A. Clarke. *Replacement Market for Residential Energy Service Equipment*. Tech. rep. Gas Research Institute, 1990.
- [234] UK Department of Energy and Climate Change. *2050 Calculator*. <http://2050-calculator-tool.decc.gov.uk/>. 2016.
- [235] E4Tech. *The Potential for bioSNG Production in the UK*. Tech. rep. 2010.
- [236] S. Moret et al. “Integration of Deep Geothermal Energy and Woody Biomass Conversion Pathways in Urban Systems”. In: *Energy Conversion and Management* 129 (Dec. 2016), pp. 305–318. ISSN: 0196-8904. DOI: 10.1016/j.enconman.2016.09.079. (Visited on 11/08/2016).
- [237] M. F. Demirbas, M. Balat, and H. Balat. “Potential Contribution of Biomass to the Sustainable Energy Development”. In: *Energy Conversion and Management* 50.7 (July 2009), pp. 1746–1760. ISSN: 0196-8904. DOI: 10.1016/j.enconman.2009.03.013. (Visited on 07/05/2016).
- [238] IEA - International Energy Agency. *Technology Roadmap - Geothermal Heat and Power*. Tech. rep. June 2011.
- [239] United Nations. *World Urbanization Prospects - The 2014 Revision*. Tech. rep. United Nations, 2014.
- [240] IEA. *World Energy Outlook 2008*. Tech. rep. IEA - International Energy Agency, 2008.
- [241] Ingrid Stober et al. *Deep Geothermal Energy - Application Possibilities in Germany*. Tech. rep. German Federal Ministry for Economic Affairs and Energy (BMWi), 2014.
- [242] E. E. (Stathis) Michaelides. “Future Directions and Cycles for Electricity Production from Geothermal Resources”. In: *Energy Conversion and Management*. Special Issue on Efficiency, Cost, Optimisation, Simulation and Environmental Impact of Energy Systems (ECOS)-2014 107 (Jan. 2016), pp. 3–9. ISSN: 0196-8904. DOI: 10.1016/j.enconman.2015.07.057. (Visited on 08/23/2016).
- [243] D. B. Fox, D. Sutter, and J. W. Tester. “The Thermal Spectrum of Low-Temperature Energy Use in the United States”. en. In: *Energy & Environmental Science* 4.10 (2011), p. 3731. ISSN: 1754-5692, 1754-5706. DOI: 10.1039/c1ee01722e. (Visited on 01/09/2016).
- [244] U. Persson and S. Werner. “Heat Distribution and the Future Competitiveness of District Heating”. In: *Applied Energy* 88.3 (Mar. 2011), pp. 568–576. ISSN: 0306-2619. DOI: 10.1016/j.apenergy.2010.09.020. (Visited on 01/07/2016).
- [245] P. E. Grohnheit and B. O. Gram Mortensen. “Competition in the Market for Space Heating. District Heating as the Infrastructure for Competition among Fuels and Technologies”. In: *Energy Policy* 31.9 (July 2003), pp. 817–826. ISSN: 0301-4215. DOI: 10.1016/S0301-4215(02)00066-6. (Visited on 01/07/2016).

Bibliography

- [246] L. Gerber, S. Fazlollahi, and F. Maréchal. “A Systematic Methodology for the Environomic Design and Synthesis of Energy Systems Combining Process Integration, Life Cycle Assessment and Industrial Ecology”. In: *Computers & Chemical Engineering* 59 (Dec. 2013), pp. 2–16. ISSN: 00981354. DOI: 10.1016/j.compchemeng.2013.05.025. (Visited on 01/20/2014).
- [247] P. Alberg Østergaard et al. “A Renewable Energy Scenario for Aalborg Municipality Based on Low-Temperature Geothermal Heat, Wind Power and Biomass”. In: *Energy*. The 3rd International Conference on Sustainable Energy and Environmental Protection, SEEP 2009 35.12 (Dec. 2010), pp. 4892–4901. ISSN: 0360-5442. DOI: 10.1016/j.energy.2010.08.041. (Visited on 01/08/2015).
- [248] C. R. Sommer, M. J. Kuby, and G. Bloomquist. “The Spatial Economics of Geothermal District Energy in a Small, Low-Density Town: A Case Study of Mammoth Lakes, California”. In: *Geothermics* 32.1 (Feb. 2003), pp. 3–19. ISSN: 0375-6505. DOI: 10.1016/S0375-6505(02)00046-9. (Visited on 01/08/2016).
- [249] I. Vallios, T. Tsoutsos, and G. Papadakis. “Design of Biomass District Heating Systems”. In: *Biomass and Bioenergy* 33.4 (Apr. 2009), pp. 659–678. ISSN: 0961-9534. DOI: 10.1016/j.biombioe.2008.10.009. (Visited on 01/08/2016).
- [250] E. Alakangas et al. *Strategic Research Priorities for Biomass Technology*. Tech. rep. European Technology Platform on Renewable Heating and Cooling, 2012.
- [251] J. W. Lund et al. “The United States of America Country Update 2010”. In: *35th Workshop on Geothermal Reservoir Engineering Proceedings*. Stanford University, Stanford, CA (USA), 2010, pp. 25–29.
- [252] A. Borsukiewicz-Gozdur. “Dual-Fluid-Hybrid Power Plant Co-Powered by Low-Temperature Geothermal Water”. In: *Geothermics* 39.2 (June 2010), pp. 170–176. ISSN: 0375-6505. DOI: 10.1016/j.geothermics.2009.10.004. (Visited on 01/08/2016).
- [253] I. Thain and R. DiPippo. “Hybrid Geothermal-Biomass Power Plants: Applications, Designs and Performance Analysis”. In: *World Geothermal Congress 2015 Proceedings*. Melbourne (Australia), 2015.
- [254] B. Kilis. “A Lignite–geothermal Hybrid Power and Hydrogen Production Plant for Green Cities and Sustainable Buildings”. en. In: *International Journal of Energy Research* 35.2 (Feb. 2011), pp. 138–145. ISSN: 1099-114X. DOI: 10.1002/er.1757. (Visited on 01/08/2016).
- [255] M. Z. Lukawski et al. “A Proposed Hybrid Geothermal-Natural Gas-Biomass Energy System for Cornell University. Technical and Economic Assessment of Retrofitting a Low-Temperature Geothermal District Heating System and Heat Cascading Solutions”. In: *38th Workshop on Geothermal Reservoir Engineering Proceedings*. Stanford University, Stanford, CA (USA), 2013.

- [256] K. F. Beckers et al. “Hybrid Low-Grade Geothermal-Biomass Systems for Direct-Use and Co-Generation: From Campus Demonstration to Nationwide Energy Player”. In: *40th Workshop on Geothermal Reservoir Engineering Proceedings*. Stanford University, Stanford, CA (USA), 2015.
- [257] M. Malik, I. Dincer, and M. A. Rosen. “Development and Analysis of a New Renewable Energy-Based Multi-Generation System”. In: *Energy* 79 (Jan. 2015), pp. 90–99. ISSN: 0360-5442. DOI: 10.1016/j.energy.2014.10.057. (Visited on 01/09/2016).
- [258] F. L.-P.R. M. Amblard. “Geothermal Energy Integration in Urban Systems. The Case Study of the City of Lausanne”. Master’s thesis. Lausanne, Switzerland: EPFL, 2015.
- [259] S. Moret et al. “Geothermal Energy and Biomass Integration in Urban Systems: A Case Study”. In: *40th Workshop on Geothermal Reservoir Engineering Proceedings*. Stanford University, Stanford, California, USA, 2015.
- [260] R. Bolliger. “Méthodologie de La Synthèse Des Systèmes Énergétiques Industriels”. Doctoral Thesis. Lausanne: EPFL, 2010.
- [261] S. L. Bungener. “Multi-Objective Optimisation of District Energy Systems”. Master’s thesis. École Polytechnique Fédérale de Lausanne, 2012. (Visited on 04/18/2016).
- [262] I. C. Kemp. *Pinch Analysis and Process Integration: A User Guide on Process Integration for the Efficient Use of Energy*. en. Butterworth-Heinemann, Apr. 2011. ISBN: 978-0-08-046826-6.
- [263] IPCC. *Climate Change 2013: The Physical Science Basis. Contribution of Working Group I to the Fifth Assessment Report of the Intergovernmental Panel on Climate Change*. Ed. by T. Stocker et al. Cambridge, UK: Cambridge University Press, 2013.
- [264] O. Jolliet et al. “IMPACT 2002+: A New Life Cycle Impact Assessment Methodology”. en. In: *The International Journal of Life Cycle Assessment* 8.6 (Nov. 2003), pp. 324–330. ISSN: 0948-3349, 1614-7502. DOI: 10.1007/BF02978505. (Visited on 04/18/2016).
- [265] R. Frischknecht and S. Büsler Knöpfel. *Swiss Eco-Factors 2013 According to the Ecological Scarcity Method. Methodological Fundamentals and Their Application in Switzerland*. Tech. rep. Bern, Switzerland: Swiss Federal Office for the Environment, 2013.
- [266] L. Gerber and F. Maréchal. “Environomic Optimal Configurations of Geothermal Energy Conversion Systems: Application to the Future Construction of Enhanced Geothermal Systems in Switzerland”. In: *Energy* 45.1 (Sept. 2012), pp. 908–923. ISSN: 0360-5442. DOI: 10.1016/j.energy.2012.06.068. (Visited on 07/16/2013).
- [267] V. Codina Gironès et al. “Optimal Use of Biomass in Large-Scale Energy Systems: Insights for Energy Policy”. In: *29th International Conference on Efficiency, Cost, Optimisation, Simulation and Environmental Impact of Energy Systems*. Portoroz, Slovenia, 2016.

Bibliography

- [268] J. Lehto et al. “Review of Fuel Oil Quality and Combustion of Fast Pyrolysis Bio-Oils from Lignocellulosic Biomass”. In: *Applied Energy* 116 (Mar. 2014), pp. 178–190. ISSN: 0306-2619. DOI: 10.1016/j.apenergy.2013.11.040. (Visited on 05/01/2016).
- [269] E. Peduzzi. “Biomass To Liquids: Thermo-Economic Analysis and Multi-Objective Optimisation, N° 6529”. PhD thesis. École Polytechnique Fédérale de Lausanne, 2015.
- [270] TRIDEL. *Rapport de Gestion 2012*. French. 2013.
- [271] BiomassEnergyCentre. *Moisture Content*. accessed 2016 Jan.
- [272] Swiss Federal Office of Energy (SFOE). *Révision technique de la consommation d’huile de chauffage extra-légère publiée dans la statistique globale de l’énergie*. French. Tech. rep. Swiss Federal Office of Energy (SFOE), 2014.
- [273] R. Edwards et al. *Well-to-Wheels Analysis of Future Automotive Fuels and Powertrains in the European Context*. Tech. rep. EUR 26237 EN - 2014. Version 4a. European Commission - Joint Research Center (JRC), 2014.
- [274] Swiss Federal Office of Statistics (SFOS). *Indice Des Prix à La Consommation, Carburants - Prix Moyens Par Litre En Francs*. Tech. rep. 2016.
- [275] WaldShewiz. *Marché Suisse Du Bois de Feu et Du Bois d’énergie*. accessed 2016 Jan.
- [276] G. Bourgault. *Implementation of IPCC Impact Assessment Method 2007 and 2013 to Ecoinvent Database 3.2*. Tech. rep. Ecoinvent centre, 2015.
- [277] L. Michel. “Complémentarité Entre Plusieurs Ressources Énergétiques Pour Une Même Prestation. Le Cas Du Réseau de Chauffage à Distance de Lausanne”. PhD thesis. Université de Geneve, 2012.
- [278] M. Gassner and F. Maréchal. “Thermo-Economic Process Model for Thermochemical Production of Synthetic Natural Gas (SNG) from Lignocellulosic Biomass”. In: *Biomass and Bioenergy* 33.11 (Nov. 2009), pp. 1587–1604. ISSN: 0961-9534. DOI: 10.1016/j.biombioe.2009.08.004. (Visited on 05/05/2016).
- [279] M. B. Shemfe, S. Gu, and P. Ranganathan. “Techno-Economic Performance Analysis of Biofuel Production and Miniature Electric Power Generation from Biomass Fast Pyrolysis and Bio-Oil Upgrading”. In: *Fuel* 143 (2015), pp. 361–372. ISSN: 00162361. DOI: 10.1016/j.fuel.2014.11.078.
- [280] W. Boie. “Fuel Technology Calculations.” In: *Energietechnik* 3 (1953), pp. 309–16.
- [281] A. Bridgwater. “Review of Fast Pyrolysis of Biomass and Product Upgrading”. In: *Biomass and Bioenergy* 38 (Mar. 2012), pp. 68–94. ISSN: 09619534. DOI: 10.1016/j.biombioe.2011.01.048.
- [282] G. Haarlemmer et al. “Second Generation BtL Type Biofuels – a Production Cost Analysis”. In: *Energy & Environmental Science* 5.9 (2012), p. 8445. ISSN: 1754-5692. DOI: 10.1039/c2ee21750c.

- [283] L. Tacher. *An Attempt of Deep Geological Stratigraphical Model in the Area of Lausanne City*. Tech. rep. EPFL, 2014.
- [284] Working group PDGN. *Programme Cantonal de Développement de La Géothermie à Neuchâtel: Rapport Final*. Tech. rep. Switzerland: Laboratoire Suisse de Géothermie - CREGE, 2010.
- [285] W. Short, D. J. Packey, and T. Holt. *A Manual for the Economic Evaluation of Energy Efficiency and Renewable Energy Technologies*. University Press of the Pacific, 2005.
- [286] Services Industriels de Lausanne (SiL). *L'aménagement hydroélectrique de Lavey*. French. (Visited on 05/01/2016).
- [287] Association des entreprises électriques suisses (AES). *Centrales à gaz à cycle combiné (CCC)*. French. Tech. rep. 2013.
- [288] P. C. Badger and P. Fransham. "Use of Mobile Fast Pyrolysis Plants to Densify Biomass and Reduce Biomass Handling Costs—A Preliminary Assessment". In: *Biomass and Bioenergy*. Proceedings of the third annual workshop of Task 31 'Sustainable production systems for bioenergy: Impacts on forest resources and utilization of wood for energy' October 2003, Flagstaff, Arizona, USA 30.4 (Apr. 2006), pp. 321–325. ISSN: 0961-9534. DOI: 10.1016/j.biombioe.2005.07.011. (Visited on 05/08/2016).
- [289] A. A. Rentizelas, A. J. Tolis, and I. P. Tatsiopoulou. "Logistics Issues of Biomass: The Storage Problem and the Multi-Biomass Supply Chain". In: *Renewable and Sustainable Energy Reviews* 13.4 (May 2009), pp. 887–894. ISSN: 1364-0321. DOI: 10.1016/j.rser.2008.01.003. (Visited on 05/09/2016).
- [290] City of Lausanne. *Statistiques de la station d'épuration des eaux usées (STEP)*. French. <http://www.lausanne.ch/en/lausanne-officielle/administration/travaux/assainissement/service/presentation/statistiques/statistiques-step.html>. (Visited on 12/10/2014).
- [291] Services Industriels de Lausanne (SiL). *Station d'épuration des eaux usées de la région lausannoise (STEP) - Remplacement de la chaudière de la ligne d'incinération des boues n° 2*. French. 2005. (Visited on 05/10/2016).
- [292] J. Oliver-Solà, X. Gabarrell, and J. Rieradevall. "Environmental Impacts of the Infrastructure for District Heating in Urban Neighbourhoods". In: *Energy Policy* 37.11 (Nov. 2009), pp. 4711–4719. ISSN: 0301-4215. DOI: 10.1016/j.enpol.2009.06.025. (Visited on 05/11/2016).
- [293] U.S. Department of Energy (DOE). *Www.Fueleconomy.Gov - the Official U.S. Government Source for Fuel Economy Information*. <http://www.fueleconomy.gov>. May 2016.
- [294]ecoinvent Centre. *Ecoinvent Report - Transport Services*. 2007.
- [295] Touring Club Suisse (TCS). *Exemple de frais pour un véhicule*. French. <https://www.tcs.ch/fr/auto-deux-roues/acheter-vendre-une-voiture/couts-et-frais-d-entretien/exemple-de-frais-pour-un-vehicule.php>. May 2016.

Bibliography

- [296] Transports Lausannois (TL). *Rapport d'activité 2013*. Tech. rep. 2014.
- [297] Ville de La Chaux-de-Fonds. *Etude comparative trolleybus – bus hybrides*. French. Tech. rep. 2013.
- [298] Canton de Vaud. *Décrets Traités Par Le Grand Conseil - 412 (20.09.11)*.



Stefano Moret

Italian, 28.01.1988

Education

- 2013–2017 **PhD Energy**, *École Polytechnique Fédérale de Lausanne (EPFL)*, Switzerland.
Strategic energy planning under uncertainty - Prof. F. Maréchal, Prof. M. Bierlaire
- 2009–2012 **MSc Mechanical Engineering**, *University of Padova*, Italy, 110/110 with honors.
GPA 29.5/30
- 2011 **Academic exchange**, *University of California, Berkeley*, USA.
- 2010 **Academic exchange**, *NTNU*, Norway.
- 2006–2009 **BSc Industrial Engineering**, *University of Padova*, Italy, 110/110 with honors.
GPA 29.3/30

Professional experience

- 2013–Present **Research and teaching assistant**, *IPESE group, EPFL*, Switzerland.
Research: modeling and optimization of urban and national energy systems. Projects:
 - Swiss-energyscope.ch - decision support for the Swiss energy strategy
 - Geotherm II - integration of deep geothermal energy in citiesTeaching:
 - Assistant to Master and PhD energy courses: lectures and exercises
 - 10+ supervised students (7 Master theses)
- 2012 **Junior Specialist**, *California Lighting Technology Center – University of California, Davis*, USA.
Building energy simulation, experimental tests for fenestration devices
- 2009–2011 **Associate, President**, *JEst - Junior Enterprise, University of Padova*, Italy.
Non-profit student association. Consultancy and event organization. Projects:
 - Start Cup Giovani (250 k€) - student start-up competition (project management)
 - President - management of 35 associates
- 2009 **Intern**, *FIAMM Spa*, Italy.
Energy storage. BSc thesis: LabVIEW application for Statistical Process Control
- 2008 **Intern**, *Aluminium Rheinfelden*, Germany.
Aluminium foundry. One-month research for development of innovative aluminum alloys
- 2006–2009 **Summer intern**, *ACC compressors*, China.
Compressor manufacturer. Quality engineer, chemical and acoustic laboratory work

Publications

Journal articles

S. Moret, V. Codina Gironès, M. Bierlaire and F. Maréchal. *Characterization of input uncertainties in strategic energy planning models*. Applied energy, 2017

V. Codina Gironès, S. Moret, E. Peduzzi, M. Nasato and F. Maréchal. *Optimal use of biomass in large-scale energy systems: insights for energy policy*. Energy, 2017

J. Unternährer, S. Moret, S. Joost and F. Maréchal. *Spatial clustering for district heating integration in urban energy systems: application to geothermal energy*. Applied Energy, 2017

S. Moret, E. Peduzzi, L. Gerber and F. Maréchal. *Integration of deep geothermal energy and woody biomass conversion pathways in urban systems*. Energy Conversion and Management, 2016

S. Moret, M. Bierlaire and F. Maréchal. *Robust optimization for strategic energy planning*. Informatica, 2016

V. Codina Gironès, S. Moret, F. Maréchal and D. Favrat. *Strategic energy planning for large-scale energy systems: A modelling framework to aid decision-making*. Energy, 2015.

Conference papers

S. Moret, M. Bierlaire and F. Maréchal. *Strategic energy planning under uncertainty: a mixed-integer linear programming modeling framework for large-scale energy systems*. 26th European Symposium on Computer Aided Process Engineering, Slovenia, 2016.

J. Rager, S. Moret, M. Pernet and F. Maréchal. *Integrating uncertainty into urban energy system design*. 26th European Symposium on Computer Aided Process Engineering, Slovenia, 2016.

V. Codina Gironès, S. Moret, E. Peduzzi, M. Nasato and F. Maréchal. *Optimal use of biomass in large-scale energy systems: insights for energy policy*. 29th International Conference on Efficiency, Cost, Optimization, Simulation and Environmental Impact of Energy Systems, Slovenia, 2016.

S. Moret, L. Gerber, F. Amblard, E. Peduzzi and F. Maréchal. *Geothermal energy and biomass integration in urban systems: a case study*. 40th Workshop on Geothermal Reservoir Engineering, USA, 2015.

S. Moret, V. Codina Gironès, F. Maréchal and D. Favrat. *Swiss-energyscope.ch: a platform to widely spread energy literacy and aid decision-making*. 17th Conference on Process Integration, Modelling and Optimisation for Energy Saving and Pollution Reduction, Czech Republic, 2014.

Languages

Mother tongue **Italian**
Fluent **English, French, Spanish**
Intermediate **German, Chinese**

✉ moret.stefano@gmail.com

